Interactions between volatile organic compounds and natural building materials

Ferreira Pinto Da Silva, Carla Florbela

Award date:
2017

Awarding institution:
University of Bath

Interactions between volatile organic compounds and natural building materials

A thesis submitted by

Carla Florbela Ferreira Pinto da Silva

for the degree of

Doctor of Philosophy

University of Bath

Department of Architecture and Civil Engineering

October 2017

Dedicated to my parents, to you, to everyone who works towards a healthy and sustainable world…

Acknowledgements

Firstly, I would like to thank my supervisory team, Dr Richard J. Ball, Dr Martin P. Ansell from University of Bath and Dr Andy Dengel from Building Research Establishment, for their guidance and constant encouragement during this PhD programme.

I would like to acknowledge the BRE Trust for funding my PhD research and the European Commission Seventh Framework Programme for research, technological development and demonstration, for funding the ECO-SEE project under grant agreement no 609234.

I was fortunate to work within the Indoor Air Quality team of scientists during my research campaigns at Building Research Establishment in Watford. Special thanks to Dr Keith Mower and Chetas Rana for their technical and experimental support and with whom it was always a pleasure to work with.

Among the partners of the ECO-SEE project, firstly I would like to thank Prof. Pete Walker (Grant holder) and Dr Andy Dengel, who supported my attendance to the very productive and interesting project meetings. I would like to thank my colleagues Sebastian Stratbücker from Fraunhofer IBP and Prof. Mukesh Khare, Dr Chinthala Sumanth and Dr Sunil Gulia from IIT Delhi for the collaborative work on the development of the design for holistic assessment of IEQ. Thanks to colleagues Dr Florian Mayer from Fraunhofer IBP, Dr Yolanda de Miguel and Dr José António Ibáñez from Tecnalia, Prof. João Labrincha and Dr David Maria Tobaldi from University of Aveiro and Andrea Giampiccolo from University of Bath for support of work on photocatalytic lime mortars. Also, thanks to Toby Dell from Kronospan for supplying photocatalytic MDF panels. From the University of Bangor, I would like to thank my colleagues Dr Graham Ormondroyd, Bronia Stefanowski and Elie Mansour for the collaborative work on wood-based panels and insulation materials. Special thanks to my colleague and friend Dr Daniel Maskell for all the encouraging conversations and scientific discussions we had since the first week of my PhD path.

Special thanks to Prof. João Labrincha who encouraged me to apply to this PhD opportunity.

Many thanks to my special friends from Aveiro: João Vieira, Vera Silva, Tiago Silva, Sandra Monteiro, Tiago Gadim, Cátia Soares e Paulo Cyhlar for their very important friendship over many years and continued support despite being two thousand kilometres apart. I would also

like to thank my friends from Bath for their friendship, understanding and patience for receiving so many '*oh sorry, I can't make it, have to work*'.

To finalise but not the least, I am very grateful to my *Mãe* (Mum) and *Pai* (Dad) for understanding how much this step of my life was important to me and of course for joining the new digital technologies - video-calls; your support and comprehension was essential! Millions of thanks to my beloved Cristiano Diogo, for being present during all moments of my PhD life. Thank you for being always inspiring and supportive.

…I am sorry my beloved *Avô* (grandpa), for not saying *até já* (see you later) in person. You will be always remembered…

Perfer et obdura

Hoc hic tibi proderit olim

Omnia causa fiunt

Sicut per gradus gradum seguitur

Abstract

There is increasing concern regarding the indoor air quality of energy efficient buildings. Indoor air pollutants, such as volatile organic compounds (VOCs) and particulates, commonly found in buildings, can be harmful to human health. Interior materials are known to be one of the main contributors to poor indoor air quality. There is a need to develop natural materials and systems in order to minimise the level of indoor air pollutants, or even reduce them to near zero through the use of VOC-free emitters and exploitation of the sink effect for airborne pollutants. Natural building materials are considered to possess low embodied energy and are environmentally-friendly.

The aim of this research was to investigate the physical and chemical interactions between natural building materials and VOCs in new or refurbished buildings (e.g. dwellings, offices, hospitals, schools and retail outlets). Key to this was the identification of low VOC emission materials with the added benefit of passively improving the indoor air quality. Comprehensive chemical and physical characterisation of materials was undertaken in order to understand the mechanisms involved in the capture of VOCs by three classes of natural building materials: insulation, coatings and wood panels.

In order to understand the interactions between VOCs and building materials, adsorption and desorption experiments were carried out in laboratory-scale environmental chambers and in a real size room with a volume of 30 m^3, all with controlled temperature, relative humidity and air flow-rate. Four organic pollutants commonly found in indoor environments were selected for this study according to their physico-chemical properties: formaldehyde, toluene, limonene and dodecane.

In the first stage of this research, TVOC and formaldehyde emissions from 18 commercially available natural building materials were analysed (six insulation materials, six coatings and six wood-based panels). These materials included natural wool, hemp fibres, wood fibres, gypsum, lime mortars, clay-based plasters and wood-based plasters. Four of these materials were selected to investigate their adsorption and desorption behaviour towards the selected organic pollutants. It was observed that, in general, all natural building materials showed very low, or even zero, VOC emissions. In the case of formaldehyde, this organic pollutant was found to be emitted by the wood-based panels due to the formaldehyde-based resins used to

glue the wood fibres. In the case of coated wood panels, the resin impregnated paper coating was shown to act as a barrier to formaldehyde emission and as a result this showed lower emission levels compared to an equivalent uncoated material. With regard to the adsorption and desorption behaviour it was observed that highly porous materials such as lime mortar and MDF panels have good capacity to remove VOCs and formaldehyde from the indoor air due to their high surface area. They allow the diffusion of the organic pollutants through their bigger pores. Natural wool, classed as an insulation material, showed good affinity to adsorb formaldehyde due to chemisorption by the proteins present in the fibres.

The later stages of this research involved the investigation of the adsorption/desorption behaviour of newly developed natural building materials incorporating bio-based additives with optimised capacity to remove VOCs from the air. The incorporations were as follows: walnut shell within MDF panels; hemp sheaves, pumice and brick powder within clay-based plasters; and cellulose flakes, natural wool and photocatalytic TiO_2 particles within lime mortar. The combination of two materials was also used because of the affinity of each material with different VOCs, for example the incorporation of natural wool in a lime mortar formulation.

The outcomes of this research demonstrate that, if careful consideration is given to materials selection when constructing a new building or during a refurbishment process, the old judgment "building materials are the main contributors to a poor indoor air quality" is not true. This is achieved by selecting materials with low- or zero-VOC emissions and with the capacity to remove organic pollutants from the indoor air. Therefore, these materials contribute to a better indoor air quality by releasing low or negligible emissions and by facilitating the removal of airborne pollutants.

Table of Contents

List of Figures

List of Tables

List of Symbols

Coefficients and variables

A	Area of the specimen exposed to the air (VOC specific emission rate, Eq. 3.5)
A	Attractive force between adsorbate and adsorbent (L-J potential, Eq. 8.1)
A_{BET}	Surface area calculated by nitrogen adsorption (BET, Eq. 3.3)
A_Q	Area specific flow rate (VOC specific emission rate, Eq. 3.4 and 3.5)
a_m	Cross-sectional area of an adsorbed gas molecules (BET, Eq. 3.3)
B	Repulsive force between adsorbate and adsorbent (L-J potential, Eq. 8.1)
C	Concentration in the chamber (VOC specific emission rate, Eq. 3.4)
C_{BET}	BET constant (BET, Eq. 3.2)
C_{ref}	VOC concentration in the reference chamber (Eq. 4.1)
C_m	VOC concentration in the test chamber (Eq. 4.1)
d	Spacing between layers of atoms (Bragg's law, Eq. 3.1)
n	Specific amount of gas adsorbed at relative pressure p/p_0 (BET, Eq. 3.2)
N_A	Avogadro number (BET, Eq. 3.3)
n_m	Specific monolayer amount of gas (BET, Eqs. 3.2 and 3.3)
p/p_0	Relative pressure (BET, Eq. 3.2)
Q	Flow rate (Eqs. 3.5 and 4.1)
r	Distance between the adsorbate and the adsorbent (L-J potential, Eq. 8.1)
λ	Wavelength of X-rays (Bragg's law, Eq. 3.1)
θ	Angle between the incident rays and crystal surface (Bragg's law, Eq. 3.1)

List of Acronyms

ach^{-1}	Air Changes per Hour
ATR	Attenuated Total Reflectance
BET	Brunauer, Emmett and Teller
BRE	Building Research Establishment
BREEAM	Building Research Establishment Environmental Assessment Method
BRI	Building Related Illness
CARB	California Air Resources Board
ECA-IAQ	European Collaborative Action for Indoor Air Quality
EDX	Energy-Dispersive X-ray spectroscopy
EPA	Environmental Protection Agency (U.S.A.)
EPDM	Ethylene Propylene Diene Monomer class M
FID	Flame Ionisation Detector
FLEC	Field Laboratory Emission Cell
FTIR	Fourier Transform Infra-Red spectroscopy
GC	Gas Chromatography
GUM	Guide to the expression of Uncertainty in Measurement
HPLC	High Performance Liquid Chromatography/Chromatographer
IAQ	Indoor Air Quality
IARQ	International Agency for Research on Cancer
IEQ	Indoor Environmental Quality
IUPAC	International Union of Pure and Applied Chemistry
JCGM	Joint Committee for Guides in Metrology
LCI	Lowest Concentration Interest
MDF	Medium Density Fibreboard
MIP	Mercury Intrusion Porosimetry
MS	Mass Spectroscopy
NIST	National Institute of Standards and Technology
OSB	Oriented Strand Board
PC	Photocatalytic
PFTBA	Perfluorotributylamine
PID	Photo-Ionisation Detector

QC	Quality Control
RH	Relative Humidity
SBS	Sick Building Syndrome
SEM	Scanning Electron Microscopy
SVOC	Semi Volatile Organic Compound
TS	Technical standard
TVOC	Total Volatile Organic Compound
UV	Ultraviolet
VOC	Volatile Organic Compound
VVOC	Very Volatile Organic Compound
WHO	World Health Organisation
XRD	X-Ray Diffraction

Chemicals and minerals

$C_3H_7NO_2S$	Cysteine
$(C_6H_{10}O_5)_n$	Cellulose monomer
C_7H_8	Toluene
$C_{10}H_{16}$	Limonene
$C_{12}H_{26}$	Dodecane
$CaCO_3$	Calcite
$Ca(OH)_2$	Portlandite
$CaSO_4 \cdot 2H_2O$	Calcium sulphate hydrate (gypsum)
HCHO	Formaldehyde
SiO_2	Silica (quartz or pumice)
$[Al_2(OH)_4(Si_2O_5]_2$	Kaolinite

Dissemination activity

A. Journal papers published or submitted

1. Da Silva, C. F., Rana, C., Maskell, D., Ansell, M. P., Dengel, A., Ball, R. J., 2016. The role of eco-materials in improving the Indoor Air Quality. ICE Green Materials Journal 4 (2), pp 72-80.
2. Da Silva, C. F., Stefanowski, B., Maskell, D., Ormondroyd, G., Ansell, M., Dengel, A., Ball, R., 2017. Improvement of Indoor Air Quality by MDF panels containing walnut shells. Building and Environment, 123, pp 427-436.
3. Giampiccolo, A., Ibánez Gómez, J. A., de Miguel, Y. R., Mair, S., Maskell, D., Casado, A. M. Da Silva, C. F., Tobaldi, D. M., Mayer, F., Ansell, M., Labrincha, J. A., Ball, R. Novel TiO2-based photocatalytic lime Plaster for indoor air quality improvement using visible light, submitted to Journal of Physics and Chemistry of Solids.

B. Conference papers published

1. da Silva, C. F., Maskell, D., Ball, R. J. and Ansell, M. P., The physical, chemical and mechanical properties of eco-materials for passive indoor environmental control. In: *Advanced Building Skins Conference Proceedings of the 9th ENERGY FORUM 2014, Bressanone - Italy*.
2. Maskell, D., da Silva, C. F., Mower, K., Rana, C., Dengel, A., Ball, R. J., Ansell, M. P., Walker, P. and Shea, A. Properties of bio-based insulation materials and their potential impact on indoor air quality. In: *1st International Conference on Bio-based Building Materials 2015, Clermont-Ferrand – France*.
3. Gulia, S., Chinthala S., da Silva C.F., Rana C., Mower K., Dengel A. and Khare M., Eco-friendly Sustainable Building Construction Materials: Emission Characteristics-Part 1. In: *Indoor Air 2016, Ghent - Belgium, July 2016*.
4. Chinthala, S., Gulia, S., Stratbücker, S., da Silva C.F., Rana C., Mower K., Dengel A., Khare M., Eco-friendly Sustainable Building Construction Materials: Emission Characteristics-Part 2. In: *Indoor Air 2016, Ghent - Belgium, July 2016*.

5. da Silva C.F., Rana C., Ansell M. A., Dengel, A. C. and Ball, R. J., Correlation between physicochemical properties and adsorption behaviour of volatile organic compounds by natural building materials. In: *Indoor Air 2016, Ghent - Belgium, July 2016*.
6. Maskell, D., da Silva, C. F., Mower, K., Rana, C., Dengel, A., Ball, R. J., Ansell, M. P., Thomson, A., Peter, U. and Walker, P., Bio-based plaster for improved indoor air quality. In: *2nd International Conference on Bio-based Building Materials 2017, Clermont-Ferrand – France*.

C. Oral communications

1. Department of Architecture and Civil Engineering Seminars 2015: "Hygrothermal behaviour and capture of volatile organic compounds by natural building materials", Bath - United Kingdom.
2. EUROMAT 2015: "The role of natural eco-materials in improving Indoor Air Quality", Warsaw – Poland.
3. Indoor Air 2016: "Correlation between physicochemical properties of natural building materials and adsorption behaviour of VOCs", Ghent – Belgium.
4. BRE Trust Research Conference 2016: "Capture of volatile organic compounds by natural building materials", Birmingham - United Kingdom.

D. Poster communications

National Women in Engineering Day (2015): "Improving the air that we breathe through building materials", Bath - United Kingdom.

E. Awards

Runner-up prize of the Best Poster Competition at National Women in Engineering Day 2015. Poster title: "Improving the air that we breathe through building materials", University of Bath - United Kingdom, June 2015.

Chapter 1

Introduction

1.1. Global context

In seeking to reduce the energy consumption of buildings, a greater level of air tightness combined with higher levels of insulation is required. A possible consequence of this approach is the deterioration of the Indoor Environmental Quality (IEQ) which involves Indoor Air Quality (IAQ) as well as acoustics, lighting levels, temperature and humidity, (Crump et al. 2009). Concerns about poor IEQ have been rising due to its effects on the health and well-being of building occupants, who typically spend more than 80 % of their life indoors.

Poor IAQ has been linked to *Sick Building Syndrome* (SBS) which in general has been defined as a range of non-specific symptoms thought to be related to spending time in a building, (World Health Organization 1989; U.S. Environmental Protection Agency 1991; Maroni et al. 1995; Crump et al. 2009; Abdul-Wahab 2011). The Environmental Protection Agency (EPA) states that the symptoms are temporally related to the time spent inside a particular building or location inside the building and should be relieved within minutes or a few hours when the person leaves that particular location, (U.S. Environmental Protection Agency 1991). On the other hand, the term *Building Related Illness* (BRI) is being used to describe symptoms that are clinically defined (Samet et al. 1988; Menzies and Bourbeau 1997; Abdul-Wahab 2011). Some researchers contend that BRI is the most appropriate term because a building cannot get sick as it is not alive (Abdul-Wahab 2011). SBS and BRI characteristics are summarised in Table 1.1.

Table 1.1 Comparison of symptoms and recovery times between SBS and BRI terms and causes.

	Sick Building Syndrome	**Building Related Illness**
Cause of the symptoms	Unknown	Known
Typical symptoms	• Headache • Eye, nose or throat irritation • Dry cough • Dry or itchy skin • Dizziness and nausea • Difficulty in concentration • Fatigue • Sensitivity to odours	• Cough • Chest tightness • Fever • Chills • Muscle aches
Recovery times	Relief soon after leaving the building	Prolonged recovery time after leaving the building
Causes	Inadequate ventilation; Low/high humidity; Low/high temperature; Temperature changes throughout the day; Airborne particles (e.g. dust); Airborne chemical pollutants (such as VOCs); Poor lighting.	

The causes of SBS and BRI are common to both, as highlighted in Table 1.1. Airborne chemical pollutants and environmental parameters, such as volatile organic compounds (VOCs), are within the scope of this PhD research. **Volatile organic compound** is a term used to classify a wide range of individual chemical compounds containing carbon atoms in their molecular composition that have low boiling point which causes their evaporation from the liquid into vapour entering the surrounding air.

The concentration of volatile organic pollutants in indoor air depends on a number of factors including:

- Volume of air contained in an indoor space;
- Rate of production/emission of VOCs into the indoor air;
- Rate of elimination of VOCs (e.g. through filtration by air conditioning or air purification systems);
- Air change rate through natural or mechanical ventilation;
- Concentration of outdoor VOCs.

The sources of VOCs found in indoor air can be classified as consumer and commercial products sources, building sources, personal sources and outdoor sources, as summarised in Table 1.2.

Table 1.2 Classes of VOCs sources in the indoor air and examples (Samet et al. 1987; Samet et al. 1988; Maroni et al. 1995; Lee et al. 2001; Raw et al. 2004; Singer et al. 2006; U.S. Environmental Protection Agency 2009; Yu and Jeong Tai Kim 2010; Abdul-Wahab 2011).

Consumer and commercial products	
Cleaners, waxes and fragrances	Aerosol cleaners, powdered abrasive cleaner, air-fresheners, deodorants, furniture and flooring waxes, oven cleaner
Paints and associated supplies	Paints, varnishes, paint brush cleaners
Pesticides	Termite treatment, mould inhibitors, insecticides, moth repellent
Adhesives	Floor tile adhesive, ceramic adhesive, carpet adhesive
Cosmetic and personal care products	Perfume, personal deodorants, hair sprays
Automotive products	Hydraulic fluids, motor oils, gasoline, automotive cleaners
Office products	Laser printers
Furnishings	Carpet, plastic and timber furniture and curtains, draperies
Building sources	
Building materials	Pressed wood fibres, plastic wall and floor coverings, adhesives
Garages	Exhaust from vehicles
Combustion appliances	Unvented heaters, gas cooking stoves, wood-burning stoves and fireplaces
Personal sources	
Tobacco smoke or ‘vape’	Cigarette, cigars, pipes, e-cigarettes
Human or biological origin	Pets, indoor plants, metabolic products
Outdoor sources	
Outdoor air	Industrial and traffic emissions, landfills

In indoor air, besides VOCs, pollutants such as ozone, sulphur dioxide, nitrogen oxides, particulates, ammonia and radon can be also found (Crump et al. 2009; Dengel 2014; Lee et al. 2001; Singer et al. 2006; Nazaroff and Weschler 2004).

Mølhave et al. (1997) suggested four exposure ranges of VOCs in indoor air (usually called TVOC – total volatile organic compounds) making impact on human health, summarised in Table 1.3. These ranges of concentrations were proposed by the authors based on the health effects of VOCs found in the literature and concentrations in air measured by Gas Chromatography (GC) equipped with Flame Ionisation Detector (FID). The GC-FID analytical technique is explained in Chapter 3.

Table 1.3 Impact of VOC concentration on human health, (Mølhave et al. 1997).

Concentrations of VOCs (μg/m^3)	**Health impact**
< 200	No irritation or discomfort expected
200 – 3000	Irritation and discomfort may be possible
3000 – 25000	Discomfort expected and headache possible
> 25000	Toxic range where other neurotoxic effects may occur

The World Health Organisation (WHO) reported that an exposure to 360 μg/m^3 of formaldehyde, classed as carcinogenic compound by IARC (International Agency for Research on Cancer), during a period of 4 hours leads to eye irritation and conjunctival redness, and an increase in the eye-blink frequency if the formaldehyde concentration is 600 μg/m^3, (World Health Organization 2010). The WHO classes benzene as another very harmful VOC, and indicates that the cancer risk due to lifetime exposure to only 1 μg/m^3 of benzene is 2.2–7.8 in a million. Due to the very high toxicity of benzene, WHO proposes that there is no recommended safe level of exposure to benzene.

The European Energy Performance of Buildings directive 2010/31/EU (published by the European Parliament and the Council of the European Union) requires the reduction of gas emissions by at least 20 % from those of 1990 by 2020. In this directive, the concept of nearly-zero energy buildings is introduced. The reduction of energy consumption and increasing the use of renewable energies are also referred to in this directive. It is suggested that the

performance criteria should include consideration of indoor air quality, thermal characteristics, application of energy from renewable sources, passive heating and cooling elements, adequate light and design of the building.

Yu and Kim (2012) reviewed the background information regarding low-carbon housing in the United Kingdom and raised the concern of the indoor pollution load due to the emissions from the building materials. The authors highlighted some implications related to the UK Government's target of zero carbon homes by 2016, such as the use of low emission materials for new build or refurbishment that would alleviate the need for higher air change rate per hour (ach^{-1}) and therefore reduce the energy cost.

1.2. Importance of the research, aims and objectives

This PhD research has focused on the study of eco-materials and components for the purpose of creating both healthier and more energy efficient buildings. This is a key objective of the European FP7 project ECO-SEE, led by the University of Bath, which aims to develop new eco-materials and components. The consortium worked towards the creation and use of natural eco-materials for healthier indoor environments through hygrothermal (heat and moisture) regulation and the removal of airborne pollutants through both passive capture and photocatalysis.

The aim of the underlying work of this PhD thesis was to contribute to the scientific knowledge of natural building materials for passive control of indoor environmental quality through the capture of volatile organic compounds. Such studies are essential to understand how the selected building materials can improve the indoor air quality either by being low-emitters or emission-free, and by removing pollutants from the air by passive sorption mechanisms. Specifically, it addresses the interaction of volatile organic compounds and formaldehyde with organic and inorganic based materials: insulation materials (natural wool, wood and hemp fibres), coatings (gypsum and lime- and clay-based plasters) and wood panels (wood fibre board, chipboard etc.).

To achieve this, the main tasks included:

- Identification of VOCs emitted by the materials and quantification of the VOC and formaldehyde emission rates;
- Measurements of the quantities of four air pollutants (toluene, limonene, dodecane and formaldehyde) adsorbed by the materials;
- Chemical characterisation in order to understand the origin of the VOCs emitted from the material and the interaction between VOCs and chemical species present in the material surface;
- Materials surface characterisation – specifically properties that will have an effect on adsorption and desorption of air pollutants.

1.3. Layout of the thesis

This thesis is composed by nine chapters including the Introduction. The following chapter, Chapter 2, includes the introduction to the Indoor Air Quality, limit guidelines for VOC concentration across Europe and literature review about VOC emissions and adsorption/desorption by building materials.

The research strategy, materials under investigation and experimental methodologies are described in Chapter 3. This included the chemical and physical characterisation of the selected natural building materials and investigation of their VOC emissions and adsorption/desorption in order to study the mechanisms of interaction between the materials and VOCs.

In first stage of this research, Chapter 4, TVOC and formaldehyde emissions from 18 commercially available natural building materials were analysed. Four of these materials were selected to investigate their adsorption and desorption behaviour of toluene, limonene, dodecane and formaldehyde. Physical and chemical properties of building materials were also characterised. In Chapter 5, 6 and 7, the adsorption and desorption behaviour of newly developed natural building materials incorporating bio-based additives with optimised capacity to remove VOCs from the indoor air as follows: Chapter 5 presents the investigation of MDF panels with walnut shells incorporated, Chapter 6 novel clay-based and lime based-plasters and Chapter 7 explores the ability of photocatalytic lime mortars to capture VOC from the air under dark conditions; Chapter 7 also presents the investigation of MDF panels coated with photocatalytic particles to remove VOC in a real sized environmental chamber. In the end of each Chapter a summary is provided, stressing their highlights.

The overall discussion about the mechanisms of interaction between natural building materials and the selected organic pollutants is presented in Chapter 8. In this section, the physical properties such as specific surface area and porosity of the materials is correlated with their VOCs adsorption and desorption behaviour. In addition, the influence of the materials chemical composition in their VOCs adsorption and desorption behaviour and physico-chemical properties of the VOCs are also explored.

Main conclusions and future recommendations are included in Chapter 9. In the Appendix, the uncertainty calculations are explained and raw data presented in tables.

Chapter 2

State of the art

2.1. Indoor air quality

Good indoor air quality can be defined as the absence of air pollutants at harmful concentrations that have a negative impact on human health and wellbeing, and where building occupants are satisfied (Berglund et al. 1997; American Society of Heating and Agency 2009; Crump et al. 2009). Concentrations of VOCs, CO_2 and particulate matter are some of the indicators for evaluating the quality of the air indoors, (Berglund et al. 1997).

Depending on the topic under discussion, VOCs can be classified into various types according to, for example, their chemical nature (alkanes, aromatic hydrocarbons, aldehydes, etc.), their physical properties (boiling point, vapour pressure) or their potential health effects (irritant, carcinogen or neurotoxic), (Berglund et al. 1997). World Health Organisation (1989) classified organic pollutants according to three types based on their boiling points, summarised in Table 2.1.

Table 2.1 Classification of Very-VOC, VOC and Semi-VOC by WHO (1989).

Type	**Boiling point (°C)**
Very Volatile Organic Compound	< 0 to 50 – 100
Volatile Organic Compound	50 – 100 to 240 – 260
Semi-Volatile Organic Compound	240 – 260 to 380 – 400

The guidelines for limits of VOC emissions or concentrations in air often refer to the term **total volatile organic compounds** (**TVOC**). This term is used to refer to a mixture of VOCs present in a sample of air which in effect is the sum of the concentrations of all VOCs present in the mixture. As different VOCs have different health effect, the term TVOC should not be used as

the only guideline tool for IAQ. However, when it comes to legislation, there is no accordance between some institutes regarding the TVOC definition for emissions limits- the so-called "*TVOC issue*" as in the phrase coined by Eurofins. As per the standards ISO 16000-6 and TS/CEN 16516, the TVOC concentration is the sum of all detected VOC samples in a Tenax TA tube which elute from a non-polar gas chromatography column, calculated as a surrogate of a calibration reference, named as 'toluene equivalent'. The reason for calculation using the toluene equivalent is to make inter-laboratory and inter-product results comparable. Each VOC has a specific health effect at different concentration ranges. In order to improve the indoor air quality guidelines for chamber emissions of products, some institutes have started to publish not only the TVOC limits, but also the LCI (lowest concentration of interest) value for each individual VOC with the potential for negative health effects. In German legislation, VOCs with their own LCI values have their concentrations expressed in their own right without using toluene equivalent, whereas others than those are calculated as toluene equivalent.

The different definitions of TVOC used by different countries make inter-laboratory comparisons difficult. This would work only if the LCI value were the same for all countries and legislations. There is a range of limits given by the different regulations and specifications, as shown in Table 2.2. The TVOC limits vary from 60 to 2000 $\mu g/m^3$ and for formaldehyde from 10 to 120 $\mu g/m^3$. The German EMICODE label serves to certificate specifically flooring products, such as adhesives, sealants and parquet varnishes, and presents the strongest requirements in terms of low VOC emissions. Some legislations present distinctions between VOCs with different health effects. In the case of carcinogenic compounds, a much lower limit is required as is the case of the Belgium and German legislation. The methodology adopted by the institutes to analyse the emissions of VOCs and aldehydes follows the ISO 16000 standard series and TS/CEN 16516. This includes emissions analysis after 3 and 28 days of storage in a ventilated environmental chamber (0.5 ach^{-1}) at a controlled temperature of 23 °C and at 50 % relative humidity (RH). It should be pointed that the emission guidelines for formaldehyde required by the EMICODE label are related to 3-day emissions. The World Health Organisation (2010) suggests 30-minute maximum exposure of 100 $\mu g/m^3$ of formaldehyde as an indoor air quality guideline.

Indoor Air Comfort and Indoor Air Comfort Gold are labels created by Eurofins for product certification regarding VOC emissions of building materials, decorative coatings and furniture. The main aim of this certification is to comply with all relevant emissions legislations used in European countries to create a single specification and to allow the use of low VOC emission

labels in European countries where no such label exists. Some of the instruments used as criteria for the Indoor Air Comfort label are Belgium legislation, French legislation, AgBB, EMICODE and BREEAM. The international standards ISO 16000-3, ISO 16000-6 and CEN/TS 16516 underlie the harmonisation of emissions testing and certification, (Yu and Crump 2010; Yu and Crump 2011).

Table 2.2 Limit values after 28 days emissions testing in a ventilated test chamber required by various regulations across Europe and proposed by the WHO.

Organisation/Institute		**TVOC ($\mu g/m^3$)**	**Formaldehyde ($\mu g/m^3$)**	**Products/Standard**
WHO		-	100	-
Belgian regulation		1000 or 1*	100	Construction products CEN/TS 16516
AgBB/DIBt (Germany)		1000 or 1*	100	Construction products CEN/TS 16516 and ISO 16000
EMICODE (Germany)	$EC1^{PLUS}$	≤ 60 or 1*	50†	Flooring products CEN/TS 16516
	EC1	100 or 1*	50†	
	EC2	300 or 1*	50†	
France regulation	Class A+	1000	10	Construction products ISO 16000
	Class A	1500	60	
	Class B	2000	120	
	Class C	> 2000	> 120	
Indoor air comfort - Eurofins	Standard	1000 or 1*	60	-
	Gold	750 or 1*	10	

* For each individual carcinogenic compound.

† Emissions after 3 days stored in a ventilated environmental chamber.

Belgian regulation – https://www.health.belgium.be/sites/default/files/uploads/fields/fpshealth_theme_file/19095734/KB Vloerbekleding.pdf

AgBB/DIBt – http://www.eco-institut.de/en/certifications-services/national-marks-of-conformity/agbb-scheme/

EMICODE - http://www.emicode.com/en/emicode-r/limit-values/

French regulation - https://www.legifrance.gouv.fr/eli/decret/2011/3/23/DEVL1101903D/jo

Eurofins - http://www.indoor-air-comfort.com/

In Table 2.3 the LCI values of toluene and limonene required by AgBB, Belgium and French legislations are given. As described in ECA report No 29, a harmonised list of VOCs and their LCI values for the assessment of emissions from building products would be the most appropriate strategy for assessing the health effects of VOCs emitted from construction products across Europe, (European Union Joint Research Centre 2013). This approach took into account the actual legislations used by several European countries such as Belgium, France and Germany. The EU-LCI values of toluene and limonene shown in Table 2.3 were taken from the EU-LCI list published in December 2016.

Table 2.3 LCI values across Europe for toluene and limonene.

Legislation		**LCI value (µg/m^3)**	
		Toluene	**Limonene**
AgBB		1900	1500
Belgium		2900	1500
France	Class A+	< 300	n/a
	Class A	450	n/a
	Class B	600	n/a
	Class C	> 600	n/a
EU-LCI		2900	5000

There are also regulations for products other than building materials such as the *Regulation for reducing emissions from consumer products* published by CARB (California Air Resources Board) in 2009, (U.S. Environmental Protection Agency 2009). This regulation prohibits the

sale of consumer products that exceeds a given percentage of VOC by weight of the product. Some examples are shown in Table 2.4.

Table 2.4 Percentage of VOC limit by weight of consumer product regulated by CARB - U.S. EPA.

Product	**% of VOC**
Air-freshener	30
Aerosol bathroom cleaner	7
Wooden floor wax	70
Paint remover	5
Non-aerosol oven cleaner	1
Aerosol wood cleaner	17
Hair colour	55
Personal fragrance	80
Shaving gel	4

A Rule document was issued by the US EPA (and starts to be effective during May 2017) entitled "*Formaldehyde Emissions Standards for Composite Wood Products*", (U.S. Environmental Protection Agengy 2016) for certification process of formaldehyde emission testing in large-scale or mid-scale test chambers at 25 °C (in contrast to 23 °C in Europe) from wood based products: hardwood plywood, particleboard, MDF and other finished products that may contain those materials. This Rule indicates that no wood based products can show formaldehyde emissions higher than 0.05 ppm for hardwood plywood, 0.08 ppm for particleboard, 0.09 ppm for MDF during the initial six-month testing period.

Kelly et al. (1999) studied the formaldehyde emission rates of building materials and consumer products, often found in California houses, in realistic chambers under typical environmental conditions: 21 °C and 50 % RH. Bare urea-formaldehyde (UF) wood products (such as particleboard, MDF and hardwood plywood), coated UF wood products (such as MDF cabinet doors, particle board with melamine laminate, recoated paper, vinyl coating and paper coating) were some of the materials studied in this work. The authors found that the formaldehyde emission rates from the unfinished wood products made with UF resin ranged from 8.6 to 1580 $\mu g/m^2h$ whereas finished products showed lower emission rates varying from 2.6 to 460 $\mu g/m^2h$.

Formaldehyde is one of the pollutants of most concern found indoors due to its carcinogenic characteristics and the vast range of formaldehyde emitting sources. The major sources of formaldehyde in indoor environments are indicated by several researchers to be building materials and consumer products. The presence of formaldehyde indoors is due to **direct sources** i.e., sources that directly emit formaldehyde into the indoor air, such as building materials with UF resins (Kelly et al. 1999; Raw et al. 2004; Park and Ikeda 2006; Salthammer et al. 2010), and **indirect sources**. Indirect sources are associated with the term indoor chemistry, and it relates to pollutants emitted by building materials or products which can react with other chemical species present in the air producing formaldehyde, (Nazaroff and Weschler 2004; Singer et al. 2006; Uhde and Salthammer 2007; Salthammer 2016; Weschler 2016). A well-known example of an indirect formaldehyde source is those air-fresheners or cleaning products that contain terpenes such as limonene, α-pinene and others, Figure 2.1, (Nazaroff and Weschler 2004; Singer et al. 2006).

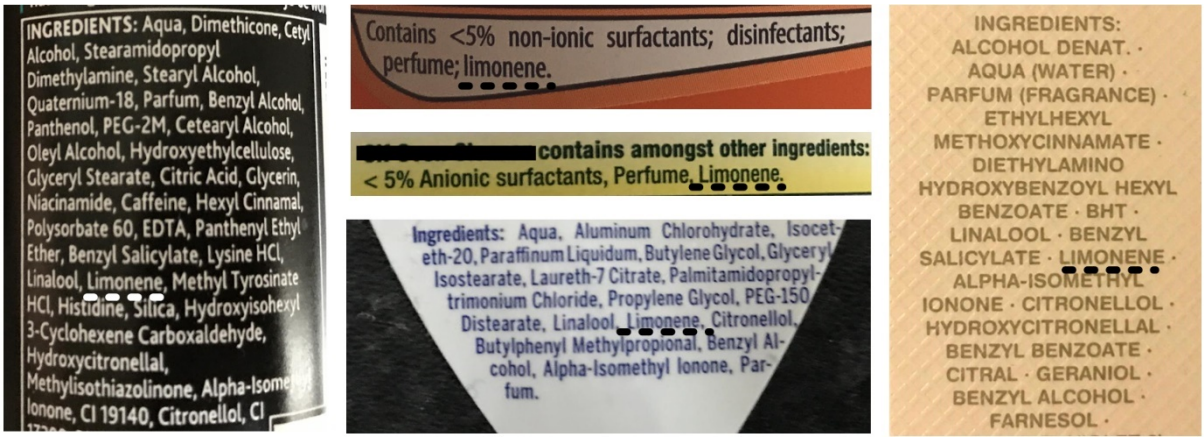

Figure 2.1 Ingredients list found in various consumer products such as deodorants, cleaners, perfume and hair care.

BRE (Building Research Establishment) carried out a large indoor air study in around 1000 English homes between October 1997 and February 1999, (Raw et al. 2004). This study included measurements of CO, NO_2, TVOC and formaldehyde throughout the four seasons, in different rooms of the dwellings. Old, relatively new and new-build houses were randomly selected for this study. It was found that rooms or areas of the houses with recent paintwork and integral garages exhibited the highest levels of TVOC. About 5 % of the houses exceeded 1000 $\mu g/m^3$ of TVOC in the air. The formaldehyde concentrations were taken in the bedrooms of 833 houses. The main factors affecting the formaldehyde levels found in the houses was the

presence of particleboard as a flooring material and the age of the house. Homes with particleboard flooring showed a mean concentration of 32.0 μg/m^3 of formaldehyde, while in homes without particleboard it was 20.3 μg/m^3. The recently built houses (less than 3 years old) showed the highest formaldehyde concentrations, around 135 μg/m^3, exceeding the WHO 30 min air quality guideline of 100 μg/m^3, as described previously. Similar findings were obtained by Park et al. (2006) which, measured concentrations around 467 μg/m^3 in new homes against 246 μg/m^3 in older homes tested in few non-specified countries. Although, after 3 years, the concentrations in new homes decayed to an average of 254 μg/m^3 and older homes showed mean TVOC concentration of 255 μg/m^3. This means that the initial levels of VOCs emitted when a house is newly-built or refurbished are higher within the first months, although these tend to decrease and reach a similar level to that in older homes after 3 years. Furthermore, the authors concluded that the decrease of VOC emissions in a new house does not depend on the ventilation rate but on the materials aging.

Lee et al. (2001) studied the TVOC and ozone emissions (μg/copy) from office equipment: laser printers, ink-jet printers and all-in-one office machines. It was found that office machines emitted more TVOC and ozone when in operation than in idle status. Laser printers emitted more TVOC and ozone due to the elevated temperatures required in the process of printing with a laser. The greatest individual VOC emitted by all office equipment were toluene, ethylbenzene, *m-p*-xylene and styrene. These four compounds are usually used as solvent in toners for printers. The highest ozone emission was also from the laser printers, again, due to the printing process.

Nowadays, air purification products for removal of VOCs from the indoor air are commonly found in shops and on the Internet. These products often use technologies involving activated carbon, HEPA filters (high efficiency particulate arrestance), photocatalytic oxidation, ionisation, and polarised-media electronic air cleaning. The drawbacks of these solutions are the cost to buy the products and the additional cost of maintaining them (filter replacement etc.), energy consumption, and the ozone which can be produced as a result of VOC degradation. The best solution for good indoor air quality would be selection of materials with very low VOC and formaldehyde emissions and a balanced design when projecting a new building, or refurbishing an old one, in terms of ventilation, light exposure etc.

Although building materials are often earmarked as the worse contributors to poor indoor air quality, if the right material is chosen for a building it can even improve the air quality by removing VOCs through physical or chemical sorption processes. Building materials are often

porous and can adsorb and desorb gases (Tichenor et al. 1991; An et al. 1999). This phenomenon is called the *sink effect* and is explained later in section *2.3 Removal of organic pollutants by sorption*.

2.2. Volatile organic compounds and formaldehyde emissions by building materials

Volatile organic compounds found in indoor air can originate from a wide range of sources as described previously in Table 1.2. For the scope of this PhD, only emissions from building materials are considered in detail. During the design stage of a new building or refurbishment there is an increased emphasis on the selection of low emission materials in order to avoid poor indoor air quality in the future. Much research is ongoing to develop new low emission materials e.g. low-VOC wood panels (Ayrilmis et al. 2009; Kim 2009; Boran et al. 2011; Paiva et al. 2014; da Silva et al. 2017) or by using nanotechnology such as photocatalytic products to clean the air through photocatalysis (Wang et al. 2007). Also, legislation, as already described in sub-chapter *2.1 Indoor air quality*, and product labelling schemes, can promote the development of low-emission building materials.

Wolkoff (1999) classified emissions of VOCs as primary and secondary. In new or refurbished buildings, the primary emissions are dominant whereas secondary emissions are associated with older buildings (although these are typically lower specific emission rates compared with primary emissions). **Primary emissions** represent the physical release of non-bound VOCs, which are present in a new product (e.g. additives, antioxidants, solvent reactants). The mechanism of emission can be evaporation from the surface, diffusion within the product or even both. **Secondary emissions** are characterised by the release of chemically or physically bound VOCs, which can be produced by chemical reactions in the product or in the indoor environment such as chemical or physical degradation, maintenance (e.g. incorrect dosing of cleaning agent), oxidation or sorption processes. The example given by Wolkoff for chemical degradation is the hydrolysis of phthalates to alcohols in PVC flooring resulted from a wet concrete underlay (high pH). An example for physical degradation is the direct sunlight that may result in thermal degradation of polymer constituents, like accelerators, or heat treated cork resulting in emissions of acetic acid and furfural (Horn et al. 1998). Oxidation and sorption processes are dependent on oxidants such as ozone and VOCs present in the indoor air, described later. Another well-known example of secondary emission is the chemical reaction between chemical species known as terpenes and ozone - creating formaldehyde as a by-

product of the reaction. Terpenes such as α- and β-pinene, 3-carene and limonene are often found in emissions from wood based materials or as ingredient in cleaning products or air-fresheners, as shown previously in Figure 2.1, (Baumann et al. 1999; Nazaroff and Weschler 2004; Singer et al. 2006). This happens because reactions between ozone (oxidising agent) with chemicals with unsaturated carbon-carbon bonds, such as C = C, are much faster, serving as a larger source for secondary emissions. In addition to the formaldehyde as a by-product of a reaction between ozone and such chemicals, hydroxyl radicals are also produced. Subsequent reactions of hydroxyl with VOCs can generate additional products, (Nazaroff and Weschler 2004).

2.2.1. Methodologies to analyse emissions of air pollutants

The methodologies to measure the TVOC concentration in the air can be divided into two types: **direct** and **indirect** measurements which differ with regard to the amount of work involved and the degree of information required. **Direct** measurement of VOCs is based in direct-reading portable devices which quickly show the real-time concentration of TVOC and also allows rapid detection of marked concentration changes. An example of this device is the *TSI Q-Trak*™ indoor air quality monitor model *7575* equipped with the TVOC probe featuring a photo-ionisation detector (PID), Figure 2.2. These devices not only show the overall concentration of VOCs but also other compounds such as VVOCs. The main drawback of this type of measurement is the limitation on the identification of the individual chemical compounds present in the air which is not possible due to the non-selectivity of the device. On the other hand, **indirect** measurement can allow the quantification and identification of each individual compound. This type of methodology is more time-consuming compared with the direct measurement although the information given is much more complete. For a research study on emissions and adsorption/desorption behaviour of known VOCs by building materials, as is the case of this thesis, an indirect measurement methodology is more suitable. This permits to evaluate the interaction between the material and each individual VOC, in some cases where the VOCs are all mixed together in the air, and also to identify and quantify each individual VOC being emitted by the material.

Figure 2.2 *TSI Q-Trak* indoor air quality monitor *7575*.

Measurement of VOC emissions often involves the use of an environmental chamber with controlled air change rate, temperature and relative humidity. Chambers of different sizes are used for emissions testing. They can be small, usually designated as a lab-scale chamber, with nominal volume varying between 2 and 150 litres (Yu and Crump 1998; Son et al. 2013; Zhang et al. 2007; Virta et al. 2005); large with a nominal volume within the range of 1 to 10 m^3 (Yu and Crump 1998; Salthammer et al. 1999; Gunschera, Mentese, et al. 2013); with specific characteristics, such as the FLEC (Field Laboratory Emission Chamber) and CLIMPAQ chambers, (Gunnarsen et al. 1994; Knudsen et al. 1999; Rizk, Verriele, Dusanter, et al. 2016; Rizk, Verriele, Mendez, et al. 2016); and even real rooms or houses (Crump et al. 1997; Yu et al. 1999; Kelly et al. 1999; Hodgson et al. 2002; Zhang 2005). The environmental chambers used for IAQ assessment are made of materials that have no or very low effect on the study, i.e. non-emitters and non-adsorbers, such as stainless steel (Haghighat and De Bellis 1998; Baumann et al. 2000; Virta et al. 2005; S. Kim et al. 2006; Son et al. 2013; da Silva et al. 2016; Jiang et al. 2017) or glass (Salthammer et al. 1999; Knudsen et al. 1999; Gunschera, Mentese, et al. 2013).

The international organisation for standardisation (ISO) published a series of standards regarding VOCs, formaldehyde and other indoor air pollutant testing, the ISO 16000 series. This includes a standard to test VOC and formaldehyde emissions a test cell such as FLEC (BS EN ISO 16000-10:2006) or in a test chamber (BS EN ISO 16000-9:2006). For specific formaldehyde emissions and analysis, BS ISO 16000-3:2011 should be followed and BS ISO 16000-6:2011 applies to VOCs.

2.2.2. Effect of air velocity, temperature, relative humidity and type of building material

Concentrations of volatile organic compounds in an indoor environment depend on several factors including the volume of air in the occupied space, primary area specific emission rate [$\mu g/m^2h$], rate of elimination (e.g. through filtration), secondary emission rate, air exchange rate and outdoor concentration of the pollutants (Haghighat and De Bellis 1998; Yu and Crump 1998; Wolkoff 1998). On the other hand, VOCs emission rates depend on the type of material (wet or dry), type of VOC (physicochemical properties), temperature, relative humidity, air velocity and stage of emission (Fang et al. 1999; Haghighat and De Bellis 1998; Wolkoff 1998; Wolkoff 1999). However, the understanding of the effect of each individual factor can be complex because they can influence each other. For example, the effect of the air velocity depends on the stage of emission (if it is primary or secondary emission) and the temperature, and RH effect depends on the type of material and the VOC.

Wolkoff (1998) observed the effect of air velocity, temperature and RH in emissions rates of dry and wet materials. For dry building materials, such as PVC flooring, during the primary emissions the air velocity does not affect the emissions rate because it is mainly due to evaporation mechanisms. However, in the later stage when the secondary emissions are predominant, higher air velocity will promote air oxidative processes because of the boundary layer between the material and air becoming smaller (Wolkoff 1998). On the other hand, in the case of wet materials, such as floor varnish or wall paint, the air velocity has a larger influence on the primary emissions when evaporation is the predominant mechanism. At higher air velocities, the mechanism of emission changes much faster to become diffusion dominated, partly due to faster formation of a dry film surface. Similar findings were observed by Knudsen et al. (1999).

The influence of the air change rate on the formation of secondary organic aerosol as a reaction product between limonene and ozone was investigated by Weschler and Shields (2000; 2003). The study demonstrated that low ventilation rates, besides allowing the accumulation of indoor pollutants, lead to a higher concentration of secondary products formed through the reaction between limonene and ozone. No secondary products were formed at the highest air change rate (12 h^{-1}).

Temperature and RH effects, again, strongly depend on the type of material and VOC (Haghighat and De Bellis 1998; Wolkoff 1998). A higher effect of temperature and RH was

observed in wet materials (Haghighat and De Bellis 1998). It is believed that a lower humidity may have resulted in a different film structure due to a faster drying-out process in this kind of material. Higher temperatures led to a faster drying process of the wet materials, thus increasing the emission rates. Similar findings were observed by Fang et al. (1999).

In general, emission rates tend to decrease with time (Wolkoff 1999; Yu and Crump 1998). Building Research Establishment (BRE) conducted a study of VOCs emissions in four newly built unoccupied houses. After 1 month, the maximum TVOC concentration in the indoor air was 9700 $\mu g/m^3$, which declined to 800 $\mu g/m^3$ after 6 months, and approximately 600 $\mu g/m^3$ after 1 year. After eighteen months the concentration stayed more or less steady, at about 200 $\mu g/m^3$ (Yu and Crump 1998).

The type of VOCs emitted from building materials depends on the material chemical composition and production processes. Table 2.5 presents a summary of VOCs emitted and the respective material type and Table 2.6 presents the same for formaldehyde. The comparison between TVOC concentrations emitted by various materials found in the literature can be difficult due to the differences in the experimental methodology, especially size of the chamber, time at which the emissions measurements were taken and air change rate per hour (ach^{-1}). Also, the pre-conditioning methodology could influence the emissions testing. In an expanded literature search, most of the materials studied for VOC and formaldehyde emissions were wood-based. One reason for this is that, wood-based materials are of concern due to their high levels of emissions contributing to a poor indoor air quality. VOC and formaldehyde emissions were studied in diverse types of wood-based materials such as uncoated MDF and uncoated particleboard, various coatings applied to the MDF and particleboards, OSB (oriented strand board) with different thicknesses, etc. The TVOC specific area emission rate measured after 48 hours of conditioning inside an environmental chamber ranged between 122 and 1146 $\mu g/m^2h$ for various building materials, with the lowest emission rate from hardwood MDF and the highest rate from southern pine particleboard. After 7 days, levels of TVOC varied between 50 and 720 $\mu g/m^2h$. The major VOC types emitted by wood-based materials were terpenes and aldehydes. Formaldehyde emission rate after 24 hours ranged between 2.7 and 442 $\mu g/m^2h$ and after 7 days between 50 and 450 $\mu g/m^2h$. In general, particleboard showed higher formaldehyde emission rates compared with MDF and coated MDF showed lower emission rates compared with uncoated MDF.

Table 2.5 Summary of VOCs and aldehydes emitted and the respective material sources.

Main VOCs released	TVOC	Material source	Exp. description & reference
α-pinene, β-pinene, camphene, limonene, 3-carene p-cymene, formaldehyde, acetaldehyde, benzaldehyde, pentanal, hexanal, octanal, nonanal, acetone, 1-pentanol, acetic acid and 2-pentylfuran.	1146 $\mu g/m^2h$	Southern pine particle board	After 48 hours in a 53-litre chamber at 1 ach^{-1} (Baumann et al. 1999)
	878 $\mu g/m^2h$	Southern pine MDF	
	659 $\mu g/m^2h$	Hardwood particle board	
	122 $\mu g/m^2h$	Hardwood MDF	
α-pinene, β-pinene, limonene, toluene, butanal, pentanal, hexanal, 2-pentanone, pentanoic acid, 2-hexanone, benzaldehyde, 3-methyl-2-pentanone.	256 $\mu g/m^3$	Recycled wood	After 48 hours in a 150-litre chamber, no information about the ach^{-1} is provided (Koivula et al. 2005)
Benzene, toluene, acetic acid, butanal, pentanal, hexanal, heptanal, 2-pentanone, xylenes, α-pinene.	29.0 $\mu g/m^3$	Flax sheet	
n/a	50 $\mu g/m^2h$	Laminated MDF	After 7 days in a 20-litre chamber at 0.5 ach^{-1} (S. Kim et al. 2006)
α-pinene, β-pinene, toluene, pentanal, hexanal, heptanal, xylene, ethylbenzene, octanal, nonanal, α-terpiol, acetaldehyde, acetone, benzaldehyde, 2-butanone, formaldehyde.	110 $\mu g/m^2h$	MDF	
	260 $\mu g/m^2h$	Particleboard	
Non-specified terpenes, aldehyde and others VOC.	4667 $\mu g/m^3$	OSB	After 7 days in a 23.5-litre chamber at 3.1 ach^{-1} (Makowski and Ohlmeyer 2006)
α-pinene, β-pinene, camphene, limonene, 3-carene cymene, benzaldehyde, butanal, pentanal, hexanal, heptanal, octanal, nonanal, 1-pentanol, acetic acid, octane and pentylfurane.	3795 $\mu g/m^3$	16 mm OBS	After 3 days in a 23-litre chamber at 3.1 ach^{-1} (Ohlmeyer et al. 2008)
	4746 $\mu g/m^3$	19 mm OSB	
	6353 $\mu g/m^3$	26 mm OSB	
Acetone, benzene, styrene, toluene, ethylbenzene and xylene.	310 $\mu g/m^2h$	MDF	After 7 days in a 20-litre chamber at 0.5 ach^{-1} (Kim et al. 2010)
	700 $\mu g/m^2h$	PVC coated MDF	
	250 $\mu g/m^2h$	Paper coated MDF	
	720 $\mu g/m^2h$	Finishing foil coated MDF	

Continued in next page.

Hexane, benzene, toluene, ethylbenzene, xylene, styrene, α-pinene, β-pinene, camphene, limonene, β-myrcene, 3-carene.□	326 µg/m^{2}h	MDF	After 7 days in a 20-litre chamber at 0.5 ach^{-1} (Son et al. 2013)
	160 µg/m^{2}h	Particleboard	
Carbonyls.	673 µg/m^{2}h	Wood flooring	After 48 hours in a 216-litre chamber at 0.5 ach^{-1} (Cheng et al. 2015)
	140 µg/m^{2}h	Green wood flooring	
	489 µg/m^{2}h	Gypsum board	
	150 µg/m^{2}h	Green gypsum board	

n/a information not available

□ quantification only carried out for the chosen compounds

Table 2.6 Summary of formaldehyde emission rates by various building materials.

Formaldehyde concentration	**Material source**	**Reference**
237 µg/m^{2}h	Particleboard	After 24 hours in a 1.43 m^3 chamber at 0.3 ach^{-1} (Kelly et al. 1999)
26 µg/m^{2}h	Paper laminate-coated particleboard	
16 µg/m^{2}h	Rigid vinyl laminate-coated particleboard	
< 2.7 µg/m^{2}h	Acrylic coated particleboard	
365 µg/m^{2}h	MDF	After 24 hours in a 51-litre chamber at 1 ach^{-1} (Brown 1999)
442 µg/m^{2}h	Particleboard	
50 µg/m^{2}h	Laminated MDF	After 7 days in a 20-litre chamber at 0.5 ach^{-1} (S. Kim et al. 2006)
320 µg/m^{2}h	MDF	
450 µg/m^{2}h	Particleboard	
400 µg/m^{2}h	MDF	After 7 days in a 20-litre chamber at 0.5 ach^{-1} (Kim et al. 2010)
90 µg/m^{2}h	Decorative veneer coated MDF	
230 µg/m^{2}h	Melamine paper coated MDF	

2.3. Removal of organic pollutants by sorption

2.3.1. Definitions and theories of sorption

Adsorption is the term used when a fluid (in liquid or gas phase) adheres into a solid surface (Masel 1996; Dabrowski 2001; Parida et al. 2006). It is also defined as the enrichment of material concentration in the vicinity of an interface and this enrichment is dependent on the extent of the interfacial area (Rouquerol et al. 2014). The adsorption phenomenon is used in a wide range of applications e.g. catalysis, liquids purification, gas separation etc. (Rouquerol et al. 2014).

A material can behave as a sink by adsorbing the gas and then re-emitting it later (Tichenor et al. 1991; An et al. 1999). This phenomenon is called the **sink effect.** The continuous interaction between air pollutants and indoor materials will influence the VOC concentrations over time by smoothing the concentration when a new condition in a room is changed by introducing new VOC sources, like wall painting, new furniture and new materials, or the ventilation is decreased. On the other hand, the sink effect may also contribute to a prolonged low level exposure to building occupants if it is a 100 % reversible phenomenon, i.e. all VOC adsorbed is desorbed later. An ideal building material for an improved IAQ would have good adsorption capacity, even irreversible, and in the case of being reversible, the desorption rate is very low, so that the concentration of VOC released is well below of the IAQ guidelines and the perceived threshold. An example of irreversible sink effect is chemisorption, explained later.

Adsorption should not be confused with absorption. The adsorption phenomenon occurs when the fluid binds only on the surface of the material while the term **absorption** is used when diffusion occurs, meaning that the fluid diffuses through the bulk material, (Masel 1996; Rouquerol et al. 2014). In general, absorption is strongly dependent on the mass of the material and adsorption is mainly dependent on the surface area of the material.

The terms adsorbent and adsorbate are often used in this field of study. **Adsorbent** is considered as material which will adsorb the gas or liquid fluid and the **adsorbate** is the substance that is or will be adsorbed by the material (Dabrowski 2001; Parida et al. 2006; Rouquerol et al. 2014).

One purpose of this PhD project is to study the interactions between building materials and volatile organic compounds. The interactions between the gas phase and the solid phase(material) for adsorption can occur through physical interactions – **physisorption**, or through chemical phenomena – **chemisorption** (Masel 1996; Dabrowski 2001; Rouquerol et al. 2014). In a physical based interaction, there is no direct bond between the gas and the material. The adsorbate is held by attractive and repulsive physical forces such as Van der Waals forces (London interaction) (Masel 1996). This attraction is resulted from fluctuations in the electron distributions in the atoms and the dipoles which are continuously changing direction are created due to the fluctuations. The strength depends on the polarity of the involved molecules. Therefore, the interaction between polar molecules is usually stronger (Atkins and De Paula 2014). Other types of attractive interactions are the dipole-dipole, ion-dipole, ion-ion interactions and hydrogen bonding. Dipole-dipole interaction is the attraction between the electric dipoles of polar molecules. The hydrogen bond can occur in a single molecule (intramolecular) or between molecules (intermolecular). This bond is stronger than a Van der Waals interaction and weaker than ion-ion interaction. The intermolecular hydrogen bond interaction occurs between molecules in which the hydrogen atom has a covalent bond with sufficiently electronegative atoms such as nitrogen and oxygen.

In the case of chemisorption, there is a direct chemical bond (electron sharing) between the gas molecules and the surface of the material. The energies involved in physisorption are much lower than those involved in a chemisorption mechanism, 2-10 kcal/mol to 15-100 kcal/mol respectively (Masel 1996). The two phenomena are compared in Table 2.7.

Table 2.7 Comparison of physisorption and chemisorption phenomena.

Physisorption	**Chemisorption**
Low degree of specificity.	Dependent on the reactivity of the adsorbent and adsorbate.
Can occur in a multilayer.	Chemisorbed molecules are linked to reactive parts of the surface and the adsorption is limited to a monolayer. In case of polymerisation, a multilayer may form, however if the chemisorption is a degradation reaction, layers are harder to define.
Physisorbed molecule keeps its identity and on desorption it can be desorbed and return to its fluid phase.	Chemisorbed molecules undergo a chemical reaction, so their chemical identity changes and it may not be recovered by desorption.
Attractive intermolecular forces between adsorbent and adsorbate. E.g. van der Waals.	Intermolecular forces involved in a chemical reaction. E.g. covalent.
Exothermic; the energy is generally not larger than the energy of condensation of the adsorbate.	Chemisorption energy is the same order of magnitude as the energy change in a comparable chemical reaction.
Reaches equilibrium fairly rapidly, but can be slow if the transport process is rate-determining.	Activation energy is often involved and at low temperature the system may not have sufficient thermal energy to reach thermodynamic equilibrium.

Masel (1996) compared the processes resulted from the collision between a molecule and solid surface with a tennis ball colliding with the ground. Depending on the nature of the solid, three possible processes were proposed: scattering, trapping and sticking, Figure 2.3. When a molecule collides with a non-deformable surface, it rebounds without losing energy or losing a very small amount of energy but not enough to stay on the surface, i.e. it is scattered as shown in Figure 2.3. In the case of a molecule colliding with a deformable surface, it loses enough of its energy and it is trapped in an adsorption site, although, in a weakly bonded state in which a small amount of thermal energy is enough to desorb the molecule from the surface. Sticking is a process where molecules collide with a surface, lose energy and remain on the surface for a reasonable time. In this case, the molecule bounces around the surface until it finds a free site to be adsorbed.

Despite in trapping and sticking the gas molecules are somehow adsorbed on the surface for some time, those two processes are quite different. In the case of trapping, the molecule loses

some energy to the solid lattice so it has no longer enough energy to be desorbed. In sticking, the molecule not only loses its energy but also forms 'strong' bond with the surface. Rates of trapping are determined by the rate at which the energy is transferred between the gas molecules and the solid surface, while sticking rates are determined by both the rate of energy transfer and the ability to find an available site on the surface where they can be physisorb of chemisorbed. The latter case, is the most probable process that can occur when building materials are exposed to VOCs and it depends on the type of gas, surface chemical composition and temperature (Masel 1996). Generally, when a solid is exposed to a certain gas, both trapping and sticking mechanisms occur.

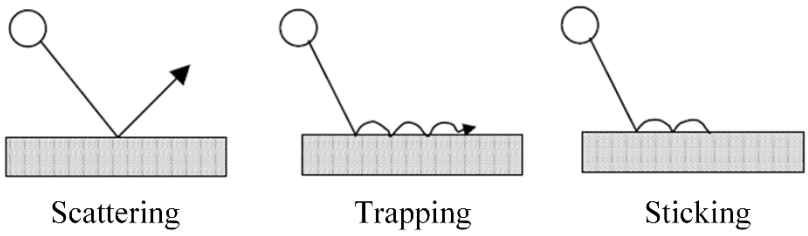

Figure 2.3 Illustration of possible mechanisms that can occur when a fluid molecule collides with a solid surface, adapted from Masel (1996).

2.3.2. VOCs adsorption and desorption behaviour in building materials

2.3.2.1. Methodologies to analyse adsorption/desorption of air pollutants

There are few methodologies found in the literature to analyse the interactions between VOCs and building materials. The most common are adsorption/desorption experiments in **dynamic conditions**. In this type of experiment, during the adsorption phase, a known concentration of VOCs is generated from appropriate source(s), and the VOCs are carried, usually by pure air, under controlled flow rates, temperature and RH, to the chamber where the material under test is placed, (Wal et al. 1998; An et al. 1999; Jørgensen et al. 1999; Won et al. 2001; Zhang et al. 2002; Elkilani et al. 2003; Uhde and Salthammer 2007; Xu and Zhang 2011; da Silva et al. 2016). The VOC concentration in the chamber is obtained by analysing the air flowing through the exhaust of the chamber. The amount of VOC adsorbed can be determined in two different ways either by performing an empty chamber experiment and comparing the results with the

material placed in the chamber or by analysing the concentration before the inlet of the chamber with that at the outlet. Once the concentration is stable, i.e. reaches equilibrium, the sources of VOCs are removed and pure air only is passed through the chamber, this being the desorption phase. In this phase, the VOCs that were previously adsorbed by the material will start to be desorbed.

Another way to study the adsorption of VOCs by the materials is to perform adsorption experiments under **static conditions**, i.e. no ventilation. In a static adsorption test, the material to be tested is placed in an airtight chamber and a known amount of VOC is introduced into the chamber through an injection port, usually in the order of µl, depending on the size of the chamber and area of the material exposed to the VOC (Huang et al. 2006; Niedermayer et al. 2013). To calculate the amount of VOC adsorbed by the material, as done in dynamic methodologies, empty chamber static experiments are performed and compared with those carried out with materials under test. It is very important that all conditions are the same when performing experiments without and with materials for comparison purposes.

The most common method for performing adsorption/desorption experiments, either under static or dynamic conditions, is by placing the testing material in an environmental chamber with controlled RH and temperature. Various sizes of chamber are used for this type of experiment, from a few litres in volume to large chambers, as described previously in section *2.2 Volatile organic compounds and formaldehyde emissions by building materials*. For the analysis of VOCs, the air exhausted from the chamber is sampled on to Tenax TA tube and analysed by GC/MS, with many studies following the standard BS ISO 16000-6:2011. For formaldehyde or other aldehydes concentrations, the air exhausted from the chamber is sampled in 2,4-DNPH cartridges and analysed by HPLC, BS ISO 16000-3:2011. A different method for analysing the concentrations, not so common, is continuous analysis, often known as on-line measurement (Meininghaus, Gunnarsen, et al. 2000; Matsumoto et al. 2009; Rizk, Verriele, Dusanter, et al. 2016; Rizk, Verriele, Mendez, et al. 2016).

Meininghaus et al. (2000) developed a gravimetric methodology to study the adsorption of *m*-xylene and n-octane by various building materials. This method involves use of a micro-balance placed inside a cell with air flow with controlled water content and adjustable VOC concentration. The test material is suspended inside the cell from a sensitive balance that registers any mass change due to VOC or water adsorption. The challenge when using this method is distinguishing the VOC adsorption from the water adsorption, since both occur simultaneously.

A third way to perform sorption studies of VOCs by building materials is by using the FLEC, although this method is not common due to the geometric limitations of the FLEC, (Meininghaus et al. 1999; Rizk, Verriele, Dusanter, et al. 2016).

2.3.2.2. Effect of physico-chemical properties of VOCs, inlet concentration of VOCs, building material, temperature and relative humidity on the adsorption/desorption behaviour

Gunschera et al. (2013) studied the physical adsorption behaviour of commercial zeolites when exposed to four VOCs: chlorobenzene, α-pinene, 2-ethoxyethylacetate and pentanal. The authors correlated the molecular 3D dimensions of the VOCs (range of 3.9 to 7.4 Å) and structure (circular or elongated) with the dimensions of the zeolite pores (range of 2.5 × 4.1 to 7.4 × 7.4 Å). It was observed that zeolites with larger pores adsorbed high quantities of VOCs independently of the size and structure of VOC molecule, while zeolites with small pores showed low capacity to adsorb large VOC molecules. Elongated VOC molecules can also be adsorbed by smaller pores, but in smaller quantities when compared with zeolites with larger pores. At the end of their studies, the authors also observed that this behaviour was not observed in some materials and they suggest that other factors, such as polarities of VOCs and specific surface area of building materials, can play an important role in the adsorption capacity of zeolites.

Niedermayer et al. (2013) studied the VOC sorption behaviour of several building materials under static conditions. The experiment used in this study is divided into parts: 1) Adsorption phase, where the building materials were placed into a glass container with certain levels of VOC concentrations, and samples of the VOCs were withdrawn every 24 h; 2) Desorption phase, where building materials tested were transferred into a cleaned glass containers. Desorption behaviour was observed after 24 h at different temperatures. Authors observed that smaller and more polar VOCs were preferably adsorbed compared with non-polar compounds. Concerning the desorption behaviour, it was observed that higher temperatures favour the re-emission of VOCs by building materials. No properties of materials or VOCs are correlated with re-emission behaviour in this research. However, the inherent emissions from wooden samples play an important role in such studies as they interfere with the sorption processes.

The effect of activated carbon surface area on VOC adsorption capacity was compared by Chiang et al. (2001). The authors explored different methods with which to characterise the main physical properties of the activated carbon, such as: specific surface area (through adsorption isotherms of nitrogen and argon – BET analyses), true density (measured by gas

pycnometer with helium) and porosity (measured by mercury intrusion porosimetry – MIP). It was observed that activated carbons with higher surface area possessed a higher capacity to adsorb VOCs.

Meininghaus et al. (1999) studied the permeability and sorption capacity of several VOCs by materials commonly found indoors such as carpet, gypsum board, PVC flooring and chipboard. In this study, the permeability factor and sorption capacity dependency on the VOC type (polarity and boiling point) was discussed. The carpet and the gypsum board showed the higher sorption capacity compared with the other two building materials. However, the lack of data on materials characteristics (such as porosity and other physicochemical properties) limited the amount of detailed analysis possible in this study, especially for the sorption capacity.

The effect of experimental parameters such as relative humidity, inlet concentrations of VOCs and air change rate on the VOC adsorption of carpet, gypsum, painted gypsum, wallpapered gypsum, wood flooring and vinyl flooring was studied by Won et al. (2001) in short term experiments (10 hours). It was observed that the sorption was highly dependent on the adsorbent (i.e. material) characteristics: good affinity was found between the carpet and non-polar VOCs, and between gypsum and highly polar VOCs; however no material characteristics are discussed. Interactions between non-polar VOCs and indoor materials were not affected by the variations in relative humidity. However, polar-polar interactions were affected by the RH. Humidity was also shown to have significant influence on the sorption capacity of unpainted gypsum with polar VOCs, maybe due to the preferable polar-polar interactions between the gypsum and water molecules. In general, there was no consistent trend between the variation of RH and the adsorption and desorption coefficients. Different observations regarding the effect of the RH on interactions between VOC and building materials were given by Colombo et al. (1993) for isopropanol and 2-butoxyethanol. Also, Colombo observed that the adsorption ability of the carpet was not influenced by either the lipophilic or hydrophilic character of the VOC or by the RH. In both studies, the authors indicate that the physico-chemical properties of VOC and building materials play an important role in the adsorption/desorption behaviour, although material characteristics are not included/explored in their studies and the comparison between different publications is difficult due to all of the experimental variants.

The effect of the relative humidity on the adsorption of toluene and formaldehyde by calcium silicate was also studied by Xu and Zhang (2011). The main observation made in this study was that by increasing the RH from 25 % to 50 % there was no significant effect on the adsorption of toluene and formaldehyde although, when increasing the RH from 50 % to 80 %

the amount of formaldehyde adsorbed increased and the amount toluene adsorbed decreased. The increase in adsorption of formaldehyde and decrease in adsorption of toluene is due to the water-solubility of formaldehyde and non-water-solubility of toluene. The formaldehyde molecules are preferably adsorbed/dissolved into the greater amount of adsorbed water under the 80 % RH condition. In the case of toluene, the decrease in the degree of desorption may be related to the competition at the adsorption sites between water and toluene molecules. Experiments with a mixture of formaldehyde and toluene against formaldehyde only were also performed in order to evaluate the effects on the adsorption of the pollutants in each case, however no clear observations were made.

Popa and Haghighat (2003) demonstrated the impact of VOC concentration, thickness of paint and type of material on sorption. The authors performed adsorption experiments with only toluene and with a mix of six VOCs (including toluene). Paint of double the thickness showed an increase of 20 % in the adsorption capacity and higher inlet concentrations of toluene led to a higher amount of toluene adsorption. In the experiments performed with a mix of VOCs, it was observed that adsorption increased with decreasing vapour pressure of VOCs. The effect of the adsorption of toluene when alone or as a part of a mixture of six VOCs was analysed. The adsorption of toluene decreased when mixed with other VOCs. Similar findings were achieved by Huang et al. (2006). A limitation of the study made by Popa and Haghighat (2003) is that no empty chamber experiments were performed in order to evaluate the sink effect of the chamber itself in the presence of several VOCs.

Jørgensen et al. (1999) tried to study the influence of the air velocity on adsorption of toluene and α-pinene by wool carpet. However, it was not possible to conclude whether the air velocity does not influence sorption in general or does not specifically influence the sorption on carpets. Contrary to the Jørgensen et al. (1999) study, Zhang et al. (2002) observed an effect of the air velocity on the sorption of VOCs by carpet. The authors observed the adsorption strength of five VOCs: ethylbenzene, benzaldehyde, decane, 1,4-dichlorobenzene and undecane. Dodecane was an exception in that its adsorption strength increased with higher air velocity. A possible reason given for this was that higher air velocity decreased the thickness of the boundary layer and thereby increased the mass transfer of dodecane across the boundary layer, resulting in a decrease of dodecane adsorption. In addition to the air velocity effect, Zhang et al. (2002) also studied the effect of temperature variation on the adsorption of painted drywall, ceiling tile and carpet. The painted drywall and ceiling tile showed such low adsorption capacity that it was difficult to observe any influence of the temperature on the adsorption

characteristics of these materials, at least within the range of experimental uncertainty. Regarding the temperature effect on the carpet, it was observed that, the adsorption strength increased when the temperature increased from 10.5 to 23 °C; however, it decreased when the temperature increased further from 23 to 35 °C. This observation was only made for three of the six VOCs tested: ethylbenzene, 1,4-dichlorobenzene and dodecane. The authors state that these observed temperature effects differ from the results obtained by Tichenor et al. (1991).

Medium density fibreboard is a well-known formaldehyde emitting material due to the formaldehyde based resin used to bind the wood fibre as already mentioned in the previous section. The current legislation and standardisation to reduce the amounts of formaldehyde that can be released from panel products has led to research been undertaken to develop low formaldehyde emission adhesives and scavengers that can been added to the panel to capture the formaldehyde that would otherwise be released into the environment (Kim 2009; Boran et al. 2011; Boran et al. 2012; Pirayesh et al. 2013). Kim (2009) investigated the addition of volcanic pozzolan to the urea-formaldehyde resin to reduce the formaldehyde emission. Pozzolans are composed of siliceous (SiO_2) and aluminous (Al_2O_3) materials and may present porosity (H. S. Kim et al. 2006). The results confirmed the reduced formaldehyde emissions from the MDF panels with increase of the pozzolan content. The capture of formaldehyde was attributed to the rough and irregular surface, with porous structure, of the pozzolanic materials. Tannin was also added as a formaldehyde scavenger in MDF panels (Boran et al. 2012). By adding 1.4 % of tannin solution, the free formaldehyde decreased by 45 %. However, the mechanical properties, such as Modulus of Rupture (MOR) and Internal Bond strength (IB), also decreased with the presence of the tannin. The lower MOR and IB was attributed to the modified fibre structure due to the presence of tannin.

Ruiz et al. (1998) investigated the interactions between soil minerals with different chemical composition (sand, limestone, clay-muscovite) and seven VOCs which, can be divided in three groups accordingly to the chemical conformation and polarity: polar ketone (methyl ethyl ketone); slightly polar aromatics (toluene, *m*-, *p*-xylene and ethylbenzene) and non-polar aliphatics (*n*-hexane, *n*-heptane and *n*-octane). To study effect of the presence of water vapour on the adsorption of VOCs two different RH were selected: 20 % and 50 %. The adsorption capacities of the minerals were related to their surface area and chemical composition. In general, it was observed that the most polar compounds showed the highest adsorption capacity on the three minerals, followed by the aromatic compounds and the aliphatics were the least adsorbed. By comparing the adsorption between the aliphatics, Ruiz et al. observed some

relationship between the length of the molecule of the VOC and the adsorption capacity where, longer molecules were adsorbed to a greater extent by the minerals. However, in the case of the sand (quartz), *n*-hexane was more adsorbed than *n*-heptane. As the three minerals have different specific surface areas, the adsorption isotherms were normalised by dividing them by the BET surface area to investigate only the effect of the chemical composition on the adsorption capacity. It was concluded that the difference in the adsorption capacity of the minerals was reduced although it can still be distinguished which, suggests that the physical characteristics of a material have a strong effect on the adsorption behaviour but their chemical composition also plays an important role. Regarding the effect of the presence of water vapour on the adsorption of VOCs, a reduction of the adsorption capacity of aromatic and aliphatic compounds was observed. In the case of the polar VOC ketone, it was observed that for a lower VOC concentration at higher RH, the adsorption capacity of the VOC was reduced. The authors suggested that VOC molecules compete with water vapour molecules for the adsorption sites in the minerals surface. Due to the high polarity of the water molecules, non-polar aliphatic and aromatic compounds are displaced, reducing their adsorption. For polar compounds at higher concentrations, the adsorption is not reduced so much due to the same intensity of polarity. As a final remark, Ruiz et al. state that the reduction of the adsorption capacity of VOCs onto minerals in the presence of water is dependent on the mineralogical composition.

An example of **chemisorption** is the reaction between the proteins in sheep's wool and formaldehyde (Alexander et al. 1951; Curling et al. 2012; Huang et al. 2007; Middlebrook 1949). Different methods have been explored with which to evaluate formaldehyde degradation by wool. Curling et al. (2012) used Dynamic Vapour Sorption (DVS) equipment. The DVS theory is based upon measurement of the sample mass change during the sorption of controlled concentrations of water vapour carried in a nitrogen gas. This study involved two experiments: 1) sorption and desorption of formaldehyde and 2) sorption and desorption of water. In the formaldehyde sorption cycle, a mass difference of 4.12 % was observed indicating the sorption of formaldehyde in wool fibres. In the water sorption cycle (performed after the formaldehyde cycle) a negative change of mass was observed, suggesting that some of the formaldehyde adsorbed in the previous experiment was released. The authors suggested that the formaldehyde released later had been physisorbed. Therefore, in a sorption system of wool and formaldehyde two phenomena may occur depending on the conditions: chemisorption and physisorption. Huang et al. (2007) placed a sheep's wool specimen inside a closed chamber with a known amount of formaldehyde. The authors measured the decreasing formaldehyde concentration

with time by using a PPM400 monitor instrument, also called a formaldemeter. The formaldehyde concentration in the chamber dropped from 1 to 0.3 ppm in 195 min. The chemical reaction scheme is proposed by several authors (Alexander et al. 1951; Curling et al. 2012; Huang et al. 2007).

2.4. Summary

In this section the main points which have been drawn from the literature review are as follows:

- ✓ Indoor Air Quality is highly affected by airborne chemical compounds, humidity and temperature;
- ✓ Building materials can emit a wide range of VOCs which can severally affect human health – hence low emissions building materials should be chosen in new build or refurbishment;
- ✓ Indoor building materials present a large exposed area which could help to remove pollutants from the air such as those used as a final coat;
- ✓ Materials with high specific surface area can act as a sink and improve the indoor air quality by reducing gas pollutant concentrations;
- ✓ There is a need to understand the interactions between actual building materials and VOCs, as the former can contribute to better Indoor Air Quality through the adsorption phenomenon;
- ✓ A correlation between chemical composition and physical properties of the materials and their adsorption/desorption behaviour needs to be established as it will help the scientific understanding of the interactions and the future development of novel materials with improved adsorption capacity.

Chapter 3

Experimental methodologies

3.1. Research strategy

Adsorption and desorption experiments were shown to be a good methodology for investigating the behaviour of building materials in real situations when there is a pollutant source present indoors (An et al. 1999; Jørgensen et al. 1999; Won et al. 2001). In this case, building materials can adsorb what is being emitted by the source, thus decreasing the pollutant concentration indoors when the emission rate is high and desorbing when the source is no longer emitting or the emission rate is significantly lower. This is known as the sink effect as described previously in Section 2.3. The testing at lab-scale may not fully represent the material's behaviour when placed in a real-scale room. For this reason, the investigation of the adsorption and desorption of some of the tested materials was carried out in lab-scale chamber and also in a real-scale room, known as a 'European Reference Room' as per the standard CEN/TS 16516:2013.

As stated previously in the literature review, the chemical composition of building materials may have an influence on their adsorption and desorption of VOCs. Therefore, it is important to understand the chemical constitution of each material to gain a more informed view of the chemical and physical interactions between molecules on the material's surface and molecules of the VOCs. In the same way, it is important to characterise the physical properties of building materials in order to study the effect of the microstructure and specific surface area of the building materials on adsorption and desorption.

Materials used in construction can have high impact on the environment. Pacheco-Torgal (2014) mentioned that buildings in Europe are responsible for more than 40 % of energy consumption and greenhouse emissions. **Eco-materials** can be defined as those materials that do not affect, or have a very low effect on the environment throughout the whole life cycle (Berge 2009). The correct selection of low energy building materials for certain applications

can reduce the embodied energy by 15 to 20 % in conventional buildings (Ashby 2013; Berge 2009). Embodied energy (MJ/kg) of a material product is the sum of the energy involved in the entire life of the product. This involves material extraction, manufacturing, transport at different stages, assembly/installation, use, disassembly and decomposition (Ashby 2013; Pacheco-Torgal and Jalali 2011). **Natural building materials** are often considered as eco-materials because of the low processing energy required after the extraction of the raw material. Melià et al. (2014) compared the environmental impacts of clay based plasters with cement based plasters. Results showed that 63 to 85 % of the embodied energy of these materials is related only to the manufacturing process, especially for the cement based plasters. It was also observed that producing plasters from crude clay and sand requires a relatively small amount of energy when comparing with cement production. Therefore, natural building materials, such as earth (clay) and lime based mortars, hemp shiv, straw, wood, sheep wool, and such, will have low impact on the environment (Ansell et al. 2017). Materials studied in this PhD are described in the following sub-section 3.2.

To study the adsorption and desorption behaviour of the natural building materials, three VOCs and a very-VOC were selected: toluene, limonene, dodecane and formaldehyde. As stated previously in section *2.3.2 VOCs adsorption and desorption behaviour in building materials*, it is known that the adsorption/desorption behaviour of VOCs is different when present in a mixture of several VOCs (Popa and Haghighat 2003; Huang et al. 2006). Because of this, only four organic compounds were selected to represent a range of molar masses and physicochemical characteristics of VOCs typically found within indoor environments. Toluene was selected to represent simple aromatic compounds such as benzene and it can be emitted by wood-based materials, fuels, oils and others. Limonene is a terpene-type compound and can be emitted by wood-based materials, cleaning products, air-fresheners etc. Limonene has a lower toxicity compared to the other three selected pollutants, although, when in presence of ozone it can react to produce formaldehyde molecules (Nazaroff and Weschler 2004). Dodecane is an alkane with long linear chain with twelve carbon atoms and it is a constituent of fuel and oil. Formaldehyde is considered a very-VOC (VVOC) due to its very low boiling point and is of particular importance as it is often found within indoor environments and classified as carcinogenic to humans (Group 1) according to IARC (International Agency for Research on Cancer). In Table 3.1 the main physicochemical properties of formaldehyde, toluene, limonene and dodecane are presented (ChemSpider database of the Royal Society of Chemistry, www.chemspider.com).

Table 3.1 Physicochemical properties and European harmonised LCI of formaldehyde, toluene, limonene and dodecane.

	Formaldehyde	**Toluene**	**Limonene**	**Dodecane**
	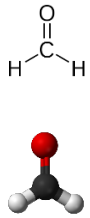	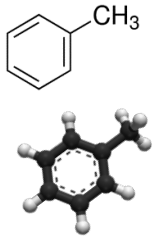	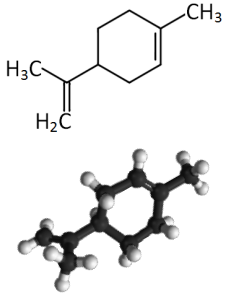	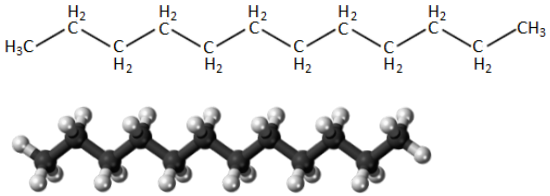
Formula	CH_2O	C_7H_8	$C_{10}H_{16}$	$C_{12}H_{26}$
Chemical conformation	Simple	Aromatic	Cyclic	Aliphatic, linear hydrocarbon chain
Polarity	Polar	Non-polar	Non-polar	Non-polar
Molar mass (g/mol)	30	92	136	170
Boiling point (°C)	-19	111	176	216
Vapour pressure at 25 °C (mm Hg)	3890	28.4	1.45	0.135
Water solubility at 25 °C (mg/l)	400000	526	13.8	0.0037
European – LCI (µg/m^3)	100	2900	5000	n/a

n/a – not available

3.2. Materials

A wide range of materials have been studied in the course of this PhD. Initial studies of the capture of VOCs and determination of chemical and physical properties were undertaken for materials which were commercially available, and classed as *Eco-materials*. In the later stages of the research, those eco-materials which showed better characteristics were further developed with the objectives of increasing their ability to capture VOCs and enhancing their moisture buffering properties.

3.2.1. Eco-materials

A range of 18 natural building materials was studied in the first stage of this PhD. These materials are classified in three types accordingly to their applications: thermal insulation, coatings and wood panels, see Figure 3.1.

All eco-materials were procured ready for use with the exception of the hemp lime insulation, lime mortars, and gypsum which were mixed and cast at the University of Bath or at the Building Research Establishment under laboratory conditions, following the manufacturers' guidance in each case.

The insulation materials can be divided into two categories, these being flexible or rigid. Flexible insulation materials are essentially loose fibres and include natural wool, hemp fibres and wood fibres. Rigid insulation materials have a higher density compared with the loose fibre products and also incorporate a binder, as is the case of the wood fibreboard and both hemp limes. Besides the natural wool, all other insulation materials are cellulose-based.

Coating materials were specified for internal use as either base (render) or finishing coats (plaster). Gypsum, Mortar_P and Clay_B are for use as finishing coats. Therefore, aesthetics are an important aspect of these materials as they will be exposed to the indoor environment. In general, coating materials for use as finishing coats have finer grains of sand and finer particles of lime to achieve a smoother final surface.

Three types of wood panels were included in this project: MDF, chipboard and clayboard. The majority of the MDF or chipboard products available, either to be used as furniture or wall covering, are covered in a resin-coated paper layer (décor finish) for both moisture resistance and aesthetic appearance. In this PhD project, a comparison between uncoated and coated wood

panels was made, allowing the effect of the coating to the evaluated with respect to the emissions and adsorption/desorption of VOCs and formaldehyde.

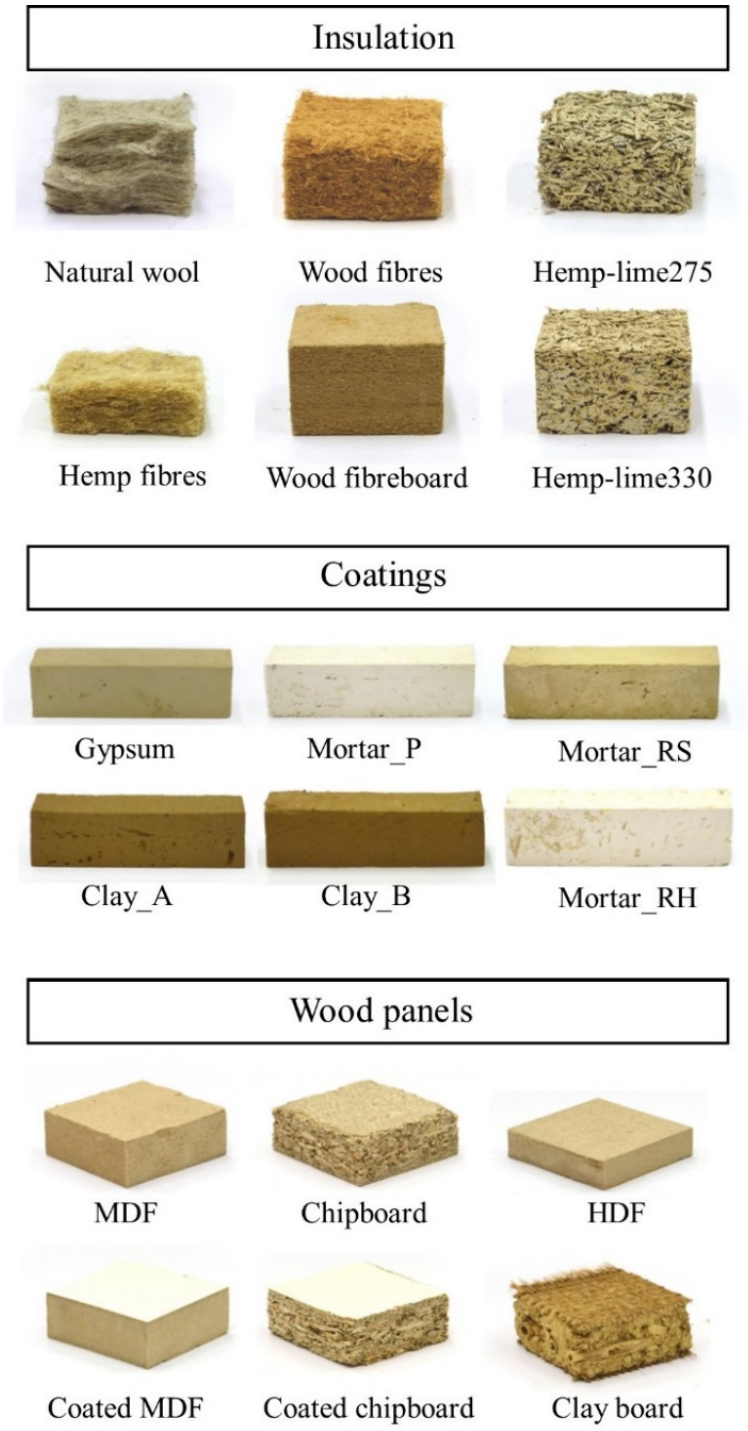

Figure 3.1 Natural building materials – *Eco-materials*.

3.2.2. Novel materials

Some of the *eco-materials* were selected for further development in order to increase their potential to capture VOC and moisture buffering capacity. The development/modifications of the eco-materials were made through the incorporation of bio-based additives or a thin coating of TiO_2 particles to enable photocatalytic activity.

The novel materials developed were:

- MDF panels with walnut shell incorporated, Figure 3.2;
- Two clay-based plasters coatings, lime-based mortars with cellulose flakes and natural wool incorporated, Figure 3.3;
- Lime-based mortar with TiO_2 particles, Figure 3.4;
- Coated MDF panels with TiO_2 particles, Figure 3.5;

A full description of the materials developed is given in Chapters 5, 6 and 7.

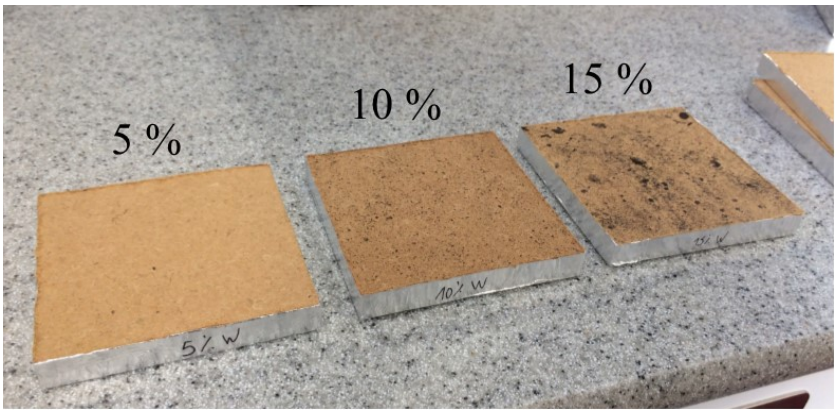

Figure 3.2 MDF panels with 5, 10 and 15% of walnut shell incorporated – Chapter 5.

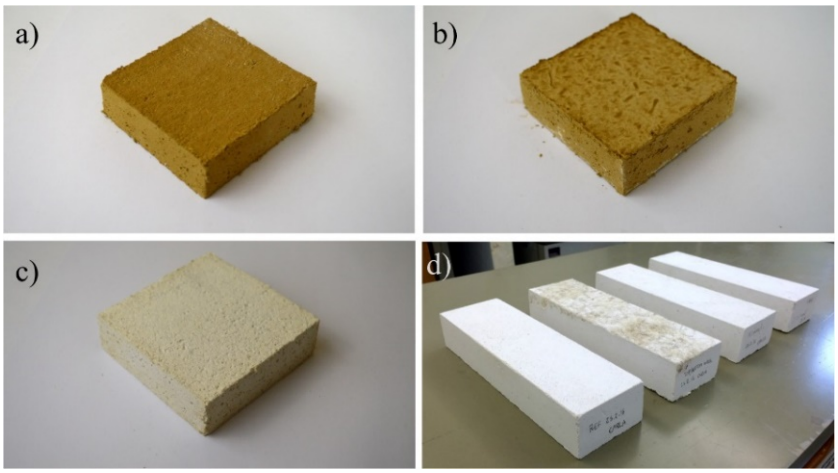

Figure 3.3 a) Clay_E14, b) Clay_H2, c) Cell_mortar and d) lime mortar with natural wool incorporated – Chapter 6.

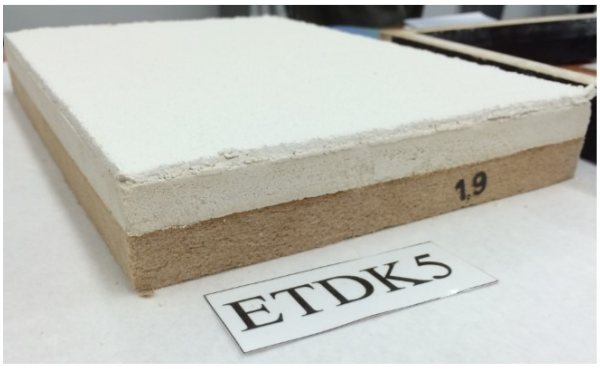

Figure 3.4 Photocatalytic lime mortar ETDK5 – Chapter 7.

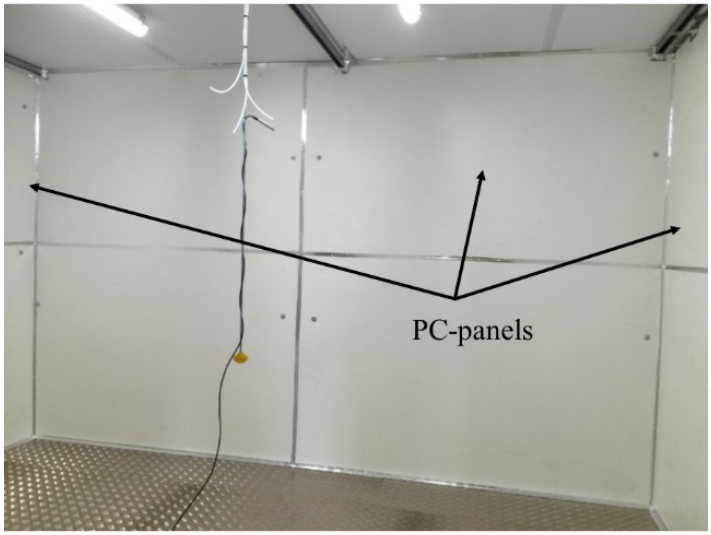

Figure 3.5 Photocatalytic panels installed in an environmental chamber – Chapter 7.

3.3. Chemical characterisation

In this section, three techniques used to characterise the chemical composition of the natural building materials are described.

3.3.1. X-ray diffraction

X-ray diffraction (XRD) allows a qualitative analysis of the crystalline or semi-crystalline phases present in materials. When a material is exposed to an X-ray beam, the X-rays are diffracted according to a certain angle (2θ) matching the characteristic crystallographic orientations of the materials as given by Bragg's law:

$$n\lambda = 2d \sin\theta \qquad \text{Eq. 3.1}$$

where λ is the wavelength of X-rays, θ is the angle between the incident rays and crystal surface, d is the spacing between layers of atoms and n is an integer (Hammond 2009).

The crystalline phases of the natural building materials were analysed using a *Brucker-AXS D8* powder X-ray diffractometer operated at 40 kV, 40 mA with a Cu-K_α X-ray source and λ = 1.5405 Å. The sweeping angles (2θ) used were between 5 and 80º with a step size of 0.016 º at ambient temperature in order to analyse all possible crystalline phases present in the natural building materials.

Depending on the material, two methods were used to prepare the samples for XRD analyses, Figure 3.6. In the case of powder samples, the sample holder was filled with powder; all other materials were fixed to the holder with an adhesive.

The identification of the peaks was carried out through the software *Match!* version 2.3.1, by using the *RRUFF.info* database for inorganic materials (Downs 2006), and by comparing with the literature.

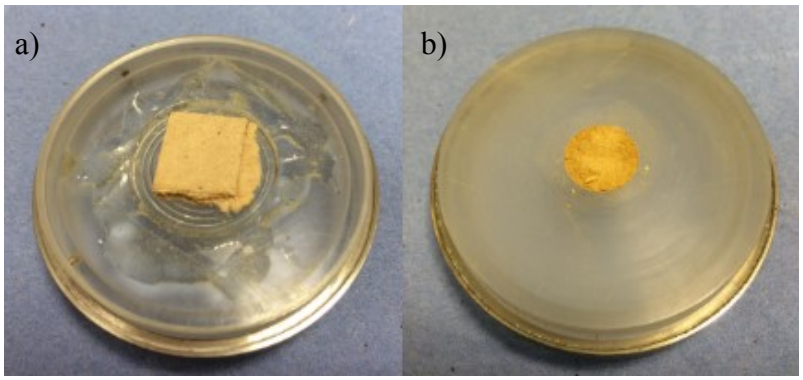

Figure 3.6 Different ways of sampling for X-ray diffraction: a) MDF sample fixed with adhesive; b) powder from clayboard panel.

3.3.2. Raman spectroscopy

Raman spectroscopy allows the identification of chemical bonds present in materials through the vibrational, rotational and other low-frequency modes caused by the interaction between the laser light and the material (Rodgers and Hampton 2003; Wojciechowska et al. 1999). When a light interacts with a material, it can be reflected, transmitted, absorbed or scattered. In the case of Raman spectroscopy, the interaction between the laser and the material results in a change in the energy of the scattered photons from the laser. This change in energy is characteristic function of the vibrational modes of the molecule which the light interacted with, and therefore it is possible to identify individual compounds present in a material.

A Renishaw System 2000 Raman spectrometer equipped with a UV-laser of wavelength 325 nm was used for the Raman studies. The analyses were carried out by focusing the laser with the objective magnification of x 50 onto the material surface, 5 seconds of exposure time and 5 accumulations. Prior to analyses, the spectrometer was calibrated using a diamond standard specimen. The identification of the peaks was carried out by using three sources: 1) *RRUFF.info* database for inorganic materials, (Downs 2006); 2) *NIST Chemistry Webbook* for organic based materials (Linstrom and Mallard 2011); and 3) by comparing with the literature.

3.3.3. FTIR spectroscopy

Fourier transform infrared spectroscopy (FTIR) is based on absorption and transmission of infrared radiation. As with the other spectroscopic techniques it is used to identify a singular component or the chemical composition of the material through the absorption peaks (Garside and Wyeth 2003; Wojciechowska et al. 1999). In an FTIR analysis, infrared radiation is passed

through a sample resulting in some wavelength being absorbed and other being transmitted through the material. This creates a spectrum that represents the molecular absorption or transmission, thus creating a fingerprint of the material (absorption peaks).

A *Perkin-Elmer Frontier* FTIR spectrometer equipped with a *MIRacle™ Single Reflection ATR* (attenuated total reflectance) with diamond crystal from PIKE technologies was used. The IR spectroscopy was carried out over a wavelength range of between 600 and 4000 cm^{-1}, with 2 cm^{-1} of resolution, 25 scans of accumulation and 0.5 $cm.s^{-1}$ of scan speed. For each material, three spectra were recorded in different zones in order to validate the data. The identification of the peaks was carried out by using three sources: 1) *RRUFF.info* database for inorganic materials, (Downs 2006); 2) *NIST Chemistry Webbook* for organic based materials (Linstrom and Mallard 2011); and 3) by comparing with the literature.

3.4. Physical characterisation

In this section, the techniques employed to characterise the physical characteristics of the natural building materials are described. The physical characterisation allows the study of important properties contributing to the sorption behaviour, such as surface area, porosity and pore size distribution, microstructure and particle morphology.

3.4.1. Surface area by BET

Adsorption measurement based on the Brunauer-Emmet-Teller (BET) isotherm is the most widely used method for the determination of the specific surface area of a powder or porous material (Sing et al. 1985).

This measurement can be done using N_2 adsorption at 77 K, by putting a solid material of a known mass in contact with a known volume of gas; adsorption creates a decrease in the gas pressure, from which the amount of adsorbed gas can be calculated. From these measurements, a plot of the amount of gas adsorbed versus the relative pressure (p/p_0, where p_0 is the saturation vapour pressure of the adsorption gas used) is obtained, which is called the adsorption isotherm. According to IUPAC (Sing et al. 1985), the shapes of adsorption isotherms are classified into six groups although the BET theory can only be applied to Type II and Type IV, Figure 3.7. The type II isotherm represents unrestricted mono/multilayer adsorption on a non-porous or macroporous adsorbent. The type IV isotherm shows a characteristic hysteresis loop and the

limiting uptake at high p/p_0: these features are associated with capillary condensation taking place in mesopores.

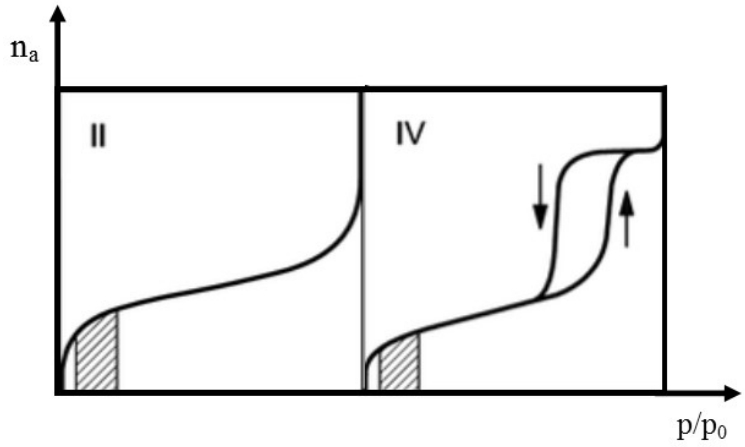

Figure 3.7 IUPAC classification of adsorption isotherms (typical BET range is indicated by the hatched area), adapted from (Sing et al. 1985).

The BET equation, which is only valid for lower values of p/p_0, is applied to the isotherm curve in the following form (Rouquerol et al. 2014):

$$\frac{p/p_0}{n(1-p/p_0)} = \frac{1}{n_m C_{BET}} + \frac{C_{BET}-1}{n_m C_{BET}} \frac{p}{p_0} \qquad \text{Eq. 3.2}$$

where n is the specific amount of gas adsorbed at relative pressure p/p_0, n_m is the specific amount of gas in the monolayer and C_{BET} is the BET constant. By this procedure, the n_m value can be calculated (from the slope and the intercept) and applied in Eq. 3.3 to calculate the surface area (Rouquerol et al. 2014):

$$A_{BET} = N_A a_m n_m \qquad \text{Eq. 3.3}$$

where A_{BET} is the surface area, N_A is the Avogadro number, a_m is the cross-sectional area of an adsorbed gas molecule, which for the nitrogen molecule at 77 K is 0.162 nm^2, (Rouquerol et al. 2014).

The surface area of the materials was measured using a *Micromeritics*® - *3Flex* instrument following the standard BS ISO 9277:2010, Figure 3.8 a). Specimens were cut into pieces with nominal diameter of approximately 0.5 cm and placed in the sample holder, Figure 3.8 b) and c). In total, a mass of approximately 0.7 g was used for each sample. Prior to the surface area measurements, all samples were degassed to remove any water or other molecules physically adsorbed on the surface. The degas phase was comprised in two steps, firstly being carried out overnight at 105 °C in a *Micrometrics*® *Flowprep* 600 under a flow of nitrogen and then in situ (in the *3Flex* instrument) at 10 °C/min until 105 °C was reached, and held at this temperature for 120 min. Following the degas phase, the adsorption and desorption cycle of nitrogen commenced. The nitrogen BET surface area values were then calculated using the 3Flex software version 3.02. Three samples of each specimen were analysed for statistical purposes.

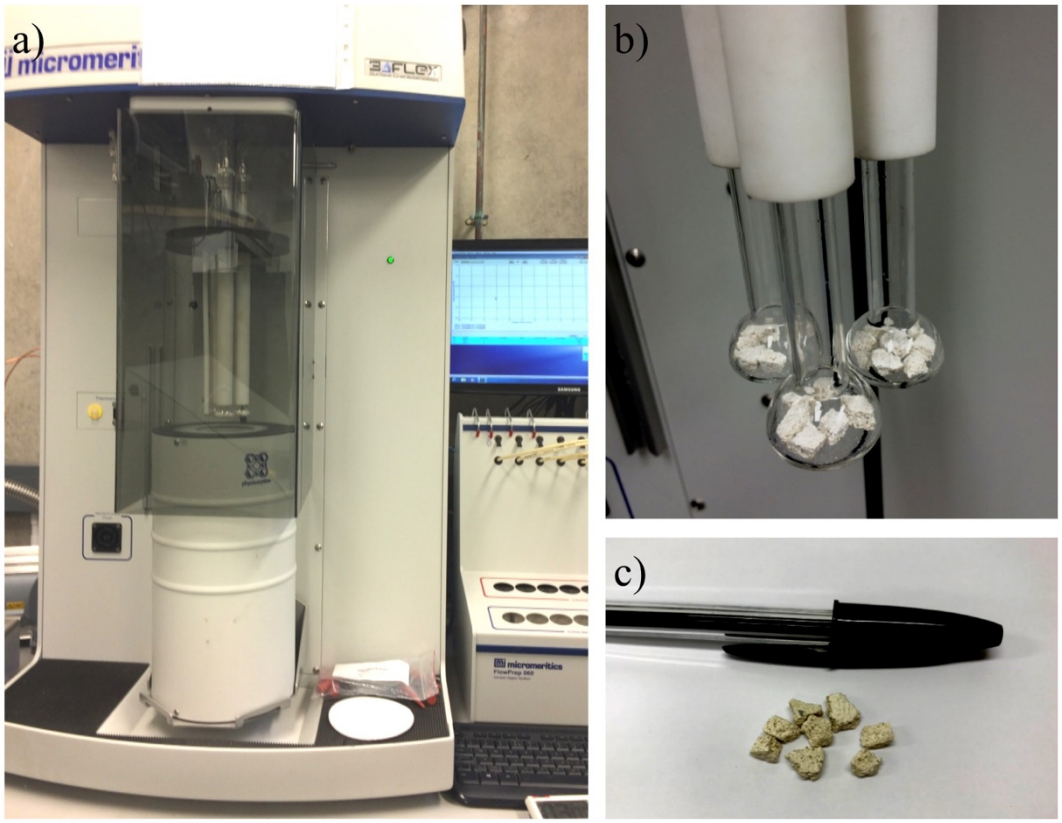

Figure 3.8 a) Micrometrics® 3Flex, b) sample holders, c) specimens for surface area measurements.

3.4.2. Mercury intrusion porosimetry

Mercury Intrusion Porosimetry (MIP) is based in an intrusion of a liquid metal (mercury) with large contact angle, under a range of pressures. At low pressures the mercury intrusion will occur in the larger pores, whereas the intrusion in the smaller pores will require higher pressures of the order of 60,000 psi (~ 413.7 MPa). Pore size distributions, bulk and true densities can be analysed through MIP. As this technique is based on intrusion and extrusion of mercury at high pressures, the process can lead to the formation of microcracks and disintegration of the pore network in samples with low mechanical strength. As this process can modify the pore structure, this must be considered when interpreting results. In addition, the analysis theory used in this technique assumes that the pores are cylindrical. This could be a source of error for the materials studied in this PhD programme which may have non-cylindrical pores (Abell et al. 1999; Diamond 2000; Hearn and Hooton 1992). Due to these limitations of MIP, the studies on porosity of building materials should be complemented by other characterisation techniques such as scanning electron microscopy.

A *Micrometrics Autopore III* instrument was used to measure the pore size distribution.

3.4.3. Electron microscopy

Scanning Electron Microscopy (SEM) is used to reveal the microstructure of the materials and particle morphology. Particle or pore size measurements can also be taken from the image obtained from SEM. The principle of this technique is based on an electron gun that generates a beam of electrons inside a vacuum column, which is then focused and scanned across the surface of the specimen (Dunlap 1997). An image is constructed by plotting the electronic signal generated from the detector. Secondary and low angle back-scattered electrons can both be used, with different detectors, to generate images relating to both morphology and atomic mass, respectively.

Elemental analysis techniques such as Energy Dispersive X-ray spectroscopy (EDX) are commonly coupled to an electron microscope, and are used for the identification of each chemical element present in a material. The electron beam stimulates the emission of characteristic X-rays from the material which allows the identification of elements by measuring their energy. EDX is mostly used for qualitative analysis and very informative 2D maps can be constructed to establish the distribution of each individual chemical element.

The microstructural and morphological analyses were carried out using a *JEOL 6480LV* scanning electron microscope, operated at an accelerating voltage of 10 kV. This microscope is equipped with an EDX spectrometer (*Oxford INCA)* for the elemental analyses/chemical characterisation.

For sample preparation, the materials were cut into small pieces of approximately 10 mm size and fixed to an aluminium sample holder with carbon tape. Prior to the analysis, all samples were degassed in a vacuum chamber for 24 h and then sputter-coated with gold-palladium to increase in the electrical conductivity and reduce the surface charging. Materials characterised by EDX were sputter-coated with carbon instead of gold-palladium. Before the elemental analyses the EDX spectrometer was calibrated using a copper standard.

3.5. IAQ assessment

In this section, the methodologies used to study the VOC and formaldehyde emissions and adsorption/desorption by the natural building materials are presented.

As discussed previously in Section *3.1 Research strategy*, experiments for IAQ assessment were carried out in lab-scale chambers (2-litre volume) and in a room-sized chamber (30 m^3 volume).

3.5.1. Rig assembly - 2-litre environmental chambers

The 2-litre chambers rig, assembled at BRE in Watford, is composed essentially of three main components: 1) pure air generator and humidification system; 2) chambers for the sources of formaldehyde and VOCs; and 3) 2-litre environmental chambers in which the materials are placed, Figure 3.9. The rig has six chambers installed in parallel, which allows the testing of five materials at the same time plus one empty chamber for reference, Figure 3.10 a) and b).

Pure air, generated at 23 ± 2 °C and kept at 50 ± 5 % RH, is introduced into the chamber and flows through the route indicated as *clean air* in the diagram, or through the route indicated as *dopant air*. The flow rate going to both lines was maintained at approximately 1200 ml/min when five chambers were in use or 1500 ml/min in the case of using all six chambers. The flow rate allows supply of 200 ml/min to the inlet of each chamber and an excess of air flow going to vent (named as exhaust in Figure 3.9). The air flow rate of the *clean air* line was controlled with a needle valve. Mass flow controllers were placed before the chambers containing the VOCs and formaldehyde sources. In order to create pollutants concentrations in the chambers

of about 2000 μg/m^3 and 1000 μg/m^3 formaldehyde, the air flow rates going to the sources chambers were set to be 800 ml/min and 400 ml/min for the VOC and formaldehyde chambers respectively. All tubes, valves and joints used in the rig assembly were made of emission-free and non/adsorbing materials to avoid extraneous influences in the experiments.

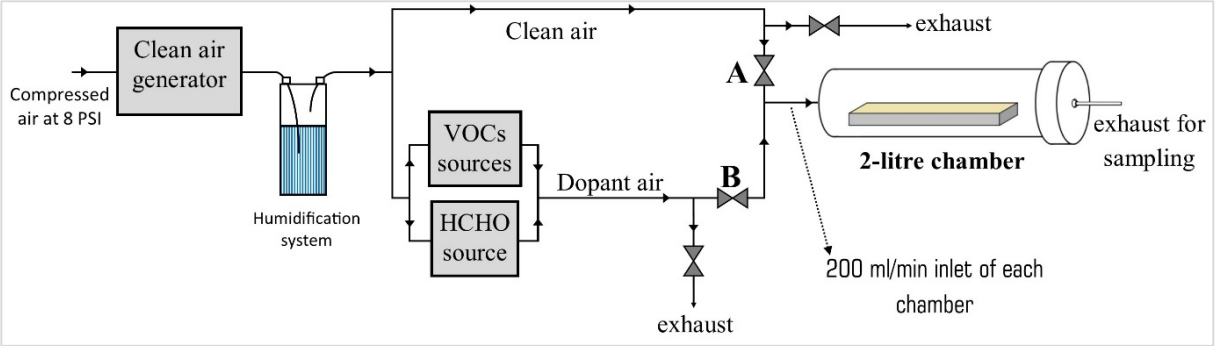

Figure 3.9 Experimental rig for measuring emissions and adsorption/desorption of formaldehyde and VOCs by building materials.

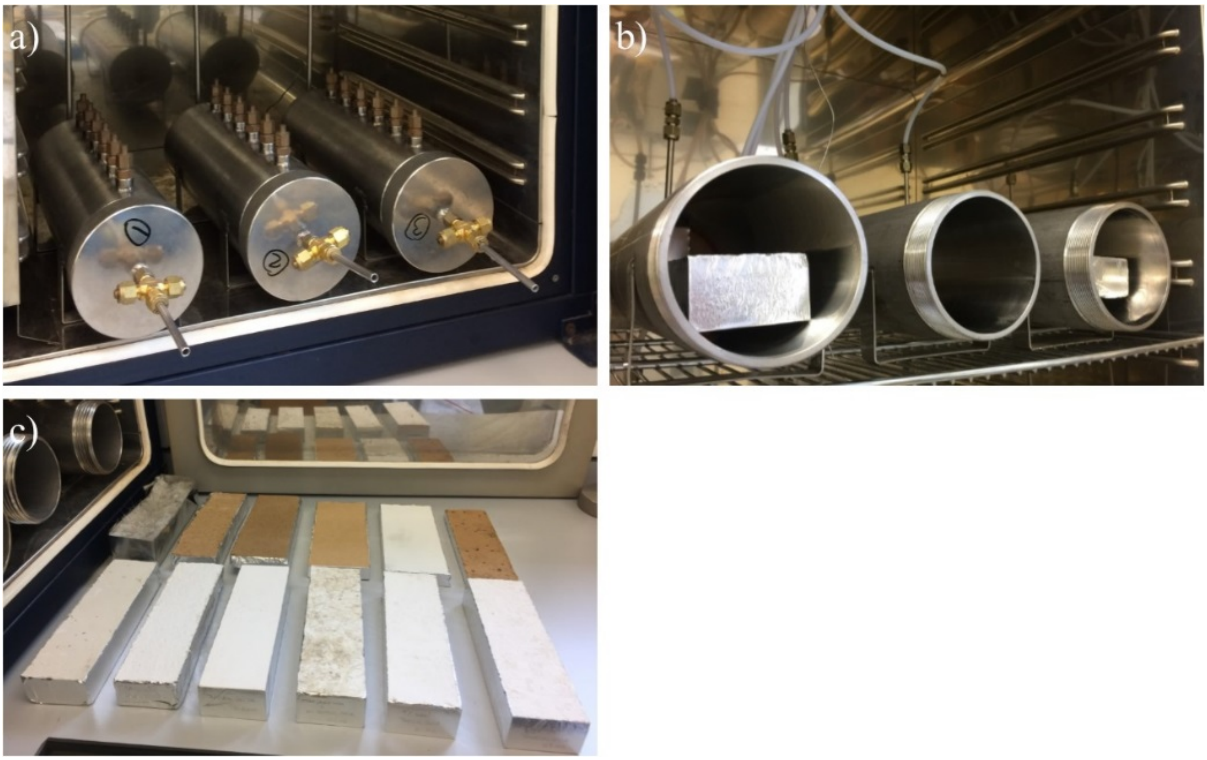

Figure 3.10 a) 2-litre chambers; b) 2-litre chambers showing samples inside; c) natural building materials enclosed in an emission-free boat for IAQ assessment.

Specimens for emissions and adsorption/desorption of VOCs and formaldehyde were cut into samples of nominal dimensions of 200 mm x 60 mm x 15-38 mm and enclosed in an emission-free boat, so that the interactions between the vapour phase the materials would occur only at the exposed surface, Figure 3.10 c).

3.5.1.1. Sources of volatile organic compounds

At the start of this project three solutions for the sources of VOCs were discussed: home-made permeation tubes, permeation tubes supplied by *KIN-TEK*™ or gas cylinders. From an economic and practical point of view, it was decided to use home-made permeation tubes as sources of VOCs.

The home-made permeation tubes were made of an aluminium tube (with 4 mm inner diameter) filled with 1.5 ml of the VOC and closed with a rubber insert at one of the ends as shown in Figure 3.11 a). The principle is based on a mass loss of milligrams per day of the source, thus creating the required level of VOC in the air flow and hence the chamber. Firstly, sources were prepared for each VOC (toluene, limonene and dodecane) with five different rubber inserts and two different lengths (6 and 12 mm) in order to evaluate the mass loss of each configuration and to observe which one exhibited the most stable mass loss. The rubbers studied, supplied by *Polymax Ltd.*, have a diameter of 6 mm and were as follows:

- EPDM (ethylene propylene diene monomer class M);
- Red oxide silicone;
- Translucent silicone;
- FKM (Viton®);
- NBR (nitrile).

For each combination of rubber type and length, three sources were prepared in order to obtain a representative result, Figure 3.11 b). From this preliminary study the following combinations of rubber cord, rubber length and VOC were selected:

- ✓ Toluene: NBR rubber with 12 mm length;
- ✓ Limonene: EPDM rubber with 12 mm length;
- ✓ Dodecane: EPDM with 6 mm length.

It is understood that the behaviour of the VOC emission stability for a specific combination of rubber and VOC is related to the ability of that particular VOC vapour to diffuse through the rubber. However, the discussion of this is outside the scope of this PhD.

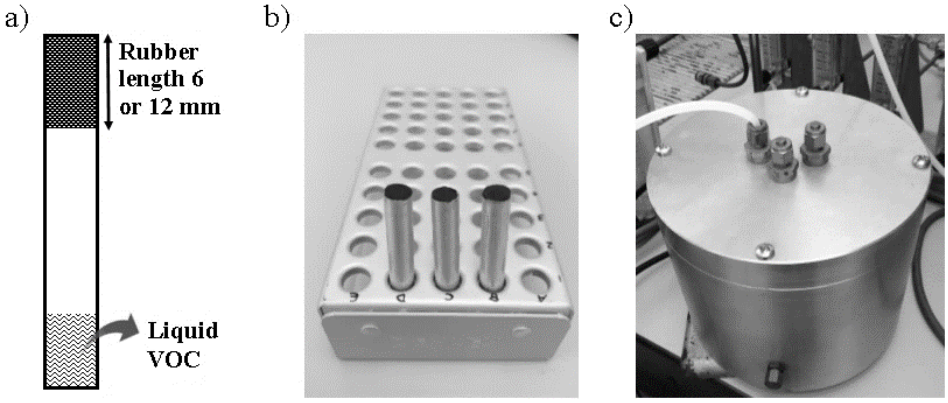

Figure 3.11 a) Schematic drawing of a home-made permeation tube, b) home-made sources and c) chamber of sources of VOCs.

Prior to the adsorption/desorption experiment, three sources of each VOC were prepared, according to the selected combination of rubber type and length, and placed within the VOC source chamber. The weight of all sources was measured on a daily basis to determine their mass loss rate and stability. In Figure 3.12, the mass loss of sources of toluene, limonene and dodecane are presented. From preliminary studies, it was observed that after placing the VOC sources inside the chamber, they would take approximately one month until reaching their maximum emission rate (maximum mass loss) and to stabilise. Therefore, the daily weightings began at least one month after placing the sources in the chamber. This shown in Figure 3.12 a) and b) where the sources of toluene and limonene were placed inside the chamber on 06/04/2016 and maximum mass loss was reached around 24/05/2016. Additionally, Figure 3.12 shows that the same combination of VOC, rubber and rubber length can show minor differences in the stabilisation of the emission rate; the sources with most stable mass loss were chosen for the adsorption/desorption experiments, these being represented by the black lines shown in the three graphs in Figure 3.12. To observe the behaviour of the sources of VOCs and formaldehyde during the adsorption/desorption experiment, the reference chamber curves are always showed in parallel with the materials curves as described later.

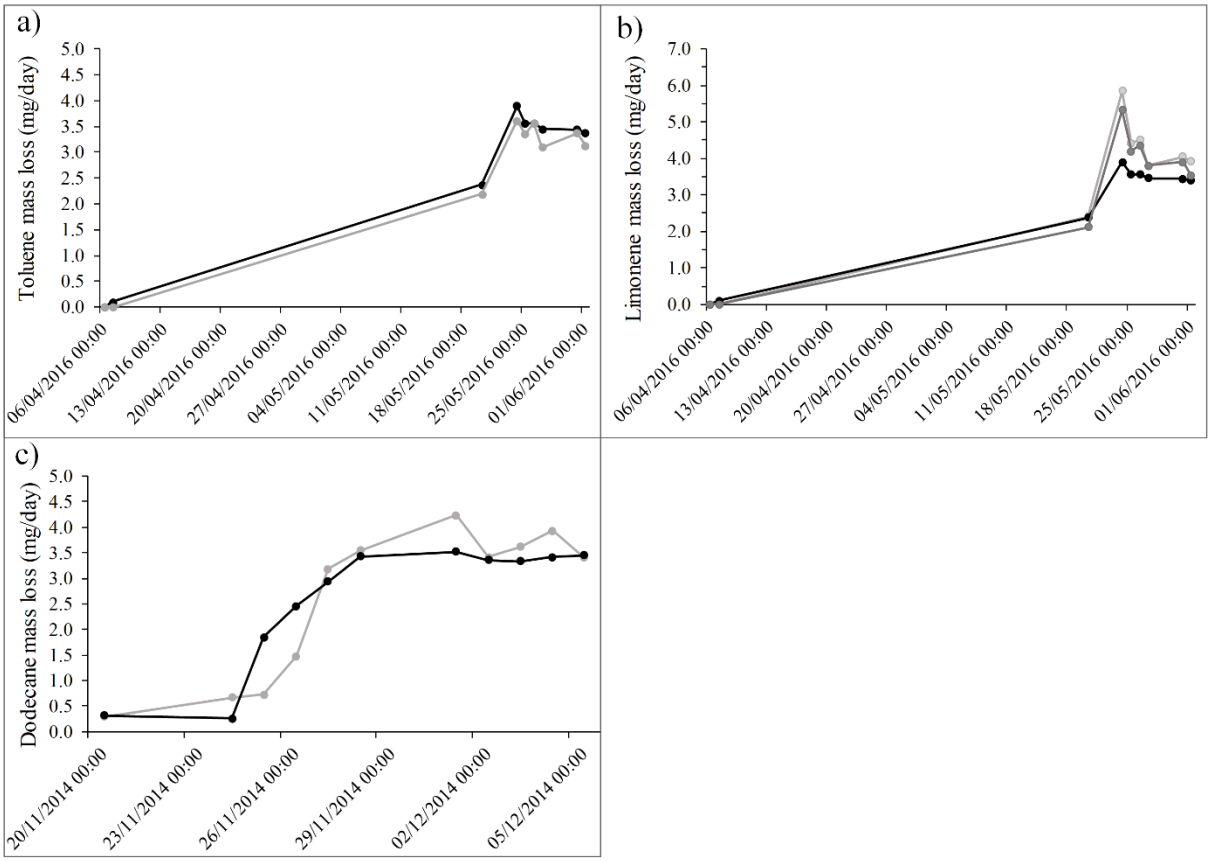

Figure 3.12 Mass loss (mg/day) of the sources of a) toluene, b) limonene and c) dodecane for the 2-litre chambers rig.

The known values of the mass loss allowed determination of the ideal flow rate going into the source chambers with which to achieve a desired concentration of VOCs in the 2-litre chambers, set to be 800 ml/min as described previously in section *3.5.1 Rig assembly - 2-litre environmental chambers*.

3.5.1.2. Formaldehyde source

The formaldehyde source used was supplied by *KIN-TEK*™. This source is a permeation tube, classified by the manufacturer as an HRT – High Rate Disposable Permeation Tube, which generates a formaldehyde emission rate of 830 ng/min when the tube is kept at 80 °C, Figure 3.13. The dosing concentration of formaldehyde in the 2-litre chambers can then be controlled using the flow rate.

Figure 3.13 Source of formaldehyde *KIN-TEK*™ inside the oven at 80 °C, to give a stable emission rate.

3.5.2. Rig assembly - 30 m^3 chamber

The real scale emissions and adsorption/desorption experiments were carried out in an environmental chamber with nominal volume of 30 m^3. This chamber, built by BRE, represents the *European Reference Room* stipulated by the standard CEN/TS 16516:2013. The internal dimensions of the chamber are 3 m × 4 m and 2.5 m height. The door is 0.8 m wide and 2 m high and the window has 2 m^2 of glazed area, Figure 3.14. Panels forming the walls of the chamber were supplied by *Kronospan*®. The inlet of the air into the chamber is at low level and the exhaust of the chamber is located in the opposite wall of the inlet at high level as shown in Figure 3.14.

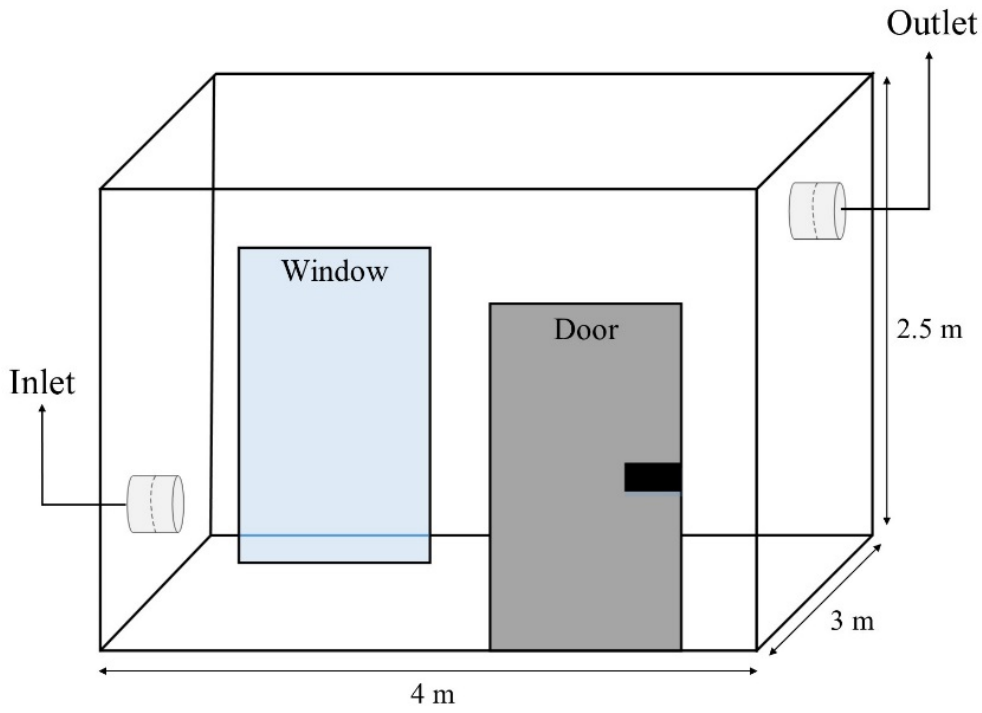

Figure 3.14 Schematic of the 30m^3 chamber showing the locations of the inlet, outlet, door and window.

A simplified schematic drawing of the 30m^3 chamber's rig is shown in Figure 3.15. The air is cleaned of any volatile compounds or particulates by passing through a chamber containing filters. Once the air is cleaned, its relative humidity is adjusted to 50 ± 5 % and the temperature to 23 ± 2 °C. After passing the filtration and humidification systems, the air flow is split into parallel lines, one going to the doping chamber 1 and another going to the doping chamber 2, represented by D1 and D2 respectively in Figure 3.15. These two chambers are used to house the sources of VOCs. The doped air resulting from the chamber D2 goes directly to vent, this chamber therefore allowing study and development of new sources of VOCs without interfering with the environmental chamber. Doping chamber D1 is where the sources of VOCs are placed to perform the adsorption/desorption experiments, Figure 3.16. Both doping chambers feature a translucent panel which allows inspection of the sources of VOCs inside, and therefore observation of the level of liquid for each source. The flow rate going to the environmental chamber is measured by forcing the air to pass through an orifice with known diameter in the doping chambers. The pressure in this location is measured and then converted to a flow rate.

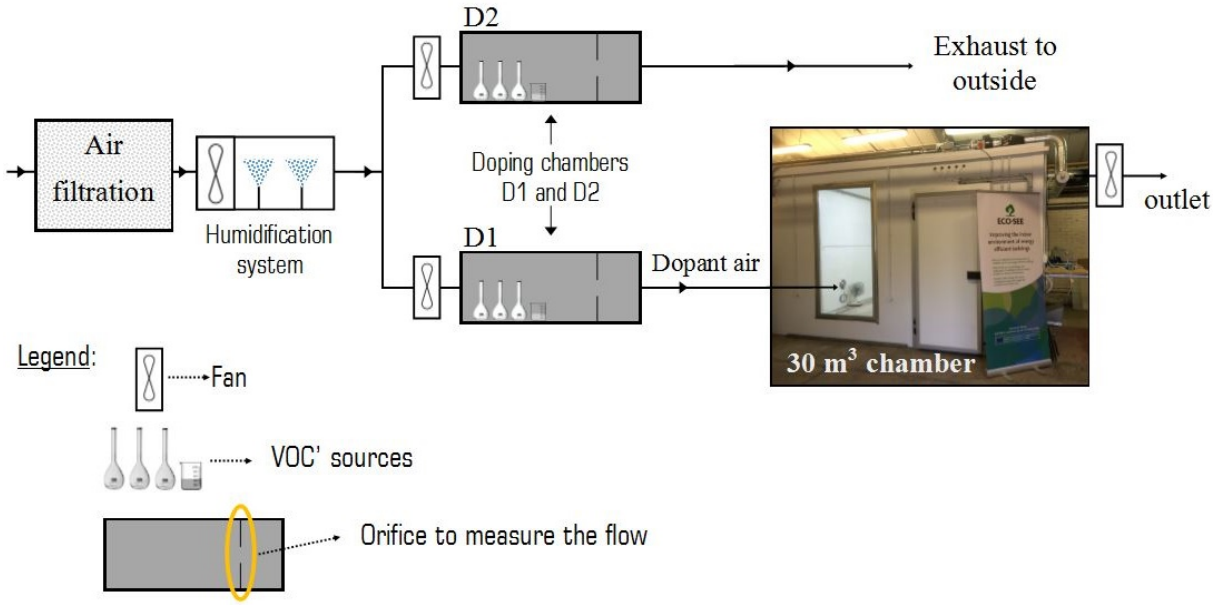

Figure 3.15 Simplified schematic drawing of the 30 m^3 chamber rig.

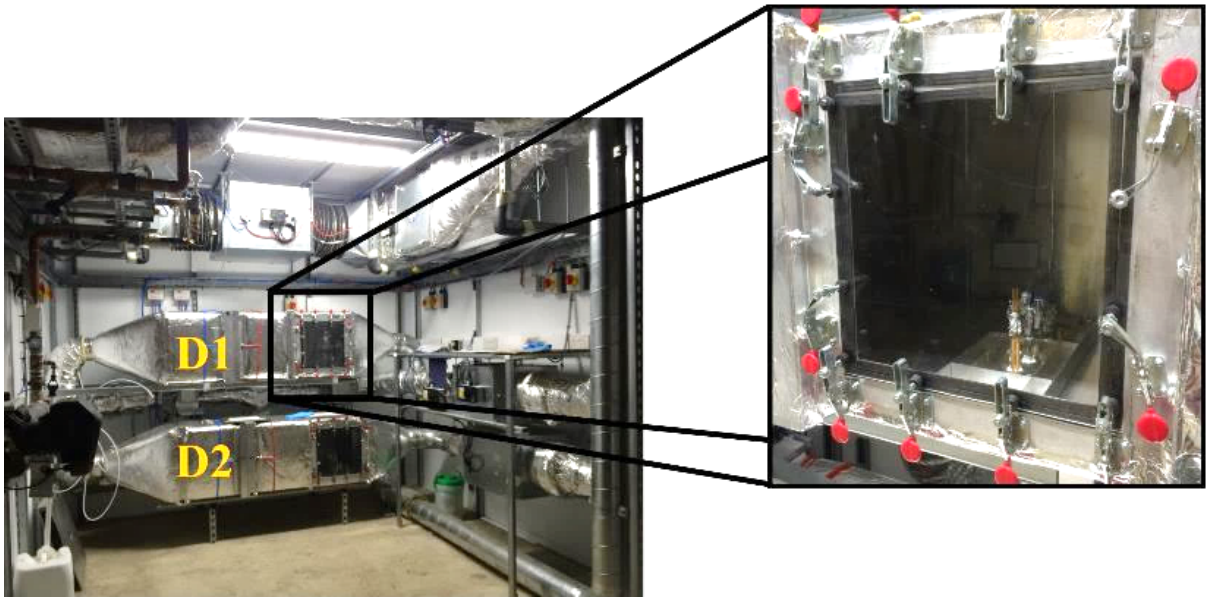

Figure 3.16 Plant room for the 30 m^3 chamber indicating the two dosing chambers where the sources of VOC sources are placed.

3.5.2.1. Development of VOC sources

The first approach taken for the development of new sources for the 30 m^3 chamber experiments was based on scaling-up the sources used in the 2-litre chambers rig. The nominal volume of this chamber is around of 15000 times higher than that of the 2-litre chamber, so VOC sources with much higher emission rate are needed in order to achieve the same level of VOC concentration inside the chamber. Thus, these sources were made of aluminium tubes closed at one end with *Swagelok*® fitting and fitted with rubber at the other end to allow the diffusion of VOC vapour, Figure 3.17. Several combinations of rubber type, rubber length and VOC were trialled. However, none of these showed enough mass loss, hence the approach was discontinued.

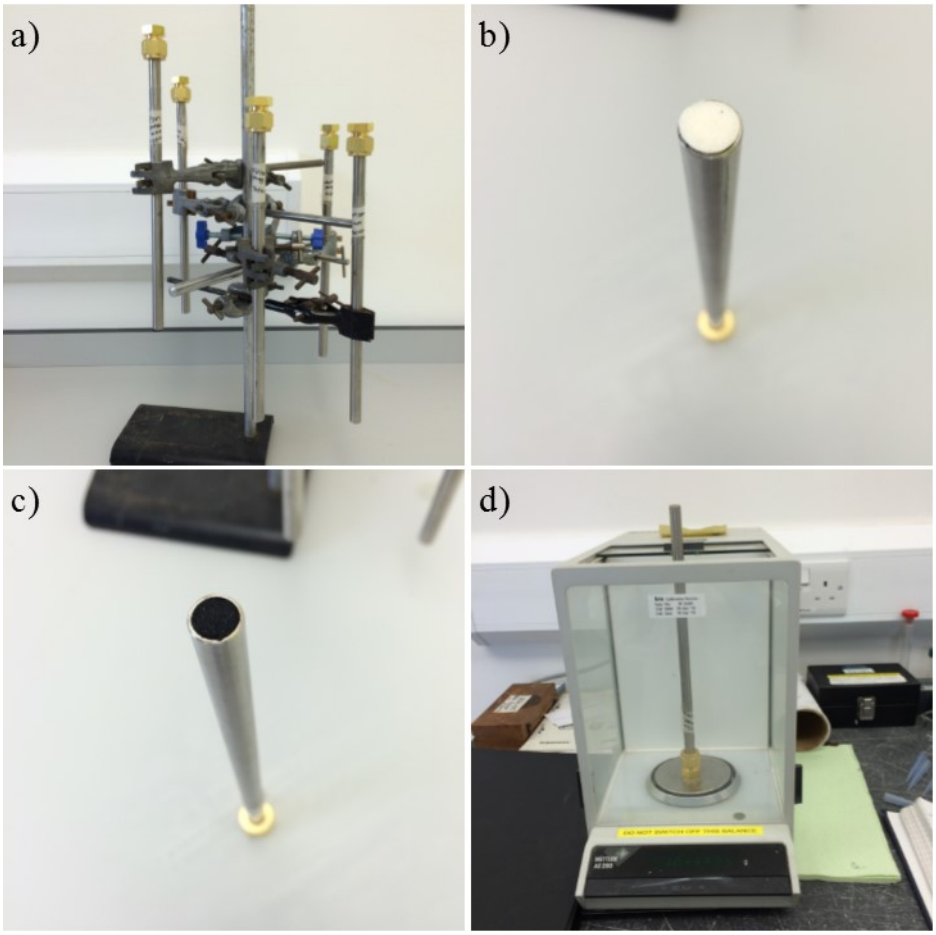

Figure 3.17 Scale-up of the VOCs sources used in the 2 litre chambers experiment.

As the scale-up of the 2-litre chambers sources did not show stable or sufficient mass loss, new sources needed to be developed. Initially, open flasks of different size were used to evaluate

the evaporation of the VOCs at laboratory ambient conditions. The emission rate of these sources relied on the vapour pressure of each VOC, boiling point, ambient temperature and humidity. Unlike the sources consisting of diffusive tubes, these new sources reach their maximum emission rate immediately after being prepared and placed inside the doping chamber (as shown in Figure 3.16). Weight measurements were taken on a daily-basis. In some cases, the identification of which source configuration showed the most stable mass loss was difficult. To help the selection of the most adequate source, the mass loss was plotted as a function of time, mean and the standard deviation of the mass loss for each VOC was calculated, Figure 3.18. The lowest standard deviation indicates the most stable mass loss and consequently the most stable emission rate. This produced a stable concentration of toluene, limonene and dodecane inside the chamber while performing the adsorption/desorption experiments.

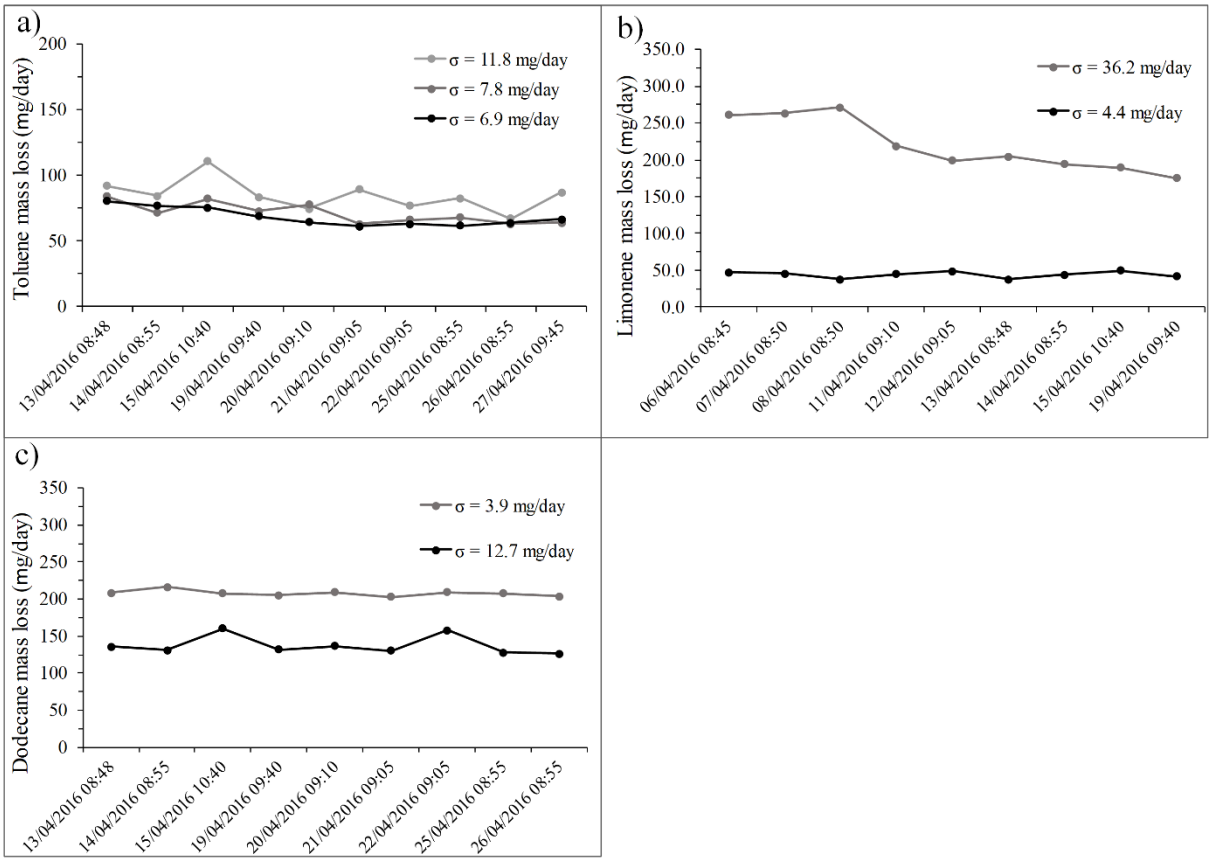

Figure 3.18 VOC mass loss as a function of time in the 30 m^3 chamber and standard deviation (σ) for each source. a) shows three examples of toluene sources, b) two examples of limonene sources and c) two examples of dodecane sources.

The photocatalytic experiment presented in Chapter 7 required VOC sources to be stable for up to two weeks. To achieve this stability, further studies were undertaken in order to understand how long the mass loss was stable without decreasing significantly. New sources were then prepared by using the same flasks as previously, although now, covered with aluminium foil and with one or more reed sticks inserted. A reed stick is used in commercial products as air-fresheners, where the stick is placed inside of a glass container with scent oil. The reed sticks feature long channels which allow the scent oil to diffuse and evaporate, creating the scent. The number of reed sticks and the length of the stick left outside of the flasks were the variable parameters studied. The sources with most stable mass loss for up to two weeks were as follows (Figure 3.19):

- Toluene: four 25 ml volumetric flasks closed with aluminium foil with two holes of 3 mm diameter;
- Limonene: four open vials with 20 ml of limonene;
- Dodecane: one 25 ml volumetric flask closed with aluminium foil with two reed sticks with 3 cm outside flasks.

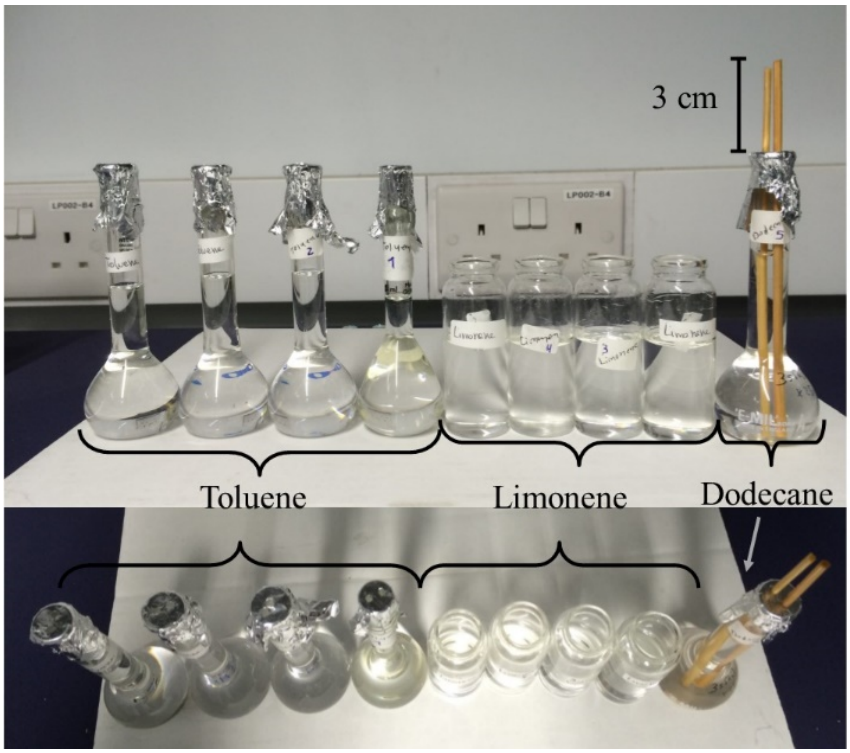

Figure 3.19 Sources of VOCs used for the photocatalytic experiments described in Chapter 7.

3.5.3. Emissions testing

Prior to all adsorption/desorption experiments, TVOC and formaldehyde emissions tests were carried out according to a procedure based on the standard BS EN ISO 16000-9:2006, in the 2-litre chambers and the 30 m^3 chamber. As required by the BS EN ISO standard, air sampling was undertaken after three and twenty-eight days of clean air passing through the chambers. In the case of the emissions tests carried out in the rig with the 2-litre environmental chambers, the exhausted air from the reference chamber was also sampled, so that it could be proved that no VOCs or formaldehyde were present in the clean air.

As an alternative to the 2-litre chambers, the Field Laboratory Emission Cell (FLEC) was also used for emissions testing following the standard BS EN ISO 16000-10:2006. However, due to the roughness of some materials, there was lack of a seal between the material surface and the FLEC and because of that the results were not considered to be accurate, Figure 3.20.

Figure 3.20 FLEC on top of the sample of H2 clay plaster covered with aluminium foil on that part of the sample surface not being tested.

Results from the emissions testing were expressed as an area specific emission rate. This was calculated by multiplying the concentration in the chamber by the area specific flow rate as shown in Equation 3.4. Area specific flow rate can be calculated by dividing the flow rate in the chamber by the exposed area of the material, Equation 3.5.

$$Area\ specific\ emission\ rate = C \times A_Q \left[{}^{\mu g}/_{m^2 h}\right] \quad \text{Eq. 3.4}$$

$$A_Q = \frac{Q}{A} \quad \text{Eq. 3.5}$$

Where C is the concentration in the chamber (µg/m^3), A_Q is the area specific flow rate, Q is the flow rate and A is the area of the specimen exposed to the air.

3.5.4. Adsorption/desorption behaviour

As stated before, the sink effect is the capacity of a certain material to adsorb VOCs from the indoor air and to re-emit them later. A way to study this effect is by challenging the materials by exposing them to polluted air, where the material will adsorb some of these pollutants, and then pass clean air so that whatever was adsorbed has the potential to be released in what is known as the desorption phase.

In Figure 3.21 the sink effect observed in the 2-litre chambers is illustrated. When the dopant air flows through the chamber with a concentration of VOCs equal to **I** $\mu g/m^3$, some of the VOCs carried by the air will be adsorbed onto the material surface (**A** $\mu g/m^3$) and the rest will flow to the outlet of the chamber (**S** $\mu g/m^3$). The concentration of VOCs in the outlet will be equal to the concentration inside the chamber (**C**). The sink effect is represented by the concentration **A**, which later will be desorbed by the materials if the process involved is physisorption.

As stated before, for comparison purposes, one of the chambers was included in all experiments without any material inside it (the reference chamber). This chamber represents the maximum concentration of VOCs and formaldehyde present in the dopant air. The amount of VOCs and/or formaldehyde adsorbed or desorbed by the natural building material under test is the difference between the reference chamber and the material chamber. The concentration in the outlet of the chamber is sampled in to the Tenax TA® tubes or 2,4-DNPH cartridges, as described in the next sub-chapter.

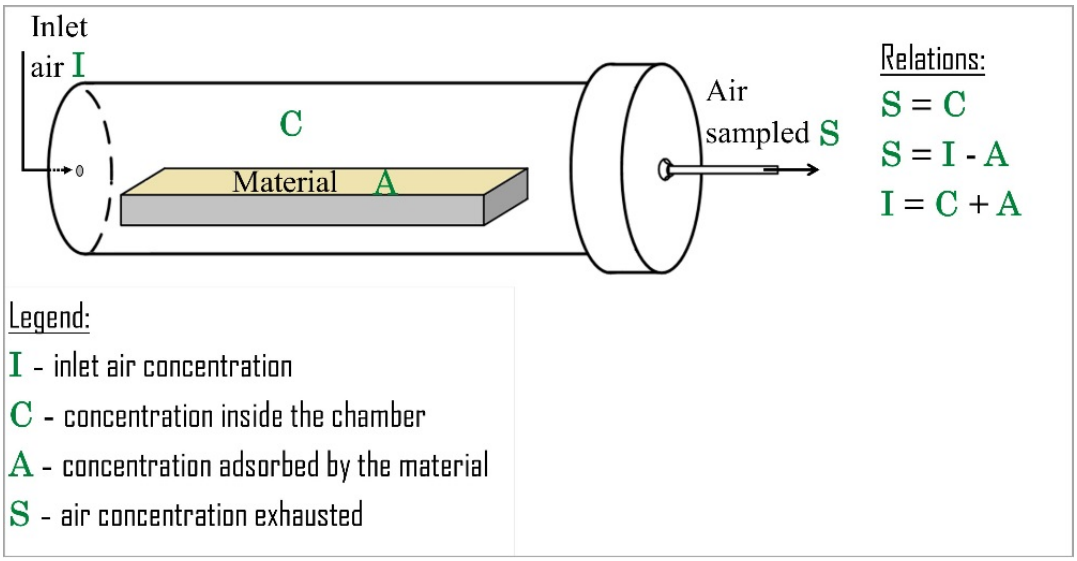

Figure 3.21 Schematic of the 2-litre environmental chamber for the VOCs and formaldehyde adsorption/desorption testing.

3.5.5. VOC and formaldehyde sampling and chemical analysis

All procedures for the analyses of VOCs and formaldehyde were carried out using procedures accredited by the United Kingdom Accreditation Service (UKAS) to BS EN ISO/IEC 17025:2005. The calculation of uncertainty of the sampling and analysis of VOCs and formaldehyde is described in the Appendix.

3.5.5.1. Volatile organic compounds

The VOC sampling and analysis procedures were carried out following the standard BS ISO 16000-6:2011. Volatile organic compounds exhausted from the chambers were sampled onto Tenax tubes assisted by a low-flow pump *Gilian LFS-113DC*, Figure 3.22. The sampling flow rate set in the sampling pump needed to be less than 80 % of the flow rate in the chamber to avoid under-pressures. Thus, the flow rate set for the sampling was approximately 150 ml/min. Tenax TA® is a porous polymer based on 2,6-diphenyleneoxide that has the capacity to sorb VOCs. The maximum capacity of a Tenax tube is 6 litres of sampling volume. After sampling, the Tenax tubes were stored and always transported inside an airtight and emission-free container, along with an activated carbon cartridge to avoid possible contamination. Also, a "travel blank tube" is required by standard BS ISO 16000-6:2011 to be stored/carried together with the sampling tubes. The VOC analysis was undertaken by gas chromatography using a flame ionisation detector (FID) coupled with a mass spectrometer (GC/MS-FID), Figure 3.22.

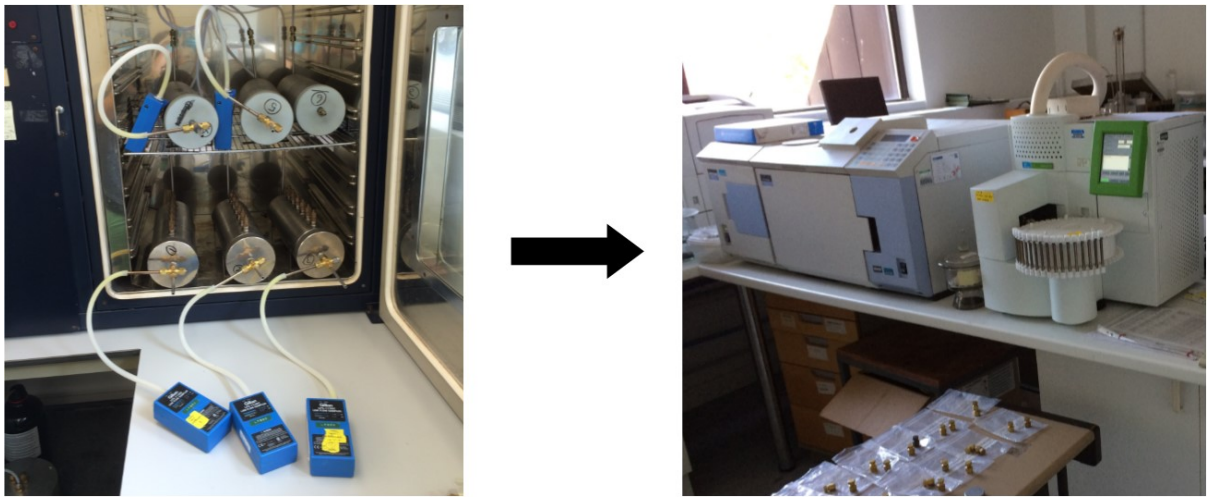

Figure 3.22 Sampling of VOCs and analysis by GC-MS/FID.

The gas chromatography technique, used in analytical chemistry, is based on a separation of the components of a mixture without decomposition. The mobile phase is the carrier gas and the sample and the stationary phase is the inlayer of the GC column with which the sample will interact. Inert gases such as helium or unreactive gases such as nitrogen are commonly selected as the carrier gas. Separation of the components in a sample is determined by the distribution of each component between the mobile phase and the stationary phase. It depends on the molecular weight of the components. Thus, a light molecule will spend a short time in the stationary phase and will elute quickly. This time is called the retention time. The separated components will then be split, passing both to the detector of the GC and to the MS. The FID detector, featuring a flame fuelled with hydrogen, is commonly used to determine organic/hydrocarbon compounds due to the ability of the carbons to form ions upon pyrolysis which generates a current between the electrodes. To detect the created ions, two electrodes are used to provide a potential difference (mVolts) which is the response that will create a peak for each detected compound - in a chromatogram, an example of which is shown in Figure 3.23. The chromatogram is plotted in retention time in hours (horizontal axis) and the response from the FID in mVolts (vertical axis).

Prior to the GC/MS analysis, the Tenax tubes were thermally desorbed using a *PerkinElmer TurboMatrix 350*. The GC, a *PerkinElmer Autosystem XL*, is equipped with an FID detector and coupled with a *PerkinElmer TurboMass* mass spectrometer. The column type installed in the GC is supplied by *Restek*, model *Rtx®-1701*, 60 meters in length.

To calculate the concentration of VOCs in the air the amount of VOC adsorbed in the Tenax tube (µg) is divided by the volume of air sampled on the tube (m^3), equation 3.6.

$$VOC\ concentration = \frac{amount\ of\ VOC\ on\ tube}{volume\ of\ air\ sampled}\left[{}^{\mu g}/_{m^3}\right] \qquad \text{Eq. 3.6}$$

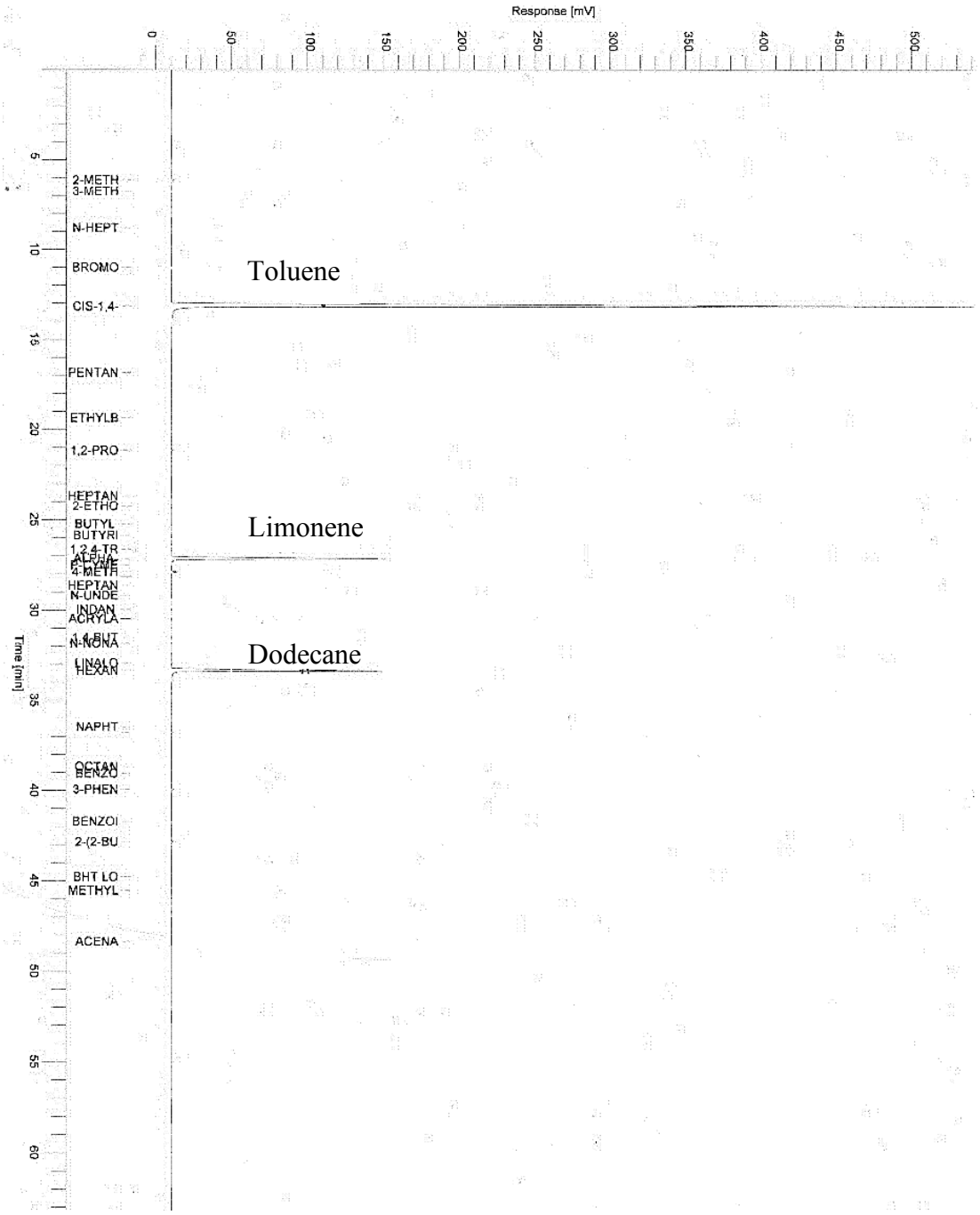

Figure 3.23 GC chromatogram showing peaks of toluene, limonene and dodecane.

To ensure high quality of the GC/MS analyses, prior to the analysis of VOCs, a quality control sample (QC) is run and analysed. The QC sample is spiked on to a Tenax tube from a liquid solution composed of a known concentration of n-hexane, toluene, limonene and hexadecane. If the concentrations in the QC chromatogram match the known concentrations of the prepared solution within the requisite limits the QC test is considered to be successful and the other samples in the batch can be analysed. If not, another QC is spiked and analysed, unless the problem is found to be related to the analytical equipment. After being desorbed and analysed, the Tenax tubes are conditioned for a subsequent reuse in a tube conditioner, *Markes TC-20*, at 300 °C for 45 minutes using nitrogen at 20 psi, Figure 3.24.

Figure 3.24 Tube conditioner.

The overall uncertainty of the VOCs sampling and analysis was 6.7 % with a level of confidence greater than 99 % (expanded uncertainty with coverage factor of 3). Further details about the uncertainty may be found in the Appendix.

3.5.5.2. Formaldehyde

Sampling and analysis of formaldehyde were undertaken following the standard BS ISO 16000-3:2011. Formaldehyde samples were collected on a 2,4-dinitrophenylhydrazine (2,4-DNPH) cartridge, supplied by *Waters*, by using the same low-flow sampling pumps as for the sampling of VOCs, Figure 3.25 1). Upon completion of the sampling the used cartridges were stored in a freezer until being desorbed and analysed. The desorption of formaldehyde from

the 2,4-DNPH cartridge was carried out in a fume cupboard by plugging the cartridge into a syringe and using 3 ml of acetonitrile as an extraction solvent, Figure 3.25 2). This solvent has a low boiling point, resulting in a fast evaporation at room temperature, and leading to high complexity for this process. To fully extract the sampler, the 3 ml of acetonitrile is passed through the cartridge at a rate of approximately one drop per second. This interval is enough to extract the formaldehyde from the cartridge without having significant evaporation of acetonitrile. Once the extraction is finished, the vial containing the formaldehyde solution is closed with a cap featuring a septum (Figure 3.25 3)) and analysed by HPLC (High Performance Liquid Chromatography), Figure 3.25 4).

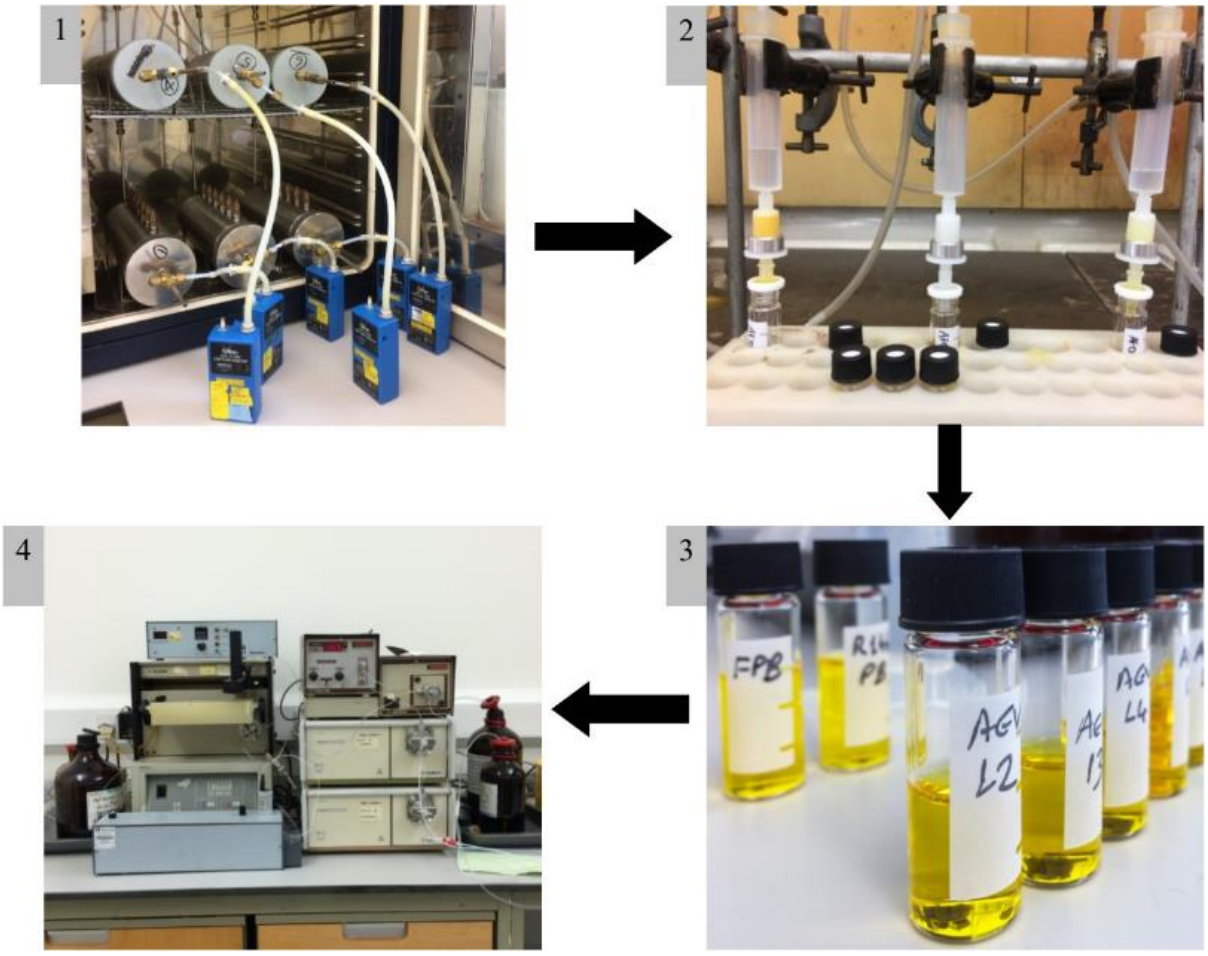

Figure 3.25 Schematic of the formaldehyde sampling and analysis. Legend: **1)** formaldehyde sampling into 2,4-DNPH cartridges, **2)** solvent extraction from the 2,4-DNPH cartridges, **3)** formaldehyde solution in acetonitrile after extraction, **4)** HPLC equipment used to quantify formaldehyde content.

High-performance liquid chromatography is a technique for analysis which allows the determination of the concentrations of a wide range of low molecular weight carbonyl compounds. It relies on pumps to pass a pressurised liquid solvent containing the sample mixture (mobile phase) through a column filled with a solid adsorbent material (stationary phase) as in the GC technique explained previously. The components of the sample (analytes) will be separated from each other due to their different interactions with the stationary phase. The mobile phase is typically a mixture of solvents such as water, acetonitrile and/or methanol. Each separated analyte is then detected using a lamp, usually UV or visible, creating a chromatogram where the analyte bands are seen as "peaks" forming the chromatogram as in the GC. The time at which a specific analyte elutes from the column is called the retention time.

A *Gilson inc.* HPLC with a UV lamp detector was used for the formaldehyde analyses. The mobile phase was pumped at 1 ml/min and was composed of 65 % of methanol and 35 % water. In the same way as the GC/MS analysis for VOCs, quality control solutions must be analysed to ensure the accuracy of the analysis. Before starting the analysis of formaldehyde, the QC samples were run and checked. The least concentrated QC had 0.04 μg/ml of formaldehyde and the most concentrated had 0.8 μg/ml. For each round of analysis, at least two QC with different concentration of formaldehyde were run. If more than 20 samples were to be analysed a QC solution was also run after the first 10 samples.

The overall uncertainty of the formaldehyde sampling and analysis was 6.3 % with a level of confidence greater than 99 % (expanded uncertainty with coverage factor of 3). Further details about the uncertainty may be found in the Appendix.

3.6. Moisture buffering

The adsorption and desorption of moisture by the materials due to humidity variation was conducted using ISO 24353:2008. The humidity was varied every 12 hours; with a step change between 75 % and 50 % relative humidity; representing the mid-level humidity cyclic test of the standard. All specimens were pre-conditioned at a relative humidity of 63 % and a temperature of 23 °C before cyclic climatic variations were started. Four cycles of 24 hours at the high and low relative humidity conditions at 23 °C were run whilst the mass of the specimen was logged.

To ensure vapour exchange only occurred through a single face of the materials, the specimens were sealed on the sides and back with aluminium tape as shown in Figure 3.26. Specimens were cut to a size of 100 mm × 100 mm, with this area exposed to the changing relative humidity environment. The specimens were placed on mass balances, logged every 5 minutes, inside an environmental chamber programmed to subject the specimens to the humidity cycles. To keep the air speed of 0.1 m/s over the specimens, a screen was placed around the mass balance to minimize the influence of air movement over the surface of the specimens during the testing. Fourth cycle moisture adsorption and desorption content values and rates were calculated in accordance with section 83 of ISO 24353:2009. Three samples of each specimen were tested.

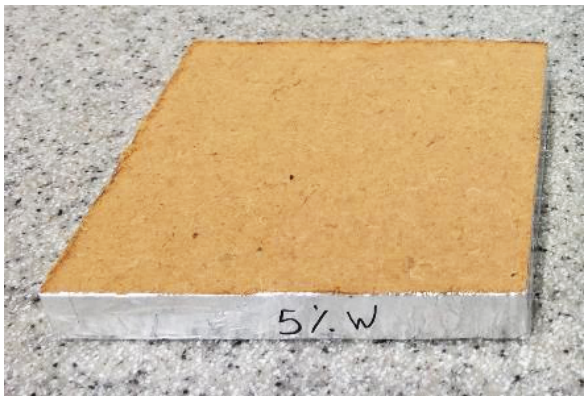

Figure 3.26 Photograph of a specimen sealed in 5 surfaces with aluminium tape.

3.7. Summary

- ✓ The methodology for the adsorption and desorption experiments of toluene, limonene, dodecane and formaldehyde will allow investigation of the sink effect of the natural building materials. This represents the behaviour of a material in an indoor environment when exposed to polluted air;
- ✓ The chemical and physical characterisation of the natural building materials will support the study of the interactions between four air pollutants and the materials surface;
- ✓ The materials characterisation is especially focussed on the surface characteristics that may have an effect on the adsorption and desorption behaviour of VOCs.

The next chapter presents the chemical and physical characterisation of the eco-materials as well as their VOCs emissions and adsorption/desorption behaviour. The sink effect is correlated with the chemical and physical characteristics of the natural building materials.

Chapter 4

TVOC and formaldehyde emissions from eco-materials and their adsorption/desorption behaviour

4.1. Introduction

The present chapter investigates the emissions of TVOC and formaldehyde from the state of the art materials, referred to as eco-materials in this thesis and their adsorption-desorption behaviour. The chemical composition of the materials and their physical properties such as microstructure and surface area have been explored and related to the emissions and adsorption/desorption behaviour.

4.2. Materials and methods

4.2.1. Materials description

In the first stage of this PhD, all 18 *eco-materials*, described in Section *3.2 Materials*, were analysed as state of the art materials, listed now in Table 4.1.

Table 4.1 List of the six insulation, six coatings and six wood-based panels reported in this chapter.

Insulation	Coatings	Wood-based panels
➢ Natural wool	➢ Gypsum	➢ MDF
➢ Wood fibres	➢ Mortar_P	➢ Coated MDF
➢ Hemp-lime275	➢ Mortar_RS	➢ Chipboard
➢ Hemp-lime330	➢ Mortar_RH	➢ Coated chipboard
➢ Hemp fibres	➢ Clay_A	➢ HDF
➢ Wood fibreboard	➢ Clay_B	➢ Clay board

4.2.2. Materials characterisation and IAQ assessment

Three different techniques were used to analyse the chemical composition of the *eco-materials* and crosscheck the results: X-ray diffraction, Raman and FTIR spectroscopies. The chemical composition of the material will support the discussion of the VOCs and formaldehyde emissions and adsorption and desorption behaviour.

The microstructure, surface area and porosity were the properties analysed in the physical characterisation by SEM.

The emissions testing of TVOC and formaldehyde was carried out on all of the 18 *eco-materials*. The adsorption and desorption behaviour in the 2-litre environmental chambers was studied on four materials: MDF, coated MDF, Mortar_P and Natural wool, Figure 4.1 a). Therefore, at least one material of each type was chosen: two wood panels, one coating and one insulation material. By studying the adsorption and desorption behaviour of the MDF and coated MDF, the effect of the paper coating on MDF could be observed. In addition, these four building materials have distinct origins and thus different chemical composition. The MDF panels were selected as a representative of the cellulosic-based materials, Mortar_P of the inorganic materials and Natural wool of the animal-based materials, allowing observation not only of the effect of the different physical properties on the adsorption and desorption behaviour but also the effect of the chemical composition. The adsorption and desorption of toluene, limonene and dodecane from the MDF was also investigated in the 30 m^3 environmental chamber at 6 ach^{-1}, in which the MDF panels were installed on one wall of the chamber, equivalent to 10 m^2 of exposed surface area.

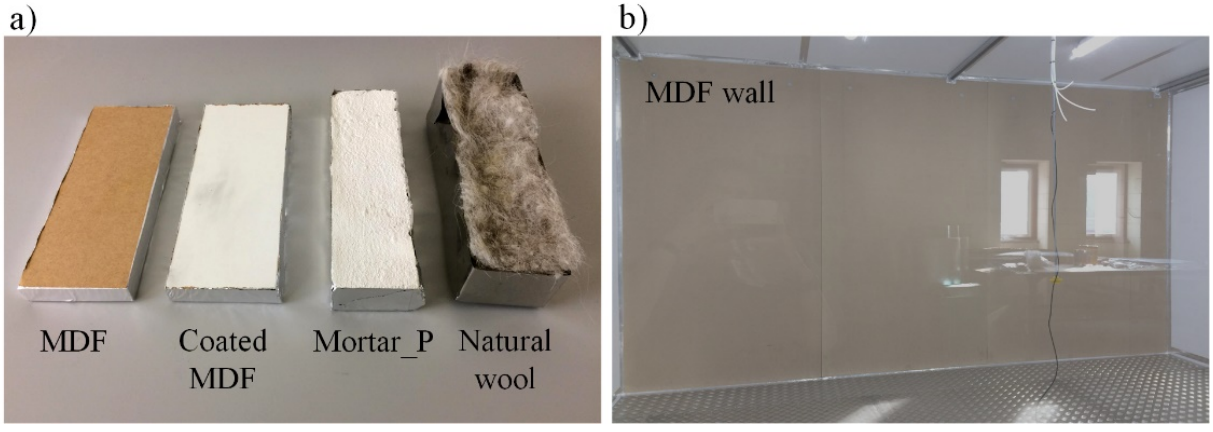

Figure 4.1 Materials selected for the adsorption and desorption studies, a) specimens tested in the 2-litre chambers (200 mm x 60 mm x 15-38 mm) and b) wall panels installed in the 30 m^3 chamber.

4.3. Results and discussion

4.3.1. Materials characterisation

4.3.1.1. Chemical characterisation

The data from chemical characterisation is divided by the type of material: insulation materials, coatings and wood panels. In this section, each diffractogram or spectrum is discussed individually in order to provide a deep understanding of the chemical composition of each material.

The X-ray diffraction patterns of the six insulation materials are presented in Figure 4.2. The results are divided according to the nature of each material as: animal (Natural wool), cellulosic (Wood fibres, Hemp fibres and Wood fibreboard) and composite (Hemp limes). Also, the X-ray diffractogram of the adhesive used in the sample holder is shown.

The Natural wool showed the presence of keratin through the broad peak around 2θ = 8° (Belarmino et al. 2012), this being the main component of the animal wool. The main crystalline phase detected on XRD patterns of Wood fibres, Hemp fibres and Wood fibreboard is cellulose (Dai and Fan 2010; Razak et al. 2014).

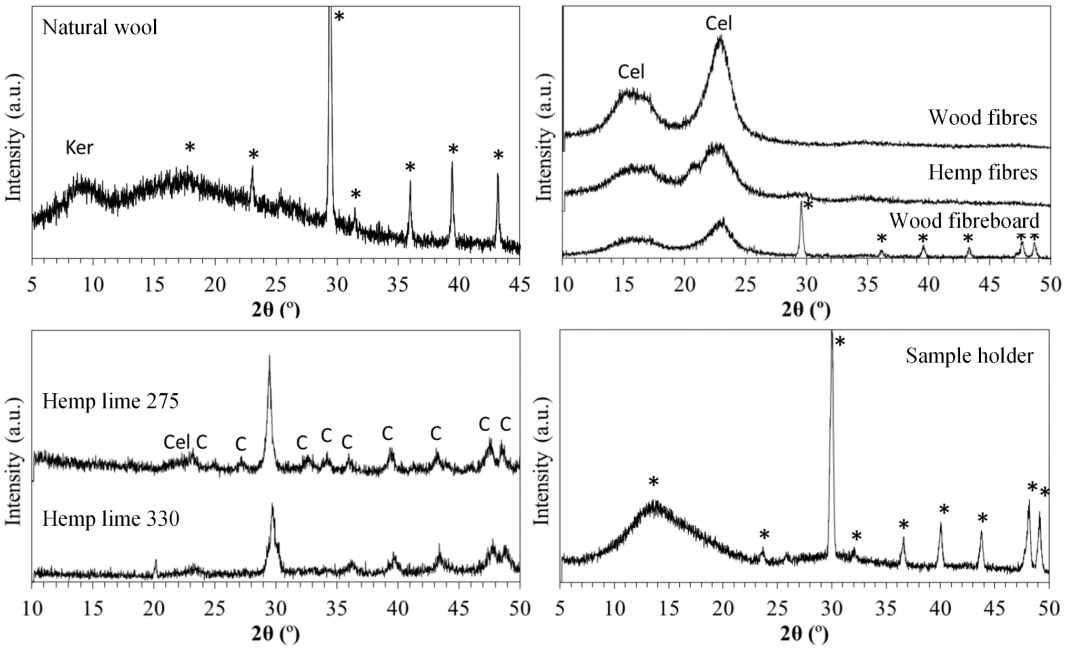

Figure 4.2 X-ray diffractograms of natural wool, wood-based insulation, hemp limes and adhesive used in the sample holder. Legend: **Ker** = keratin, **Cel** = cellulose $(C_6H_{10}O_5)_n$ and **C** = Calcite ($CaCO_3$).

Cellulose, Figure 4.3, is the most common organic polymer in nature but its crystallinity is quite variable depending on the order of the polymer chains. Usually, the X-ray diffraction main peaks from cellulose are broad and appear at 2θ values of 16 and 23° (Dai and Fan 2010; Razak et al. 2014).

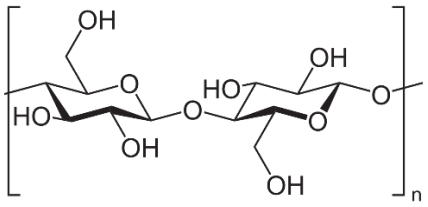

Figure 4.3 Monomer of cellulose.

The Hemp lime insulation materials showed the presence of an inorganic material, calcium carbonate (commonly known as calcite), prevenient from the carbonation of the lime and also cellulose peaks from the hemp shives.

The analyses of these types of insulation materials demand the use of an adhesive in order to fix the specimens onto the sample holder as described in *3.3.1 X-ray diffraction*. In some XRD patterns extra peaks were detected that do not correspond with the insulation material. In order to determine if this peaks were from the adhesive or not, an XRD of the adhesive was carried out. With this pattern the extra peaks present in the XRD of both Hemp limes, Wood fibreboard and Natural wool are shown to be from the adhesive, identified with an asterisk * in Figure 4.2. The peaks of calcite and cellulose on both Hemp limes were barely visible due to the intensity of the adhesive peaks.

The Raman spectra of the Hemp lime, Hemp fibres, Wood fibreboard and Wood fibres are presented in Figure 4.4. The Raman spectrum of Natural wool was inconclusive due to the absence of relevant peaks in the spectrum, so it is not presented here. This can be attributed to the difficulty in handling this kind of loose fibrous material for Raman spectroscopy or the absence of characteristic peaks (Wojciechowska et al. 1999). Peaks from cellulose were detected in all analysed insulation materials around 350 and 1610 cm^{-1} (Agarwal 2006). In addition to cellulose, the presence of calcite in the Hemp lime specimen was also successfully detected at 280, 711, 1087, 1748 cm^{-1}. One extra peak was detected for Wood fibreboard around 1420 cm^{-1}.

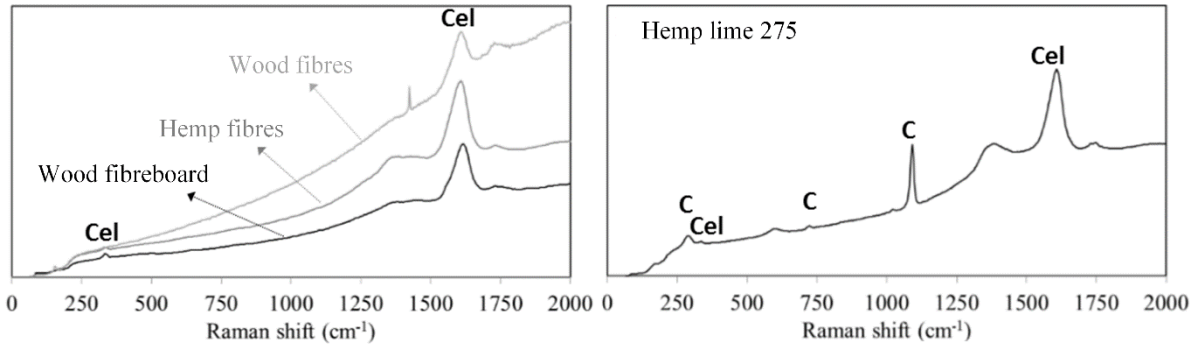

Figure 4.4 Raman spectra of wood based insulation materials and hemp lime 275. Legend: **Cel** = cellulose $(C_6H_{10}O_5)_n$ and **C** = Calcite ($CaCO_3$).

The FTIR spectra of the six insulation materials are presented in Figure 4.5. The peaks identified in the spectra correspond to different inter-atomic bonds. Through the identification of these peaks, the chemical composition of the materials can be characterised. Natural wool is composed essentially of a complex fibrous protein, keratin, with amino acid molecules along its chain (Belarmino et al. 2012; Wojciechowska et al. 1999). Bands at 3060 and 1513 cm^{-1} are related to the amide group (COHN and NH respectively) with bands at 2940 and 1441 cm^{-1} representing the presence of CH_2 bonds and one at 2880 cm^{-1} due to CH. The presence of the C=O bond is confirmed by the band at 1710 cm^{-1}.

Comprehensive analyses of FTIR spectra from wood-based materials can be very complex due to the high number of absorption peaks. Wood fibres are composed mostly of cellulose, hemicellulose, pectins and lignin (Dai and Fan 2010; Garside and Wyeth 2003). Hemp fibre, Wood fibre and Wood fibreboard showed the expected bands indicating the presence of cellulose, hemicellulose and lignin (Dai and Fan 2010). The two mixes of Hemp lime also showed bands from cellulose, hemicellulose and lignin, although they are not as notable as in the wood-based samples. This could be related to the presence of calcite within the lime composite as detected by peaks at 1394, 872 and 712 cm^{-1} (Downs 2006).

Water molecules adsorbed on the fibres are indicated by bands at 3280 and 1634 cm^{-1}. The insulation materials that showed through FTIR a higher amount of adsorbed water molecules were Natural wool and Hemp fibre, indicating the enhanced potential of both materials to adsorb and store water compared with the other materials.

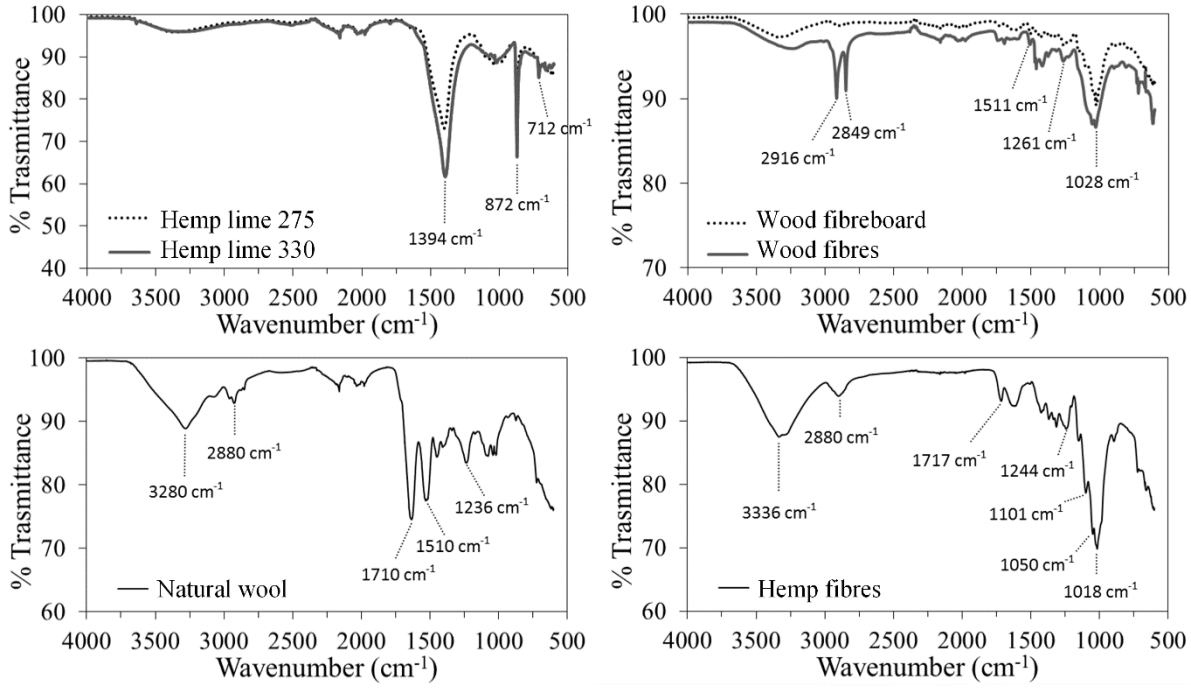

Figure 4.5 FTIR spectra of all insulation materials.

X-ray diffraction was used to identify the crystalline phases present in each coating, Figure 4.6. The X-ray diffraction patterns of the three lime based coatings showed the presence of portlandite and calcite. Very sharp peaks of quartz can be observed in spectra of Mortar_P, Mortar_RS and both clays. Clay_A showed the presence of calcite in its composition. The presence of high intensity peaks from the quartz were difficult to distinguish from the other crystalline phases. The XRD pattern of gypsum did not show any additional crystalline phases apart from that of calcium sulphate.

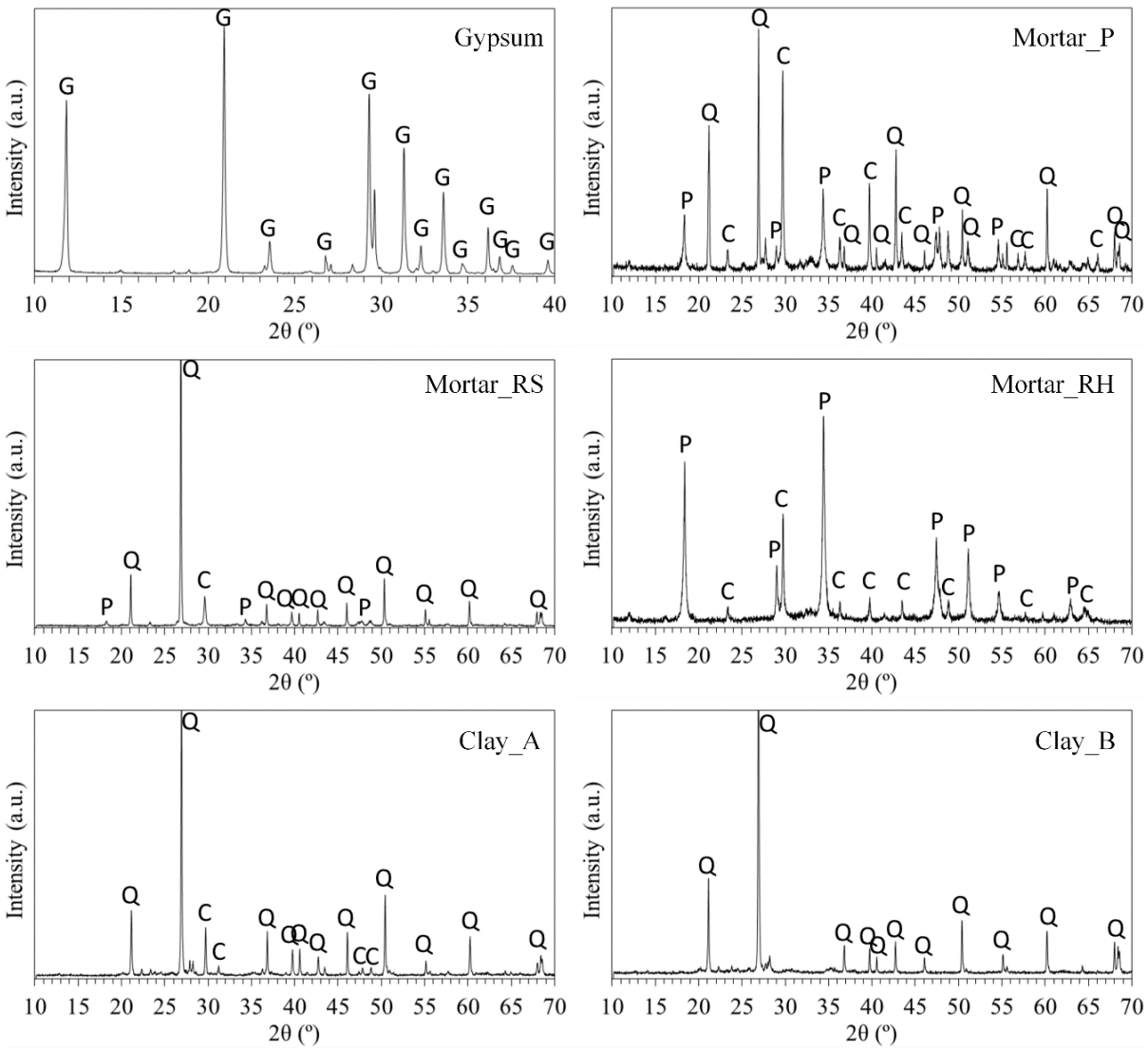

Figure 4.6 X-ray diffractograms of the six coating materials. Legend: **G** = gypsum ($CaSO_4 \cdot 2H_2O$), **C** = calcite ($CaCO_3$), **P** = portlandite ($Ca(OH)_2$), **Q** = quartz (SiO_2) and **Cel** = cellulose $(C_6H_{10}O_5)_n$.

Raman spectra recorded from the surface of fractured specimens of the Gypsum, Mortar_P, Mortar_RS, Mortar_RH, Clay_A and Clay_B are presented in Figure 4.7. The Gypsum was identified through bands assigned to vibrations of [SO_4^{2-}] at wavenumbers of 425, 496, 635, 677, 1024 and 1087 cm^{-1} (Dickinson and Dillon 1929; Deng et al. 2002). The Raman spectra of Mortar_RS and Mortar_P show the presence of calcite ($CaCO_3$), identified through the peaks at 280, 711, 1087, 1435 and 1748 cm^{-1} (Ball et al. 2011). The weak peak at 359 cm^{-1} observed in spectra of both limes is assigned to [OH^-] vibration of portlandite - $Ca(OH)_2$ (Deng et al. 2002). Mortar_RS showed a broad peak around 1640 cm^{-1} which could be attributed to amorphous carbon present in the sand grains (Edwards et al. 2007). A spectrum was recorded

from a sand grain of Mortar_P and shows the vibrations bands of quartz SiO_2 (Rodgers and Hampton 2003; El-Turki et al. 2010).

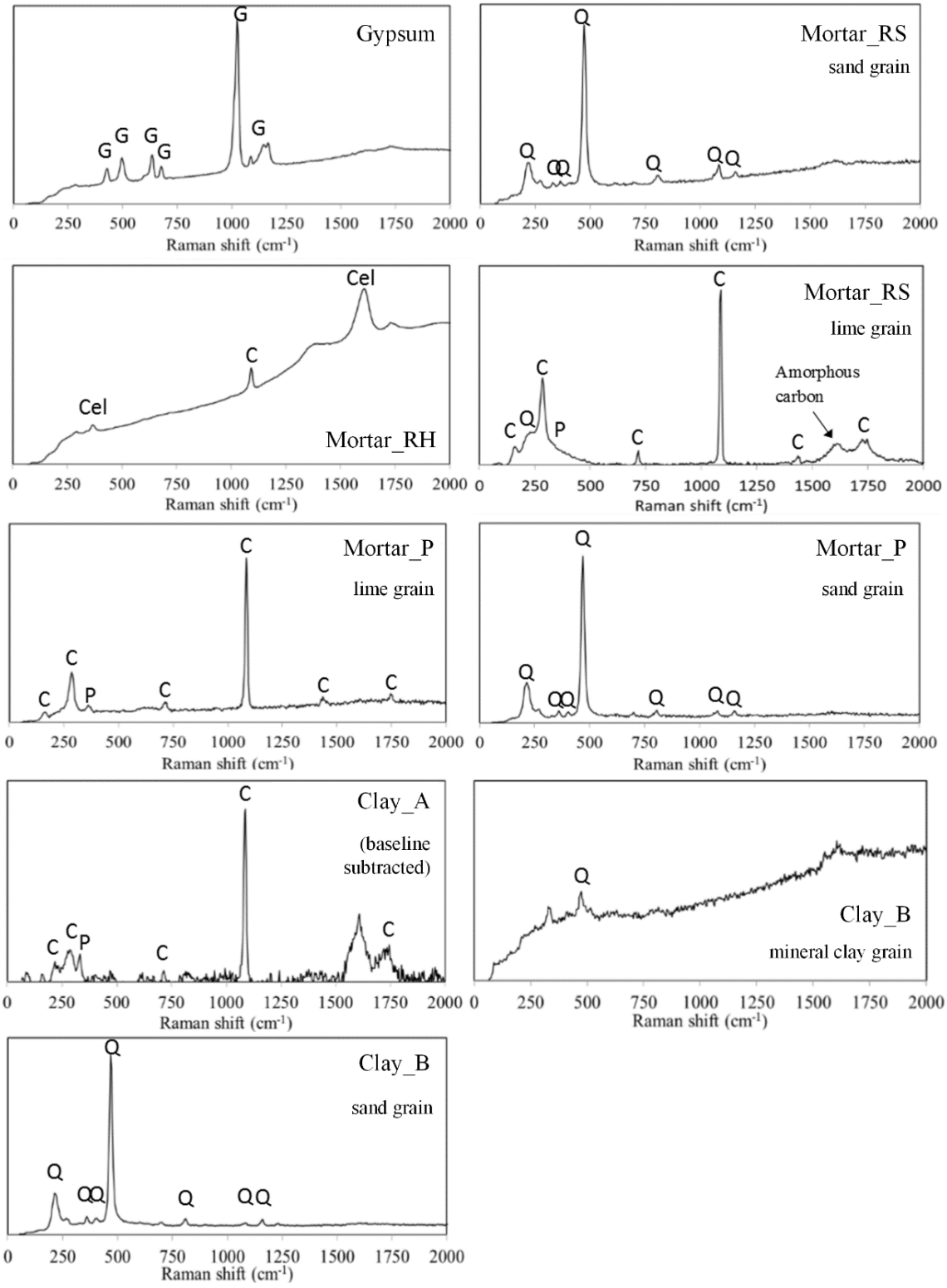

Figure 4.7 Raman spectra of the six coating materials. Legend: **G** = gypsum ($CaSO_4{\cdot}2H_2O$), **C** = calcite ($CaCO_3$), **P** = portlandite ($Ca(OH)_2$), **Q** = quartz (SiO_2) and **Cel** = cellulose $(C_6H_{10}O_5)_n$.

The FTIR spectra of Gypsum, Mortar_P, Mortar_RS, Mortar_RH and Clay_A and Clay_B are presented in Figure 4.8. The IR spectrum of gypsum includes peaks assigned to [SO_4^{2-}] at wavenumbers of 671, 716 and 1118 cm^{-1}. The peaks 1623, 1689, 3388 and 3500 cm^{-1} are assigned to the group -OH from the water molecule (Anbalagan et al. 2009). The presence of calcite is identified through the peaks at wavenumbers 713, 873 1422 and 1815 cm^{-1} and they were detected in Mortar_P, Mortar_RS, Mortar_RH and Clay_A. Quartz is identified by peaks at 691, 773, 795, 1081 and 1150 cm^{-1} and they are present for all of the coating materials except the Gypsum, as expected. On Mortar_RH, besides the presence of calcite, the peaks of cellulose from hemp were also detected at 896, 995, 1019, 1048, 1155, 1202, 2887, 3336 cm^{-1} (Dai and Fan 2010). In addition, peaks from the background of the FTIR equipment (between 2340 and 2373 cm^{-1}) were detected on Mortar_RS, Mortar_RH and both clays, circled zones in Figure 4.8.

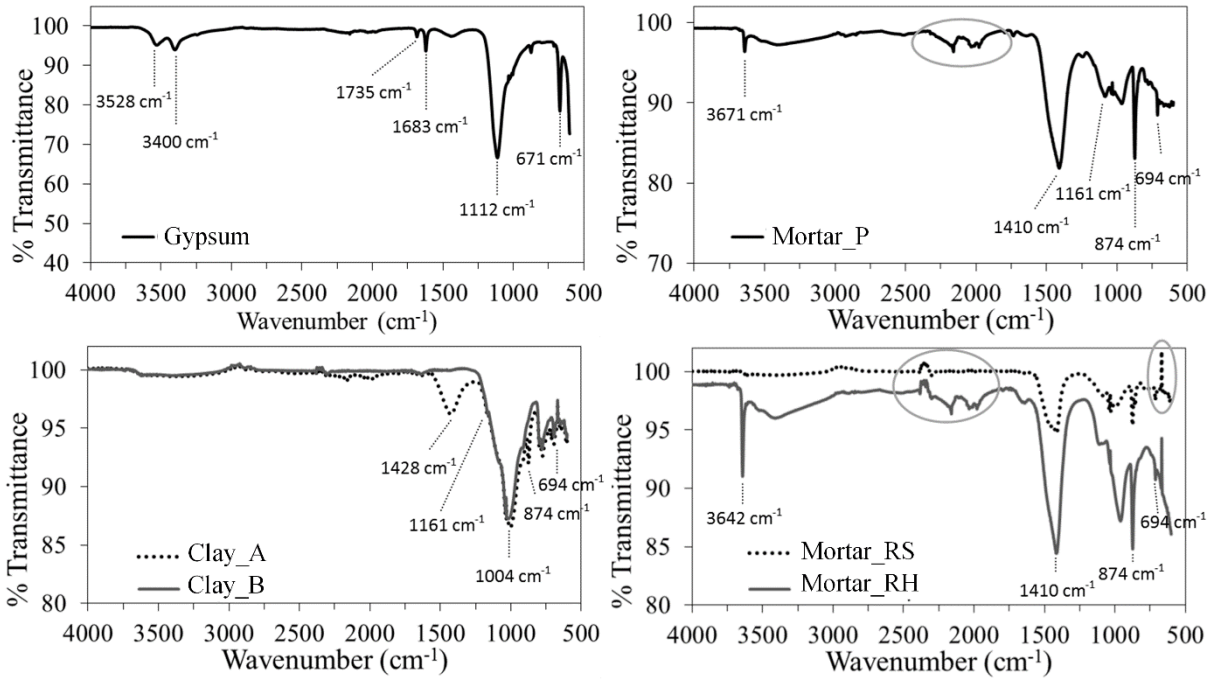

Figure 4.8 FTIR spectra of the six coating materials.

The elemental analyses obtained from EDX are presented in Table 4.2. Mortar_P, Mortar_RS and both clays showed the presence of silicon (Si) in their composition, belonging to quartz (SiO_2) from the sand. The amount of iron present in the Clay_A and Clay_B is different. Clay_B has a higher concentration of iron than Clay_A, which is in agreement with the natural

appearance of the material as shown previously in Figure 3.1. A higher amount of iron leads to a darker appearance of the clay. Besides the presence of the iron-based compounds and quartz in clays, the presence of other elements can be observed such as magnesium (Mg), potassium (K), chlorine (Cl) and phosphorous (P) which are associated with typical clay minerals (Montana et al. 2014). Due to the high crystallinity of the quartz, the XRD peaks of these minerals were at the noise level and thus could not be identified in Figure 4.6. As expected, the EDX analysis of the gypsum showed the presence of calcium and sulphur, which are elements from calcium sulphate - $CaSO_4$. Traces of silicon and aluminium were also detected in the gypsum analysis.

Table 4.2 Chemical elements present in coating materials and respective atomic weight (%) obtained by EDX.

Element	Atomic weight (%)					
	Gypsum	**Mortar_P**	**Mortar_RS**	**Mortar_RH**	**Clay_A**	**Clay_B**
Al	0.2	1.0	0.8	0.3	4.3	3.6
Si	0.4	5.0	4.4	1.1	11.9	11.5
Ca	13.8	17.9	22.3	25.4	2.8	0.6
S	13.9	0.5	0.2	-	-	-
K	-	0.2	-	-	0.6	0.5
Ti	-	1.7	-	-	-	-
Fe	-	-	0.3	-	2.5	21.9
Mg	-	-	-	-	1.4	0.5
P	-	-	-	-	-	0.8
Cl	-	-	-	-	-	0.4

In Figure 4.9 the XRD patterns of the wood based panels are presented. These include MDF (medium density fibreboard), HDF (high density fibreboard), chipboard and clayboard. MDF and HDF are manufactured from the same raw material, the only difference is the processing procedure employed to obtain different densities (panel thickness). As observed in Figure 4.9, the XRD patterns of MDF and HDF are very similar. Chipboard showed the 3 peaks from cellulose, however it is more amorphous compared to the MDF and HDF material. Clayboard showed a more complex XRD pattern due to its composition. It is known from the supplier that the Clayboard is composed of clay minerals, sand, reed, hemp, wood chip and jute fabric. The presence of high intensity peaks from the quartz makes identification of the other crystalline phases more difficult, in the same way as seen for the coatings Clay_A and Clay_B.

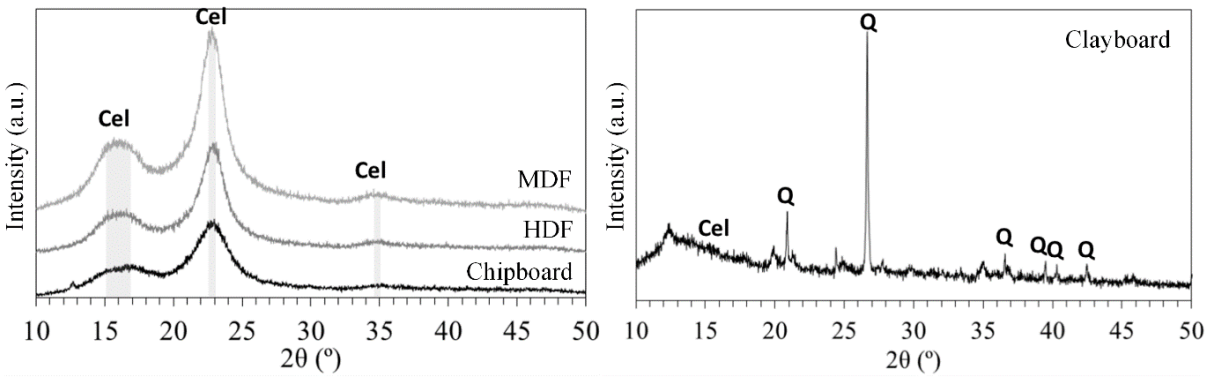

Figure 4.9 X-ray diffractograms of wood panels. Legend: **Cel** = cellulose $(C_6H_{10}O_5)_n$ and **Q** = quartz (SiO_2).

The Raman spectra were difficult to record from the wood based panels. Peaks from cellulose at wavenumber 1610 cm^{-1} were detected from the HDF panel, Figure 4.10.

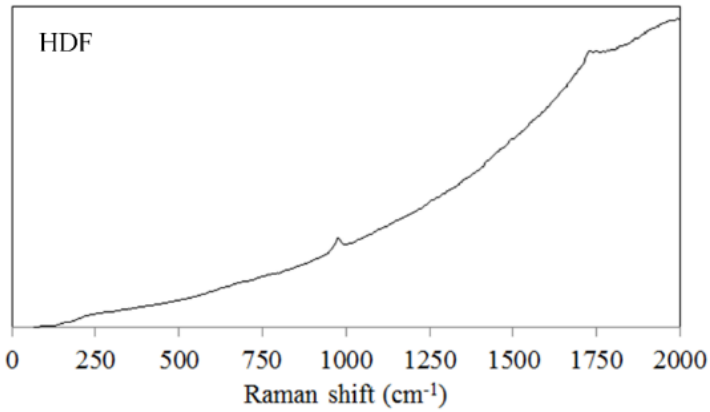

Figure 4.10 Raman spectra of HDF panel.

FTIR spectra of the wood-based panels are presented in Figure 4.11. All panels showed the presence of cellulose in their composition through the peaks at 896, 995, 1019, 1048, 1155, 1202, 1317, 1362, 1368, 1420, 2887 and 3336 cm^{-1}. On Clayboard, peaks from quartz were also detected.

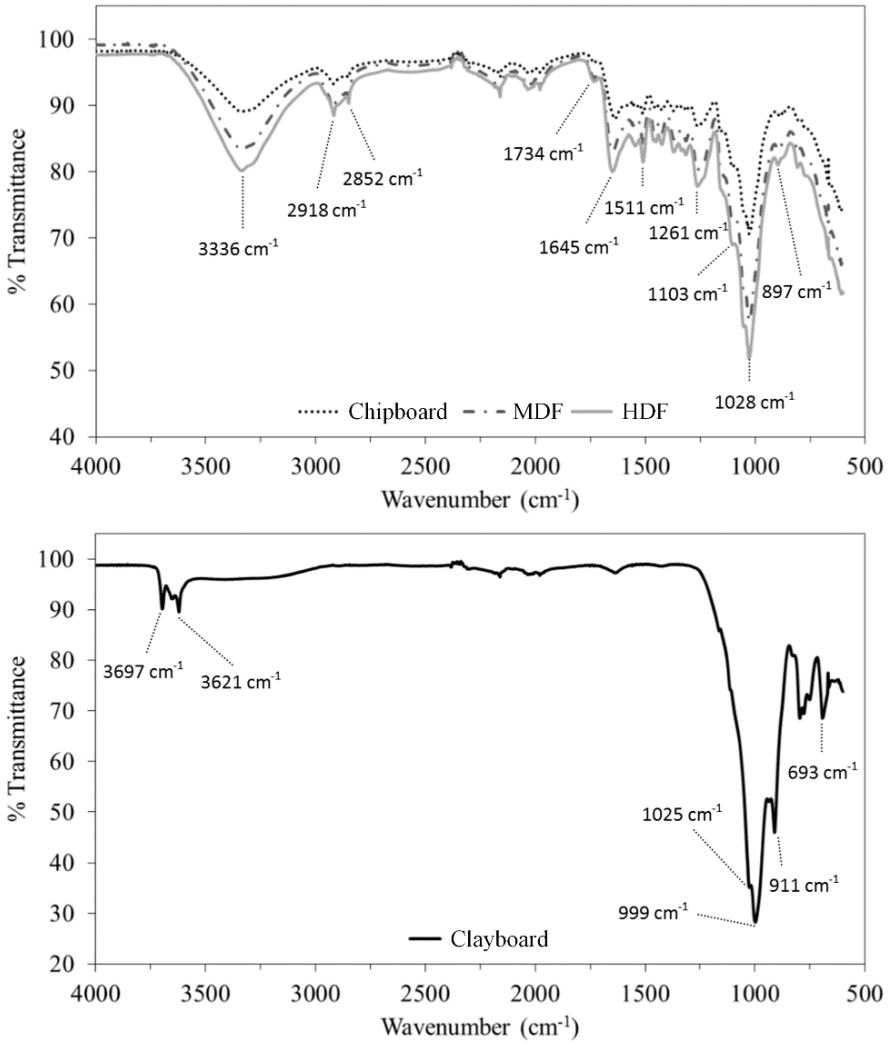

Figure 4.11 FTIR spectra of wood panels.

Figure 4.12 shows the molecular structures of the chemical compounds present in the *eco-materials*. The 3D drawings of the portlandite, calcite and quartz shown in Figure 4.12 were adapted from Barak and Nater (2005). All other molecular structures and 3D drawings were made by using the software *ChemDraw Professional* and *Chem3D* version *16.0*.

Keratin was the main component detected by the analytical techniques used for chemical characterisation of the Natural wool. This protein represents approximately 82 % of the composition of the wool and has a high content of cysteine (Belarmino et al. 2012; Wang et al. 2016). Cysteine is an amino acid composed of a central linear chain of carbon atoms with thiol (-SH), carboxyl (-COOH) and amine ($-NH_2$) groups attached, Figure 4.12.

Cellulose is a polysaccharide ordered as a semi-crystalline polymer due to the partial order of its linear chains, which allows detection in the X-ray diffraction analysis. Due to the presence

of the -OH group in the cellulose monomer, which is composed of two molecules of glucose, this compound has the ability to have inter- and intramolecular hydrogen bonds.

Calcite present in the lime mortars and both hemp limes is a product of the carbonation of the calcium hydroxide (portlandite), (Van Balen and Van Gemert 1994; Van Balen 2005). Quartz crystals found in sand are composed of silicon and oxygen atoms in a framework composed of SiO_4 tetrahedra although, the chemical formula of the quartz is SiO_2.

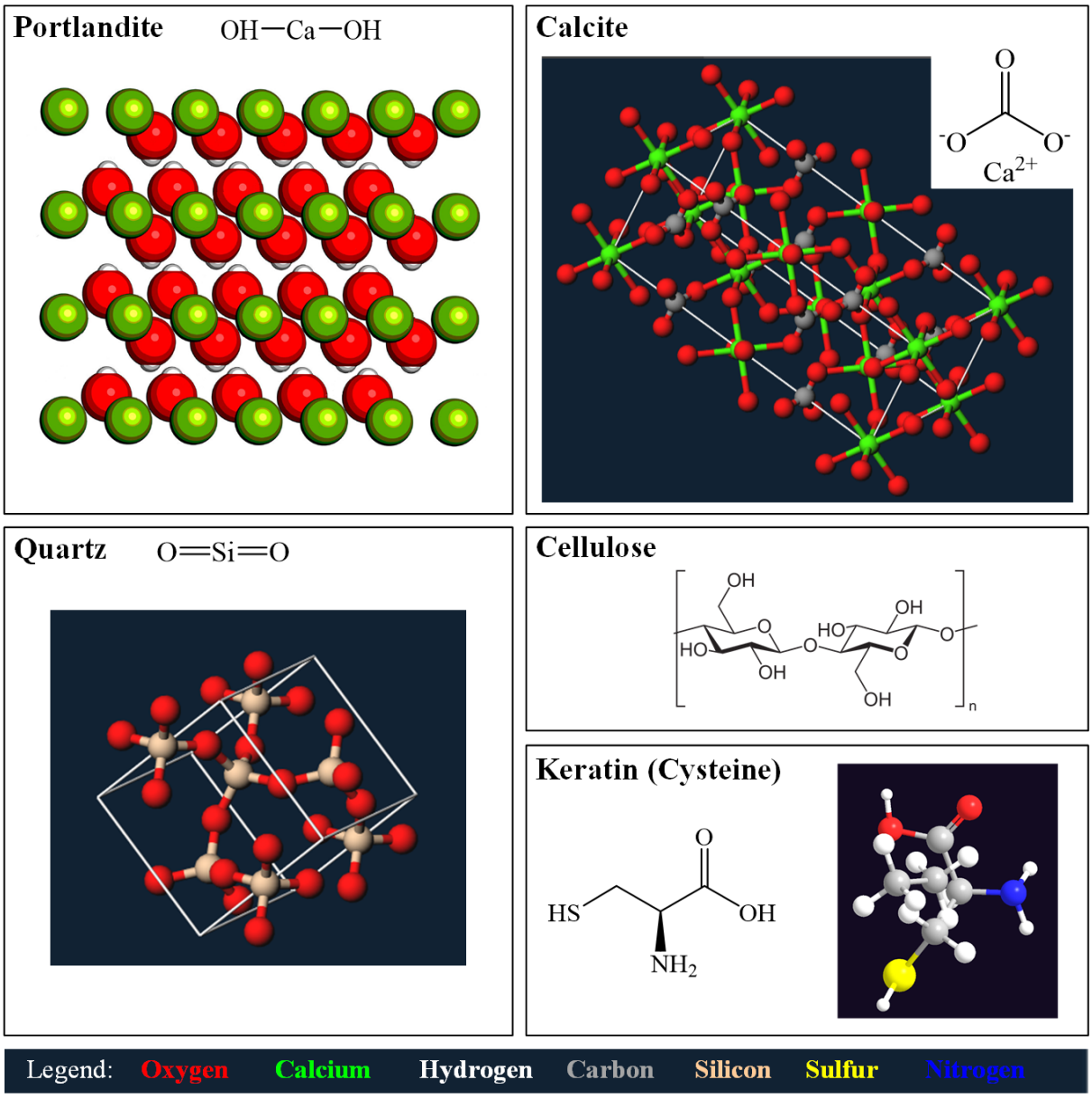

Figure 4.12 Molecular and crystal structures of portlandite, calcite, quartz, cellulose (monomer) and cysteine present in keratin.

4.3.1.2. Physical characterisation

Electron microscopy images of MDF, Coated MDF and Mortar_P are presented in Figure 4.13. Two magnifications were recorded for each material in order to analyse the macrostructure (top images) and the microstructure in detail (bottom images). For the purpose of this study, only the surface of the material that is in contact with organic pollutants was analysed. Each material showed distinct porosity. At the macro scale, MDF showed some porosity due to the fibre packing. The irregular shape and size of the cellulose fibres is evident at the macro and micro levels and leads to a wide pore size distribution. The top image of Coated MDF shows a cross-section where the flat surface of the paper coating can be seen, and the cellulose fibres underneath. No open porosity is observed at macro or micro levels in the paper coating of the Coated MDF. The porosity of Mortar_P, composed mainly of air lime and sand particles, can be observed at the micro level. The particles size is less than 1 μm, leading to smaller pore sizes compared with MDF.

The specific surface area (m^2/g) can be predicted from these SEM images where: Mortar_P has the higher specific surface area and Coated MDF the lower specific surface area.

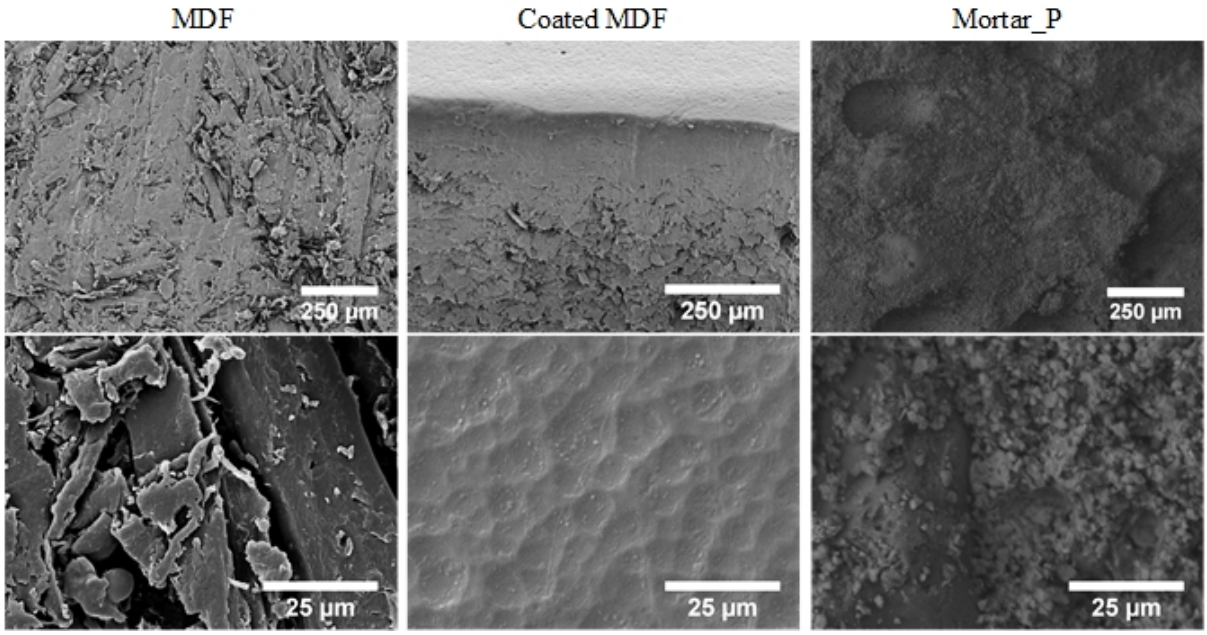

Figure 4.13 SEM images of MDF, coated MDF and Mortar_P.

In Figure 4.14, the macrostructure of the Natural wool and the microstructure of its fibres are presented. Natural wool is not considered a bulk material as it is composed of loosely packed

fibres, Figure 4.14 a). Fibre size and surface roughness are important characteristics that influence the physical adsorption of VOCs and formaldehyde. The fibre diameter varies between 20.6 and 80.5 µm (measured by using the software ImageJ 1.48v). Figure 4.14 b), a cross-section of a Natural wool fibre shows its internal porosity. In Figure 4.14 c) shows the surface of two individual fibres. The layers on the fibre surface are called the cuticular scale, and this surrounds the cortical cells (Rogers 1959).

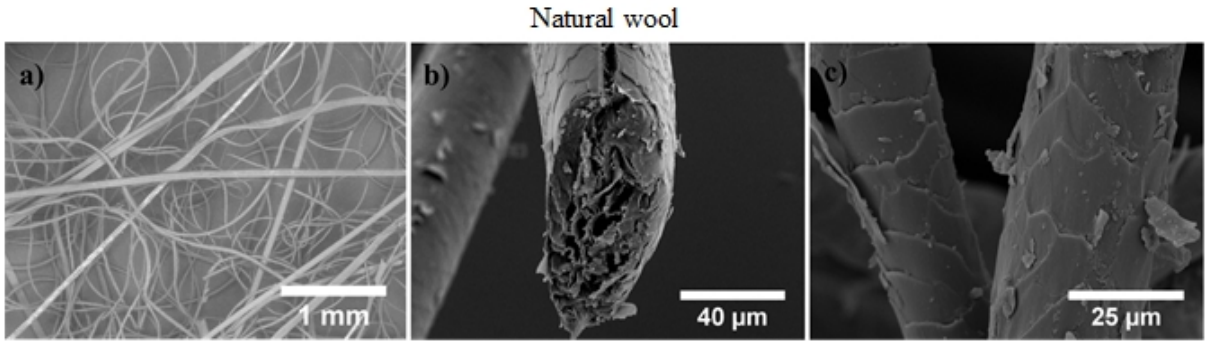

Figure 4.14 SEM images of natural wool.

The summary of the physical characterisation, specifically fibre and particle sizes and pore size distribution of MDF, coated MDF, Mortar_P and Natural wool are presented in Table 4.3. All measurements were determined using the software *ImageJ* version 1.48.

Table 4.3 Fibre/particle size range measured in the SEM images.

Material	Fibre/particle size range	Pore size distribution
MDF	10 to 200 µm	Wide
Coated MDF	Not applicable	Not applicable
Mortar_P	< 1 µm (air lime)	Narrow. < 1 µm
Natural wool	20 to 80 µm	Not applicable

4.3.2. IAQ in 2-litre chambers

4.3.2.1. Emissions testing

The specific emission rates of formaldehyde and TVOC (μg/m^{2}h) after 3 and 28 days of the 18 state of the art materials are shown in Figure 4.15 and Figure 4.16, respectively. All materials were grouped according to their classification of either insulation, coatings or wood-based panels, for a better comparison. All materials showed a decay of the formaldehyde and TVOC emissions from 3 to 28 days.

Insulation materials and coatings showed a very low emission rate of formaldehyde, lower than 20 μg/m^{2}h. However, this figure changed when looking at the emissions from the wood-based materials. The highest formaldehyde emission rates were observed for the chipboard, 290 μg/m^{2}h after 3 days, reducing to 270 μg/m^{2}h after 28 days. Coated chipboard showed a lower formaldehyde emission rate than the chipboard, this being 162 μg/m^{2}h and 110 μg/m^{2}h after 3 and 28 days respectively. The same effect was observed for MDF and coated MDF, with 94 μg/m^{2}h being emitted by MDF and 78 μg/m^{2}h by the coated MDF after 3 days testing. This indicates that the paper coating on the surface of the wood panels may act as a barrier to the diffusion of formaldehyde through the material up to the surface. Comparing the MDF emissions with the chipboard, the former showed lower emissions after 3 and 28 days. This may be attributed to the MDF being composed of smaller wood fibres than the chipboard which is composed of large wood chips. The smaller wood fibres provide higher surface area and thus better ability to adsorb the formaldehyde that is emitted by the material. Similar results were observed by Kim et al. (2006), Kelly et al. (1999) and Brown (1999). Kim et al. (2006) tested coated MDF, MDF and chipboard in a 20-litre environmental chamber and observed that coated MDF emitted less formaldehyde than the MDF, and that chipboard emitted more formaldehyde than MDF. Kelly et al. (1999) also studied the emissions of formaldehyde from wood-based materials such as flooring and furniture. The results showed that the paper coatings applied to chipboard reduced the formaldehyde emissions by 60-90 % and vinyl coating reduced it by 90-93 %. Brown (1999) tested MDF, chipboard and office furniture in a 51-litre environmental chamber. After 7 days of testing, the MDF material showed an average emission rate of 330 ± 23 μg/m^{2}h and chipboard of 362 ± 82 μg/m^{2}h. The common fact between these three studies is that, in each case, the discussion regarding the structure of the material (small fibres versus chips) or the coating acting as a barrier for the formaldehyde emissions was beyond of the scope of the studies and therefore these areas were not explored by the authors.

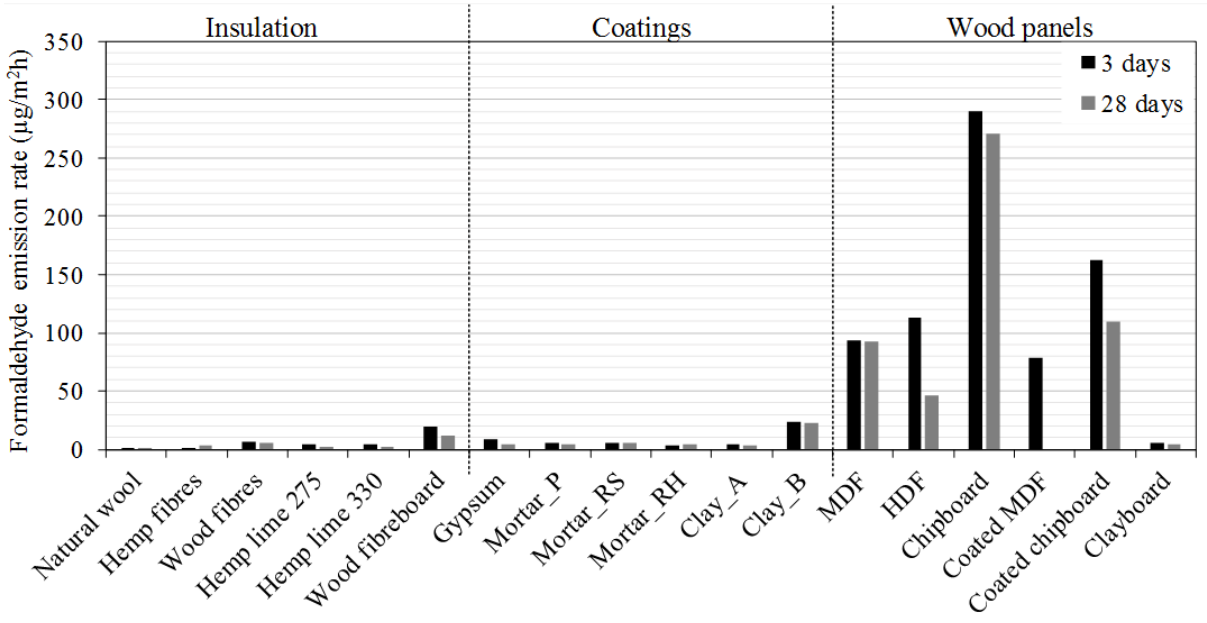

Figure 4.15 Formaldehyde area specific emission rate of insulation, coatings and wood-based panels after 3 and 28 days of testing.

In general, TVOC emission rates were low for all materials except the Wood fibre insulation, as shown in Figure 4.16. In Table 4.4, the main VOCs emitted by the 18 materials are shown. Wood-based panels and cellulosic insulation materials emitted natural VOCs such as terpenes (α-pinene and 3-carene), linear aldehydes, a cyclic aldehyde (furfural), a ketone (acetone) and acetic acid. Similar results were obtained by several authors as shown previously in Section *2.2 Volatile organic compounds and formaldehyde emissions by building materials*, Table 2.5. The emissions of acetic acid and furfural by these materials are associated with the degradation of the hemicellulose. The origin of the acetic acid is associated with the elimination of acetyl groups and furfural is formed from pentoses and hexoses by elimination of water (Horn et al. 1998; Uhde and Salthammer 2007). This could be caused by the heat-treatment applied to the panels during the manufacturing processes. Inorganic based materials such as lime mortars and hemp limes showed emissions of aldehydes and alcohols such as 1-butanol and 2-ethylhexan-1-ol. Both alcohols are often found in solvents and fuels. 1-Butanol can also be used in the manufacture of the melamine-formaldehyde resins as a reactant, which explains its emission from some wood-based materials.

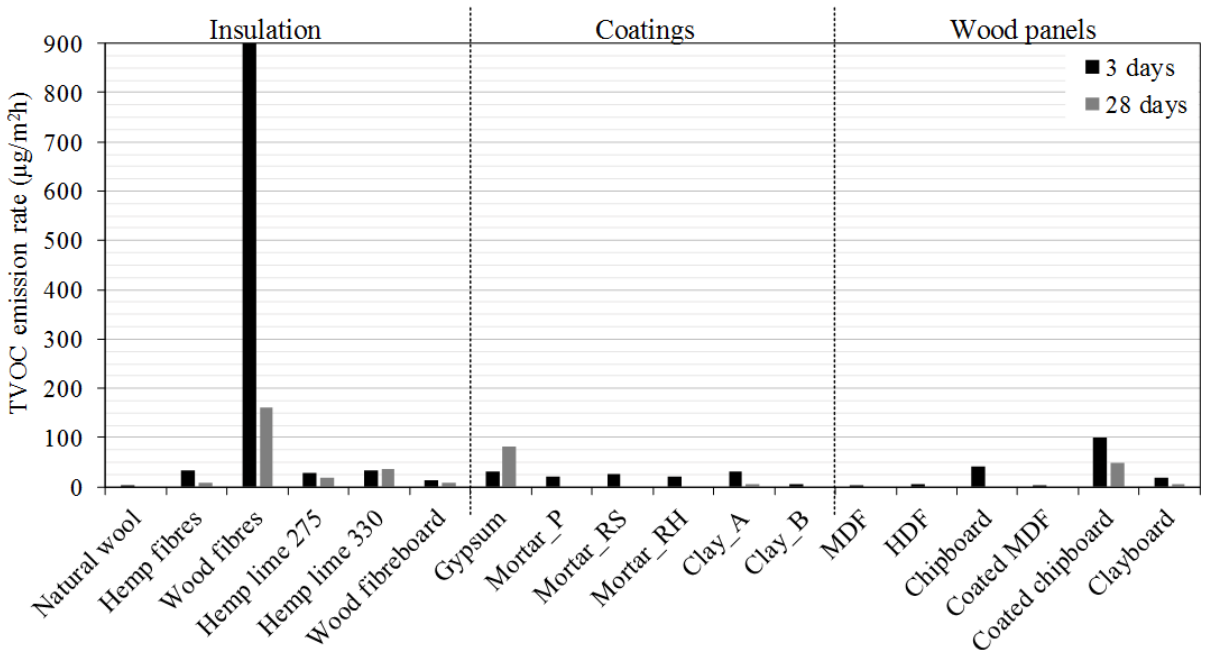

Figure 4.16 TVOC area specific emission rate of insulation, coatings and wood-based panels after 3 and 28 days of testing.

Table 4.4 Main VOCs emitted by the *eco-materials*.

VOC	Insulation	Coatings	Wood panels
Acetone	✓		✓
Acetic acid	✓		✓
Benzaldehyde	✓		✓
Toluene	✓		✓
Furfural	✓		✓
Hexanal	✓	✓	✓
Nonanal	✓	✓	✓
Decanal	✓	✓	✓
1-Butanol	✓	✓	✓
2-Ethylhexan-1-ol		✓	
α-Pinene	✓		✓
3-Carene			✓

4.3.2.2. Adsorption and desorption behaviour

In Figure 4.17, concentrations of toluene, limonene, dodecane and formaldehyde during the adsorption and desorption phases are shown. The concentrations during the adsorption phase represent the dosing levels of these compounds in the chambers where the testing materials are placed. The maximum dosing concentrations were controlled through the air flow passing in the doping chambers, as shown previously in Figure 3.9, and simulate the worst-case scenario where toluene, limonene and dodecane are present at concentrations of around 2000-2500 $\mu g/m^3$ and formaldehyde at about 700 $\mu g/m^3$. Formaldehyde quickly reached its maximum concentration in the reference chamber, just 1 hour after turning on the doping air. The other three VOCs reached their maximum concentration only after approximately 24 hours. During the adsorption phase, the emissions from the sources of VOCs and formaldehyde were fairly stable which led to a stable dosing concentration throughout the adsorption phase. In the desorption phase, all concentrations dropped to almost 0 $\mu g/m^3$ within 1 hour of turning on the pure air. In this stage, the concentration of VOCs adsorbed onto the surface of the materials was higher than in boundary layer on the surface and the reversibly adsorbed (physisorbed) VOCs began to be desorbed (Tichenor et al. 1991; An et al. 1999).

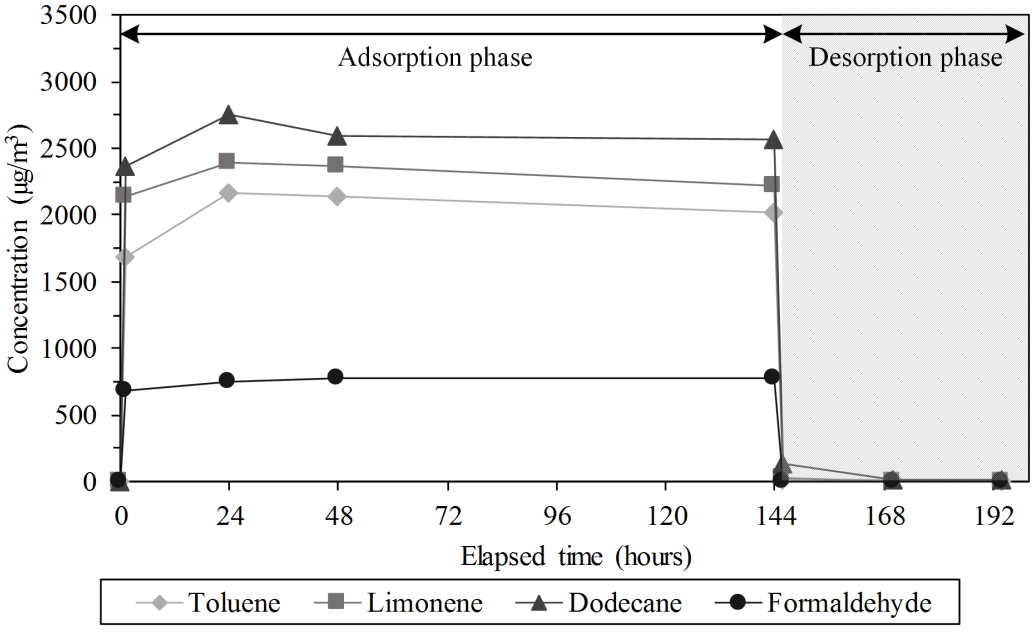

Figure 4.17 Adsorption and desorption curves of toluene, limonene, dodecane and formaldehyde in the reference 2-litre chamber.

The adsorption and desorption behaviour of the four selected eco-materials with regard to toluene, limonene, dodecane and formaldehyde is shown in Figure 4.18, where the black line without any symbol represents the concentration in the reference chamber. The main objective of this specific study is to investigate the quantity of VOCs and formaldehyde that these materials can adsorb and then desorb and to correlate their adsorption/desorption behaviour with their chemical composition and physical characteristics, such as porous microstructure and surface area. From Figure 4.18 it is clear that these four materials exhibit different adsorption/desorption behaviour when exposed to the same organic pollutant and that each individual material has a different ability to interact with various organic pollutants. This allows these results to be discussed on the basis of the materials' characteristics or the physico-chemical properties of the VOCs/formaldehyde.

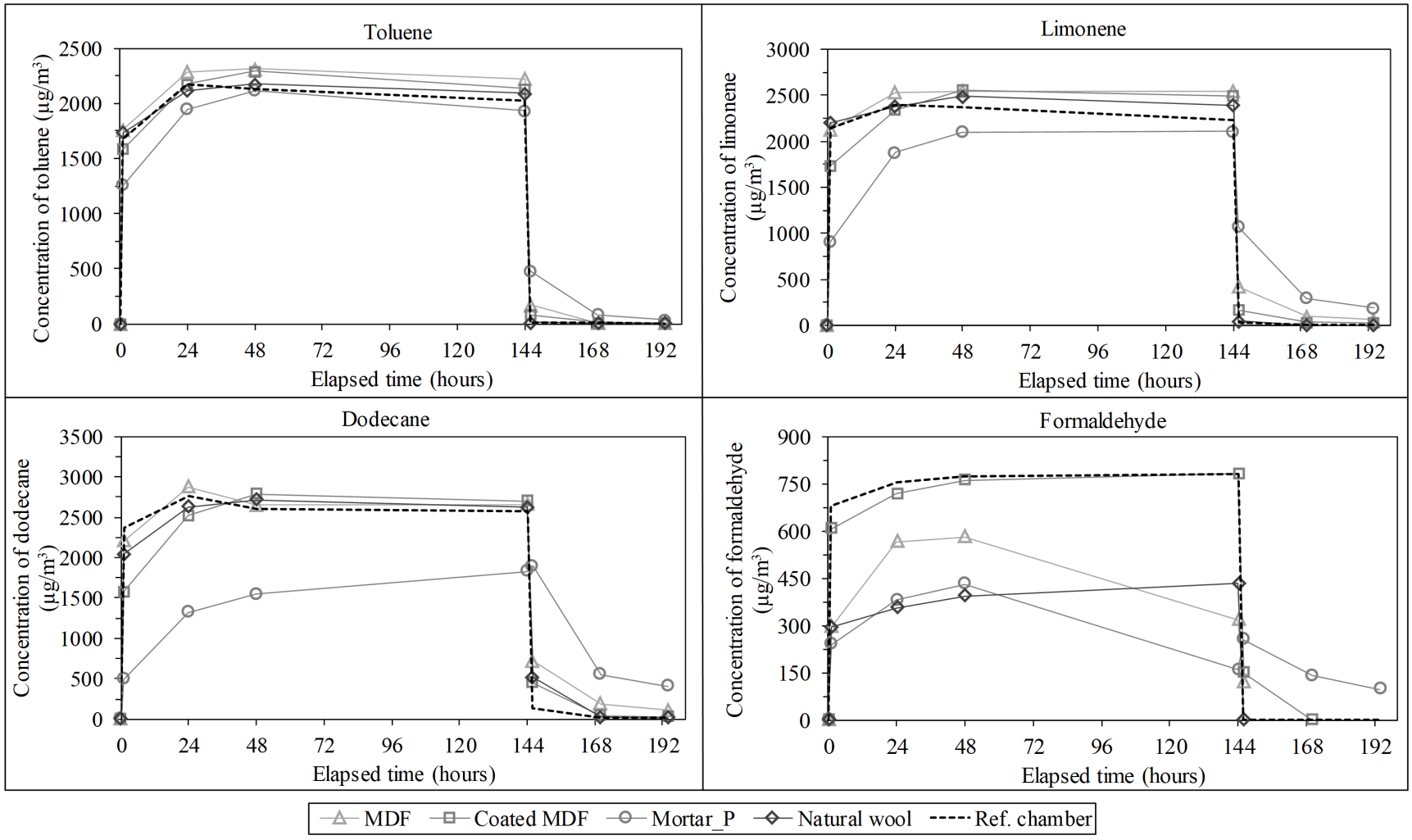

Figure 4.18 Adsorption and desorption curves of VOCs and formaldehyde by MDF, coated MDF, Mortar_P and Natural wool.

The most readily adsorbed organic compounds were dodecane and formaldehyde followed by limonene; the least adsorbed was toluene for each of the four tested materials. There is no correlation between vapour pressure or boiling point of the organic compounds and their ability to be adsorbed by the different materials, although their polarity, chemical conformation and water solubility may explain this. Formaldehyde was one of the most adsorbed compounds and this may be due to its polarity and water solubility. If a material has good ability to adsorb moisture, in principle it will also have good ability to adsorb formaldehyde by dissolving this in the already-adsorbed water molecules. Dodecane is a non-polar compound, like toluene and limonene, although it is an aliphatic compound. Its molecular structure consists of a large linear hydrocarbon chain and so it has more oscillating charges associated with its electron cloud that can interact with electron clouds from the surface of the materials. This facilitated the diffusion through pores and capillaries of the materials by physisorption compared with toluene and limonene (Gunschera, Markewitz, et al. 2013). Aromatic and cyclic compounds, such as toluene and limonene, were the least adsorbed. Ruiz et al. (1998) have different observations regarding the adsorption capacity of aliphatic compounds and aromatic compounds. In their studies, aromatic compounds (toluene, *m- and p*-xylene and ethylbenzene) were more adsorbed than the aliphatic compounds (*n*-hexane, *n*-heptane and *n*-octane). This conflicting observation may be because of the smaller aliphatic compound used in their studies compared with the longer-chained dodecane in the present PhD work. In Figure 4.18 the concentration of toluene and limonene in the chambers containing materials is higher than the reference chamber for some periods of time. This may be related to the uncertainty of the experiment (less than 7 %) and the saturation point of the material, which should equal the concentration in both chambers (chamber with testing material and reference chamber).

In Figure 4.19 a) the total mass of formaldehyde adsorbed and desorbed by the four materials is presented. These masses were calculated as a product between the volumetric air flow through the chambers (Q) and the difference between the concentrations in the test chamber C_m and reference chamber C_{ref}, integrated over the period t_i to t_f hour period for the adsorption and desorption phases, Eq. 4.1.

$$\text{Mass adsorbed or desorbed} = \int_{ti}^{tf} Q \times \left(C_{ref} - C_m\right) dt \qquad \text{Eq. 4.1}$$

In the adsorption phase, the specimen Mortar_P gave rise to the lowest concentrations in the chamber for all VOCs and formaldehyde. This means that this material has a good capacity to adsorb VOCs quickly, thereby having the potential to improve the IAQ in a real case. The highest sink effect of Mortar_P was observed for dodecane and formaldehyde, followed by limonene and toluene, Figure 4.19 b). In Figure 4.18, at 48 hours of elapsed time, the concentration of dodecane in the reference chamber was around 2600 $\mu g/m^3$ while in the chamber containing Mortar_P it was approximately 1450 $\mu g/m^3$, some 40.4 % lower than in the reference chamber. In the case of formaldehyde, the concentration in the chamber containing the Mortar_P was 44.2 % lower than in the reference chamber. This good sink effect can be attributed to the large surface area of the lime mortar porous matrix with pore sizes in the order of nanometres, as shown previously in Figure 4.13, and the chemical affinity between organic pollutant molecules and silica from quartz (Parida et al. 2006), calcium cations and oxygen atoms from the surface of the calcite crystals, and hydroxyl groups from portlandite. When the VOC and formaldehyde molecules approach the surface of the Mortar_P particles, the Van der Waals forces and the hydrogen bonding will keep the VOC and formaldehyde molecules adsorbed onto the surface of the particles (Rouquerol et al. 2014). If any chemisorption mechanism is taking place during these interactions, the adsorption is irreversible. This is measured by calculating the mass of organic compound adsorbed during the adsorption phase and the amount of desorbed organic compound in the desorption phase using Eq. 4.1. As shown in Figure 4.19 b), Mortar_P adsorbed a total mass of dodecane of 1856 µg and then desorbed 460 µg until 48 h into the desorption phase (192 hours elapsed in total). If the concentration of VOC in the chamber with material reaches 0 $\mu g/m^3$ in the desorption phase and the mass of VOC desorbed is lower than the mass adsorbed this means that some of the VOC has been irreversibly adsorbed on the surface of the material. As shown in Figure 4.18, the concentration of the three VOCs and formaldehyde in the chamber with the Mortar_P did not reach the same level of concentration of the reference chamber at the end of the allotted adsorption phase. This means that this material was still adsorbing VOCs and formaldehyde after 144 hours of elapsed time.

MDF exhibited similar concentrations in the reference chamber during the experiment for the three VOCs, showing that this wood panel has a low capacity to adsorb these gases. In the case of the coated MDF, the adsorption was low for all four organic compounds. The lower adsorption capacity of the coated MDF in comparison with the MDF may be related to its very flat surface, as shown previously in Figure 4.13.

Natural wool showed a high capacity to adsorb formaldehyde, confirming the chemisorption phenomenon between its proteins and formaldehyde as observed by Middlebrook (1949), Huang et al. (2007) and Curling et al. (2012). The chemical interactions between Natural wool proteins and formaldehyde proposed by Curling et al. (2012) is shown in Figure 4.20. The authors suggest that formaldehyde has high reactivity towards the proteins within the wool, reacting with functionality in the side chains of the amino acids, the amido groups. The MDF panel also showed good capacity to adsorb formaldehyde. This may be explained by the hygrothermal properties of the MDF (i.e. the capacity of this material to adsorb moisture). As formaldehyde is a water-soluble compound, its adsorption will be favoured in materials with good hygrothermal properties such as MDF (da Silva et al. 2017), also shown in Chapter 5 of this thesis.

In the desorption phase, the effect of the toluene, limonene and dodecane relative molecular masses on desorption rates can be observed in all materials. VOCs with small molecular mass such as toluene (92.14 g/mol) were completely desorbed from the surface of the materials after 24 h. On the other hand, dodecane (170.34 g/mol) was not totally desorbed from Mortar_P and MDF even after 48 h of the desorption phase. As an exception, formaldehyde has a smaller molecular mass and was not completely desorbed by the Mortar_P after 48 hours. This may be due to the polarity of the formaldehyde molecule which does not allow this compound to be desorbed easily. Natural wool did not show any desorption of formaldehyde, indicating the high affinity to adsorb this compound chemically and indicating that this phenomenon is irreversible.

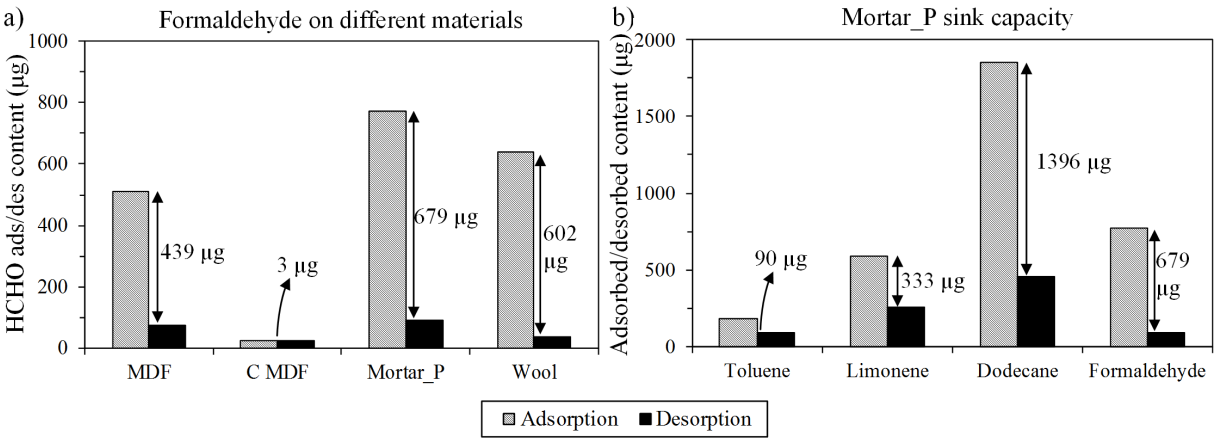

Figure 4.19 a) mass of formaldehyde adsorbed and desorbed by MDF, Coated MDF, Mortar_P and Natural wool and b) VOCs and formaldehyde adsorbed and desorbed by the Mortar_P. Arrows and values represent the quantities of VOC retained in the material surface (difference between the adsorbed and desorbed mass).

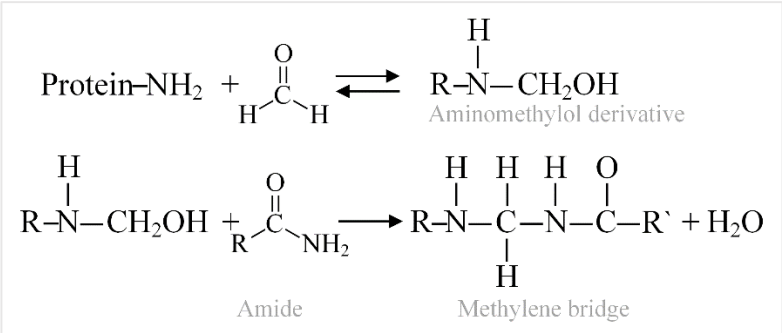

Figure 4.20 Reaction mechanism between wool proteins and formaldehyde adapted from Curling et al. (2012).

4.3.3. IAQ in 30 m^3 chamber

Figure 4.21 shows the concentration curves of toluene, limonene and dodecane in the inlet and outlet of the 30 m^3 chamber during the adsorption and desorption phase of the MDF. For this study, the wall opposite to the window and door of the chamber was covered with MDF panels, equivalent to approximately 10 m^2 of exposed area of the material.

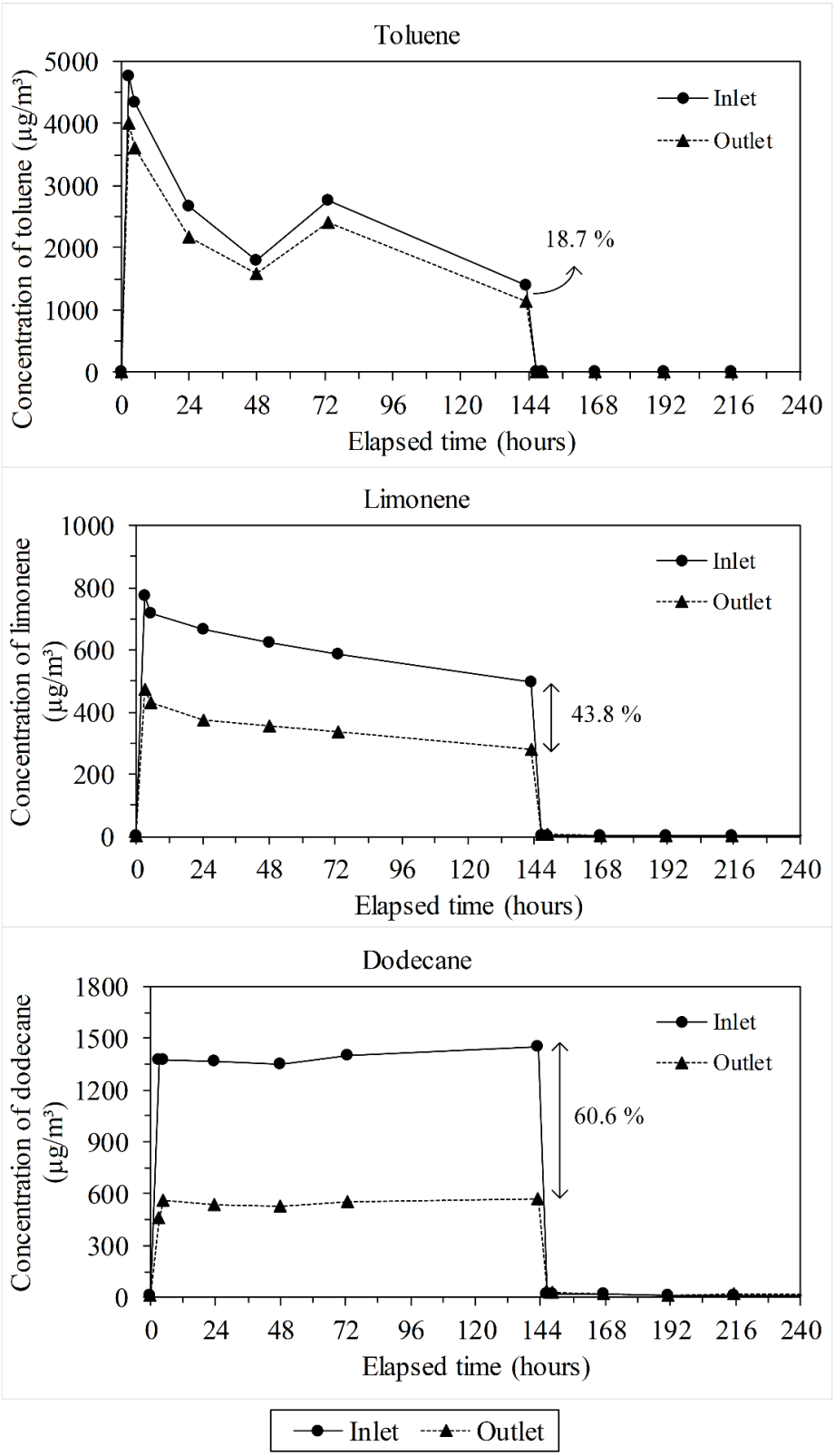

Figure 4.21 Concentration of toluene, limonene and dodecane in the inlet and outlet of the 30m^3 chamber with MDF panels placed in one wall of the chamber (~10 m^2).

The curve showing the concentration of toluene in the inlet of the chamber during the adsorption phase shows that the emission rate of the source of toluene was too high leading to a quick depletion of the source. This is observed from the start of the experiment until 48 hours where, the concentration of toluene in the inlet reached almost 5000 µg/m³ and then started to decrease. After 48 hours, the source of toluene was topped up and the concentration subsequently increased again. The concentration of toluene in the outlet of the chamber followed the path of the emission rate of the source. The source of dodecane showed the most stable emission rate with the inlet concentration of the chamber varying between 1400 and 1450 µg/m³. In the case of limonene, the source showed a fairly stable emission rate, although with a decay of 1.6 µg/m³/h between 5 and 144 hours of elapsed time. As occurred for toluene, the concentration of limonene and dodecane in the outlet of the chamber followed a parallel behaviour to the inlet concentration. At the end of the adsorption phase, at 144 hours, the difference between the inlet and outlet concentrations is indicated in Figure 4.21. Toluene showed the lowest difference between concentrations in the inlet and outlet, at 18.7 %. On the other hand, the concentration of dodecane in the outlet was 60.6 % lower than in the inlet. The same was observed in the 2-litre chambers experiment, where the dodecane was preferably adsorbed compared to toluene or limonene. The difference between the concentrations in the inlet and outlet of the chamber may indicate the amount of VOC adsorbed. However, as there is no parallel analysis for the same chamber under same conditions without any material in (i.e. chamber background/reference), the difference between the inlet and outlet of the chamber may not fully represent the uptake of VOCs by the material.

During the desorption phase, concentrations of the three VOCs in the inlet dropped to almost 0 µg/m³ after 3 hours. However, Figure 4.22 shows that very low levels of toluene, limonene and dodecane were still being exhausted through the outlet of the chamber. This may mean that either the MDF panels were desorbing the physisorbed compounds very slowly, or that the remaining VOCs within the internal volume of the chamber were still being exhausted out of the chamber. Six days after the desorption phase started, there were still some VOCs being exhausted through the outlet of the chamber, supporting the theory of very slow desorption of the physisorbed VOCs.

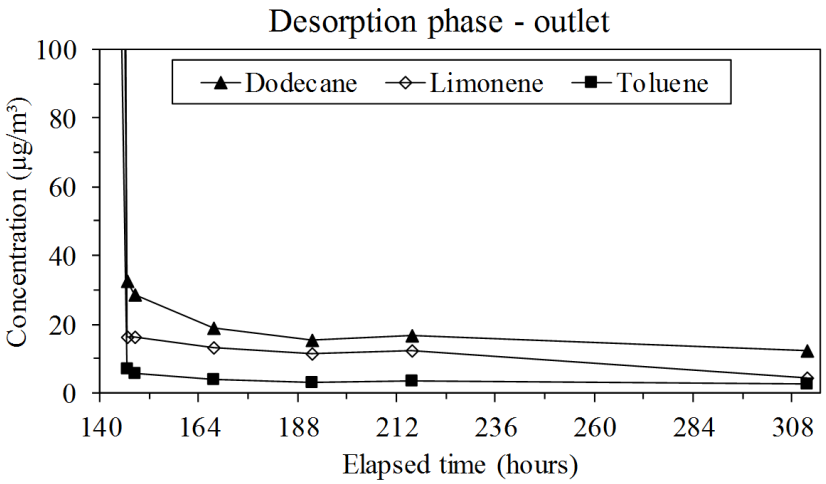

Figure 4.22 Concentrations of toluene, limonene and dodecane in the outlet of the chamber during the desorption phase.

4.4. Summary

- ✓ The chemical composition of all 18 *eco-materials* is summarised in Table 4.5. Wood-based materials have a chemical composition based on cellulose and derivatives. The coatings group are composed of the inorganic crystalline phases of calcite, portlandite and quartz in the case of the lime-based mortars, calcium sulphate in gypsum, and clay minerals and also quartz in the Clay plasters. The chemical detected in the Natural wool was keratin;

Table 4.5 Summary of the chemical compostion of all *eco-materials*.

	Material	Chemical composition
Insulation	Natural wool	Keratin
	Wood fibres	Cellulose, hemicellulose and lignin
	Wood fibreboard	Cellulose, hemicellulose and lignin
	Hemp fibres	Cellulose, hemicellulose and lignin
	Hemp limes	Cellulose and calcite
Coatings	Gypsum	Calcium sulphate
	Mortar_P	Calcite, portlandite and quartz
	Mortar_RS	Calcite, portlandite and quartz
	Mortar_RH	Calcite, portlandite and cellulose
	Clay_A	Calcite, quartz and clay minerals
	Clay_B	Quartz and clay minerals
Wood panels	MDF	Cellulose, hemicellulose and lignin
	HDF	Cellulose, hemicellulose and lignin
	Chipboard	Cellulose, hemicellulose and lignin
	Clayboard	Cellulose, quartz and clay minerals

- ✓ Physical investigation of the microstructure of the MDF, Coated MDF, Mortar_P and Natural wool showed that these materials have very distinct morphologies which will affect the adsorption and desorption of VOCs and formaldehyde;
- ✓ Emissions of formaldehyde and TVOC are well below the current IAQ guidelines for all eco-materials described in Table 2.2 of the Section 2.1. In a 30 m^3 European Reference Room (CEN/TS 16516:2013) with all four walls covered with the material (~31.4 m^2) with the highest TVOC emission rate (Wood fibres), the concentration of TVOC in the chamber after 28 days at 0.5 ach^{-1} would be up to 76.4 $\mu g/m^3$. In the case of formaldehyde, the material with the highest emission rate (Chipboard) would give a concentration in the chamber up to 128.8 $\mu g/m^3$ which is slightly higher than the guidelines described previously in Table 2.2. The type of VOC emitted is related to the chemical composition of the material and manufacturing process;
- ✓ Paper coatings on MDF panels act as a barrier to formaldehyde and TVOC emissions;

- ✓ Adsorption and desorption behaviour strongly depends on the physical properties and chemical composition of the building materials. Specimens with a flat surface such as Coated MDF adsorbed fewer or no VOCs, including even the more polar formaldehyde. Mortar_P presented a highly porous microstructure with pore size < 1 μm and the highest specific surface area of the four studied materials, leading to it exhibiting the highest adsorption capability for each of the three VOCs and for formaldehyde. This indicates that higher specific surface area leads to a higher adsorption capacity. The chemical composition of the Mortar_P, MDF and Natural wool had an influence on the adsorption mainly due to the presence of dipoles, and the -OH and -NH_2 groups;
- ✓ With reference to the physico-chemical properties of the organic compounds, in the group of non-polar compounds (toluene, limonene and dodecane), dodecane was the most adsorbed by the four materials tested. This may be attributed to the dodecane chemical conformation being a straight chain of 12 carbons surrounded by 26 atoms of hydrogen in the same plane, leading to a strong hydrogen bonding interactions when compared with toluene and limonene. Formaldehyde was the most adsorbed compound in this study due to its polarity;
- ✓ In Table 4.6, the correlation between the chemical composition and microstructure and the adsorption and desorption behaviour is given.

Table 4.6 Correlation between material properties and adsorption behaviour.

Material	**Microstructure**	**Chemical composition**	**Adsorption behaviour**
MDF	Large pore size distribution	Cellulose	Good with regard to formaldehyde
Coated MDF	Flat surface/no porosity	Cellulose	Weak
Mortar_P	Pore size < 1 μm	Calcite, portlandite, quartz	Very good in general
Natural Wool	Loose fibres	Keratin	Good with regard to formaldehyde

Chapter 5

Effect of the incorporation of walnut shell on VOCs adsorption/desorption of MDF panels

5.1. Introduction

In Iran, walnut and almond shells are considered as agricultural by-products with no significant industrial usage and as a result they are often incinerated or dumped. Pirayesh (2013) studied the formaldehyde emission reducing effect of walnut and almond shells when added to particleboards. When 10, 20, 30 and 100 % of shell was added, results showed that the presence of the shells decreased the formaldehyde emission by up to 42.8 %. The authors attributed the reduction of the formaldehyde emission to the high amounts of extractives in the shells, and therefore the presence of large number of polar hydroxyl and phenolic groups. Wood panels could be produced with up to 20 % of walnut shell particles without falling below the minimum EN standard requirements of mechanical properties for general purpose use (Pirayesh et al. 2012).

This chapter demonstrates the potential of MDF modified with walnut shell to improve IAQ by not only reducing the formaldehyde emissions but also by capturing VOCs and formaldehyde from the air. MDF panels with 5, 10 and 15 % walnut shell incorporated were compared to a control sample with no shell content. VOCs, formaldehyde and moisture adsorption/desorption properties were quantified. Additionally, the microstructure of the modified panels was investigated and correlated with the adsorption/desorption behaviour.

5.2. Materials and methods

5.2.1. Materials description

MDF panels were made to a density of 760 kg/m^3, with thickness of 12 mm by the ECO-SEE project partner Bangor University. The resin loading was 14 % of urea formaldehyde (UF). A commercial mix of spruce, pine and fir chips was refined at 8 bar at the BioComposites Centre's Technology Transfer Centre following the protocols described in Skinner et al. (2016). The fibre, scavenger and resin were individually weighed and combined in a drum blender. The resinated fibre was weighed out again and formed into a mat which was subsequently pre-pressed by hand before finally being pressed between two heated platens at 200 °C for 5 minutes following the standard press profile (controlled by the Pressman control program) used by the BioComposites Centre. All samples were transported and stored in sealed bags prior to characterisation and IAQ assessment. The scavenger loading for the panels was 5, 10 and 15 % of fibre, Table 5.1.

Table 5.1 Percentage of walnut addition to MDF fibre.

%	Walnut weight (kg)	MDF fibre (kg)
0	0	1.61
5	0.07	1.27
10	0.13	1.20
15	0.20	1.14

5.2.2. Materials characterisation and IAQ assessment

The porous microstructure of the MDF panels with walnut, surface of the MDF fibres and surface of the walnut shell were analysed by SEM. For the IAQ assessment, MDF panels with 0, 5, 10 and 15 % walnut were tested for the emission rates of TVOC and formaldehyde after 3 and 28 days. The adsorption and desorption behaviour of VOCs, formaldehyde and water vapour were also investigated.

5.3. Results and discussion

5.3.1. Materials characterisation

Scanning electron microscope images of the MDF panels with walnut shell are presented in Figure 5.1 a) to d). MDF panels were manufactured to achieve a density as close to 760 kg/m^3 as possible. It became apparent however that packaging of the wood fibres in the MDF panels with higher contents of walnut shell led to a more compact structure than expected. This resulted in the voids between each single wood fibre in the MDF matrix being smaller for the panels with higher contents of walnut shell, which led to a higher surface area, Figure 5.1 d). Figure 5.2 shows the walnut shell particles embedded in the MDF matrix, with sizes varying between approximately 200 and 600 μm.

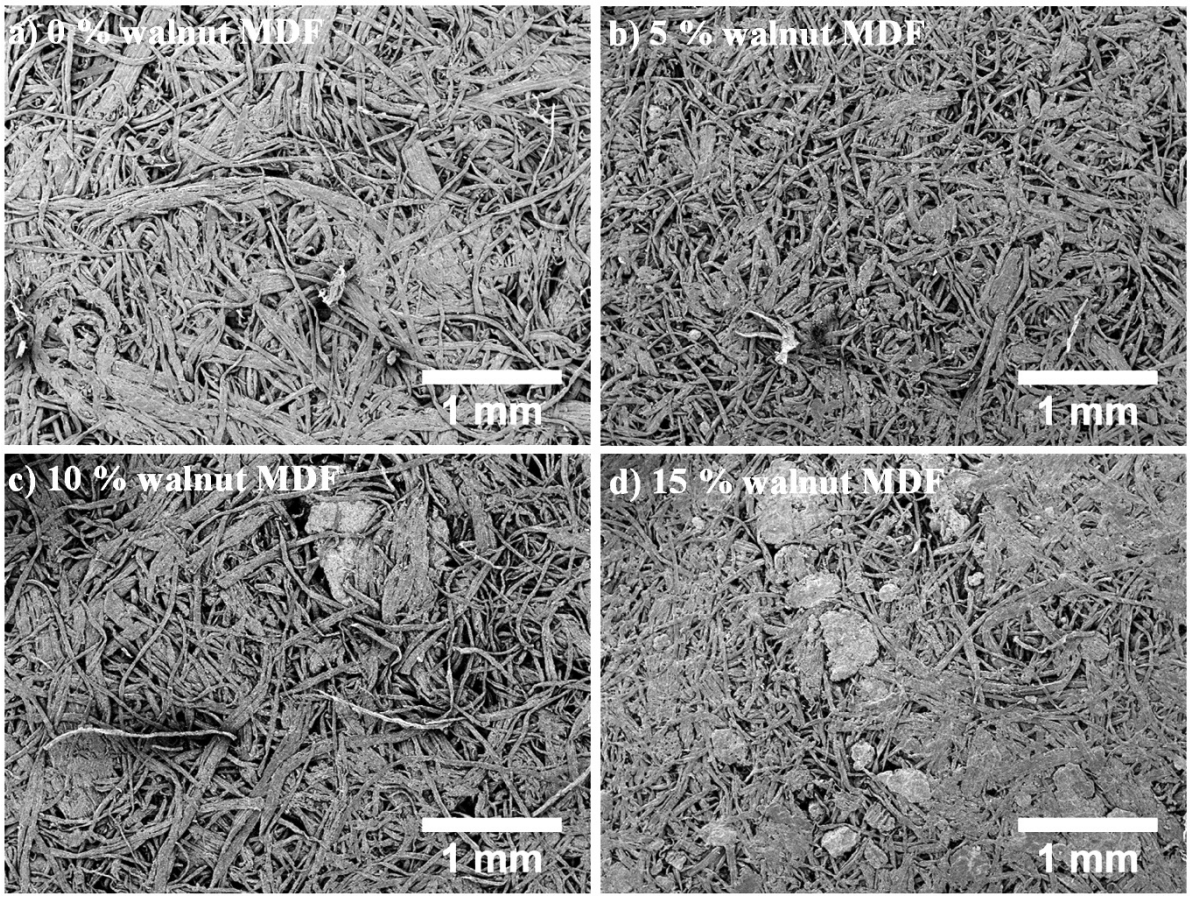

Figure 5.1 Scanning electron microscope images of the MDF panels prepared with different amounts of walnut shell.

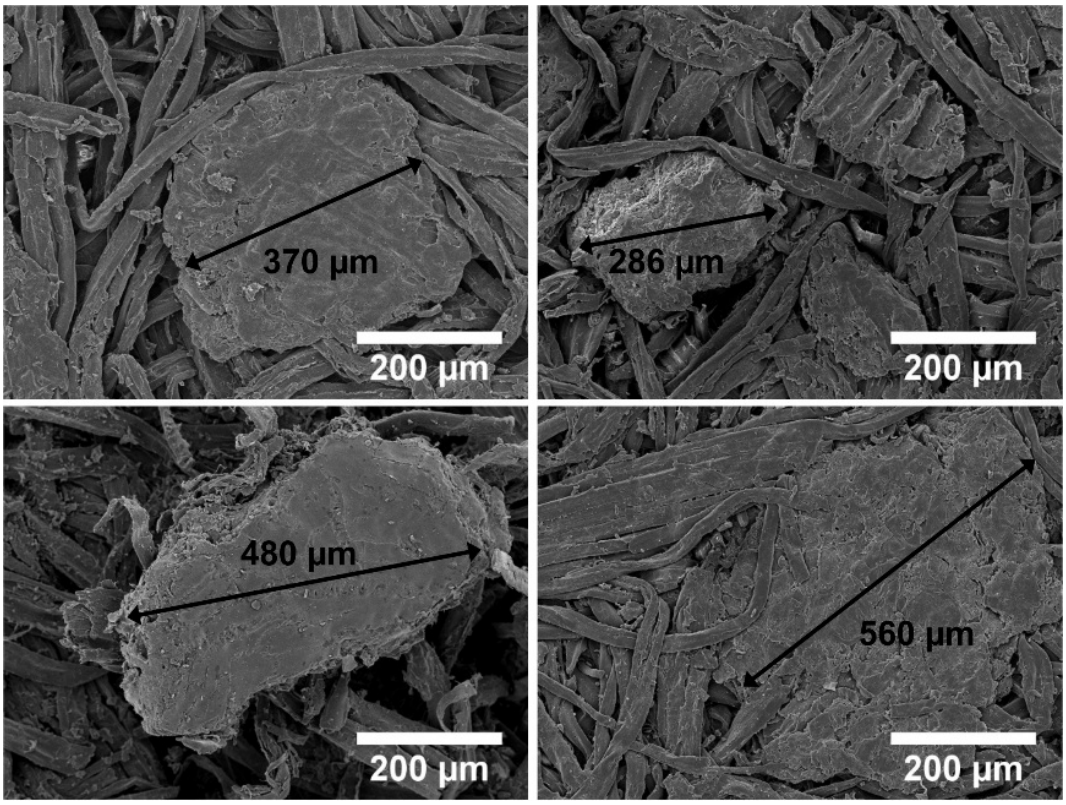

Figure 5.2 A number of representative scanning electron microscope images of walnut shell particles of varying size.

Macroscopically, walnut shell does not show porosity as seen in Figure 5.2 although, at higher magnifications, a highly porous structure can be observed, Figure 5.3 a) and b). The wood fibre surface is shown in Figure 5.3 c) and d). The average size of the pits in the wood fibre is 1.42 µm.

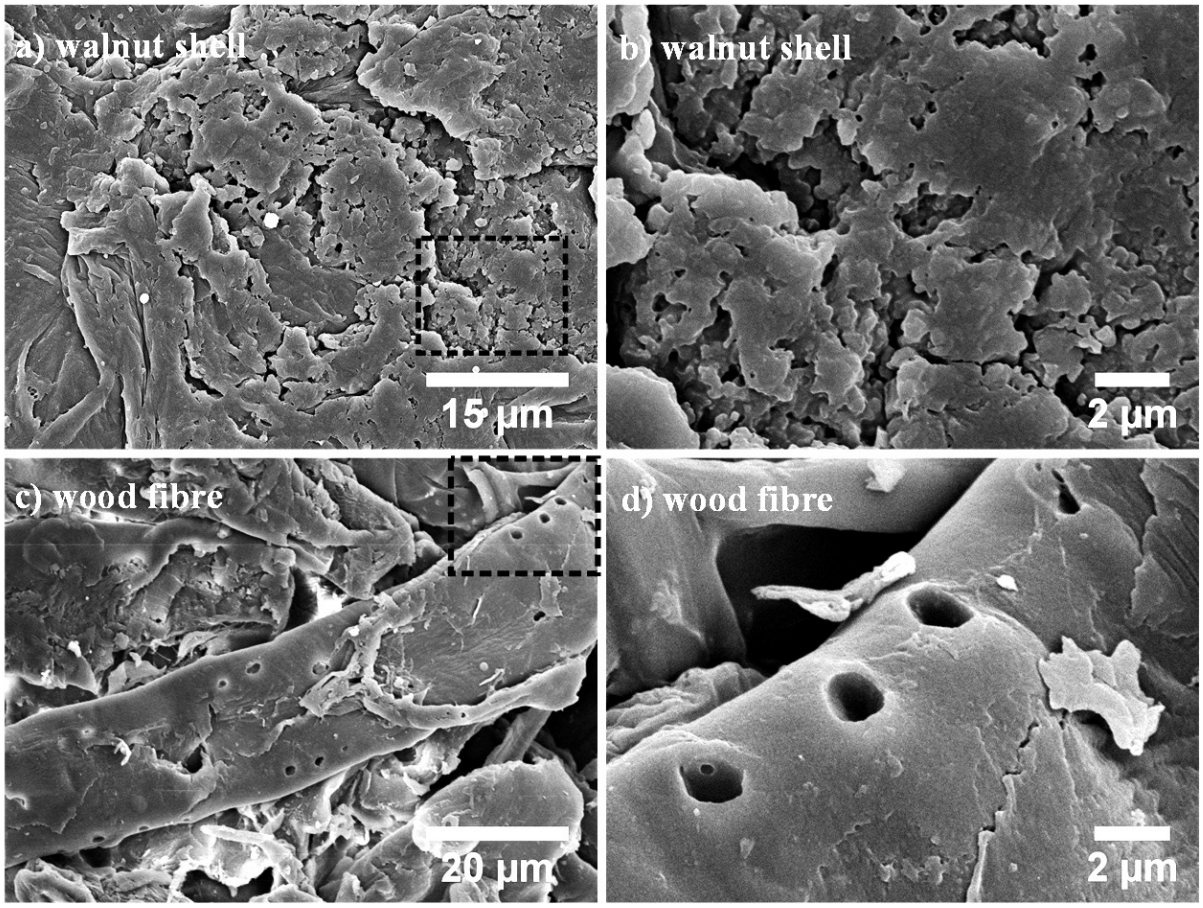

Figure 5.3 Scanning electron microscope images of (a) and (b) walnut shell surface, (c) and (d) MDF wood fibre surface. Images (b) and (d) are higher magnifications of the dashed areas indicated in (a) and (c), respectively.

Walnut shell presents an irregular porous surface with pore sizes ranging from 25 nm to 1224 nm. The pore size of the walnut shell was measured using ImageJ version 1.48 image analysis software. An average pore size of 330 nm was obtained from a sample of two hundred measurements. As the pore size distribution is wide the average is not representative and thus it is plotted as a size distribution, Figure 5.4. In a sample of 200 pore size measurements, 20 % of the pores exhibited sizes between 25 and 74 nm. Overall, 65 % of all measured pores showed sizes below 374 nm.

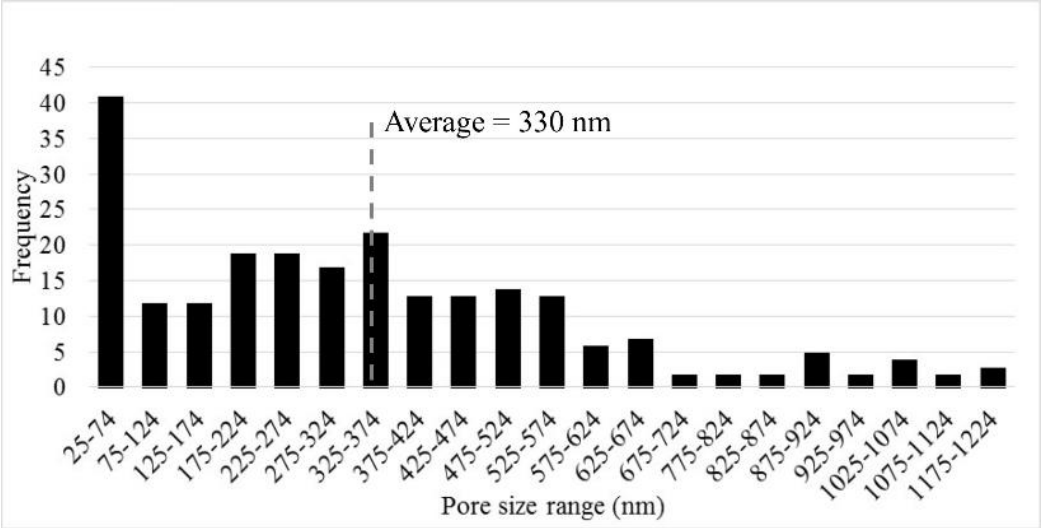

Figure 5.4 Pore size distribution of the walnut shell in the form of counts (frequency) and intervals of pore size (pore size range).

5.3.2. IAQ in 2-litre chambers

5.3.2.1. Emissions testing

The area specific emission rates (μg/m^{2}h) of formaldehyde and TVOC are presented in Figure 5.5. The main VOCs identified during emissions testing were acetic acid and 2-ethylhexan-1-ol. Acetic acid emitted by the MDF panels can be associated with the degradation of the hemi-cellulose by the elimination of acetyl-groups (Horn et al. 1998; Uhde and Salthammer 2007). This could be attributed to the heat-treatment applied to the MDF panels during the manufacturing process, as described in the experimental section.

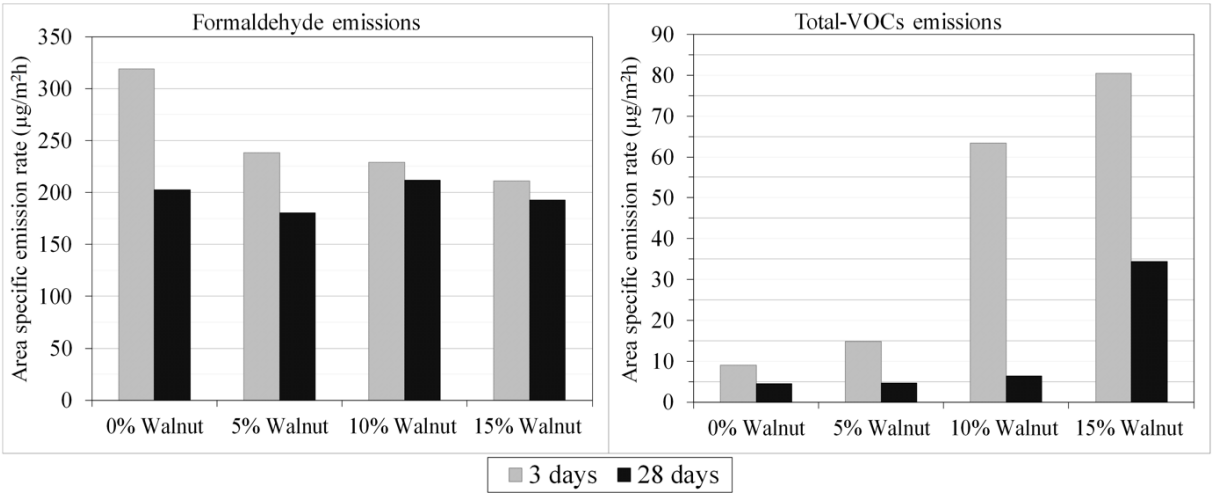

Figure 5.5 Area specific emission rate of formaldehyde and total-VOC from the wood panels with walnut after 3 and 28 days. Major VOCs emitted: acetic acid and 2-ethylhexane-1-ol.

The formaldehyde emission rate was lowest for the MDF panel with 15 % walnut shell content after 3 days. In comparison, the MDF panel with the highest walnut content emitted 34 % less formaldehyde than the MDF without walnut. Pirayesh et al. (2013) also observed a decrease in formaldehyde released by the particleboard with higher walnut content, using the BS EN 717-3 standard methodology. Similar observations were reported in other studies (Boran et al. 2011; Ayrilmis et al. 2009). After 28 days, the MDF panel with 5 % walnut showed the lowest emission rate at 180 µg/m^2 h, followed by the MDF with 15 % walnut at 193 µg/m^{2}h. Notwithstanding the decreasing emission rate with increasing walnut content at 3 days, for the 28-day testing the difference between all samples was reduced, with only a 15.1 % difference between the samples with the highest and lowest emission rates (180 to 212 µg/m^{2}h). Kim et al. (2010) reported slightly higher 3-day formaldehyde emissions from MDF panels, at 400 µg/m^2 h.

Unlike the formaldehyde emissions, TVOC emissions increased with the addition of walnut from 9 to 80 µg/m^{2}h with 15 % of walnut added after 3 days of testing. After 28 days, MDF with 0 %, 5 % and 10 % showed very low emissions, less than 6 µg/m^{2}h. The respective concentrations in the chambers were almost within the range of the lowest limit of quantification (LOQ) of the GC/MS system, 3 µg/m^3. Further investigation is required to fully understand why the TVOC emission increases with the addition of walnut, despite being very low. Significantly higher 3-day TVOC emissions from MDF were reported by Kim et al. (2010) and Son et al. (2013) of 300 µg/m^{2}h and 460 µg/m^{2}h respectively. In an adsorption process two types of interactions can occur between the solid and fluid phase: physisorption and

chemisorption (Rouquerol et al. 2014). As discussed previously in Chapter 4, the chemical nature of the material and its physical characteristics (e.g. open porosity, pore size distribution etc.) will determine if the interaction between the material surface and the organic pollutants is physical, chemical or even a combination of both. Materials such as cellulose from the wood fibres which have high surface area and chemical components with negative/positive charges or hydroxyl groups typically exhibit a combination of physisorption and chemisorption when exposed to organic pollutants. In the case of MDF panels, the reduction of formaldehyde emissions with the increase in walnut shell content can be attributed to the porous microstructure of shell surface, leading to a higher specific surface area, and hydroxyl groups present in the material as discussed previously.

5.3.2.2. Adsorption and desorption behaviour

The adsorption and desorption behaviour of MDF panels with walnut shell is shown in Figure 5.6. Adsorption/desorption curves represent the concentration of formaldehyde and VOCs in the chambers of each material plotted against the elapsed time. The difference of concentrations in the reference chamber and a chamber containing the material represents the amount of VOC adsorbed on to the material surface. Concentrations shown by the black line with squares represent the adsorption/desorption phase in the reference chamber. These concentrations are dependent on the emission rate of the VOC and formaldehyde sources. Toluene and formaldehyde sources showed a stable emission rate, but the emission rates of limonene and dodecane sources increased over the elapsed time, reaching their maximum after 215 hours. Considering the adsorption and desorption behaviour of all samples with respect to the four pollutants, toluene was the least adsorbed volatile compound and formaldehyde was the most. As observed in the previous chapter, less polar molecules have a lower affinity for adsorption compared to those with higher polarity such as formaldehyde. Aromatic and cyclic compounds, including toluene and limonene, were the least adsorbed. Similar observations were made in Chapter 4 of this thesis and also by Mansour et al. (2016) and Niedermayer et al. (2013). Within the non-polar group organic compounds (toluene, limonene and dodecane), dodecane was more preferentially adsorbed compared to toluene and limonene because it has a larger linear hydrocarbon chain and so has more oscillating charges associated with its electron cloud that can interact with electron clouds from the materials, as already discussed in Chapter 4. This facilitated the diffusion through pores and capillaries of the walnut shell and wood fibre by

physisorption (Gunschera, Markewitz, et al. 2013). Also, the lower vapour pressure would facilitate the physisorption of dodecane compared with toluene and limonene. At the end of the adsorption phase, the MDF sample with 15 % of walnut showed higher concentrations of limonene and dodecane in the chamber than the reference chamber. Further research needs to be undertaken to understand this finding.

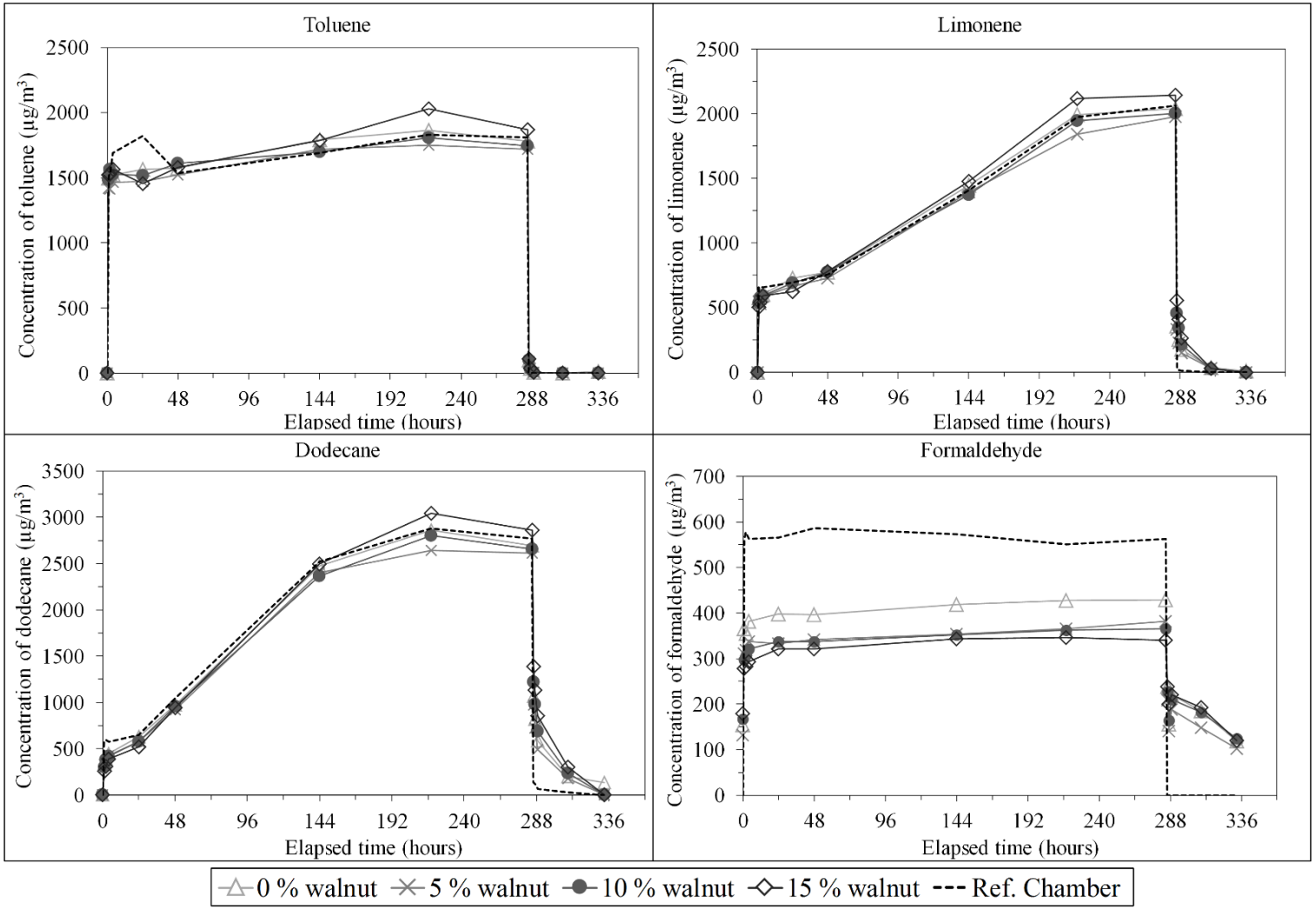

Figure 5.6 Adsorption and desorption curves of toluene, limonene, dodecane and formaldehyde.

The detail of the desorption behaviour is shown in Figure 5.7. During the desorption phase, the concentration of toluene, limonene and formaldehyde dropped immediately to 0 $\mu g/m^3$ in the reference chamber. Dodecane may have remained in the reference chamber slightly longer due to its higher molar mass compared with the other organic compounds. No toluene was detected in any chamber at five hours from the start of the desorption phase. The same was observed for limonene 24 hours after desorption began. At 48 hours, dodecane was still being desorbed by the pure MDF and formaldehyde was still being desorbed by all of the materials. Interestingly the MDF containing 15 % walnut exhibited the lowest concentration of formaldehyde during the adsorption phase in Figure 5.6, indicating that the MDF with higher content of walnut shell has a strong adsorption efficiency with regard to formaldehyde. A small perturbation at the beginning of the desorption phase of formaldehyde, at 285 hours, is visible in Figure 5.7. For all samples the formaldehyde concentration in the chamber dropped to a minimum at 287 hours before increasing again to a slightly higher value at 290 hours. This behaviour is consistent with two desorption processes taking place on/in the sample surface over these first few hours of desorption. It is beyond the scope of this investigation to confirm the exact nature of these observations, however it could be hypothesised that a proportion of the formaldehyde is surface adsorbed and can be released quickly into the pure air atmosphere. In addition, there may be formaldehyde present in the sub-surface pore network of the sample which must negotiate a certain diffusion path before final release into the chamber atmosphere, which would take more time. This behaviour may be a consequence of the difference in chemical and physical properties of the wood fibre and walnut shell phases present in the test specimens.

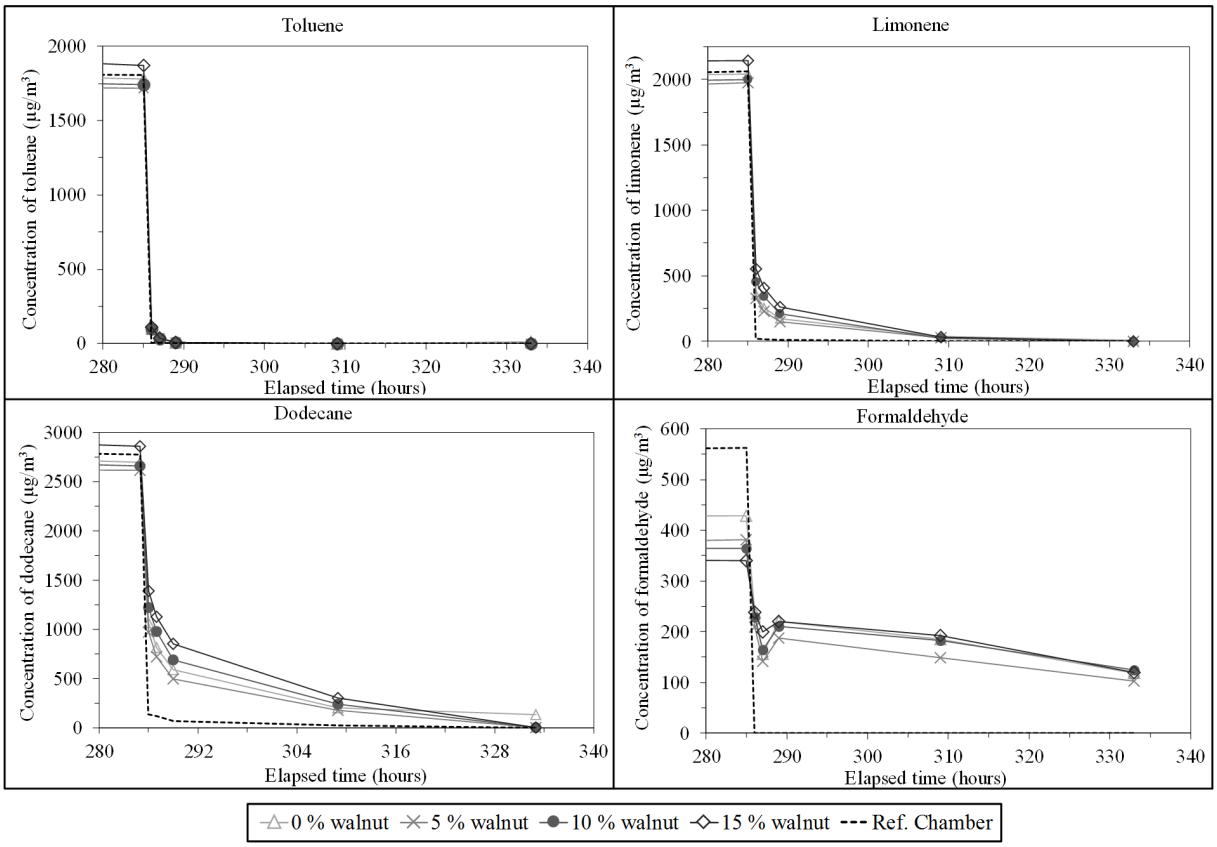

Figure 5.7 Desorption curves of formaldehyde in detail of by the wood panels with walnut.

The amount of formaldehyde and dodecane adsorbed and desorbed by the MDF panels during the adsorption and desorption phases is shown in Figure 5.8 a) and b), respectively. The mass of VOC adsorbed or desorbed was calculated as a product between the volumetric air flow through the chambers and the difference between concentrations in the test chamber and reference chamber, integrated over the period 0 to t hours; this being t = 285 hours for the adsorption phase and t = 48 hours for the desorption phase, using Eq. 4.1, as described in the previous chapter. The amount of formaldehyde adsorbed by the MDF panels increased from 528 µg to 798 µg when 15 % of walnut shell was added. MDF samples with 5 and 10 % walnut shell showed a similar amount of formaldehyde adsorbed, at 729 and 745 µg respectively. The difference between the mass of formaldehyde adsorbed and desorbed is the amount of formaldehyde that is still adhered to the material surface. If the desorption phase was carried out until the concentration in all chambers was 0 µg/m^3, this difference would represent the irreversible adsorption of formaldehyde. Although, as shown in Figure 8, at 333 hours of elapsed time (48 hours since the desorption phase started) all materials were still desorbing formaldehyde. On the other hand, in the case of dodecane, Figure 5.6, all chambers showed a

concentration of 0 µg/m^3 (except 0 % walnut MDF showing 134 µg/m^3), which means that MDF panels with 5, 10 and 15 % walnut desorbed all physisorbed dodecane by 48 hours from the start of the desorption phase. In this case, Figure 5.8 b) presents the amount of dodecane irreversibly adsorbed by the MDF panels with 5 and 10 % of walnut (i.e. a good sink effect). Pure MDF desorbed almost the same amount of dodecane as that adsorbed. In the case of MDF with 15 % of walnut, the amount of dodecane desorbed is higher than the amount adsorbed. This is the result of the concentration of dodecane in the chamber containing MDF with 15 % walnut being higher than the concentration in the reference chamber. Further research must be carried out to fully understand this finding.

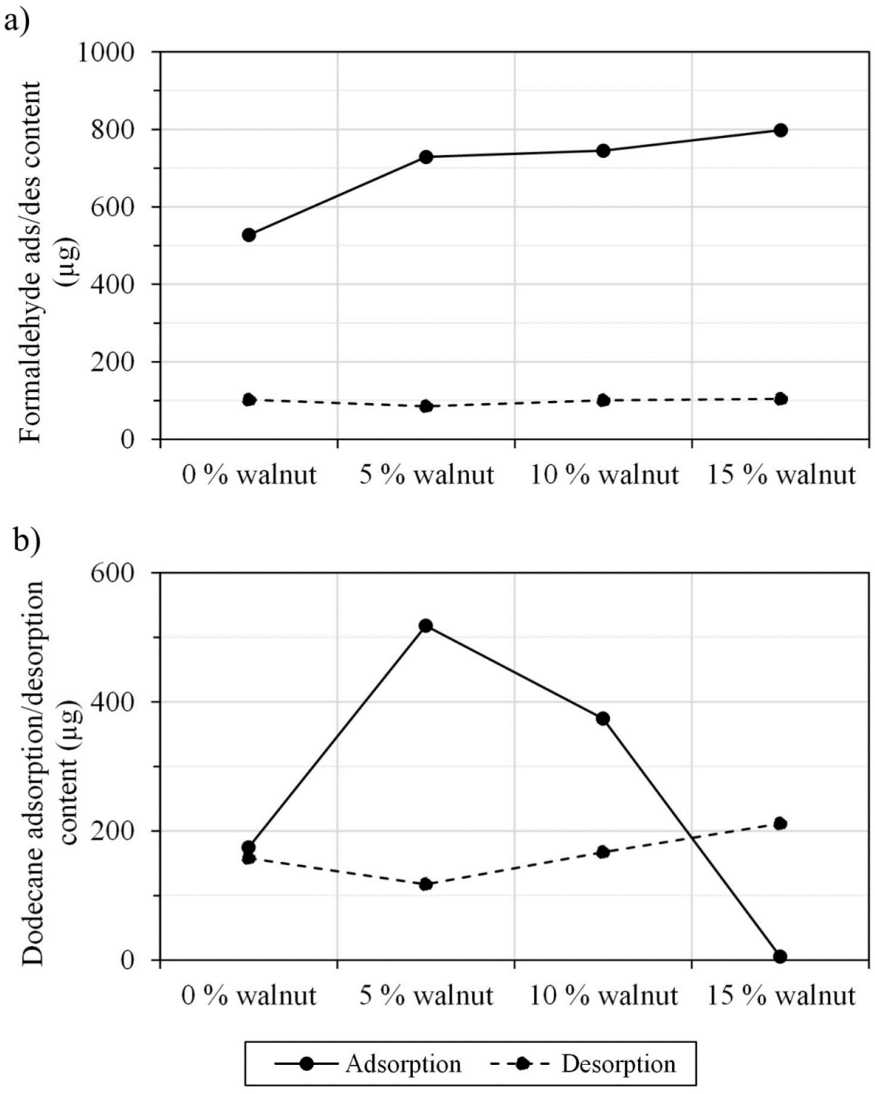

Figure 5.8 Amount of (a) formaldehyde and (b) dodecane adsorbed after 285 hours and desorbed after 48 hours for MDF panels containing 0, 5, 10 and 15 % walnut shell.

The MDF panel with 15 % walnut reduced the formaldehyde concentration in the chamber by 40 %. In contrast, the reference MDF (no walnut added) adsorbed 24 % of the formaldehyde. The results show that by adding 15 % of walnut to the MDF matrix the formaldehyde uptake is almost doubled, increasing from 24 to 40 %.

5.3.3. Moisture buffering

The moisture adsorption and desorption characteristics of the MDF control specimen (0 % walnut) and specimens with 5, 10 and 15 % walnut shell are presented in Figure 5.9. Three specimens of each type were tested and the error bars represent the 95 % confidence interval. Although an alternative method was used, the results can be compared against classifications for moisture buffering of materials proposed by (Rode et al. 2005). The MDF panel without any modification would be classified as *good*. Panels containing 10 % and 15 % walnut shell exhibited improvements of 34 % and 44 % respectively, leading to a moisture buffering material classification of *excellent*.

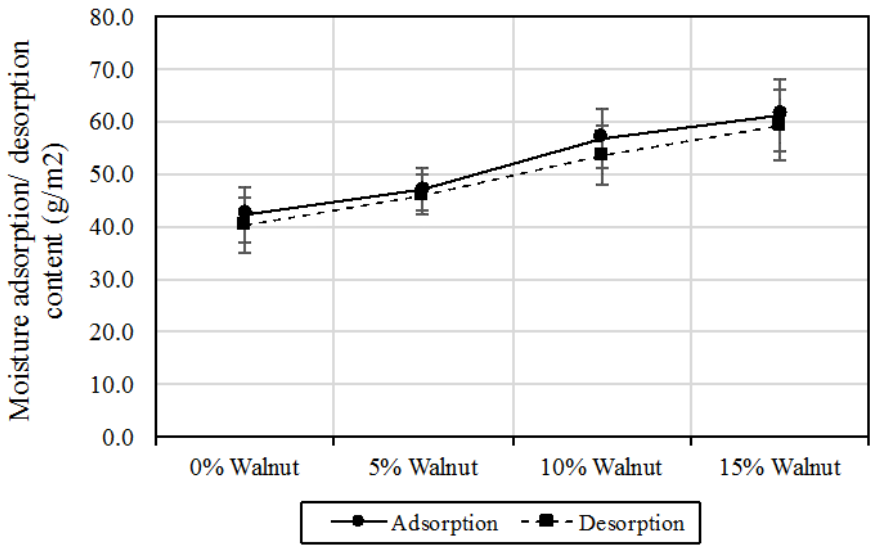

Figure 5.9 Moisture adsorbed by MDF panels with walnut shell.

5.4. Summary

- ✓ The surface of the walnut shell is very porous, leading to an increase of the surface area of the MDF panels with walnut shell added;
- ✓ The addition of walnut shell to the MDF matrix leads to a more compact microstructure, with smaller voids between the wood fibres;
- ✓ MDF panels with higher walnut shell content showed a greater ability to adsorb formaldehyde and moisture from the air;
- ✓ Polar compounds, such as formaldehyde and water, and aliphatic compounds with long linear molecular chains, such as dodecane, were adsorbed more readily by all materials when compared with the aromatic or cyclic compounds such as toluene and limonene;
- ✓ The removal of formaldehyde from the air was observed not only during the adsorption/desorption tests but also during the emissions testing. As well as the polarity of formaldehyde, its solubility in water may explain the better ability of the MDF with walnut shell to adsorb this compound, since the same material adsorbed more water during the moisture buffering analysis;
- ✓ MDF panels with 5 and 10 % walnut shell showed irreversible adsorption of dodecane which is an irreversible sink effect;
- ✓ The incorporation of walnut within the MDF panels showed excellent promise for the future of MDF as a building material. This is particularly important as MDF might often be identified as a problematic material due to its high formaldehyde emissions and perceived negative impacts on the health and wellbeing of humans exposed. Adoption of walnut shell as an additive in fibre-based building materials will not only improve indoor air quality, but also provide an alternative to landfill or incineration of the shell, with an associated reduction in embodied CO_2;
- ✓ Despite the present study being focused on the environmental performance of the MDF panels modified with walnut under ambient conditions to simulate the real conditions inside a building (i.e. 23 °C and 50 % RH), an interesting study would be to perform the VOCs and formaldehyde adsorption/desorption experiment at much lower relative humidity, i.e. dry conditions, to avoid the effect of water solubility of VOCs.

Chapter 6

Passive control of the IAQ with novel clay-based plasters and cellulosic- and wool-based lime mortars

6.1. Introduction

The development of novel building materials with improved properties such as hygrothermal control, thermal conductivity and acoustic isolation are important factors in optimising the performance of energy efficient buildings. The ECO-SEE project aimed to maximise the environmental performance of clay-based plasters and mortars by incorporating a range of bio-based products within commercially available materials.

Natural clays are often defined as materials resulting from the weathering of rocks. Their consistency is plastic at an appropriated water content and they harden if dried or fired (Bergaya and Lagaly 2013; Rouquerol et al. 2014). These materials have different origins and can be volcanic, hydrothermal, sedimentary etc. (Bergaya and Lagaly 2013). Being natural earthen materials, the chemical composition and particle shape of clays vary from one geological location to another. However, all clay minerals are the mineralogical constituents of hydrated phyllosilicates (*phyllo* = leaf shape) resulting from the fine-grained fraction of rocks, sediments and soils, e.g. kaolinite and montmorillonite. The thickness of each layer of the phyllosilicates may vary between 0.7 nm and 1 nm according to their molecular structure (Bergaya and Lagaly 2013; Rouquerol et al. 2014). Clay minerals with tetrahedral molecular arrangements may have Si^{4+}, Al^{3+} and Fe^{3+} as coordinating cations placed in the centre; the coordinating cations in an octahedral-like mineral are usually Al^{3+}, Mg^{2+}, Fe^{3+} or Fe^{2+}. Graphic representations of the structure of two common clay minerals are shown in Figure 6.1.

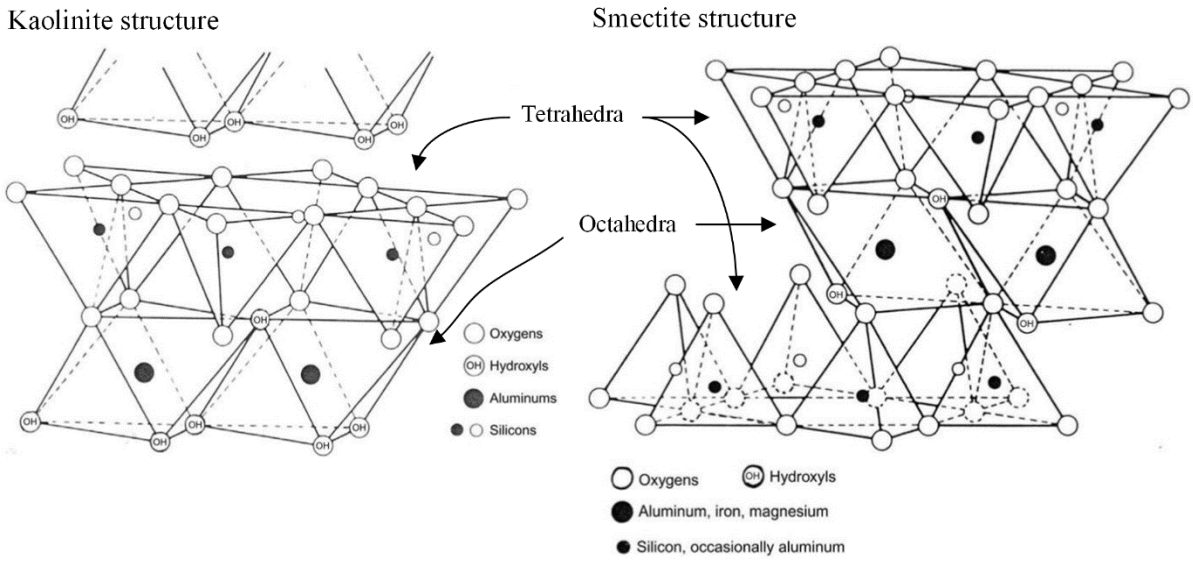

Figure 6.1 Structure of kaolinite and smectite showing the tetrahedral and octahedral arrangements. Adapted from Rouquerol et al. (2014).

Individual particles of clay minerals consist of multilayers, with some of these being separated by interlayer materials. The individual layers are held together by Van der Waals forces, hydrogen bonding or weak electrostatic attraction. The complex chemical composition of clay minerals and characteristic shape of the clay particles may be interesting features that have a bearing on the adsorption and desorption of VOCs. It is postulated that a favourable interaction would require materials with high specific surface area available with small pores and also surfaces with electronic charges which would attract the VOCs molecules in order to physisorb them.

Mortars are often used as a final coating (plaster) or as a base coat (render) and are composed of a binder (lime or cement) mixed with an aggregate (sand) and water (Gonçalves and Margarido 2015). These materials are available in the market as a pre-formulated mix or as just a binder (lime) ready to be mixed. The effect of some additives or modifiers is being investigated to either improve the environmental performance of the mortars, such as hygrothermal performance (Lucas et al. 2010; Gonçalves et al. 2014; Vieira et al. 2014; Maskell et al. 2017); or adding photocatalytic particles for indoor pollution control (Senff et al. 2013; Vieira et al. 2014; Giampiccolo et al. 2017); or to use of industrial waste to decrease their disposal in the landfill (Edwards et al. 2007; Senff et al. 2011; Labrincha et al. 2014; Modolo et al. 2013).

The effect of the addition of cellulosic flakes on the hygrothermal performance of lime mortars was investigated by Maskell et al. (2017). Contents of 2.5 % and 5 % by weight of cellulosic flakes were added to the lime matrix and compared to an unmodified reference lime mortar. The presence of the cellulosic flakes led to a decrease of the mortar's density, which had a negative influence on the mechanical properties. Despite this, the hygrothermal performance increased by over 25 %.

Natural wool fibres have been shown to have good ability to capture formaldehyde from the indoor air as shown in Chapter 4 and by other authors including Huang et al. (2007) and Curling et al. (2012). On the other hand, lime mortar showed good ability to adsorb toluene, limonene, dodecane as well as formaldehyde when compared with materials such as MDF and laminated MDF (see Chapter 4).

The present chapter presents the assessment of the potential for IAQ improvement by two novel clay plasters and pre-formulated lime mortars with cellulosic flakes and natural wool additions. The physical characteristics of the materials, such as porous microstructure and specific surface area, were investigated and correlated with their adsorption/desorption behaviour.

6.2. Materials and methods

6.2.1. Materials description

6.2.1.1. Clay based plasters and lime mortar with cellulosic flakes added

Clay plasters Clay_A and Clay_B, presented in Chapter 4, were further developed under the ECO-SEE project in association with project partners resulting in Clay_H2 and Clay_E14 formulations, Figure 6.2 a) and b), with the materials content as presented below:

- Clay_H2 – natural earthen clay (60 %), sand, brick powder, hemp sheaves, cellulose;
- Clay_E14 – natural earthen clay (43 %), pumice, brick powder, straw, cellulose;
- Cell_mortar – 5 % of cellulosic flakes (by weight) embedded in the pre-formulated lime mortar matrix.

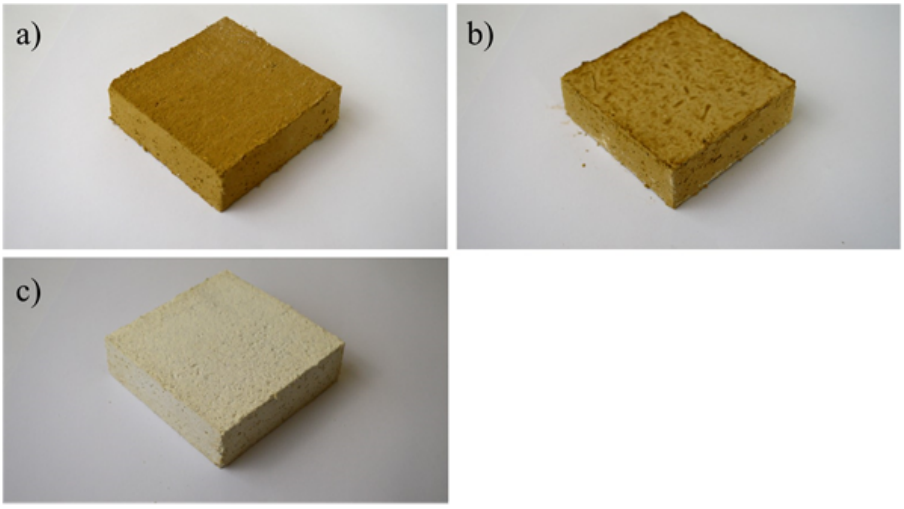

Figure 6.2 a) Clay_H2, b) Clay_E14 and c) Cell_mortar.

6.2.1.2. Lime mortar with natural wool additions

Wool lime mortars were prepared at the University of Bath, externally to the ECO-SEE project, following the standards BS EN 1015-2:1999 and BS EN 1015-11:1999. The formulation of these materials (pre-formulated lime + water) followed the suggestions given by the manufacturer (BCB). The amount of lime and water used was maintained as constant for all samples, and thus the effect of the wool on the porous microstructure could be studied. The amount of wool added as a proportion of the weight of lime was 1 and 2.5 %, Figure 6.3. One extra specimen was prepared, the TL w_mortar. This specimen had the same formulation as the reference mortar, although in this particular case a thin layer of wool was added to the top of the specimen straight after mixing (TL – top layer).

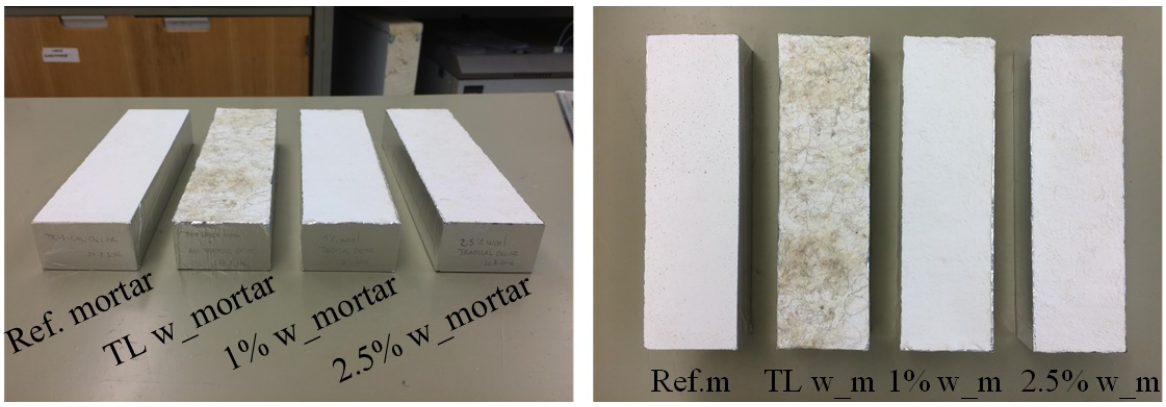

Figure 6.3 Photographs of the lime mortars with different amounts of natural wool added.

The workability of a fresh mortar was characterised by its flowability. The effect of the wool fibres on the flowability of the mortars, measured in a flow-table following the standard BS EN 1015-3:1999, is presented in Table 6.1. Clearly, the presence of the wool fibres had an influence on the workability of the fresh mortar. As expected, the higher the wool content, the lower the flowability of the mortar. The addition of the wool fibres required a higher amount of water for the mixture, which in fact was kept constant for all formulations, and therefore its flowability decreased.

Table 6.1 Effect of the wool fibres on the flowability of the pre-formulated lime mortar.

Material	Flowability (mm)
Ref mortar / TL w_mortar	200 × 205
1 % w_mortar	160 × 165
2.5 % w_mortar	140 × 140

6.2.2. Materials characterisation and IAQ assessment

The porous microstructure of all materials was investigated by SEM and specific surface area by nitrogen adsorption BET isotherms. As the materials studied in this chapter resulted from development of those presented in Chapter 4 and no unknown chemical additives were added, a chemical characterisation was not carried out. TVOC and formaldehyde emissions and adsorption/desorption test for all materials were performed in the test rig containing 2-litre chambers described previously in section *3.5.1 Rig assembly - 2-litre environmental chambers*. The formaldehyde adsorption/desorption testing of the lime mortars with wool was also compared with traditional Gypsum plaster. The IAQ assessment of the specimen Clay_E14 was also carried out in the 30 m^3 chamber, described previously in section *3.5.2 Rig assembly - 30 m3 chamber*. In this case, a panel with two opposite surfaces of 1 m^2 each was placed in the centre of the room. This was decided in collaboration with other partners of the ECO-SEE project.

The following results and discussion section of this chapter considers the testing of each group of materials, i.e., clay based plasters and mortar with cellulosic flakes, mortars with natural wool added in the 2-litre chambers and the Clay_E14 specimen in the 30 m^3 chamber.

6.3. Results and discussion

6.3.1. Clay plasters and lime mortar with cellulosic flakes – 2-litre chambers

6.3.1.1. Materials characterisation

The SEM images of the Cell_mortar, presented in Figure 6.4 a) and b), show that the incorporation of the cellulosic flakes into the mortar matrix did not cause any noticeable changes in the macro- and microstructure of the mortar. This is confirmed by comparing the Cell_mortar SEM images with those of the Mortar_P presented previously in Figure 4.13 of section *4.3.1.2 Physical characterisation*. The cellulosic flakes are evenly spread in the mortar matrix and completely surrounded by the lime mortar particles, see Figure 6.4 a). The macrostructure of Clay_E14 and Clay_H2 are shown to be similar, Figure 6.4 c) and e) respectively. The bio-based additives incorporated in the specimen Clay_H2 are shown in Figure 6.4 e) and g), these being hemp shiv and cellulosic fibre. At the macro scale, only the pores between big particles/aggregates of the clay-based plaster matrix are noticeable. However, at higher magnifications, it is possible to identify smaller particles and pores of sizes under 500 nm, Figure 6.4 f) and h). A mineral clay particle may possess a wide range of shapes including: platelets, tubules, laths, fibres and needle-like structures (Bergaya and Lagaly 2013). The natural earthen clays used to produce the materials Clay_E14 and Clay_H2 have particles with irregular shapes although these are somewhat similar to platelets, Figure 6.4 h).

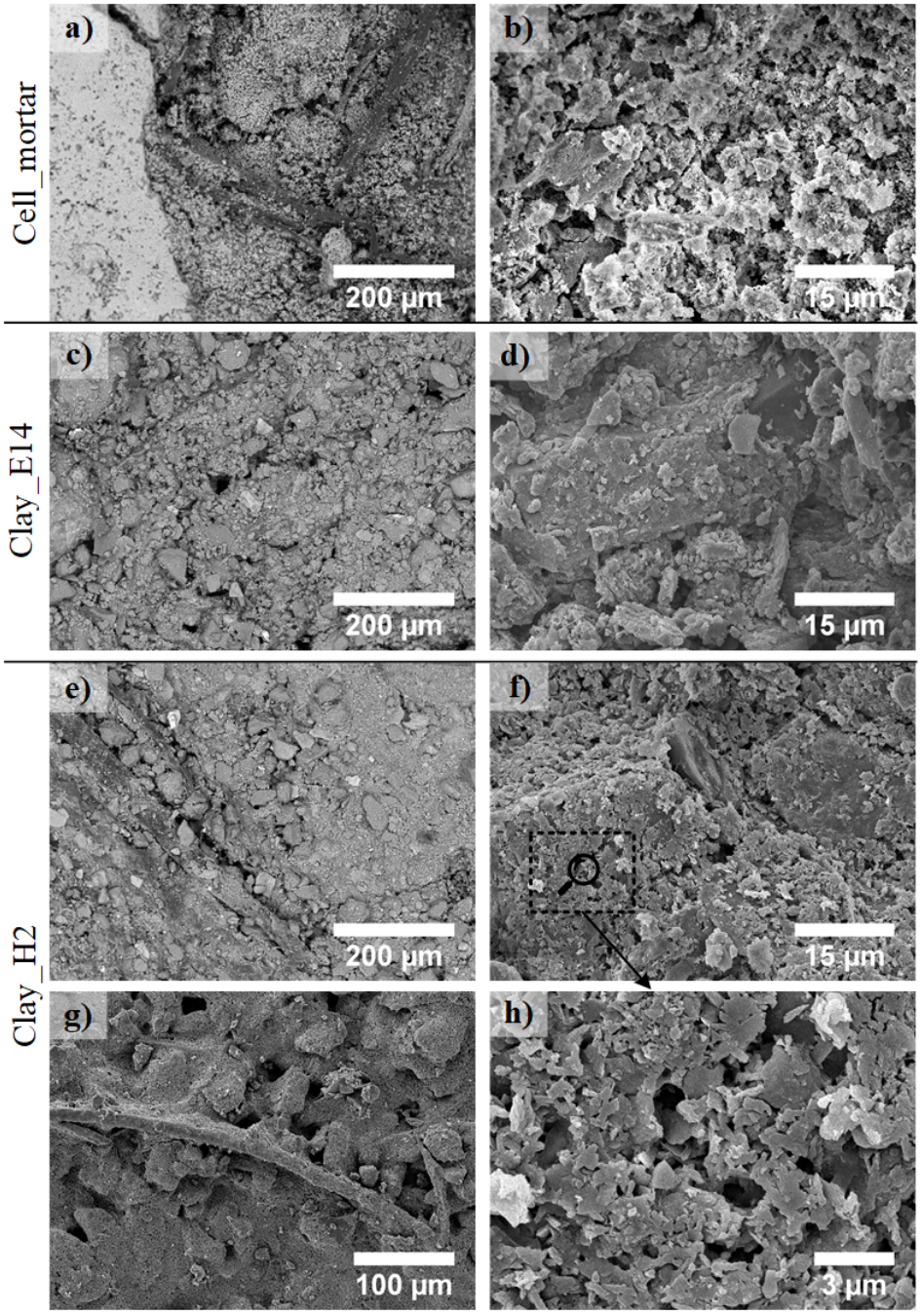

Figure 6.4 Scanning electron microscopy images of the Cell_mortar, Clay_E14 and Clay_H2. Two or more different magnifications are shown for each specimen type.

The specific surface area of both clay plasters and the Cell_mortar is shown in Figure 6.5. Clay_E14 and Clay_H2 have the same average specific surface area of 4.6 m^2/g. However, the standard deviation of Clay_E14 is slightly higher than the Clay_H2. These results are in accordance with the SEM images shown in Figure 6.4 which show the similarities between the microstructure of both clay plasters. Cell_mortar has a lower specific surface compared to the clay plasters, at 3.1 m^2/g.

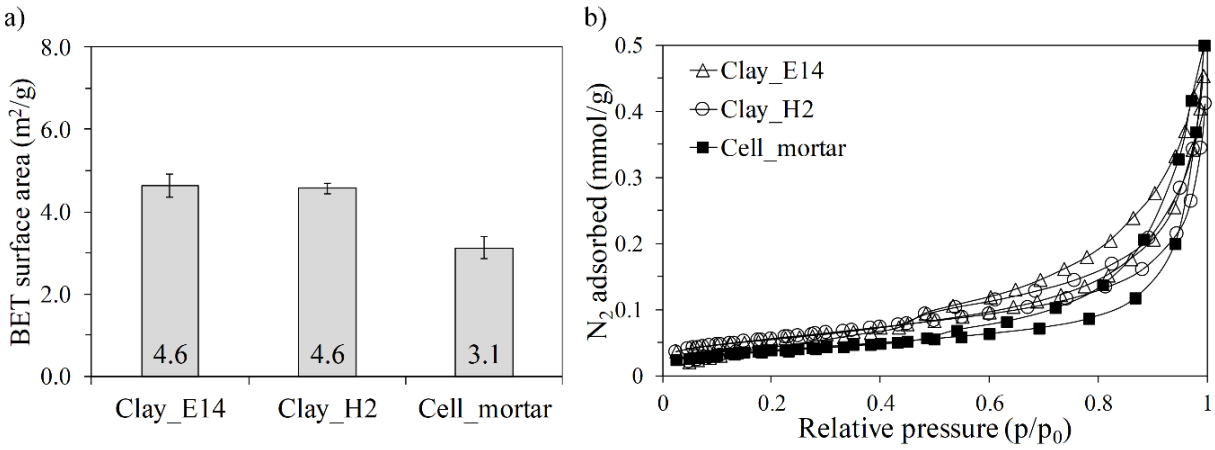

Figure 6.5 a) BET surface area and b) nitrogen adsorption isotherms of Clay_E14, Clay_H2 and Cell_mortar.

6.3.1.2. IAQ - Emissions testing

The TVOC and formaldehyde area specific emission rates, after 3 days of testing, of both clay plasters were very low, less than 3 µg/m^{2}h of TVOC and less than 2 µg/m^{2}h formaldehyde, Table 6.2. These values of emission rate are of the same order of the GC/MS and HPLC detection limits used for the analysis of the emission samples. The Cell_mortar specimen showed a slightly higher emission rate, about 21 µg/m^{2}h for TVOC and 7 µg/m^{2}h for formaldehyde. After 28 days, no emissions of TVOC or formaldehyde were detected in any material.

Table 6.2 TVOC and formaldehyde area specific emission rate after 3 and 28 days of Clay_E14, Clay_H2 and Cell_mortar.

Material	**TVOC (µg/m^{2}h)**		**Formaldehyde (µg/m^{2}h)**	
	3 days	28 days	3 days	28 days
Clay_E14	2.9	nd	nd	nd
Clay_H2	2.6	nd	1.9	nd
Cell_mortar	20.9	nd	6.9	nd

nd – not detected.

6.3.1.3. IAQ - Adsorption and desorption behaviour

Figure 6.6 shows how the Cell_mortar, Clay_E14 and Clay_H2 behave when exposed to gaseous toluene, limonene, dodecane and formaldehyde. Concentrations of the three VOCs and formaldehyde were fairly constant over the time in the reference chamber. Both clay plasters showed very similar adsorption/desorption behaviour for toluene, limonene and dodecane, in fact, the curves of both materials almost overlap. This may be due to the similarities in the microstructure and specific surface area of both clay-based materials. In the case of the formaldehyde, the Clay_H2 specimen showed a higher ability to adsorb this organic pollutant compared to the Clay_E14. This may be due to the interactions between the VOC's molecules and the sand or pumice (so-called volcanic glass) particles present in the Clay_H2 and Clay_E14, respectively, indicating that polar molecules such as formaldehyde may be more preferentially adsorbed onto crystalline silica (quartz) from the sand grains than onto the amorphous silica within the pumice. In general, the mortar with cellulosic flakes incorporated showed a lower capacity to capture VOCs. During the desorption phase, all VOC concentrations dropped to 0 $\mu g/m^3$ after 1 hour of exposure to clean air. At the end of the adsorption/desorption experiment, all materials had already desorbed all the toluene, limonene and formaldehyde that was previously adsorbed, but dodecane was still being desorbed at very low concentrations, less than 50 $\mu g/m^3$.

Considering a real-scale situation, i.e. a room being polluted with formaldehyde as an example, the levels of the concentrations in the reference chamber to those in the testing chambers should be considered. If the room had the Cell_mortar or one of both clays with the same loading factor as used in the 2-litre chambers (m^2/m^3), these materials would have the capacity to reduce the concentration of dodecane from 1200 $\mu g/m^3$ to 500 $\mu g/m^3$ which equates to 58 % less, despite still being higher than the proposed guidelines discussed in Chapter 2. In cases like this, where the source of the organic pollutant is not found and removed, other strategies can be applied such as increased ventilation. Usually, in real buildings the formaldehyde concentrations are not as higher as those used in this research. Such high concentrations of toluene, limonene, dodecane and formaldehyde were chosen here in order to 'simulate' the worst possible case scenarios.

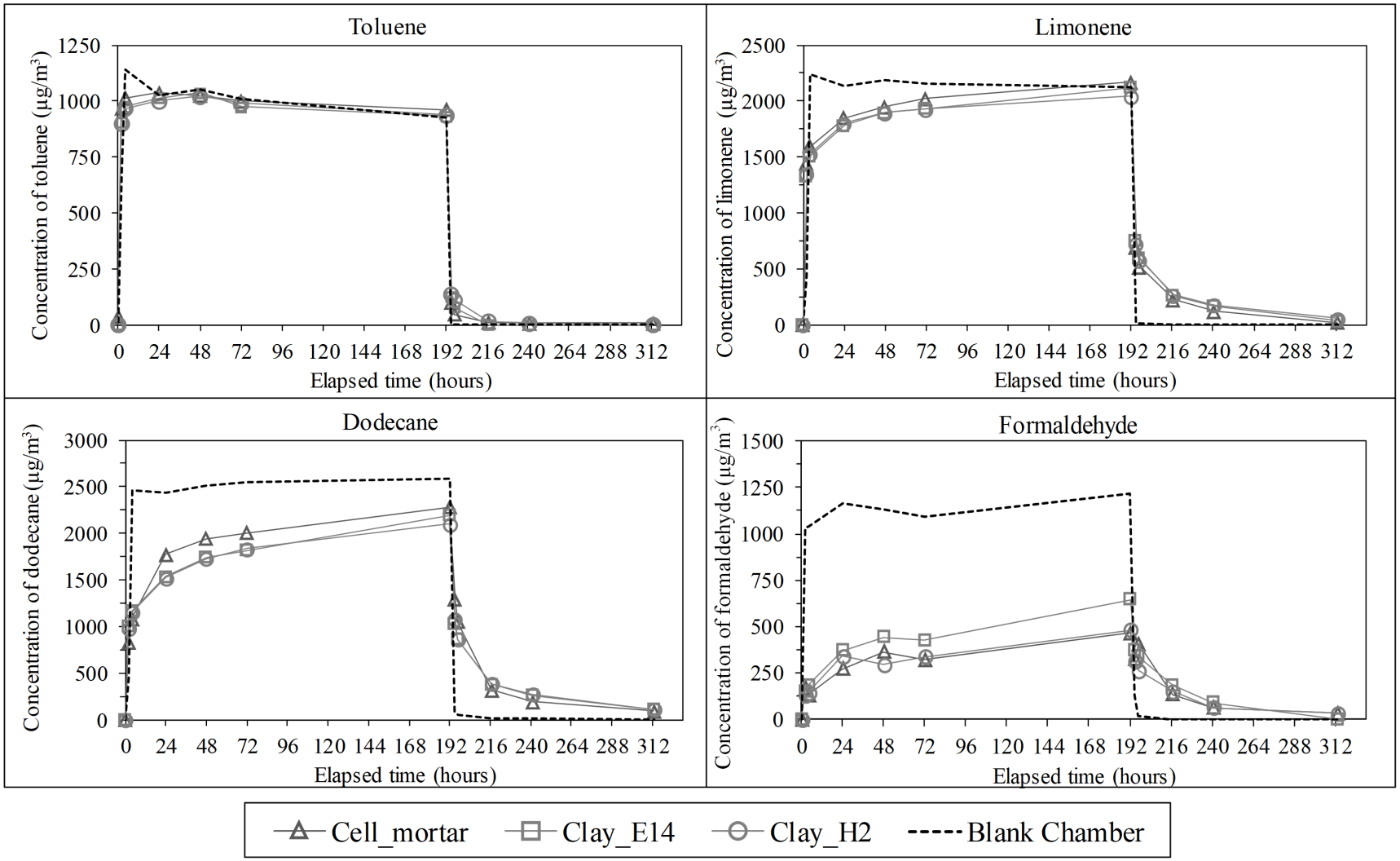

Figure 6.6 Adsorption and desorption curves of VOCs and formaldehyde by Clay_E14, Clay_H2 and Cell_mortar.

The mass of dodecane and formaldehyde adsorbed and desorbed by both clay plasters and the lime mortar with cellulosic flakes is shown in Figure 6.7. When the adsorption/desorption experiment finished, concentrations of formaldehyde in the testing chambers were 0 μg/m^3 (or very close), so it may be assumed in the calculation that of the mass of formaldehyde desorbed was the exact quantity of formaldehyde desorbed. Therefore, the difference between the mass adsorbed and desorbed is the amount of formaldehyde that was irreversibly adsorbed onto the material surface. In the case of the clay-based materials, this may be due to the strong Van der Waals forces and hydrogen bonding between the surface of the clay particles and the VOC molecules. The cations present in the top layers of the clay particles would attract the VOC molecules due to the presence of positive charges. Also, hydroxyl groups play an important role in attracting VOCs molecules, especially the most polar such as formaldehyde. When it is said that an organic compound is irreversibly adsorbed onto the material surface this means that, under steady conditions, i.e. where temperature, RH and ventilation are kept constant, the molecules of VOC will remain adsorbed.

At the end of the experiment, dodecane was still being desorbed by the material's surface, although in very small concentrations. Therefore, the mass of dodecane desorbed by the materials is not the real figure but it can be considered to be close to the real value as it is almost all desorbed. Therefore, both clay plasters showed the capacity to remove (without desorbing) approximately 1000 μg of VOC. The specimen Cell_mortar showed a slightly lower capacity to capture dodecane, around 800 μg. The better ability of both clay plasters to adsorb and keep the VOCs molecules adsorbed on the material surface may be due to the complex structure of clay mineral layers, within which the VOC molecules could diffuse through nanosized pores if exposed to polluted air for enough time. Schematics of the assembly of a clay particle composed of several layers of clay minerals are shown in Figure 6.8.

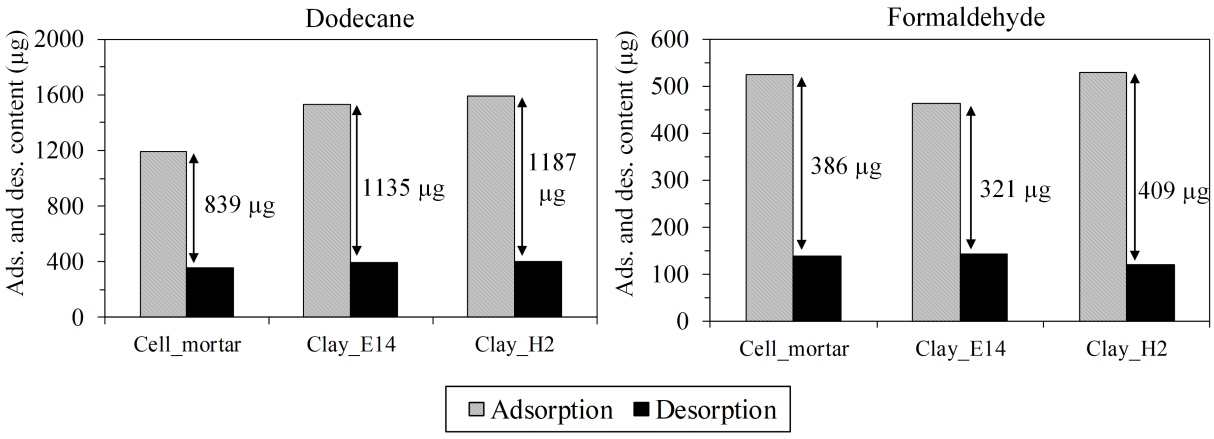

Figure 6.7 Mass of limonene, dodecane and formaldehyde adsorbed and desorbed by Cell_mortar, Clay_E14 and Clay_H2.

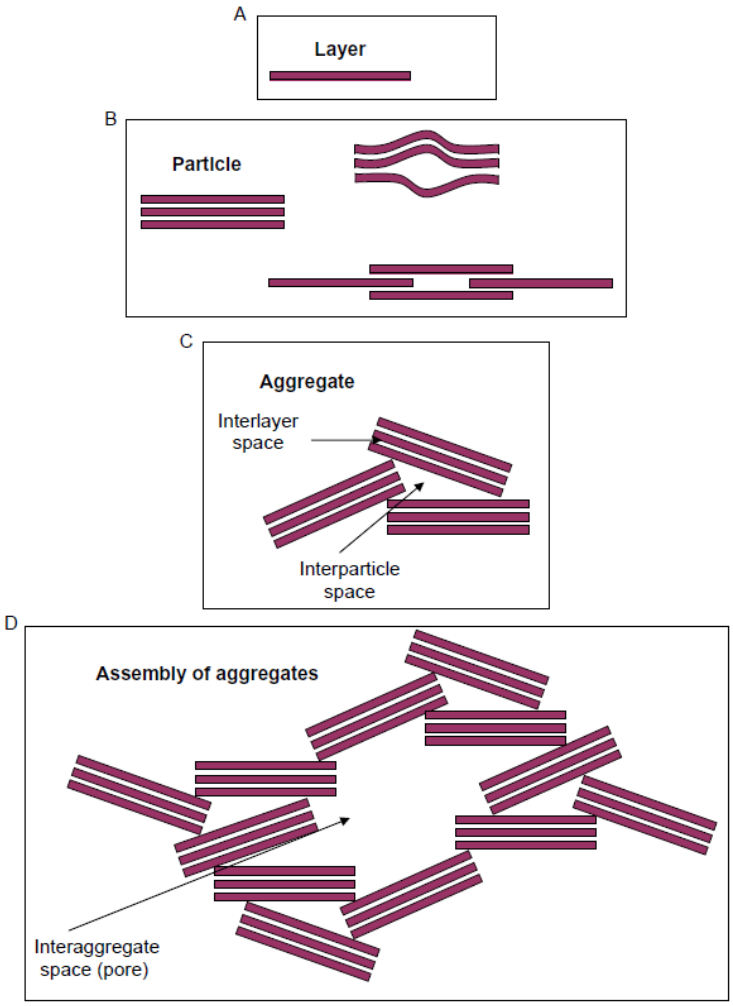

Figure 6.8 Illustration showing: a) clay mineral layer, b) clay particle composed by several layers, c) aggregate composed by several particles and d) assembly of aggregates. Figure taken from Bergaya and Lagaly (2013).

6.3.2. Lime mortar with natural wool – 2-litre chambers

The effect of the incorporation of Natural wool on the VOCs and formaldehyde adsorption/desorption behaviour of lime mortars is discussed in this section. In the case of the formaldehyde adsorption and desorption, lime mortars with wool added were also compared to the widely-used traditional plaster – gypsum.

6.3.2.1. Materials characterisation

The comparison between the porous macrostructure of gypsum and mortars with wool incorporated is shown in Figure 6.9 and the effect of the wool fibres on the microstructure of the mortar in Figure 6.10. At low magnifications, the differences in the macrostructure of the gypsum and Ref. mortar are only slightly noticeable, Figure 6.9 a) and b). However, at higher magnifications, by comparing Figure 6.10 a) and b), it is observed that the microstructures of both materials are completely distinct. Gypsum is composed of big particles of calcium sulphate (~ 5 - 20 μm) whereas the Ref. mortar specimen is comprised of various different particles shapes, such as round, elongated, rod and thin fibres (see Figure 6.10 b), c), d) and f), respectively).

The effect of the wool fibres on the microstructure of the lime mortar is primarily analysed in Figure 6.9. The arrangement of the fibres within the lime matrix is random, due to the good dispersion of the fibres during the mixing of the fresh mortar; as shown in Figure 6.9 c) and d), the fibres are placed horizontally or vertically in relation to the surface of the mortar. With regard to the lime microstructure surrounding the wool fibres, it remains very similar, no significant changes are observed. By investigating the interface between the wool fibre and the lime matrix, Figure 6.9 c) and e), it is observed that there is a gap between the lime particles and the wool fibre surface due to less than 100 % being in contact. This effect led to the creation of ‘tunnels’ throughout the lime mortar microstructure which, may help the diffusion of VOCs when the material is exposed to polluted air.

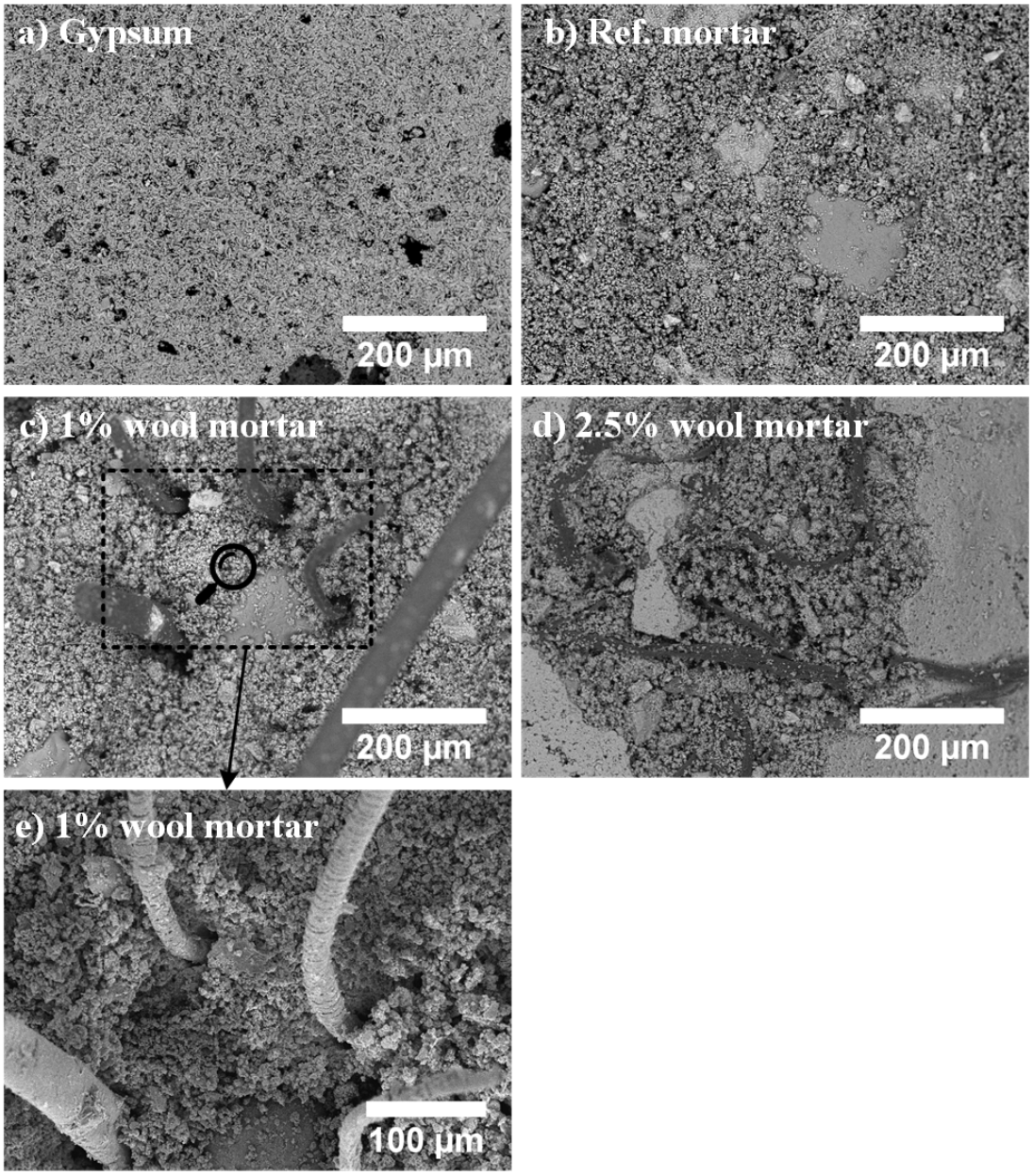

Figure 6.9 Scanning electron microscopy images of the Gypsum plaster, Reference mortar, 1 % wool lime mortar and 2.5 % wool lime mortar.

The microstructure of the lime mortars with 1 % and 2.5 % wool were shown to be very similar with no major differences, see Figure 6.10 g) to k). This means that the major effect of the incorporation of the wool fibres is the creating of tunnels where the fibres are placed but it does not change the original microstructure of the lime mortar. In Figure 6.10 k) it is possible to see pores with sizes under 300 nm.

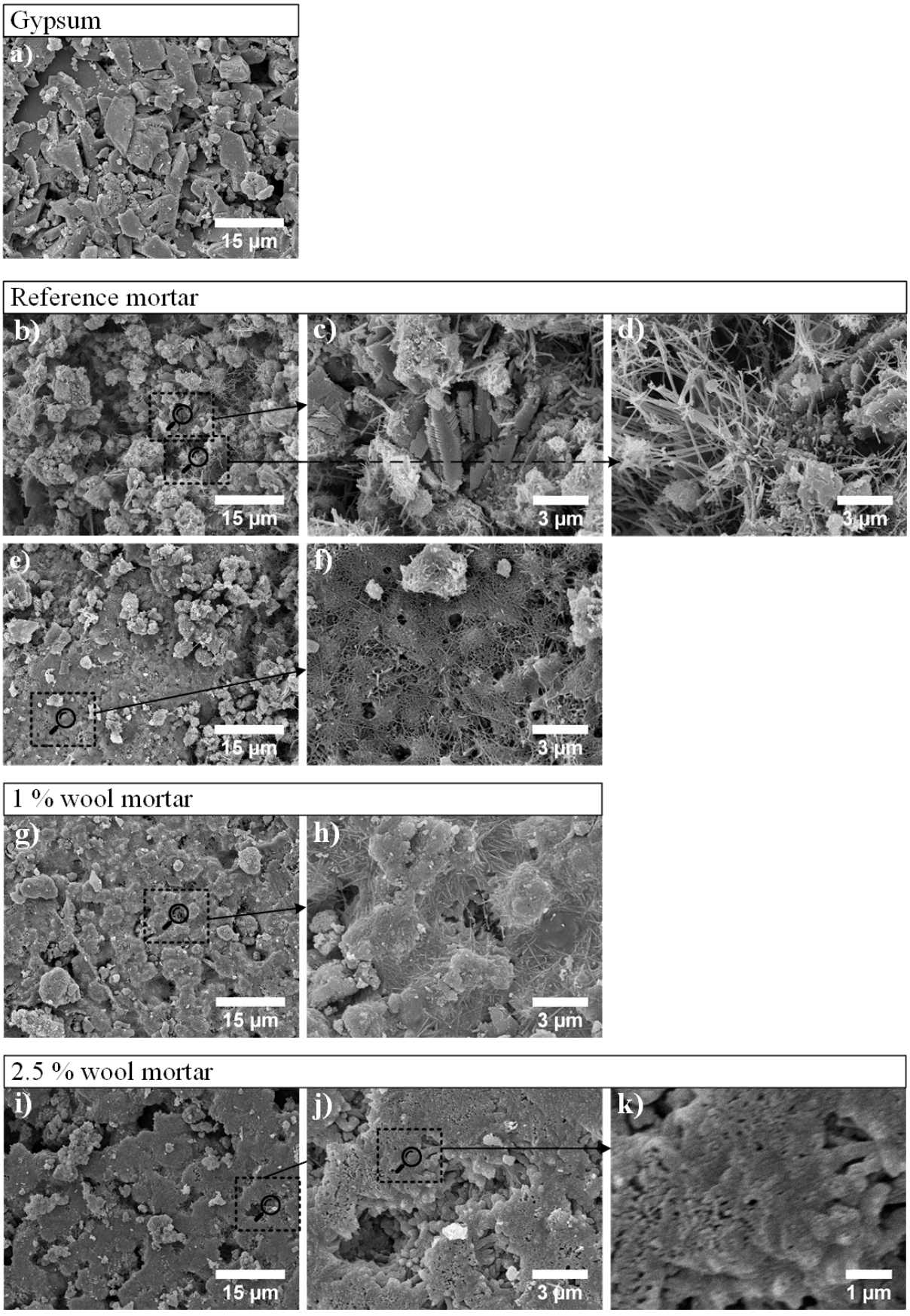

Figure 6.10 Scanning electron microscopy images of the Gypsum, Reference mortar, 1 % wool lime mortar and 2.5 % wool lime mortar.

The influence of the incorporation of natural wool fibres on the specific surface area of the lime mortar is shown in Figure 6.11. The results for the mortars were also compared to gypsum. By adding 1 % natural wool the specific surface area of the resulting mortar did not change, however when 2.5 % was added the specific surface area decreased slightly from 5.3 to 4.7 m^2/g. As shown previously in the SEM images of Figure 6.9 and Figure 6.10, the incorporation of the wool fibres into the lime mortar matrix did not cause significant changes in the microstructure. The presence of the fibres only created tunnels in the lime mortar matrix where the fibres were placed. The surrounding particles of mortar have the same microstructure as the Ref. mortar. This explains why the addition of the fibres had only a slight influence on the specific surface area of the lime mortar. The reason why it decreased with the addition of 2.5 % of wool fibres is because of the lower surface area of the fibres in relation to the lime mortar matrix.

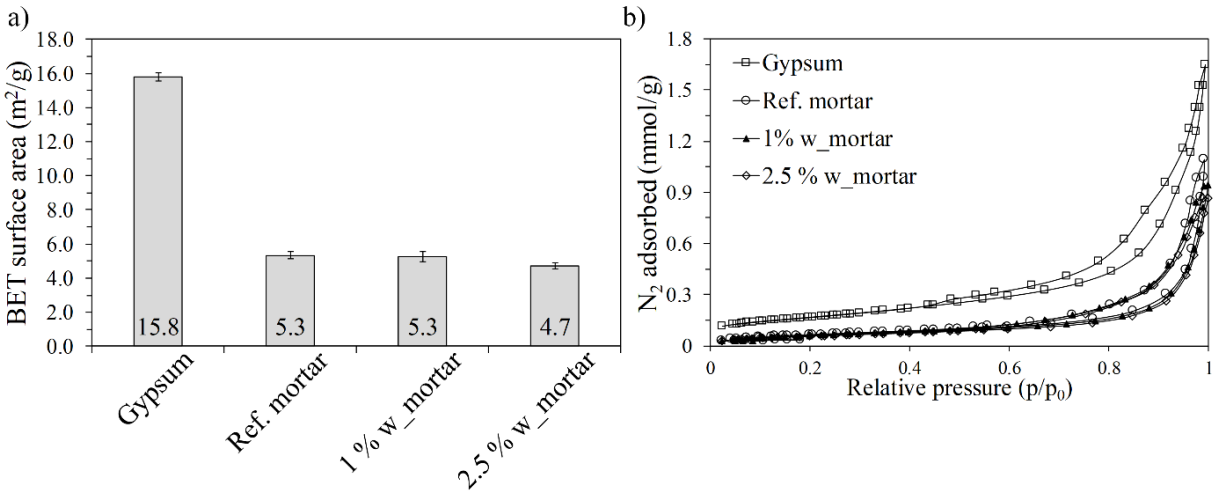

Figure 6.11 a) BET surface area and b) nitrogen adsorption isotherms of gypsum and lime mortar with different amounts of natural wool.

The pore size distribution, porosity and average pore diameter, analysed by mercury intrusion porosimetry, of the Ref. mortar and the gypsum specimens is presented in Figure 6.12 and Table 6.3. The wider pore size distribution of Ref. mortar, see Figure 6.12, is due to its greater variety of particles sizes and shapes as shown previously in Figure 6.10 c), d) and e). In addition to this, its percentage of porosity and average pore size are lower than those measured in the gypsum specimen. The results for the physical characteristics of the Ref. mortar and gypsum

obtained by MIP are in accordance with the microstructures analysed by SEM shown in Figure 6.9 and Figure 6.10.

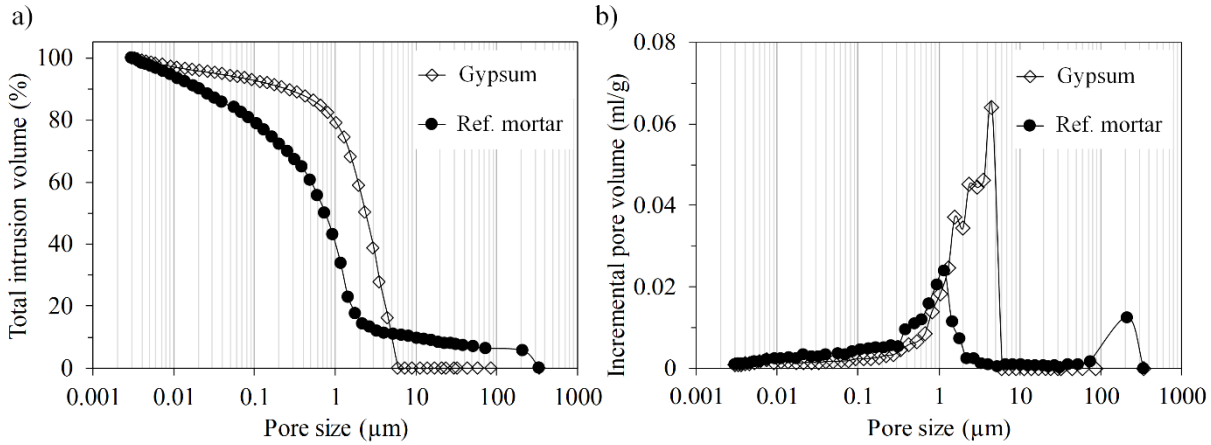

Figure 6.12 a) Cumulative pore size distribution and b) pore size distribution analysed by MIP.

Table 6.3 Physical characteristics analysed by MIP.

Material	**Gypsum**	**Ref. mortar**
Porosity (%)	38.5	35.4
Average pore diameter (µm)	2.37	0.67

6.3.2.2. IAQ - Emissions testing

In Table 6.4 the TVOC emissions rates of the wool lime mortars and gypsum are presented. After 3 days of placing the samples in the 2-litre chambers, the TVOC area specific emission rate was very low, near 0 µg/m^{2}h, for all samples. The results of the emissions from the gypsum specimen were taken from Figure 4.15 and Figure 4.16 from Chapter 4 of this thesis. After 28 days, no TVOC or formaldehyde was detected. The major compound emitted, n-undecane, is commonly found in fuels and solvents and thereby can be related to the calcination of the air-lime during its manufacturing.

Table 6.4 TVOC and formaldehyde area specific emission rate after 3 days for gypsum and mortar samples with different amounts of natural wool.

Material	TVOC ($\mu g/m^2h$)	Formaldehyde ($\mu g/m^2h$)
Gypsum*	31	9
Ref. mortar	0.15	nd
TL w_mortar	0.15	nd
1 % w_mortar	0.15	nd
2.5 % w_mortar	0.15	nd

* Data presented in Chapter 4.
nd – not detected

6.3.2.3. IAQ - Adsorption and desorption behaviour

The toluene, limonene, dodecane and formaldehyde adsorption/desorption behaviour of the lime mortars with natural wool is shown in Figure 6.13. In the case of formaldehyde, the adsorption/desorption behaviour of the modified lime mortars was also compared to the gypsum plaster. The average maximum concentration of organic pollutants in the reference chamber was 2000 $\mu g/m^3$ for toluene, 2100 $\mu g/m^3$ for limonene, 1800 $\mu g/m^3$ for dodecane and 300 $\mu g/m^3$ for formaldehyde.

24 hours after the adsorption phase had started, concentrations of toluene in the chambers with testing materials were higher than the reference chamber. This can be related to the saturation of the material's surface. The same behaviour was observed in other materials as shown previously Chapter 4, Figure 4.18 and Chapter 5 in Figure 5.6. The effect of the wool incorporation on adsorption/desorption of the lime mortar was not noticeable. Limonene was adsorbed until the desorption phase started; however, at 192 hours (last adsorption sampling point) concentrations in the chambers with materials were approaching values similar to that of the concentration in the reference chamber. Ref. mortar, TL w_mortar and 1% w_mortar specimens were showed to have a similar behaviour in the adsorption and desorption phases. The sample of 2.5% w_mortar adsorbed less limonene than the other materials. Dodecane was the most adsorbed VOC of all the materials. This may be related to the physicochemical properties of the VOCs as discussed in Chapter 4 of this thesis. After 48 hours of adsorption, TL w_mortar and 1% w_mortar specimens followed the same trend during the adsorption phase

observed for limonene. Mortar with 2.5 % wool adsorbed less dodecane than the other materials.

By looking at the adsorption and desorption curves of formaldehyde, it is clear that gypsum has less ability to adsorb formaldehyde and thereby the concentration in its chamber was higher than the other materials (closer to that in the reference chamber). After 144 hours of the adsorption phase the concentration in the chamber of the gypsum plaster was similar to the reference chamber concentration, meaning that this material was reaching its saturation point. Lime mortars with natural wool incorporated showed a higher ability to adsorb formaldehyde. The concentration in the chambers of 1% w_mortar and 2.5 % w_mortar specimens were always below 20 $\mu g/m^3$ compared to 300 $\mu g/m^3$ in the reference chamber.

In the desorption phase, the Ref. mortar and TL w_mortar exhibited similar behaviour after 24 hours. This is related to the formaldehyde being physisorbed on the lime mortar surface; the porous microstructure of the lime is the same for both materials, and thus the desorption rate is similar. Those formaldehyde molecules that were chemisorbed by the natural wool fibres would not be desorbed if the experimental conditions were kept the same. Mortars with 1 % and 2.5 % of wool incorporated behaved similarly in the formaldehyde desorption phase.

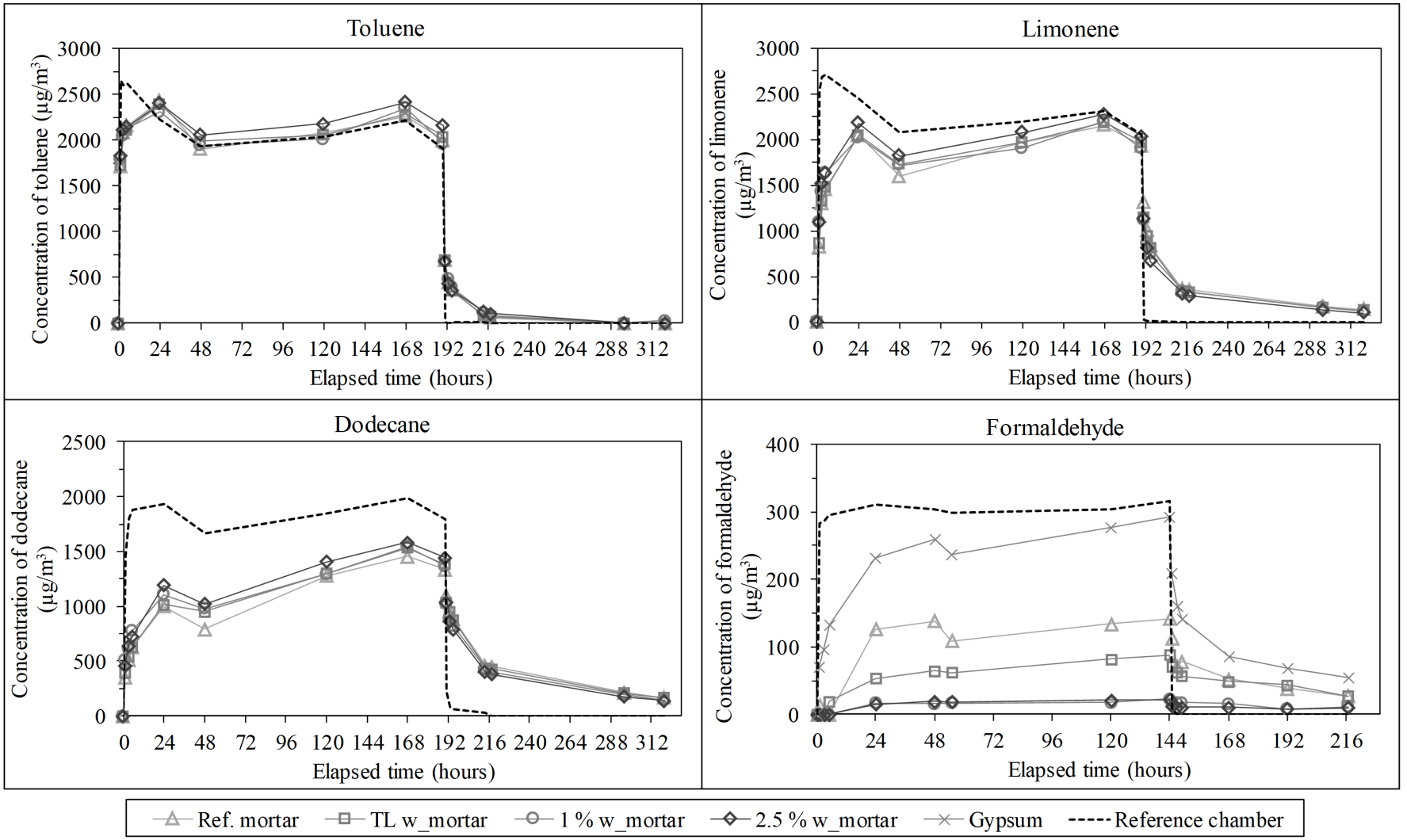

Figure 6.13 Adsorption and desorption curves of VOCs and formaldehyde by lime mortar with different natural wool content. In the case of the formaldehyde adsorption and desorption, gypsum was also compared with the wool lime mortar samples.

The mass of limonene, dodecane and formaldehyde adsorbed and desorbed by the lime mortars with wool incorporated and gypsum is presented in Figure 6.14. The adsorption/desorption of limonene and dodecane were affected by the incorporation of the wool fibres in the lime mortars, with a slight decrease. In Chapter 4, the adsorption and desorption of toluene, limonene, dodecane and formaldehyde by natural wool was investigated and it was observed that this material had a very low ability to capture toluene, limonene or dodecane, although it showed very good capacity to adsorb formaldehyde. Transferring this knowledge to the current discussion, the interactions between the lime mortars with wool incorporated is governed by the mortar characteristics, namely specific surface area. Therefore, as the incorporation of the wool fibres led to a slight decrease in the specific surface area of the mortars, their capacity to adsorb VOCs had also decreased slightly.

In the case of the mass of formaldehyde adsorbed and desorbed by the modified mortars and gypsum, the incorporation of the natural wool led to an increase of the formaldehyde adsorbed. The difference between 1 % w_mortar and 2.5 % w_mortar is negligible indicating that 1 % is the ideal content of wool in order to improve the capacity of lime mortar to capture formaldehyde from the indoor air. All wool contents higher than 1 % would be a waste of resources as the adsorption and desorption capacity of the modified material is not improved. In addition to the outstanding ability of the 1% w_mortar to capture formaldehyde, the desorbed mass of formaldehyde is very low, less than 10 μg - which indicates irreversible adsorption. In a real case, if this material is installed in a room which will be polluted with formaldehyde, this material would have the capacity to quickly remove the formaldehyde from the indoor air without desorbing it later or desorbing at very low concentrations which would not affect human health. The formaldehyde that would be desorbed is the component which is physisorbed by the lime mortar.

Despite the higher specific surface area measured by BET, the gypsum showed a much lower adsorption capacity of formaldehyde and also a lower sink effect compared with the modified lime mortars. This indicates that, for a more comprehensive investigation of the adsorption and desorption behaviour of the building materials, several characterisation techniques should be taken into account to fully analyse the physical and chemical characteristics of the materials. Each characterisation technique complements the other.

From these results, it is concluded that the specific surface area or porosity (physical characteristics) do not always play the main role in the capacity to adsorb and desorb, as is the case for the adsorption/desorption of formaldehyde by gypsum and the Ref. mortar. As shown

previously in the physical characterisation section of these materials in section *6.3.2.1 Materials characterisation*, gypsum possesses a three times higher specific surface area than the Ref. mortar as well as higher porosity. However, by looking at the formaldehyde mass adsorbed and desorbed, the specimen Ref. mortar showed a better sink effect, i.e. it adsorbed more and desorbed less.

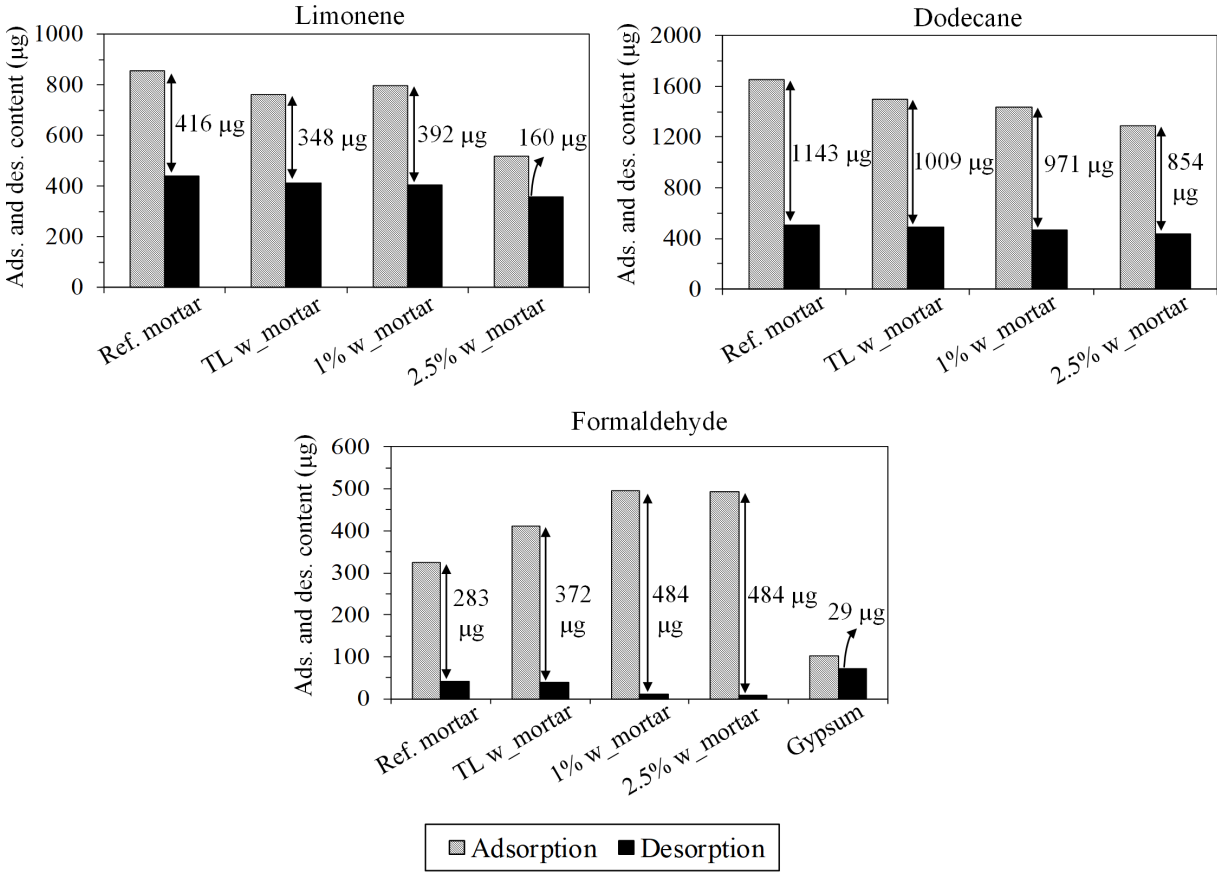

Figure 6.14 Mass of limonene, dodecane and formaldehyde adsorbed and desorbed by the lime mortars with natural wool added.

6.3.3. Clay E14 plaster - 30 m^3 chamber

The adsorption and desorption behaviour of VOCs by the Clay_E14 plaster was also tested in the 30 m^3 environmental chamber in addition to the testing carried out in the lab-scale 2-litre chambers. Concentrations of toluene, limonene and dodecane were measured at the inlet and centre of the chamber. After 120 hours of elapsed time, the concentration of toluene was almost at the same level as that measured at the inlet of the chamber (see Figure 6.15) meaning that the material was reaching its saturation point. In the case of limonene and dodecane, both

organic pollutants were still being adsorbed by the material surface. At the end of the adsorption phase, the difference of limonene concentration between the inlet and the centre of the chamber was 21.6 % and 44.7 % in the case of dodecane. Comparing with the IAQ guidelines presented in Chapter 2, the source of dodecane was emitting around 2000 µg/m^3, although in the centre of the room the concentration was reduced to approximately 1000 µg/m^3 which is the limit of the Belgium regulation or the German AgBB/DIBt guidelines.

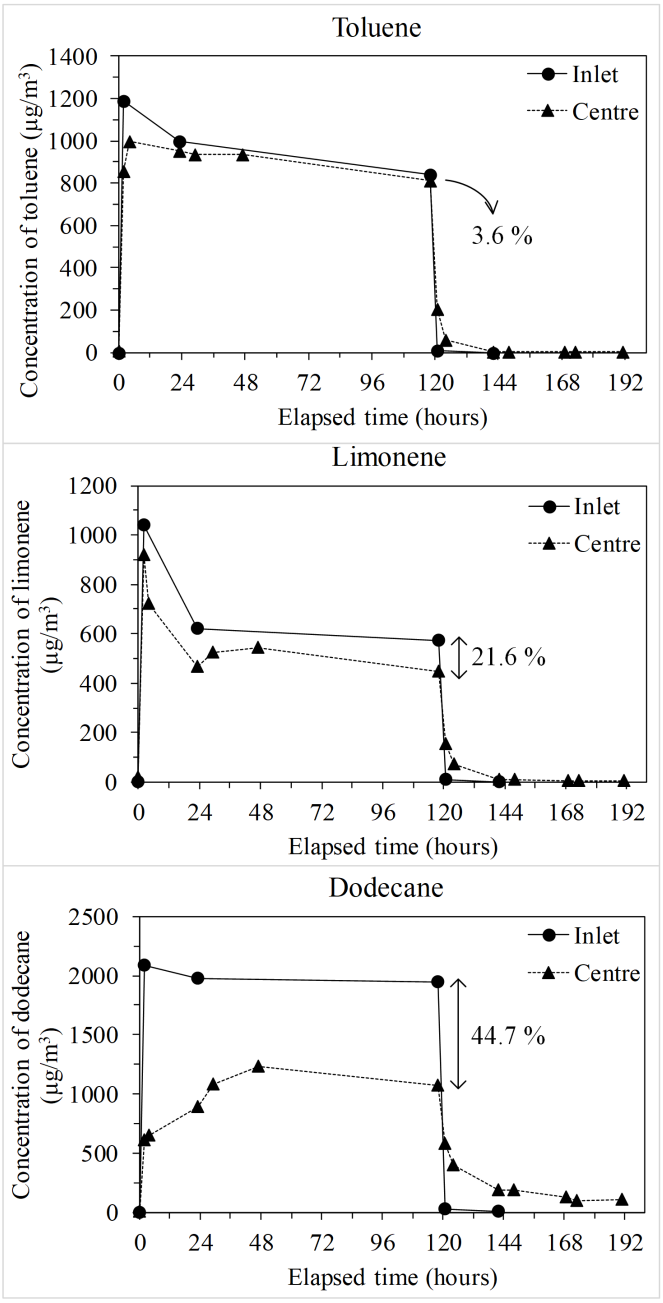

Figure 6.15 Concentration of toluene, limonene and dodecane in the inlet and centre of the 30 m^3 chamber with Clay_E14 panel placed in the centre of the chamber (~2 m^2 of total area exposed).

6.4. Summary

6.4.1. Clay-based plasters and lime mortar with cellulose flakes

- ✓ The porous microstructure and specific surface area of both clay plasters were similar despite the different bio-based additives incorporated;
- ✓ TVOCs and formaldehyde emissions of all materials were negligible;
- ✓ Clay_E14 and Clay_H2 showed comparable adsorption/desorption behaviour for toluene, limonene and dodecane;
- ✓ The difference in the adsorption/desorption of formaldehyde between both clays may be due to the different additives incorporated, specially the silica in form of pumice (amorphous) and quartz from the sand (crystalline).

6.4.2. Lime mortar with Natural wool incorporated

- ✓ All lime mortars showed similar behaviour with regard to the adsorption of VOCs. No evident effect of the presence of wool was observed;
- ✓ The presence of wool fibres in the lime matrix greatly improved the adsorption of formaldehyde;
- ✓ Lime mortars adsorbed more formaldehyde than the traditional gypsum irrespective of the presence of wool;
- ✓ Lime mortars with 1 % and 2.5 % of wool showed the same ability to capture formaldehyde, suggesting that at these concentrations there is no significant difference;
- ✓ Considering a linear scaling-up of this experiment to the real world, a room polluted with levels of formaldehyde three times higher than the limits suggested by WHO and other legislations (100 $\mu g/m^3$) where the walls have lime mortar incorporating natural wool, the indoor concentration of formaldehyde would not exceed 20 $\mu g/m^3$ for at least 6 days (144 hours).

Chapter 7

Photocatalytic lime mortars and wood panel for passive and active control of the IAQ

7.1. Introduction

Photocatalysis can be simply defined as a photochemical reaction occurring at the solid surface of a material with is usually a semiconductor (Fujishima and Honda 1972; Fujishima et al. 2000; Agrios and Pichat 2005). This reaction is composed of two steps which happen simultaneously, the first involving oxidation and the second reduction, Figure 7.1. When the light radiation hits the surface of the photocatalyst, electron-hole pairs (e^- and h^+) are created that can either recombine or react with the adsorbed molecules. Examples of chemical equations of the photocatalytic transformations can be found in publications by Diebold (2003) and Agrios and Pichat (2005). Titanium dioxide (TiO_2) has been a well-known and widely studied photocatalyst since its photocatalytic activity was discovered by Fujishima and Honda in the 70's by splitting water into hydrogen and oxygen (Fujishima and Honda 1972).

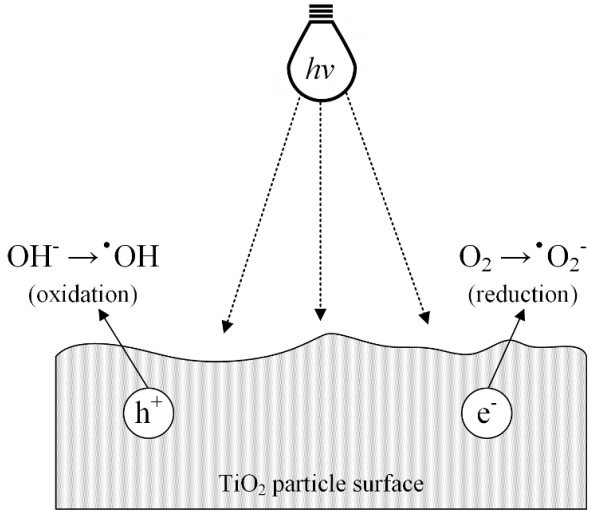

Figure 7.1 Simplified schematic of the photocatalysis on a TiO_2 particle surface.

Titanium dioxide has various applications such as self-cleaning surfaces, sterilisation, air or water purification systems and others (Agrios and Pichat 2005; Nakata and Fujishima 2012; Nakata et al. 2012; Giampiccolo et al. 2016; Tobaldi et al. 2016). TiO_2 exists in various crystalline phases, however, only those containing the rutile and anatase phases show the more efficient photocatalytic activity (Agrios and Pichat 2005; Fujishima et al. 2008; Tobaldi et al. 2016; Giampiccolo et al. 2016).

The incorporation of photocatalytic TiO_2 particles in mortars has being studied for the purposes of NOx degradation under the action of light (Senff et al. 2013; Vieira et al. 2014). Other studies are being carried out in order to improve the photocatalytic activity at higher wavelengths in the visible spectrum. A common approach includes the doping of the TiO_2 with other metallic atoms such as cobalt (Giampiccolo et al. 2016), copper and zinc (Tobaldi et al. 2016). Also, rare-earth metals, such as lanthanum, europium and yttrium are used to dope TiO_2 particles and their photocatalytic activity under visible light can then be compared to the un-doped TiO_2 (Tobaldi et al. 2014). Other ways to improve the photocatalytic activity of TiO_2 is the addition of high-surface area adsorbent materials such as activated carbon, zeolites and clays (Sampath et al. 1994; Takeda et al. 1997). The objective of adding these types of additives is to increase the adsorption capacity of the TiO_2 particles and therefore their photocatalytic efficiency, i.e. activated carbon and zeolites will attract the pollutants molecules due to their high specific surface area and then TiO_2 will degrade those pollutants. This mechanism is called a synergetic mechanism. Salthammer and Fuhrmann (2007) stated that TiO_2 particles present in wall paints shown no photocatalytic degradation of 1,2-dichrolobenzene under simulated sun light although, the authors pointed out a possible reversible sink effect which probably resulted from the high dipole moment of the VOC molecule (2.5 Debye) and the compound's high boiling point (181 °C). Besides the photocatalytic activity of the building materials with TiO_2 particles incorporated, its capacity to remove VOC from the indoor air under dark conditions has not yet been explored.

In this chapter, the VOCs and formaldehyde adsorption/desorption behaviour of lime mortars with 0, 2, 3 and 5 % of TiO_2 commercial particles added is investigated. The atomic concentration of titanium on the surface of the mortars is analysed by EDX and the specific surface area is measured by nitrogen adsorption isotherms (BET).

In Chapter 4, the MDF panel with a décor paper coating (Coated MDF) was shown to exhibit a very low capacity to adsorb toluene, limonene, dodecane and formaldehyde due to its very flat surface (low specific surface area). In the present chapter, a coating of TiO_2 particles was

applied to the surface of the Coated MDF in order to test its photocatalytic activity. The TiO_2 particles were applied to large panels by the manufacturer of the panels, to be tested in the 30m^3 chamber. In this way, such Coated MDF panels may have an important role in improving the indoor air quality despite the flat surface of the panels.

7.2. Materials and methods

7.2.1. Materials description

7.2.1.1. ETDKx materials

The ETDK*x* specimens, prepared in partnership between University of Bath, Tecnalia and University of Aveiro, were the first prototypes of the ECO-SEE project. These panels consisted of an MDF substrate coated with a 15 mm thick layer Mortar_RS and the top layer made of Mortar_P, see Figure 7.2 a) and b). Photocatalytic particles, *KRONOClean 7000*, were added to the material used in the 3-millimetre top layer only, as this layer is in direct contact with the indoor air. The content of photocatalytic particles added to the Mortar_P mixture (prior the casting) was 0 %, 2 %, 3 % and 5 % by weight related to the Mortar_P. The specimens were named accordingly to the TiO_2 content as follows: ETD, ETDK2, ETDK3 and ETDK5, respectively.

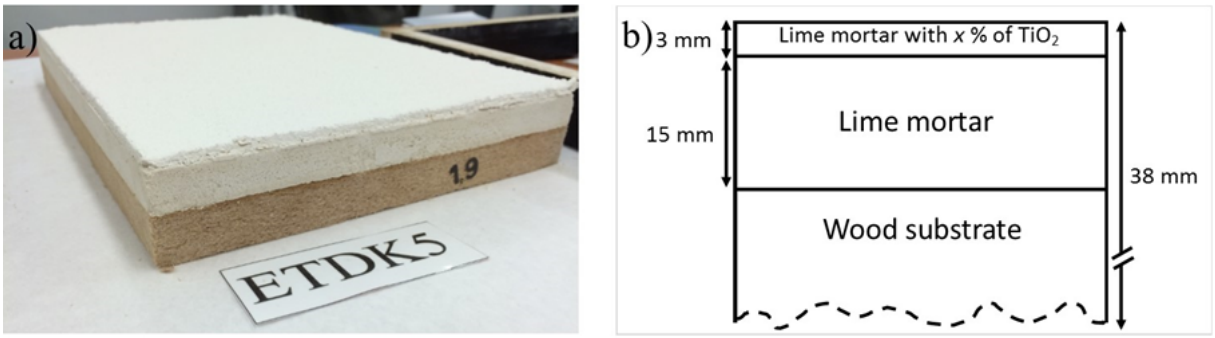

Figure 7.2 a) ETDK5 specimen and b) schematic of the layer composition of ETDK*x* material series.

7.2.1.2. PC panel

Photocatalytic (PC) panels, prepared at *Kronospan* (Chirk, Wales), consist of Coated MDF coated with photocatalytic particles. The particle coating was applied by the manufacturer of the panels. Approximately 35 m^2 of PC panels were installed on four walls of the chamber and all edges were sealed with aluminium tape as shown in Figure 7.3.

Figure 7.3 PC panels installed on 4 walls of the 30 m^3 chamber.

7.2.2. Materials characterisation and IAQ assessment

The ETDK*x* specimens were tested in the 2-litre chambers for TVOC and formaldehyde emissions and their adsorption/desorption behaviour under dark conditions. In order to investigate the effect of the TiO_2 particles on the adsorption/desorption characteristics, the specific surface area of the top layer (Mortar_P with and without photocatalytic particles) was measured by nitrogen adsorption isotherms (BET) and the microstructure analysed by SEM. The atomic content of titanium present in this same layer of the specimens was analysed by EDX and correlated with the TiO_2 content added to the lime matrix experimentally. The EDX spectrum was recorded in three different locations in the same sample for statistical purposes.

In the 30m^3 chamber, the TVOC and formaldehyde emissions were analysed. In the case of the investigation of the adsorption/desorption behaviour, the objective of this experiment was to evaluate the adsorption of VOCs and photocatalytic activity of PC panels in a real scale room

at an air change rate of 0.5 ach^{-1}. The experiment was divided into three phases: adsorption, photocatalysis and desorption.

Before the adsorption phase, the LED lights were turned off and the window of the chamber was covered with cardboard to keep the interior of the chamber under completely dark conditions, Figure 7.4. At this stage, only the physical interactions between VOCs and the surface of the PC panels were expected to occur. The experiment was started as soon as the VOCs sources were placed in the dopant chamber. After one week from the start of the experiment, the LED lights were turned on and the photocatalytic phase started. One week later, VOCs sources were removed and the desorption phase was allowed to take place. In this later phase, any VOC molecules that were physically adsorbed onto the material surface would be expected to be re-emitted into the air in the course of time.

Figure 7.4 30 m^3 chamber with the window covered for IAQ assessment under dark conditions.

7.3. Results and discussion

7.3.1. ETDK - 2-litre chambers

7.3.1.1. Materials characterisation

The atomic weight of titanium present in the ETDK*x* is shown in Table 7.1. The values shown in the table are the average resulting from three measurements recorded over a selected area and the respective standard deviation. The sample without TiO_2 particles in its formulation, ETD, showed an average of the Ti atomic weight of 1.8 % ± 0.2 %. This can be associated with impurities or small additives of the air-lime used to formulate the Mortar_P. To check the origin of the titanium present in the ETD specimen, an EDX spectra was recorded on a lime particle. The content of titanium found on the lime was 1.7 % which confirms that the origin of the titanium present in the specimen without any TiO_2 particles added is from the lime. Thereafter, in general, all samples showed a Ti atomic weight between 1.2 and 1.8 times higher than the TiO_2 content added.

Table 7.1 Average of the titanium atomic weight (%) obtained by EDX.

Material	**TiO_2 weight added in to the mortar (%)**	**Titanium atomic weight (%)**
ETD	0	1.8 ± 0.2
ETDK2	2	3.4 ± 0.1
ETDK3	3	4.5 ± 0.1
ETDK5	5	6.2 ± 0.2

The correlation between the amount of TiO_2 particles added to the lime matrix and the atomic titanium content measured by EDX (with the respective standard deviation) is shown in Figure 7.5.

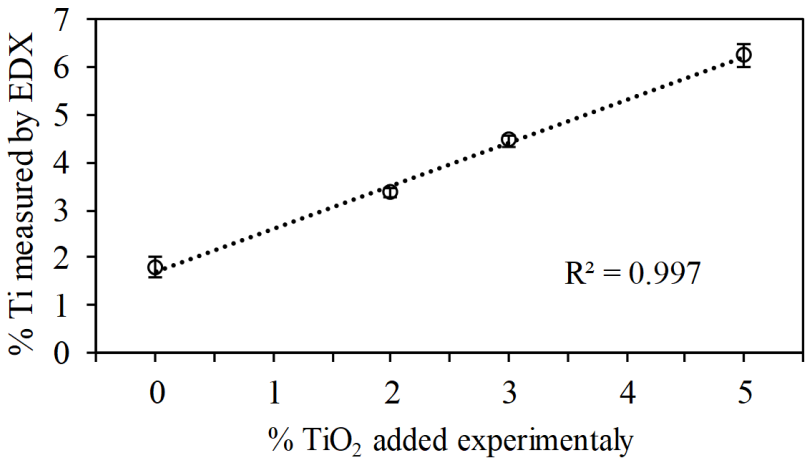

Figure 7.5 Correlation between the TiO_2 particles added to the lime matrix and the Ti content measured by EDX.

The high R^2 value shown in Figure 7.5 indicates the very good correlation between the amount of TiO_2 particles added in to the lime matrix and the Ti content measured by EDX. Also, by measuring the titanium content in three different locations on the sample surface it is possible to indicate the good dispersion of the particles. To confirm this, EDX mapping was carried out over the ETDK5 sample surface for 1.5 hours in order to achieve good resolution. EDX maps of carbon, oxygen, titanium and calcium are presented in Figure 7.6. Carbon, oxygen and calcium were detected spread throughout the entire map. The brighter blue colour in the titanium map shows the good spread of the TiO_2 particles.

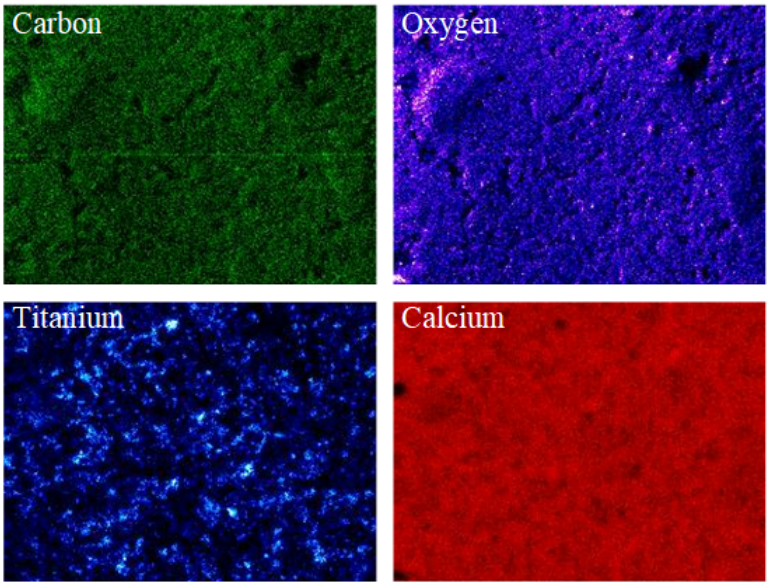

Figure 7.6 EDX maps of carbon, oxygen, titanium and calcium recorded on ETDK5 specimen.

The effect of the TiO_2 particles on the microstructure of the ETD specimen is shown in Figure 7.7. By comparing the four SEM images, the effect of the TiO_2 particles on the porosity of the mortars is clear, where, as can be seen, the ETD specimen is composed of a smaller number of bigger pores while the ETDK5 specimen contains a greater number of pores which were generally smaller. Specimens ETDK2 and ETDK3 gradually follow this trend. By looking closer at the microstructure of the ETD and ETDK5 specimens, Figure 7.8, it is observed that the size of the "original" pores of the lime mortar matrix in the ETDK5 may be similar to those in the ETD although, in the former case, the pores are occupied with TiO_2 particles which, by themselves are spread into the whole matrix, as was shown before in the titanium EDX map of Figure 7.6. The EDX mapping of the titanium is thereafter in good agreement with the SEM image of the ETDK5 specimen. In a study carried out by other partners of the ECO-SEE project (Giampiccolo et al. 2017), the porosity of the ETDK*x* was analysed by MIP. The authors found an increase in the porosity from 28.8 % to 33.1 % by adding 5 % of TiO_2 particles resulting in a decrease in pore size from 1.04 µm to 0.82 µm. The MIP results obtained by Giampiccolo et al. (2017) are in agreement with the microstructure analysed by SEM, shown in Figure 7.7 and Figure 7.8.

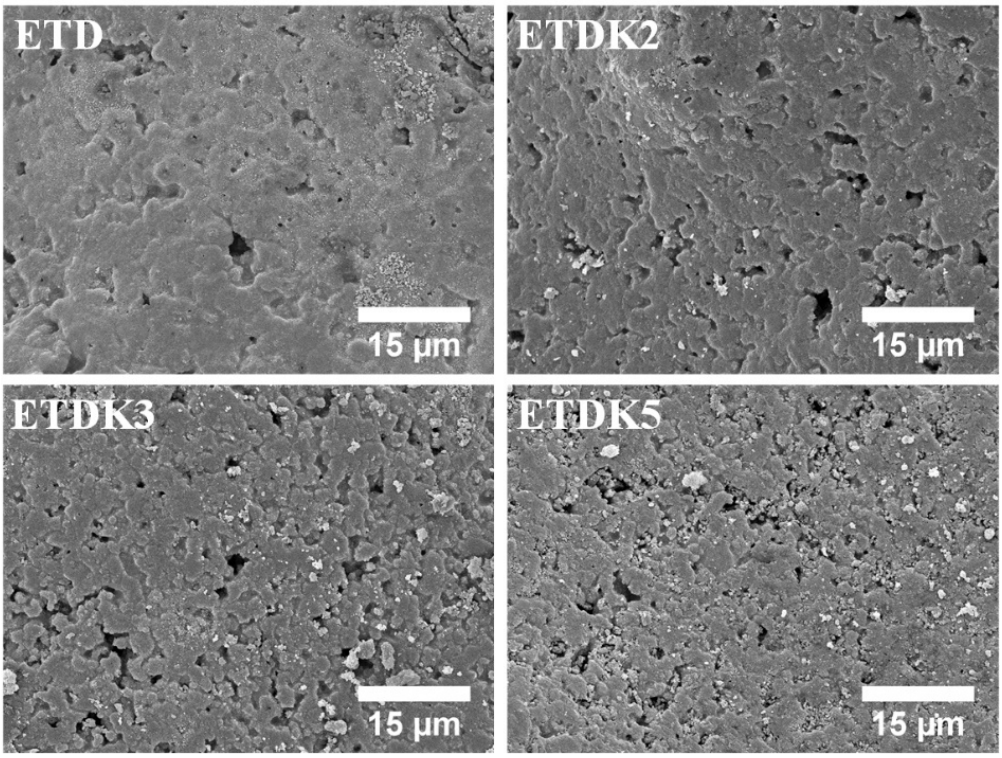

Figure 7.7 SEM images of the ETDK*x* specimens.

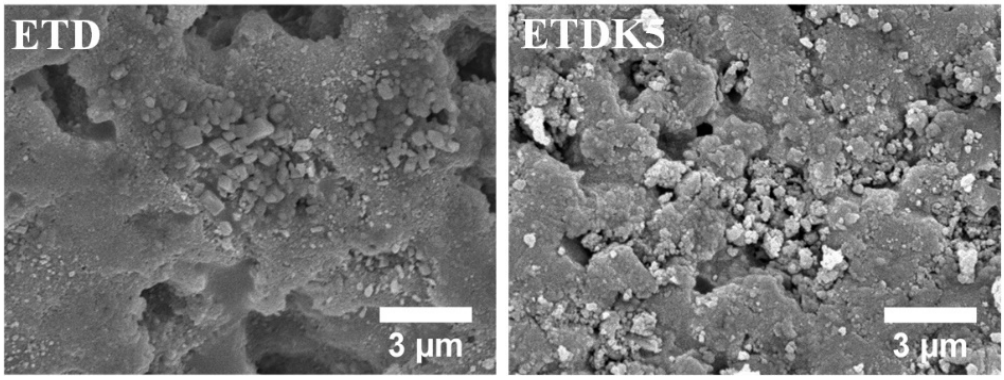

Figure 7.8 SEM images at higher magnification of the ETD and ETDK5 specimens.

To further study the physical characteristics of the ETDK*x* materials, BET nitrogen adsorption isotherms were drawn to calculate the specific surface area of these materials, Figure 7.9. A change in the N_2 adsorption/desorption isotherms is observed for the different amounts of TiO_2 added to the lime mortars, Figure 7.9 a), which led to a different specific surface areas (Figure 7.9 b)). The reference mortar, ETD, showed the lowest surface area of 1.6 m^2/g in comparison to 4.5 m^2/g for ETDK5, a result of the addition of 5 % of TiO_2 particles to the lime mortar with led to an increase of 65 % in the surface area. These results demonstrate that, the addition of TiO_2 particles refines the pore structure, by being located in the large pores between the lime particles leading to smaller pores in the final product as was already observed by the SEM results.

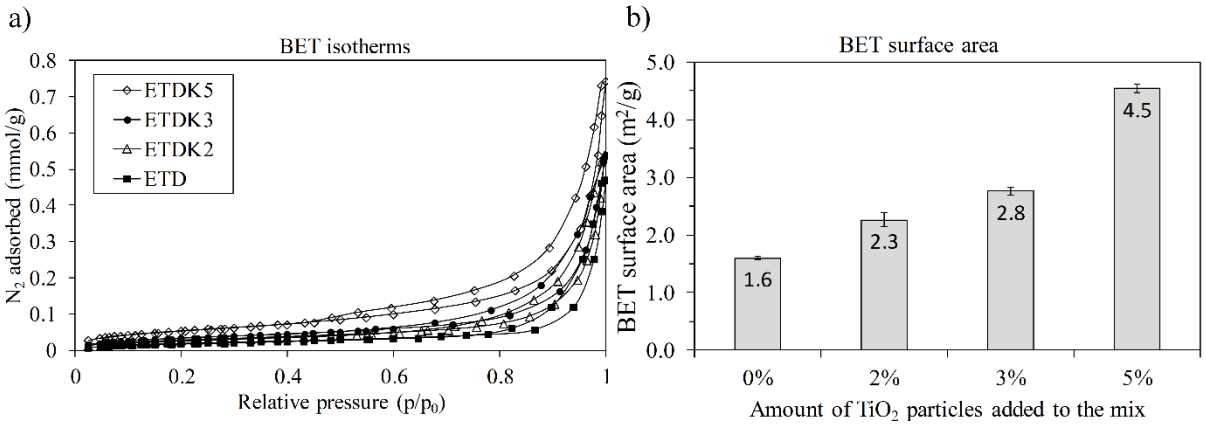

Figure 7.9 a) BET surface area and b) nitrogen adsorption isotherms.

7.3.1.2. Emissions testing

The area specific emission rates (μg/m^{2}h) of formaldehyde and TVOC, presented in Figure 7.10, show that emission rates are very low in general, the maximum formaldehyde emission rate being around 11 μg/m^{2}h (ETDK2) and approximately 30 μg/m^{2}h for TVOC (ETD). Due to the emission rate being so low, it is difficult to see a clear effect of the presence of the TiO_2 particles on the emissions. However, in the particular case of the formaldehyde emission rate, the two specimens with highest TiO_2 content showed the lowest formaldehyde emission rates, or even no emissions at all. After 28 days of testing, emission rates decreased considerably with the highest rate being 3 μg/m^{2}h in the case of the formaldehyde and 9 μg/m^{2}h in the case of TVOC.

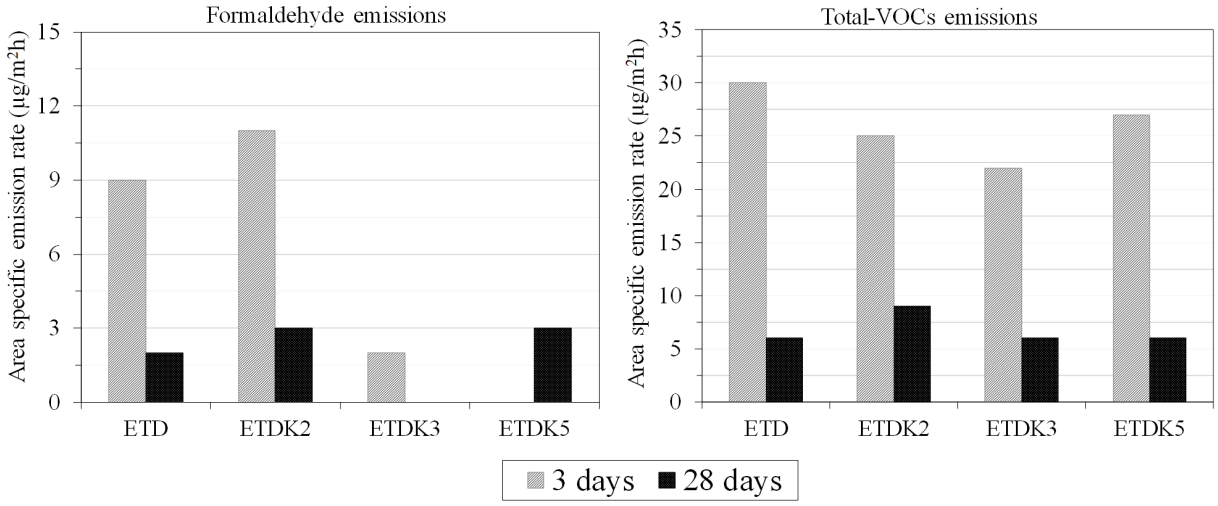

Figure 7.10 Area specific emission rate of formaldehyde and TVOC from the photocatalytic lime mortars with different content of TiO_2. Main VOCs emitted: 1-butanol and hexanal.

7.3.1.3. Adsorption and desorption behaviour

The adsorption and desorption behaviour of the ETDK*x* materials is shown in Figure 7.11. The toluene adsorption and desorption curves are very similar for the four materials, indicating that the presence of the TiO_2 particles may only have a small effect on the toluene adsorption/desorption, which is hardly detectable. The same is observed for limonene but only during the adsorption phase. In the case of the desorption of limonene some differences in the materials' curves can be noticed. The most adsorbed organic pollutants were dodecane and formaldehyde. In both cases, 168 hours after the adsorption phase had started, all materials

were still adsorbing these compounds. The concentration of formaldehyde in the reference chamber at 168 hours was around 625 $\mu g/m^3$, and being approximately 350 $\mu g/m^3$ in the testing chambers which, it is almost 50 % less in concentration. This indicates the good capacity of these materials to adsorb formaldehyde.

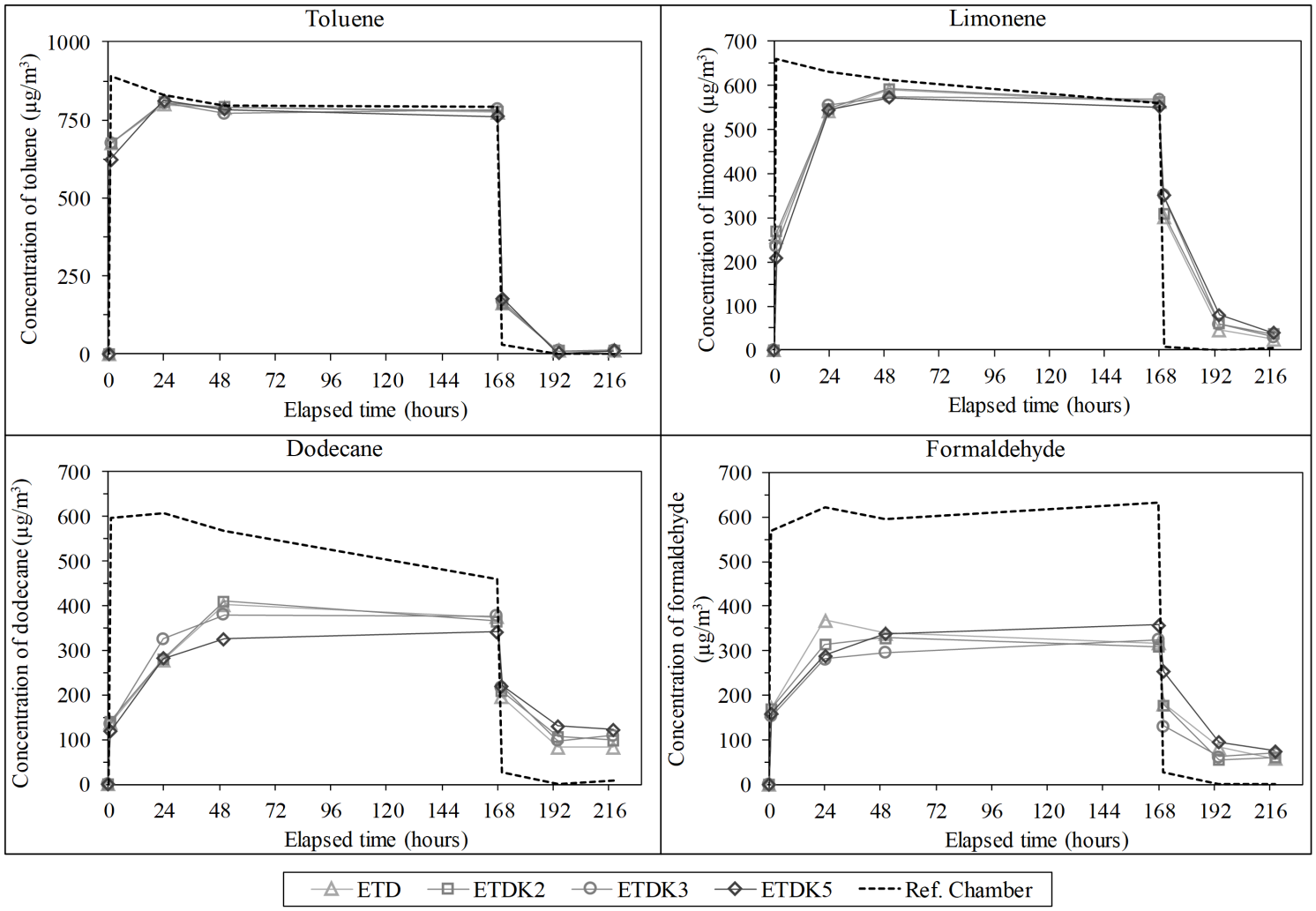

Figure 7.11 Adsorption and desorption curves of toluene, limonene, dodecane and formaldehyde.

For an improved impression of the effect of the TiO_2 particles on the adsorption and desorption of toluene, limonene, dodecane and formaldehyde, the mass adsorbed during the adsorption phase and then desorbed is shown in Figure 7.12. The results also demonstrate the capacity of these materials to remove the organic pollutants from the air under dark conditions, i.e. through only passive mechanisms. As already observed before but now quantified, toluene was the least adsorbed compound, approximately 80 µg, and dodecane and formaldehyde were the most adsorbed, up to 413 µg and 613 µg, respectively. By looking at the effect of the TiO_2 particles on the uptake of the four organic pollutants, the ETDK5 showed the highest ability to adsorb gases with the exception of formaldehyde for which, the ETDK2 and ETDK3 specimens showed a slightly higher adsorbed content, 565 µg and 613 µg respectively, against 544 µg adsorbed by the ETDK5. In terms of the difference between the adsorbed and desorbed mass which represents the amount of organic compound captured by the material, the ETDK5 specimen showed the highest uptake for toluene, limonene and dodecane. However, it should be stressed that the desorption values for dodecane and formaldehyde do not fully represent what the materials have desorbed because at the end of the experiment all materials were still desorbing as seen previously in Figure 7.11.

As a final remark, in the course of this investigation it was observed that the presence of the TiO_2 particles led to a change in the capacity of the lime mortars to adsorb and desorb toluene, limonene, dodecane and formaldehyde. This change may be caused by the effect of the TiO_2 particles on the porous microstructure of the lime mortars, leading to a greater porosity and also higher specific surface area which, in turn improved the sink effect of the material. Another possible reason, in combination with the effect of the physical characteristics, may be the physical interaction between the VOC molecules and the surface of the rutile and anatase crystals of the TiO_2 particles through Van der Waals forces and hydrogen bonding (Parida et al. 2006; Rouquerol et al. 2014).

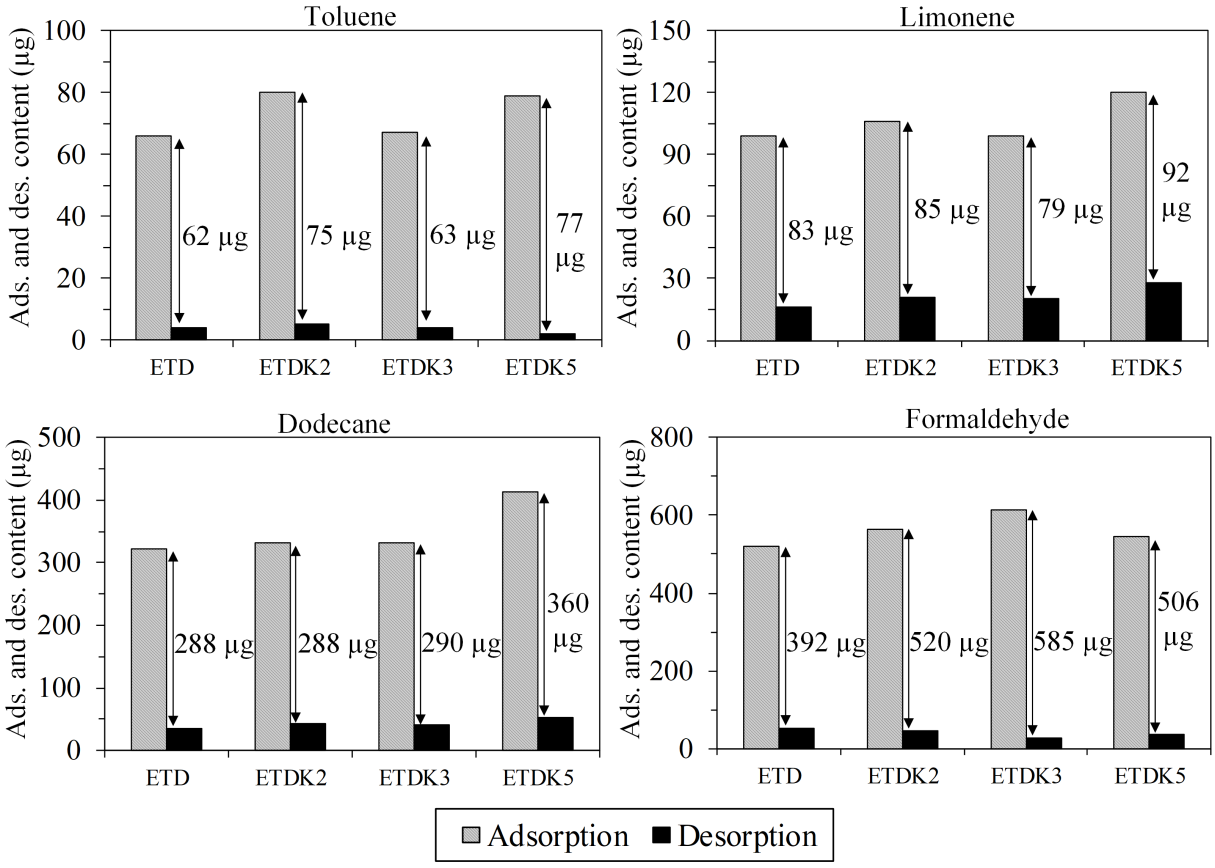

Figure 7.12 Mass of toluene, limonene, dodecane and formaldehyde adsorbed and desorbed by the ETDK*x* materials.

7.3.2. Photocatalytic coated MDF panel - 30 m^3 chamber

7.3.2.1. Emissions testing

Three-day area specific emission rates of VOCs and formaldehyde are shown in Table 7.2. As levels of formaldehyde and TVOC emitted by the PC panels were very low, the 28-day emission testing was not necessary. Sampling was carried out in the centre and outlet of the chamber using PTFE lines to avoid interfering with the chamber air chemistry. Both locations showed very similar emission rates of VOCs (~ 14 µg/m^{2}h) and formaldehyde (~ 9 µg/m^{2}h). The difference between the concentrations sampled in the centre of the room and the outlet was only 4 % in the case of TVOC and 3 % in the case of formaldehyde. The major VOC emitted by the PC panels was α-pinene. This chemical compound is commonly emitted by natural wood

materials, and in this case, the source is thought to be from the Coated MDF, as observed previously in Chapter 4.

Table 7.2 Three-day formaldehyde and TVOC area specific emission rate of the photocatalytic coated MDF panel.

Sampling location	**Formaldehyde ($\mu g/m^2h$)**	**TVOC ($\mu g/m^2h$)**	**Main VOCs**
Centre	9.4	14.1	α-pinene
Outlet	9.1	14.7	

7.3.2.2. Adsorption-photocatalysis and desorption behaviour of the coated MDF panel

Figure 7.13 shows the concentration curves during adsorption, photocatalysis and desorption phases for toluene, limonene and dodecane. Samples of VOCs were drawn from the inlet, centre and outlet of the chamber. One graph for each chemical compound was drawn, so that the concentration in each of the different sampling locations could be compared (inlet, centre and outlet). The adsorption phase ran for 190 h. Thereafter, the LED lights were turned on and the photocatalysis phase started. The highlighted sections in Figure 7.13 represent when the LED lights were on and the VOC sources were in the doping chamber. During the desorption phase, which started after 360 hours of elapsed time, the LED lights were kept on, although the VOC sources were removed. In this later stage, despite the absence of VOC sources, the photocatalytic activity may have also occurred due to the desorption/re-emission of those VOCs previously physisorbed by the material's surface.

In the adsorption phase, VOC concentrations reach their maximum value and become fairly stable in the chamber after approximately 24 hours. The difference between VOC concentrations in the inlet and in the other two locations may indicate the adsorption/photocatalytic activity. After turning the LED light on (at 192 hours) an increase in the VOC concentrations is observed in all sampling locations. This behaviour is not yet fully understood; however, it is known that it is not related to the material because the inlet concentration is also increasing. After 24 h of the photocatalysis phase, the VOC concentrations in the inlet return to their stable adsorption phase values.

Once the VOCs sources were removed from the doping chamber, concentrations of the three VOCs in the inlet of the chamber dropped to 0 $\mu g/m^3$ after 5 h whereas, in the centre and outlet of the chamber, limonene dropped to 0 $\mu g/m^3$ only after 24 h and dodecane was still being desorbed when the experiment was ended, showing approximately 20 $\mu g/m^3$ in the outlet and 40 $\mu g/m^3$ in the centre of the chamber.

Only peaks that correspond to toluene, limonene and dodecane were seen in the GC chromatograms and MS spectra. Therefore, no secondary products resulting from the photocatalytic degradation were detected.

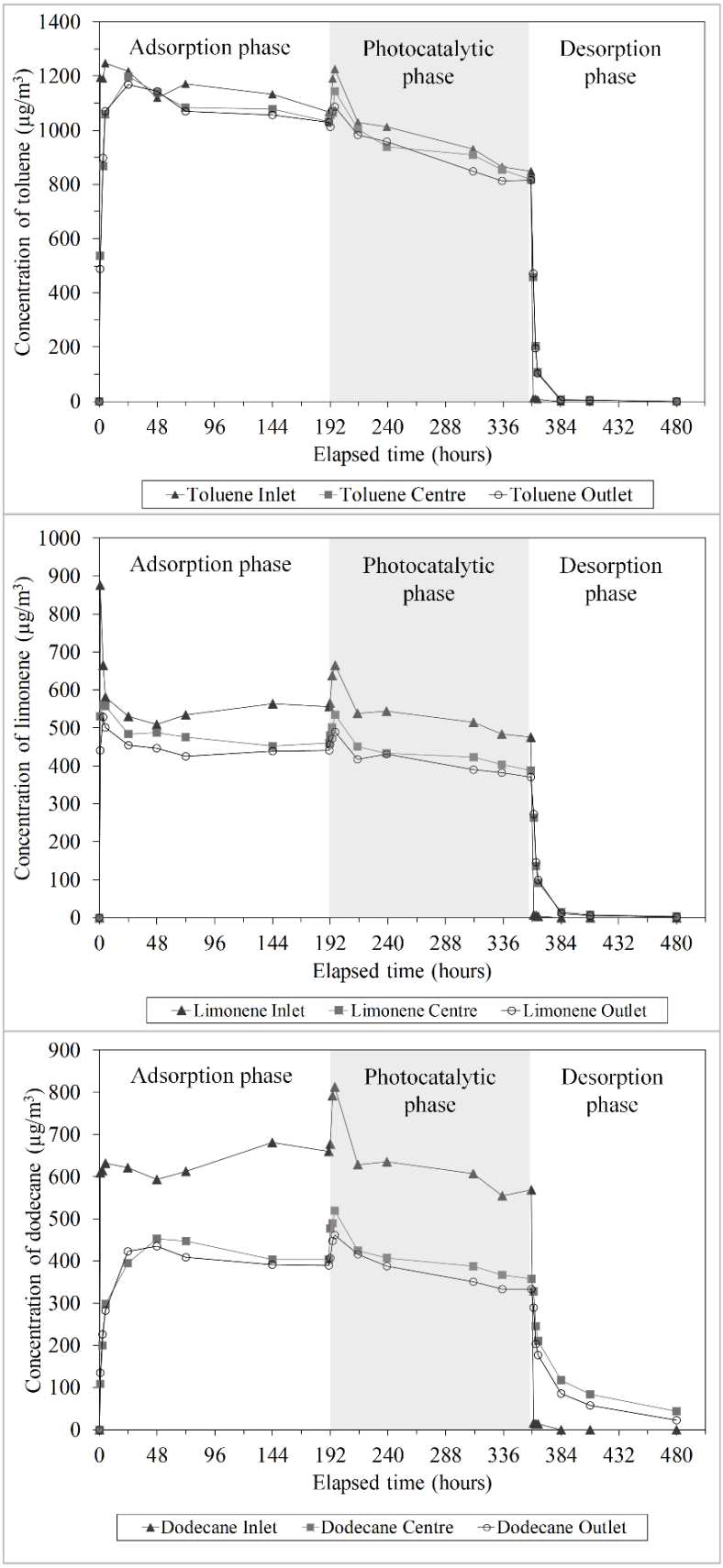

Figure 7.13 Adsorption, photocatalysis and desorption curves of the PC MDF panel in the 30m^3 chamber for toluene, limonene and dodecane.

From Figure 7.13, it is not possible to observe if the photocatalytic activity had taken place or not. In order to fully investigate this, the amount of VOC reduction by the material (either by adsorption and/or photocatalysis) was calculated. To do this, the quantity of VOC reduced up to144 hours during the adsorption and photocatalytic phases was calculated in the inlet and centre of the room. The reason behind the period of 144 hours is that the experimental durations of the adsorption phase and the photocatalytic phases were different. For the comparison of the VOC mass reduced by adsorption or photocatalysis, the period of time should be the same, otherwise incorrect observations and therefore inappropriate conclusions could be made. The curve of VOC concentration in the centre of the chamber was chosen instead of the outlet of the chamber because, in a real case, it is where a building occupant would spend most time inside the building. The periods of time used for these calculations are highlighted in Figure 7.14, taking limonene as an example.

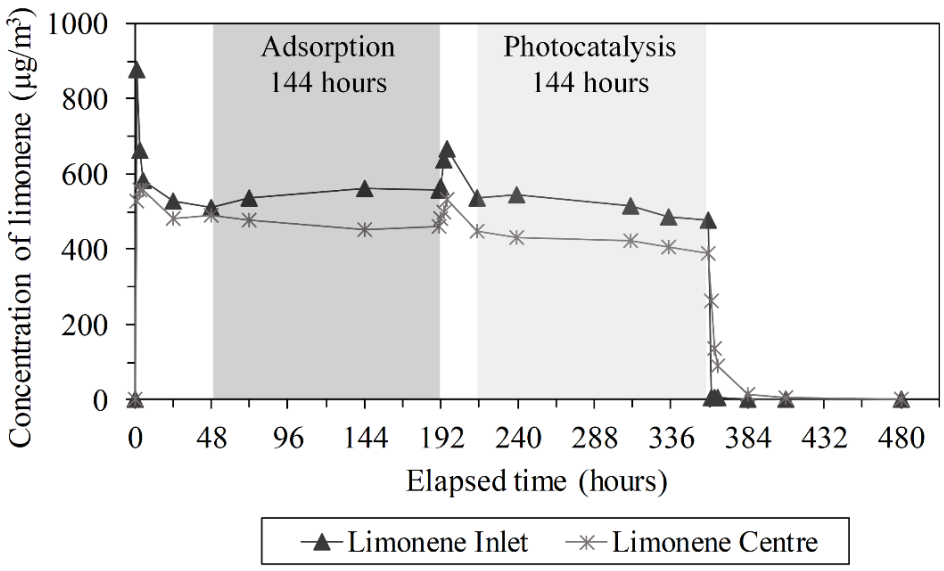

Figure 7.14 Limonene curves to illustrate the periods of time used to calculate the mass of VOC reduced during the adsorption and photocatalysis phases for the MDF panel.

The masses of toluene, limonene and dodecane reduced during the adsorption and photocatalytic phases are thereafter shown in Figure 7.15. Following the same trend as observed in Chapters 4, 5 and 6 of this thesis, dodecane had the greater reduction and toluene the least. This occurred under both conditions, in dark (adsorption) and with LED lights on (photocatalysis). For the three VOCs analysed in this experiment, the photocatalytic phase

showed the highest reduction, being toluene 67 µg, limonene 166 µg and dodecane 371 µg. In terms of the difference between the VOC reduction during the adsorption and photocatalytic phase, toluene showed the highest difference, being 40 µg to 67 µg respectively, and dodecane showed the lowest, 330 µg to 371 µg respectively. This difference represents, in percentage terms, 40.3 % for toluene and only 11.1 % for dodecane. This may be related to:

1) the adsorption occurring under dark conditions took place on the surface of the panel paper coating and also on the surface of the TiO_2 particles. When the LED lights were turned on, the photocatalytic activity was the dominant mechanism (related to the physisorption) and therefore the reduction of VOCs that usually were not adsorbed (as the case of toluene) is higher;
2) the photocatalytic degradation of toluene is preferential or less energy demanding compared with the other two VOCs.

As a final and the most important remark, the fact that the reduction of the three VOCs is higher for the photocatalytic phase, may indicate the photocatalytic activity took place when the LED lights were turned on, or even a combination of both mechanism, i.e. physical adsorption and photocatalytic activity. This is supported by the observations made in the previous section about the ETDK materials, where it was shown that the addition of TiO_2 particles led to an increase of the capacity to adsorb VOCs, even under dark conditions.

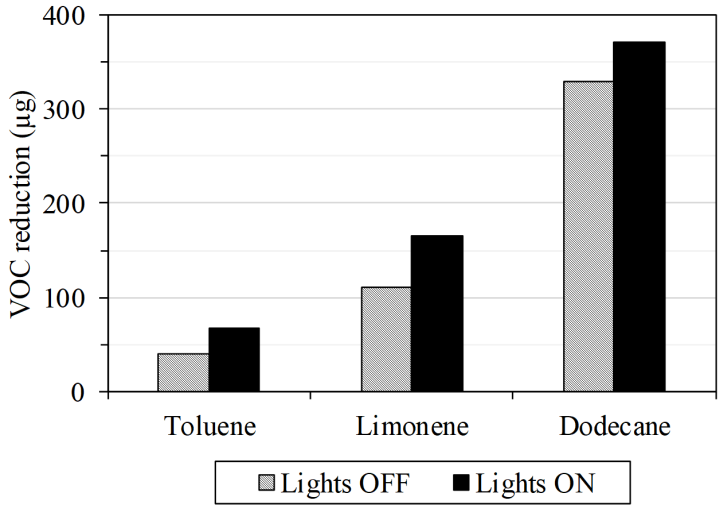

Figure 7.15 VOCs reduction the adsorption phase (dark conditions) and photocatalytic phase (lights on) for the PC MDF panels.

7.4. Summary

7.4.1. ETDK*x* – 2-litre chambers

- ✓ The addition of TiO_2 particles to the lime mortar matrix led to an increase in the porosity and specific surface area and to a decrease in the pore size;
- ✓ The changes in the physical characteristics of the lime mortars were attributed to the TiO_2 particles being well spread throughout the lime mortar matrix and also being located in its bigger pores, thus creating smaller pores;
- ✓ There was a good correlation between the amount of TiO_2 added to the lime matrix and the atomic weight of titanium analysed by EDX;
- ✓ TVOC and formaldehyde emissions of the ETDKx materials were very low with no detectable effect in the case of TVOC. For formaldehyde emissions, materials with higher TiO_2 content emitted less formaldehyde;
- ✓ The sequence of the least and most adsorbed VOCs applies and is confirmed once again: toluene < limonene < dodecane < formaldehyde;
- ✓ Materials with the highest amount of TiO_2 particles, therefore with higher surface area, showed a higher capacity to adsorb organic pollutants, confirming the effect of the surface area on the sink effect of porous building materials;
- ✓ ETDKx lime mortars with photocatalytic particles added were shown to have good capacity to passively remove (i.e. without light) toluene, limonene, dodecane and formaldehyde from the air, behaviour which would be even greater under the action of light.

7.4.2. Photocatalytic Coated MDF – 30 m^3 chamber

- ✓ TVOC and formaldehyde emissions were very low, being similar to the limit of the detection of the analytic techniques used to quantify these organic compounds;
- ✓ Coated MDF with no TiO_2 particles added showed a very low ability to adsorb organic compounds due to its flat surface. However, by applying a photocatalytic coating, this ability increased;

- ✓ The percentage VOC uptake during the photocatalytic phase was on average higher for all three VOCs when compared to the adsorption phase. This observation is consistent with a photocatalytic process occurring on the surface of the panels, thus promoting the removal of VOCs from the chamber atmosphere.

Chapter 8

Mechanisms of interaction between volatile organic compounds and the surface of natural building materials - general discussion

In the previous chapters, the adsorption/desorption behaviour of toluene, limonene, dodecane and formaldehyde towards various natural building materials is presented and discussed. The physical and chemical characteristics of the building materials, namely chemical composition, specific surface area, porosity and pore size distribution, were correlated with their adsorption and desorption behaviour. Also, the mass of dodecane and formaldehyde adsorbed and desorbed was calculated.

In this chapter, a general discussion about the mechanisms of interaction between the selected organic pollutants and the natural building materials is presented. The discussion is informed by consideration of the physical properties and chemical composition of the materials. At the end of this chapter, the influence of the physico-chemical properties of toluene, limonene, dodecane and formaldehyde on the adsorption and desorption behaviour is also discussed.

8.1. Influence of the physico-chemical characteristics of the materials on the adsorption of VOCs and formaldehyde

In Table 8.1 the various materials characteristics and the mass of dodecane and formaldehyde adsorbed and desorbed is presented, providing the basis for the general discussion. Various materials were grouped according to the experiment in which they were tested.

Table 8.1 Chemical composition, physical characteristics and adsorbed/desorbed mass of dodecane and formaldehyde by natural building materials, tested in 2-litre chambers.

Material	Principal chemical constituent(s)	BET surface area (m^2/g) or microstructure	Dodecane (µg)		Formaldehyde (µg)	
			Ads	Des	Ads	Des
MDF	Cellulose	Large pores	n/a	n/a	511	72
Coated_MDF	Cellulose	Flat	n/a	n/a	26	23
Mortar_P	Calcite, portlandite	Pores < 1 µm	1856	n/a	771	92
Natural wool	Keratin	Loose fibres	n/a	n/a	639	37
0 % walnut MDF	Cellulose	Large pores	174	158	528	102*
5 % walnut MDF	Cellulose	Pores of the walnut shell < 1 µm	518	117	729	85*
Clay_E14	43 % clay, amorphous SiO_2, cellulose	4.6	1531	396	463	142
Clay_H2	60 % clay, crystalline SiO_2, cellulose	4.6	1591	404	529	120
Cell_mortar	Calcite, portlandite, cellulose	3.1	1196	357	524	138
Gypsum	Calcium sulphate	15.8	n/a	n/a	102	72
Ref. mortar	Calcite, portlandite	5.3	1651	508	324	42
TL w_mortar	Calcite, portlandite, keratin	n/a	1499	490	411	39
2.5 % w_mortar	Calcite, portlandite, keratin	4.7	1286	464	492	8
ETD	TiO_2, calcite, portlandite	1.6	323	35	521	53
ETKD2	//	2.3	331	43	565	45
ETDK5	//	4.5	413	53	544	38

// - same as above n/a - not applicable

* - formaldehyde was not fully desorbed at the end of the experiment

Analysis of the results has demonstrated that a direct comparison between the adsorption and desorption of VOCs by natural building materials and the direct correlation between the accessible (open) porosity and the sink effect is not possible. This is because natural building materials have a complex microstructure with a range of chemically different components. The measured open porosity in a material may indicate its bulk density, however, there is insufficient data relating to the specific pore sizes which strongly influence the adsorption and desorption characteristics. According to IUPAC, in relation to adsorption science, pore size can be classified into three groups: micropores for those with size inferior to 2 nm, mesopores includes sizes between 2 and 50 nm and macropores for those larger than 50 nm (Dabrowski 2001; Rouquerol et al. 2014). In the case of micropores, the size of the pores can be comparable with the molecular size of the gases (VOCs) and the adsorption mechanism is based on a pore-filling process in which the pore volume is the main factor. The surface of mesopores are composed of a greater number of atoms and molecules of the adsorbent material than that of micropores, therefore they have a greater surface area/sites available to adsorb molecules in the gas phase. This is the major difference between the micropores and mesopores. The mono-layer and multi-layer adsorption takes place successively on the surface, and in the final stage capillary adsorbate condensation occurs. This corresponds to the point at which the pore is completely full of the adsorbate molecules. In this case, the main parameters involved are the pore-size distribution and specific surface area. The adsorption mechanisms on macropores are considered similar to adsorption on a flat surface. Therefore, capillary condensation does not occur in macropores. Although these pores of greater size (including mesopores) play an important role for the diffusion of the VOC molecules through the microstructure, the adsorption occurs in the micropores.

For example, MDF panels contain large inter-fibre pores, greater than 100 μm, and also smaller pores (fibre pits) around 1.4 μm in the fibre cell wall, see Figure 8.1. The large pores represent the macroporous structure of the MDF where the pores are voids between the wood fibres. The pits are the main contributor (regarding the available surface area) to the adsorption of VOCs and are paths for the diffusion of the VOCs into the interior of the material, Figure 8.1 c). This effect is increased when walnut shell is added to the MDF panel due to the very porous surface of the walnut shell with average pore size of 330 nm, Figure 8.1 b). By adding 5 % walnut shell, the mass of adsorbed dodecane increased from 174 μg to 518 μg and formaldehyde from 528 μg to 729 μg, as shown in Table 8.1.

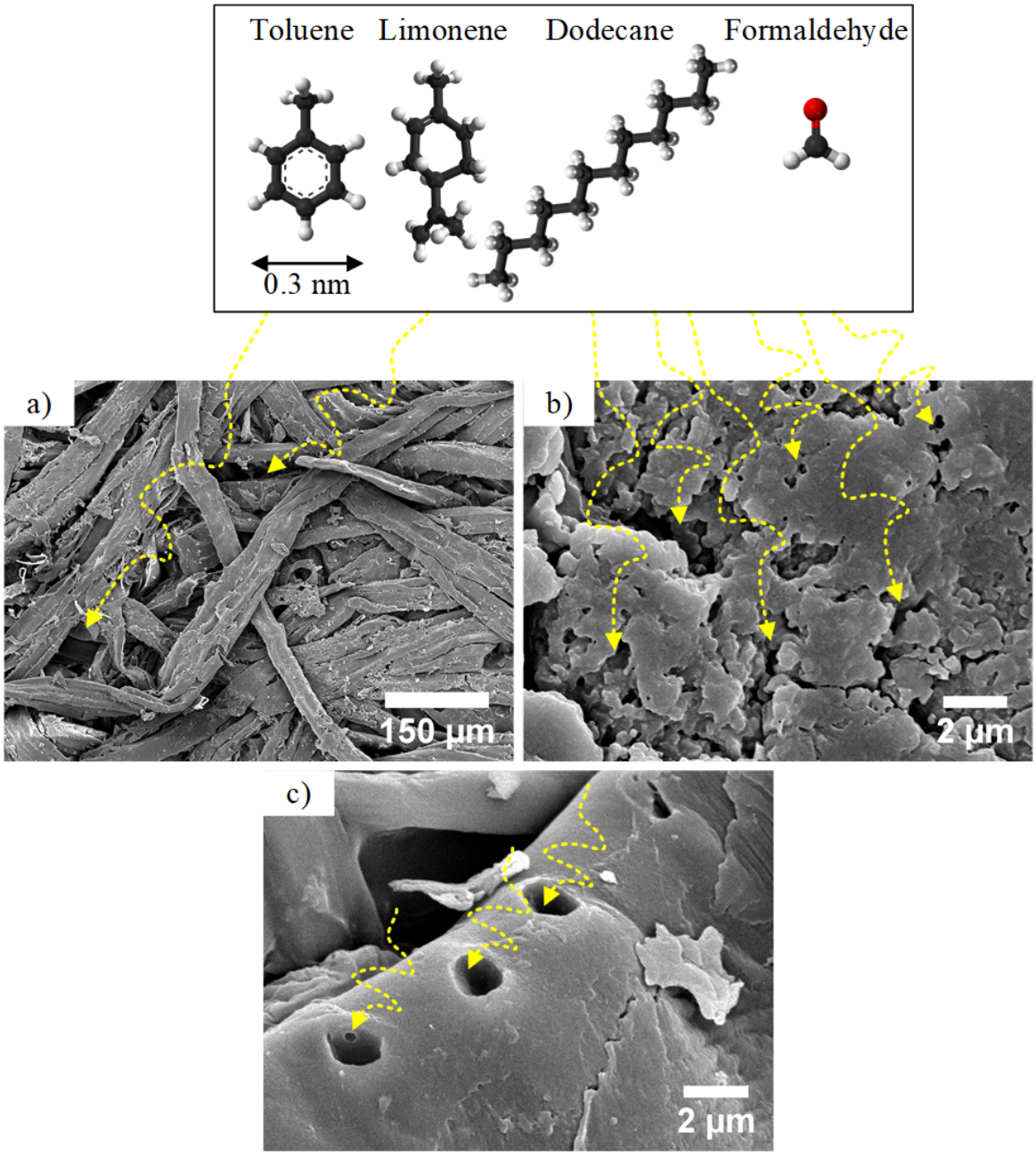

Figure 8.1 Illustration of the diffusion (yellow arrows) of toluene. limonene, dodecane and formaldehyde through the a) pores between wood fibres in the MDF panel, b) pores of the walnut shell surface and c) pits of the wood fibres.

A second example, illustrating the effect of the physical properties on the adsorption and desorption behaviour, is the comparison between the gypsum and Ref. lime mortar with regard to their interaction with formaldehyde. Intuition suggests that materials with higher porosity and specific surface area would exhibit a greater capacity to adsorb formaldehyde. However, the opposite was observed. The measured porosity and average pore diameter was 38.5 % and 2.37 µm for gypsum, and 35.4 % and 0.67 µm for Ref. mortar respectively. In addition to this,

gypsum also showed a specific surface area approximately three times higher than the Ref. mortar, 15.8 m^2/g and 5.3 m^2/g respectively. Results from the formaldehyde adsorption and desorption testing showed that, despite the Ref. mortar featuring lower specific surface area and porosity, the capacity to adsorb formaldehyde was three times higher. The calculated mass of formaldehyde adsorbed by the Ref. mortar was 324 µg compared to 102 µg adsorbed by the gypsum specimen. This supports the conclusions that the pore size has a very important role to play in the interactions between the material surface and the molecules of VOCs. Despite the gypsum specimen having higher porosity and specific surface area, its average pore diameter was also greater than that measured for the Ref. mortar and the pore size distribution was narrower. By having a narrower pore size distribution, a great number of pores present in the gypsum microstructure had sizes around the calculated average, 2.37 µm. In the case of the Ref. mortar, the pore size distribution was wider meaning that this material had pores significantly larger or smaller than the calculated average of 0.67 µm. Relating this to the interactions between both materials and formaldehyde, and their capacity to adsorb this compound, it appears that microstructures with smaller pores have a great capacity to adsorb formaldehyde. In addition to this, a wider pore size distribution means that the lime mortar has pores with higher diameter than the calculated average. This would promote the diffusion of gases throughout the material increasing the number of potential adsorption sites. This discussion is made assuming that the chemical composition of both materials has no influence on their respective adsorption and desorption characteristics.

The specific surface area can be correlated with the adsorption and desorption characteristics of building materials. However, there are exceptions for some particular materials as there are other processes involved such as chemisorption. If no chemisorption is occurring, the specific surface area is one of the main factors influencing the capacity of a materials to adsorb and desorb VOCs, called the sink effect. This is clearly shown through the investigation of the adsorption and desorption of the lime mortars with different amounts of TiO_2 particles incorporated (ETDK*x*). The presence of TiO_2 particles in the lime mortar led to an increase in specific surface area and a corresponding decrease in the number of larger pores attributed to the deposition of TiO_2 in the region within the lime mortar microstructure. Specimens with higher surface area contained a higher adsorbed mass of dodecane as shown in Table 8.1. In the case of formaldehyde, the ETDK2 adsorbed slightly more formaldehyde compared to the specimen ETDK5. This may be related to the uncertainty of the adsorption/desorption testing of formaldehyde.

Another example of the effect of the specific surface area on the adsorption of VOCs is the comparison between the MDF, Coated MDF and Mortar_P investigated in Chapter 4, Figure 8.2. Materials with low specific surface area, as is the case for the Coated MDF, have deeper adsorption sites accessible to VOC molecules.

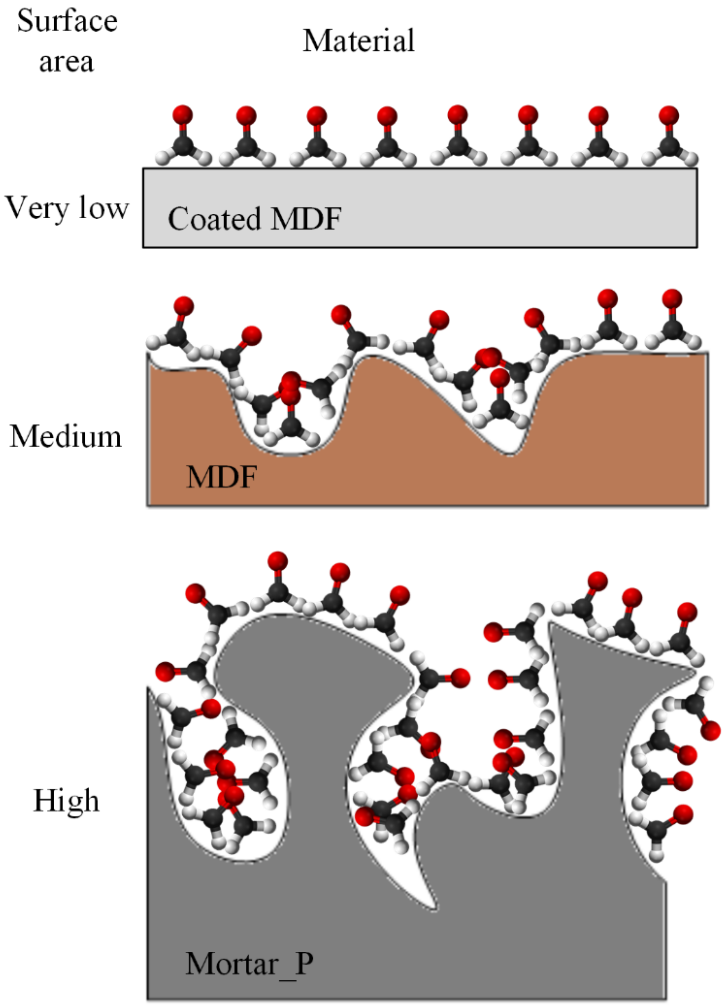

Figure 8.2 Effect of the surface area on the adsorption of formaldehyde. Greater surface area → greater number of adsorption sites → greater adsorbed formaldehyde content.

The main purpose of incorporating natural wool into the Mortar_P formulation was to increase the capacity of the mortar to adsorb formaldehyde, as it was known that wool has the ability to chemisorb this organic pollutant, Figure 8.3. However, by adding wool to the lime mortar matrix, the specific surface area decreased. The lower specific surface area of the lime mortars with natural wool incorporated led to a slight decrease of the adsorption of VOCs. The capacity of the mortar with wool additions to adsorb formaldehyde increased significantly. The very

low mass of formaldehyde desorbed strongly suggested that for practical purposes this effect was irreversible, as only 1.6 % of the adsorbed formaldehyde was desorbed thereafter. This means that approximately 1.6 % of the adsorbed formaldehyde was physisorbed on the surface of the lime mortar and the remainder was chemisorbed by the wool fibres.

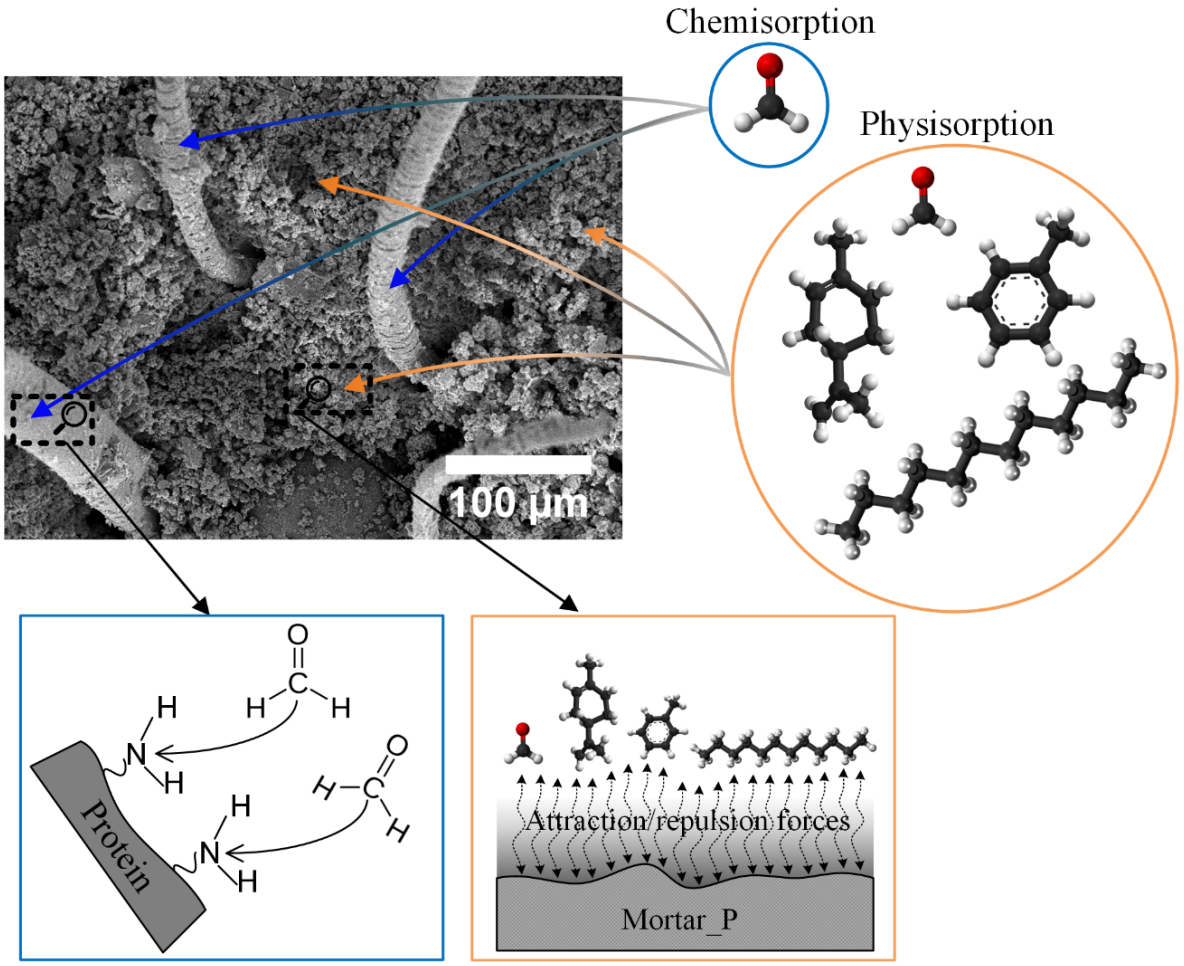

Figure 8.3 Illustration of the interactions between toluene, limonene, dodecane and formaldehyde and the lime mortar with Natural wool incorporated.

When a gas molecule (adsorbate) is flowing near a solid surface (adsorbent), the energy resulting from the interaction between the gas molecule and the molecules at the surface of the solid material depends on the distance between them. At larger distances (short enough to provoke interactions between the two species), the resulting force is attractive, generally Van der Waals. At shorter distances, the forces are repulsive due to the overlapping of the electron orbitals of the two-interactive species (Lennard-Jones 1931; Young and Crowell 1962; Masel 1996). Lennard-Jones (1931; 1937) developed a mathematical expression, known as *Lennard-*

Jones potential, which reflects the resulting potential of a gas molecule approaching a solid surface involving attractive and repulsive forces (Young and Crowell 1962; Rouquerol et al. 2014). The simplified expression of the Lennard-Jones potential function of the distance (*r* in Å) between the interactive species is given by equation 8.1:

$$L.J.potential\ (r) = -A.r^{-m} + B.r^{-n} \qquad \text{Eq. 8.1}$$

Where, $A.r^{-m}$ is the energy related to the attractive forces and $B.r^{-n}$ is the energy related to the repulsive forces, in which, A and B are the attractive and repulsive forces, respectively. In most of the cases, the constants *m* and *n* are 6 and 12 respectively, and in this case the Lennard-Jones potential is referred as L-J 6-12 potential (Young and Crowell 1962; Rouquerol et al. 2014).

Considering a flat (non-porous) surface, or pores with different sizes (micropores or mesopores) present in the microstructure of a certain solid material, the plot of Lennard-Jones potential will have different profiles, that are dependent on the microstructure as shown in Figure 8.4. Examining the L. J. plot of the case a) in Figure 8.4, the potential is positive at shorter distances between the adsorbate and the adsorbent, in which case, the dominant forces are repulsive. The distance between the two-interactive species is never 0 Å. The negative values of potential energy occur at greater distances where the dominant forces are attractive. The minimum potential represents the balance between the repulsive and attractive forces. In the case of porous solid structures with micropores, there is a favourable minimum value for the potential energy, due to the short distance between the walls of the pore, Figure 8.4 b). The adsorbate molecule is adsorbed at the respective distance *r* where the potential energy is a minimum. When the adsorbate molecules are flowing in a wider pore (mesopore) the potential is similar to a non-porous surface when the molecule approaches a wall of the pore, Figure 8.4 c).

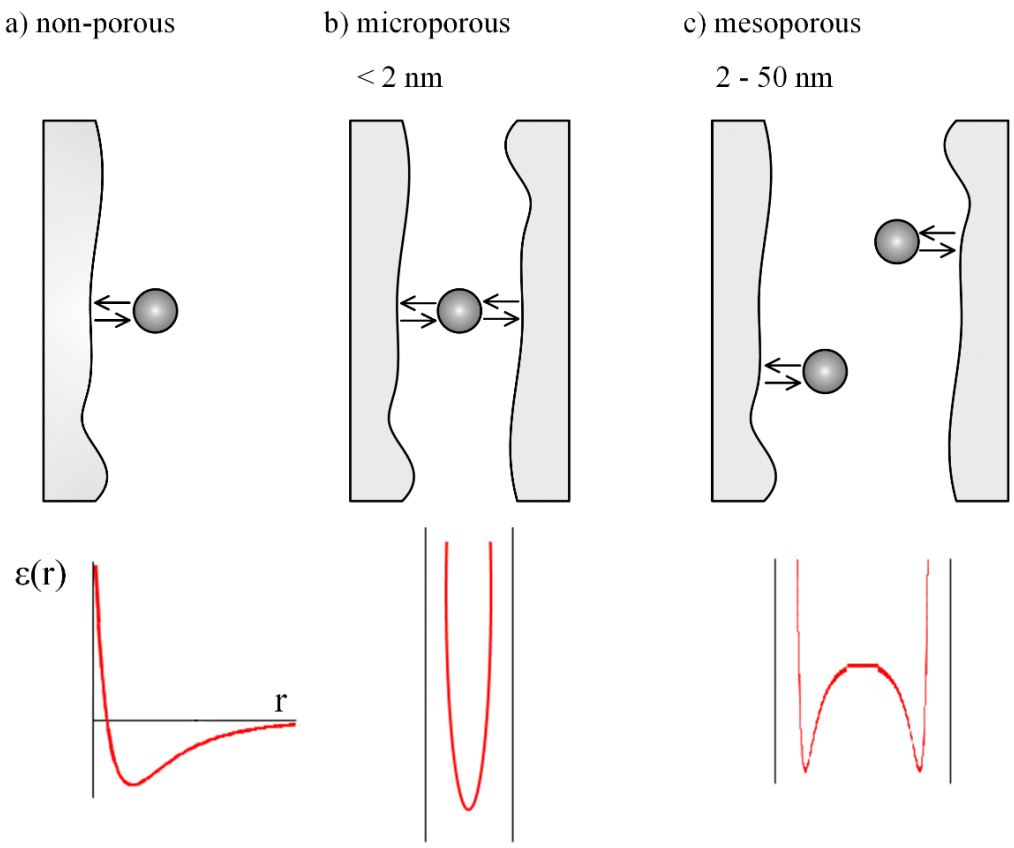

Figure 8.4 Plot of the adsorption Lennard-Jones potential function in a) non-porous, b) microporous and c) mesoporous materials as a function of the distance between the gas molecule and the solid surface.

The Lennard-Jones potential can be related to the Scattering, Trapping and Sticking processes described by Masel (1996) and introduced previously in section 2.3.1 *Definitions and theories of sorption*. In the case of the Trapping and Sticking mechanisms, the adsorbate molecules approach the solid surface and bounce for some time until trapping or sticking to the surface occurs. However, the adsorbed molecule being trapped or stuck to the solid surface does not mean that it is in a fixed state, i.e. it is continuously under repulsive and attractive forces which sustains slight bouncing of the molecule without leaving the surface but at the same not being in physical contact with the surface.

The Lennard-Jones potential supports the greater ability of materials with smaller pore size to adsorb VOCs, even if they have lower surface area measured by BET. This was the case for the comparison between gypsum and Ref. mortar (Mortar_P) in which, Ref. mortar showed a wider pore size distribution and greater ability to adsorb formaldehyde despite the lower specific surface area. Therefore, larger macropores (size greater than 50 nm) would have the ability to adsorb some VOCs and also would promote the diffusion of the VOCs into the inner

microstructure of the material, Figure 8.5. The mesopores (2 – 50 nm) also have the capacity to diffuse some VOCs, although, the molecular size of the VOCs can limit this process since once there are molecules adsorbed on the pore wall, the pore size is no longer the distance between the walls of the pore, but the distance between the adsorbed molecules on the pore walls. Therefore, the bigger the size of the adsorbed VOC molecule, the smaller will be the resulting free space in the pore for diffusion. This mechanism is exemplified in Figure 8.5, which shows the reduction of the pore size after VOCs have been adsorbed onto the pore walls in the case of a system with a single VOC (Figure 8.5 a) for formaldehyde) or when there is a mixture of four VOCs, Figure 8.5 b). The reduction of the pore size after the monolayer adsorption occurred is shown by the dashed line. It is clear that the size of the VOC molecules adsorbed influences the diffusion of additional VOCs. In the case of the multi-VOC system, there is insufficient free space for diffusion after a monolayer of VOC's has been adsorbed onto the walls of a micropore. In a single VOC system, or even a multi-VOC system of smaller molecular size, after a monolayer of VOCs has been adsorbed, there is still some free space available for diffusion.

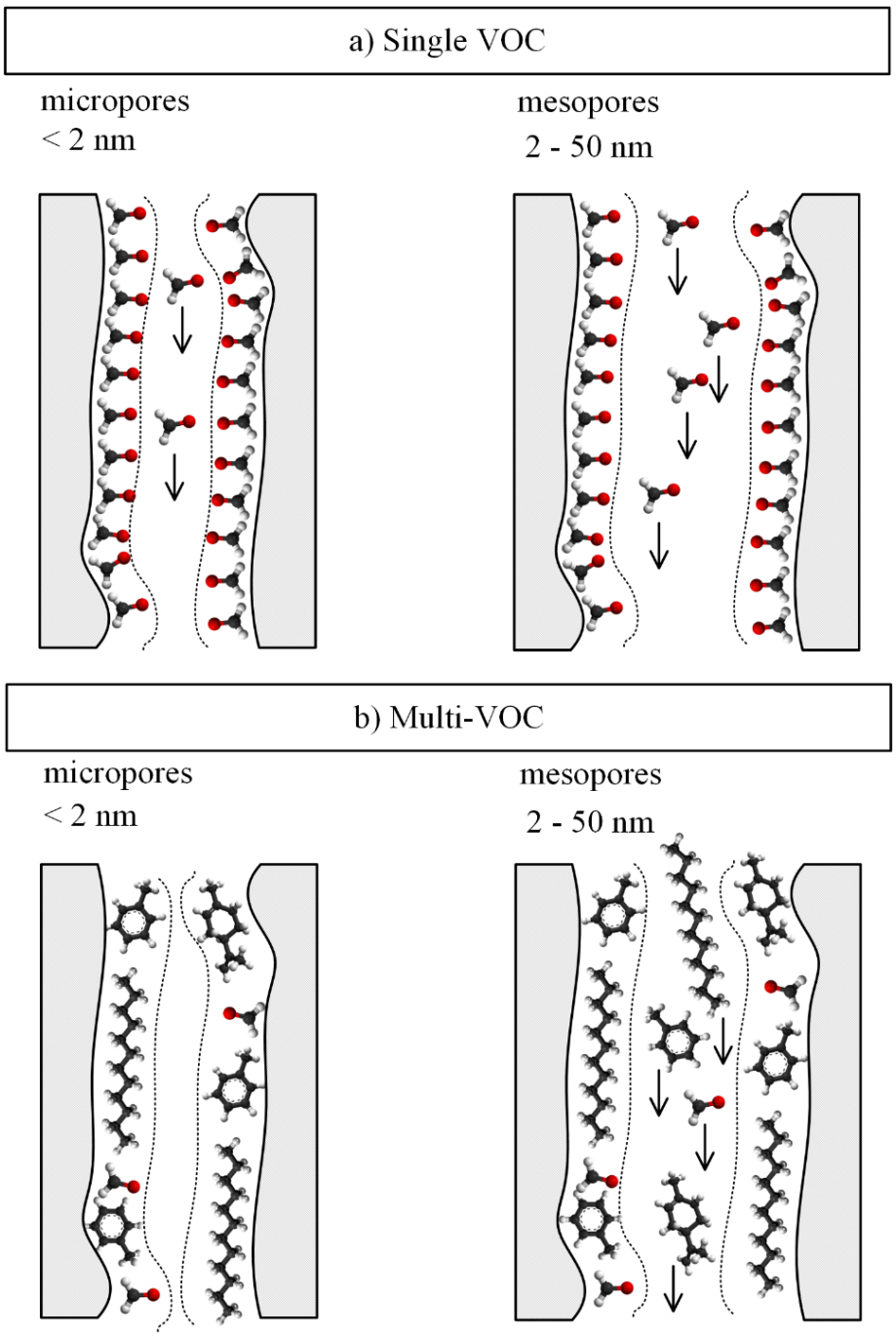

Figure 8.5 Diffusion of VOCs through the macro and mesopores after a monolayer of VOCs have been adsorbed. Dashed lines show the reduction of the pore size after the monolayer adsorption.

The fairly flat surface of the wool fibres is favourable for the chemisorption of formaldehyde to occur. Masel (1996) stated that the bond scission in a chemisorption process depends on the type of bond being broken and also on the orientation of that bond relative to the surface of the adsorbent. Masel named this issue as the **proximity effect**. It is said that bond scission would only occur if the adsorbate molecule is close enough to the adsorbent surface. Figure 8.6, taken from Masel (1996), illustrates two examples of how the sites where the chemical reaction between the adsorbent and the adsorbate occur and roughness of the adsorbent surface influences the chemisorption. Figure 8.6 a) shows that, if the adsorbate molecule is chemisorbed on the top of the steps of the adsorbent surface, the chemisorption efficiency would decrease compared to the case where the adsorbate molecules react in the valleys. The same surface would chemisorb six adsorbate molecules in the case of these reacting in the valleys of the surface while, in the other configuration, the surface would chemisorb only three molecules. Figure 8.6 b) illustrates how the roughness of a surface influences its chemisorption capacity; an atom X in an adsorbate molecule reacts on an available adsorption site at the bottom of the step. On the left-hand side diagram, the step density is lower and thus the atom X of the adsorbate molecule is able to get closer to the available adsorption site. If the step density is higher (right-hand side diagram), the adsorbate molecule will be chemisorbed at the top of two steps, creating a *bridge* over two steps.

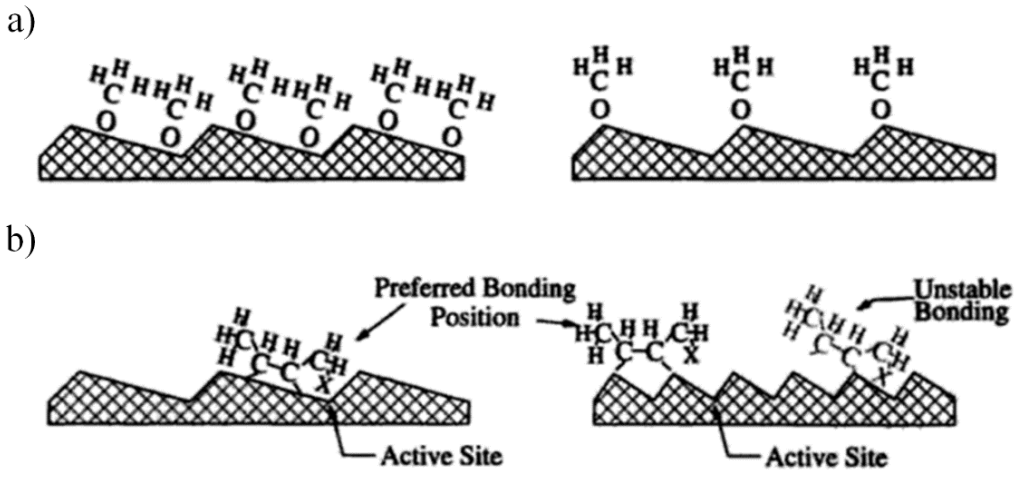

Figure 8.6 Illustration showing how an increase in step density can influence the reactivity on the surface. Figure taken from Masel (1996).

The proximity effect may be the reason why the specimen 2.5 % w_mortar adsorbed more formaldehyde compared to the TL w_mortar. The lime mortar matrix plays an important role in attracting the formaldehyde molecules closer to the wool fibres prior to their chemisorption. While in the case of the TL w_mortar, the wool fibres are placed on top of the lime mortar and therefore the attractive forces of the lime mortar particles are lower. This is demonstrated by the 2.5 % w_mortar where the wool fibres are embedded into the lime matrix. The formaldehyde adsorption process in the lime mortars modified with natural wool is a combination of physisorption and chemisorption, as already discussed in the previous section *6.3.2 Lime mortar with natural wool – 2-litre chambers*. In the previous chapters, the adsorption/desorption behaviour of toluene, limonene, dodecane and formaldehyde towards various natural building materials is presented and discussed. The physical and chemical characteristics of the building materials, namely chemical composition, specific surface area, porosity and pore size distribution, were correlated with their adsorption and desorption behaviour. Also, the mass of dodecane and formaldehyde adsorbed and desorbed was calculated.

In this chapter, a general discussion about the mechanisms of interaction between the selected organic pollutants and the natural building materials is presented. The discussion is informed by consideration of the physical properties and chemical composition of the materials. At the end of this chapter, the influence of the physico-chemical properties of toluene, limonene, dodecane and formaldehyde on the adsorption and desorption behaviour is also discussed.

Influence of the physico-chemical characteristics of the materials on the adsorption of VOCs and formaldehyde, where the main mechanism occurred on the surface of the wool fibres is chemisorption and that occurring in the lime mortar particles is physisorption. However, before the chemisorption can occur, the physisorption has to take place - allowing formaldehyde molecules to approach the surface of the wool fibres. Figure 8.7, from Masel (1996), shows an example of how this process occurs. This illustration represents the adsorption of methane on a nickel surface. Firstly, the molecule of methane is physisorbed on the surface of the material. Afterwards, the attractive energy between the carbon atom from the methane and the material surface is sufficiently high to cause stretching of the bonds between the hydrogen atoms and carbon. This allows the carbon atom to move closer to the nickel surface, thereby allowing it to be chemisorbed. It is however noteworthy that the author points out that the activation energy for adsorption is the same as the energy needed to move the hydrogen atoms, so that the carbon atom approaches the adsorbent surface in order to be chemisorbed.

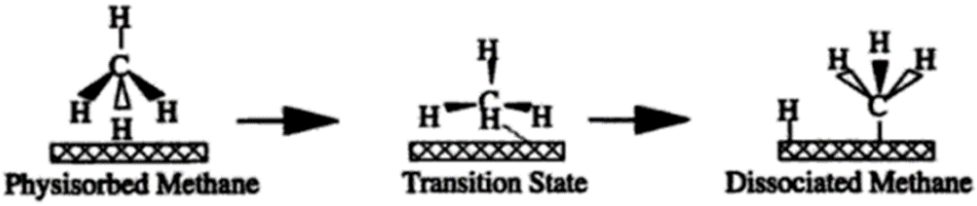

Figure 8.7 Sequence of stages prior to chemisorption of methane on a nickel surface proposed by Masel (1996).

A different example of molecular distortion upon adsorption is also given my Masel (1996) based on the data of Lin et al. (1987). This example is shown in Figure 8.8 and represents the distortion of a benzene molecule when adsorbed onto the surface of a metallic material. In this case, there is not bond scission as was observed previously in Figure 8.7. This example may reflect what happens when a molecule of toluene or limonene is physisorbed onto a natural building material surface.

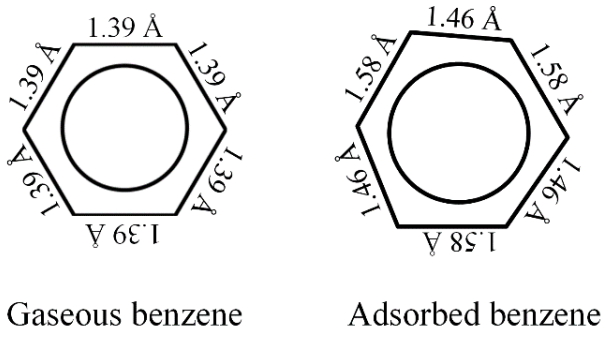

Figure 8.8 Distortion of the benzene molecule after being adsorbed on a rhodium surface. Adapted from Masel (1996).

The effect of the chemical composition of the natural building materials on the adsorption of VOCs is clearly seen when comparing the mass of dodecane and formaldehyde adsorbed by both clay plasters, presented in Table 8.1. Despite both clay plasters featuring the same measured specific surface area, Clay_H2 adsorbed more dodecane and formaldehyde. The main difference in the chemical composition of the two clays is that Clay_H2 contains 60 % of clay minerals and sand (crystalline SiO_2 - quartz), while Clay_E14 contains only 43 % of clay minerals and, instead of quartz, includes pumice in its composition. Pumice is a very

porous volcanic rock composed essentially of volcanic glass, i.e. amorphous silicate. In a crystalline material, atoms, molecules or ions are arranged in a highly ordered three-dimensional pattern, forming the crystalline lattices, Figure 8.9. On the other hand, a material with the same chemical composition in a non-crystalline/amorphous state has an irregular molecular arrangement.

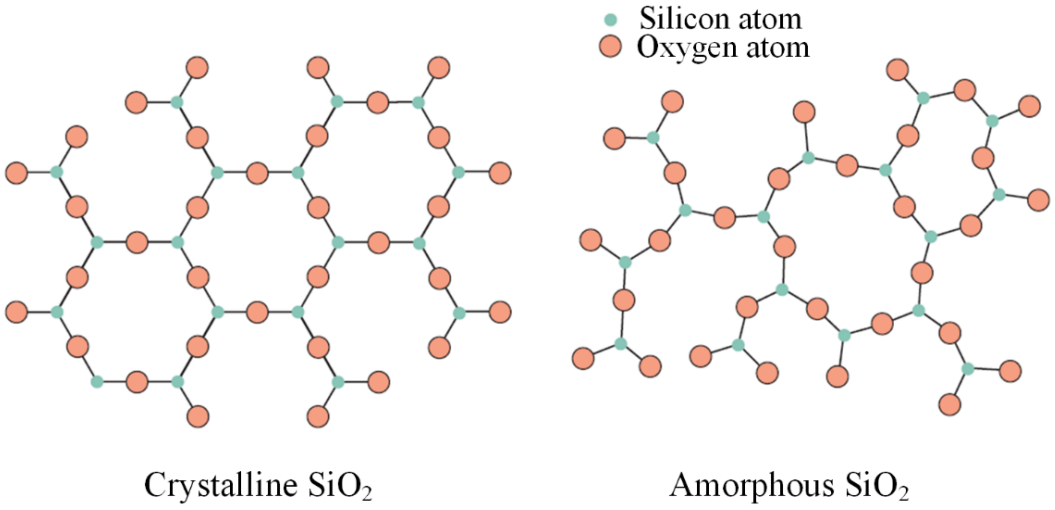

Figure 8.9 Two-dimensional diagrams illustrating the atomic arrangement in a crystalline and amorphous structure of the SiO_2. Adapted from Callister (2007).

The organised molecular structure of crystalline SiO_2 provides a flatter surface compared to amorphous SiO_2. By relating this to the proximity effect proposed by Masel (1996), it is proposed that materials in crystalline form would have lower step density and thus higher capacity to adsorb gaseous molecules compared to those with a higher step density. By comparing the physisorption of dodecane on the surface of a crystalline or amorphous material, it is possible to observe that by having lower step density, the material has the capacity to physisorb more dodecane molecules than those surfaces with higher step density, Figure 8.10.

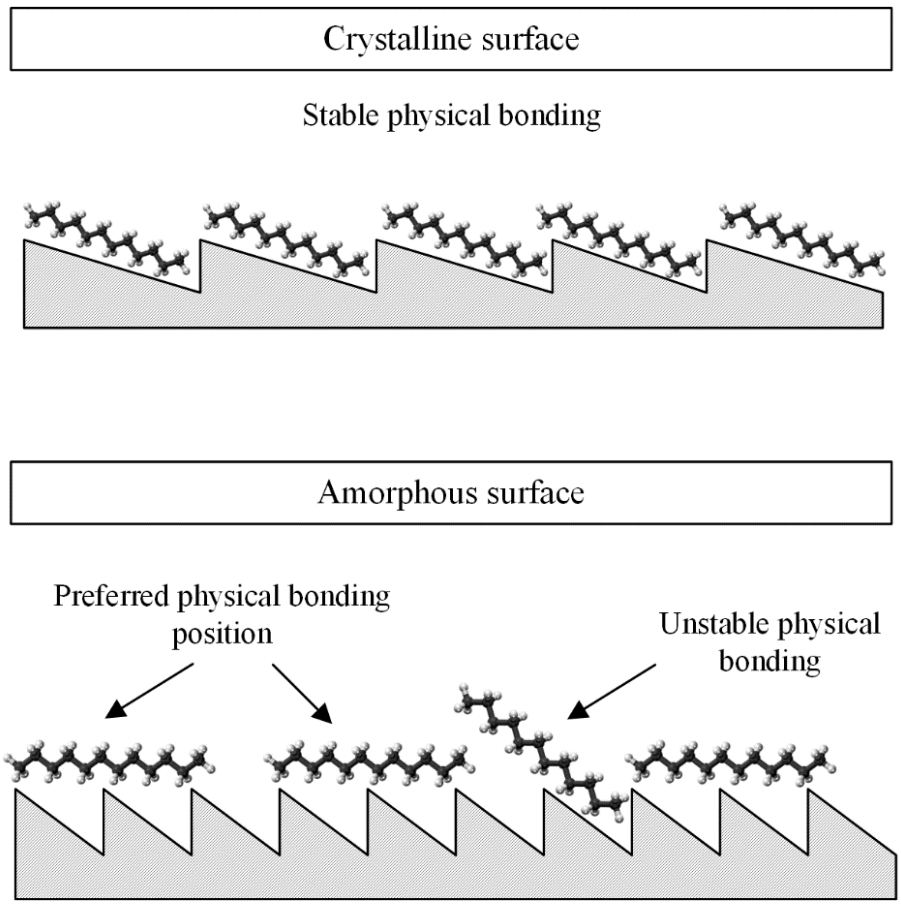

Figure 8.10 Proximity effect in the physisorption of dodecane onto the surface of quartz (crystalline) and pumice (amorphous).

As discussed previously in section *6.4.1 Clay-based plasters and lime mortar with cellulose flakes*, clay particles are composed of multilayers of clay minerals, which may in turn have a tetrahedral or octahedral molecular arrangement. Cations are located in the centre of the tetrahedron or octahedron, as shown in Figure 8.11 for the case of the kaolinite; a well known clay mineral with a $[Al_2(OH)_4(Si_2O_5)]_2$ unit cell, (Bergaya and Lagaly 2013). Depending on the electronegativity of the cation in the clay mineral (Table 8.2), the charge of the oxygen atoms changes as follows: $O(Si^{4+}) < O(Al^{3+}) < O(Mg^{2+})$. The charges of the oxygen atoms placed on the surface of the clay minerals will favour their interaction with VOCs, especially polar compounds, as is the case with formaldehyde. A similar approach can be applied to calcite crystals found in lime mortars, where a cation of calcium is placed in the centre of carbonate group (CO_3) as shown in section *4.3.1.1 Chemical characterisation*.

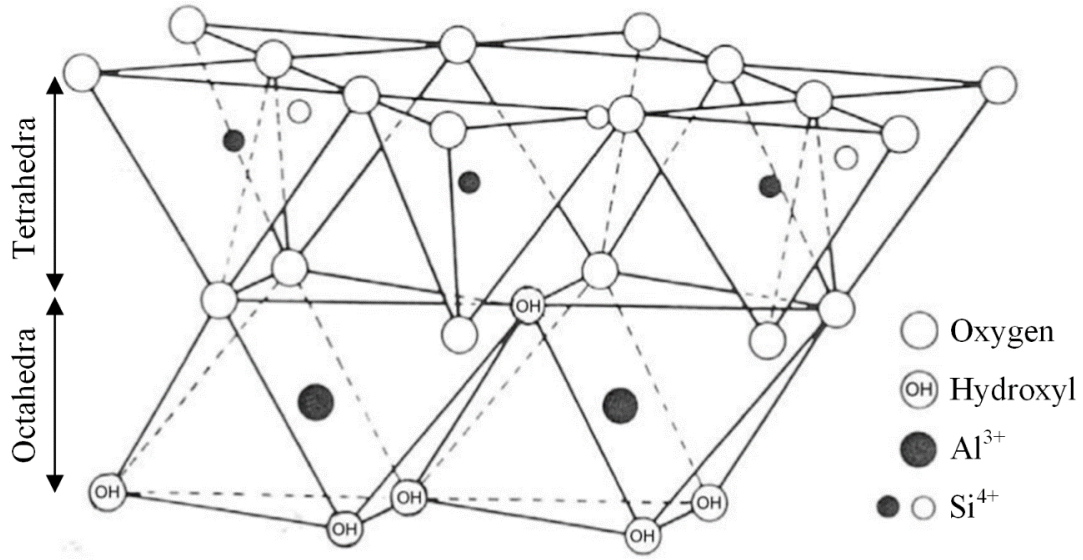

Figure 8.11 Kaolinite structure showing the atomic arrangement of the cations in the centre of the tetrahedra and octahedra. Adapted from (Rouquerol et al. 2014).

Table 8.2 Electronegativity of oxygen, silicon, aluminium and magnesium cations commonly found in molecular structures of clay minerals.

Atom	Electronegativity
Oxygen	3.44
Silicon	1.90
Iron	1.83
Aluminium	1.61
Magnesium	1.31

In addition to the discussion with regard to the passive capture of the selected organic pollutants, it is also important to describe the mechanism involved in the passive adsorption and photocatalysis of the Coated_MDF with TiO_2 particles added. The experiment started under dark conditions in which the interactions occurring were only of physical nature, i.e. Van der Waals forces etc. At this stage, the VOC molecules were captured on the surface of the TiO_2 particles, Figure 8.12. Once the LED lights were turned on, those VOC molecules that were previously adsorbed will have been degraded though photocatalytic activity and the forthcoming VOCs will follow the same path. Therefore, in such an experiment, the VOC molecules are constantly being attracted to the material surface and then degraded by photocatalytic activity.

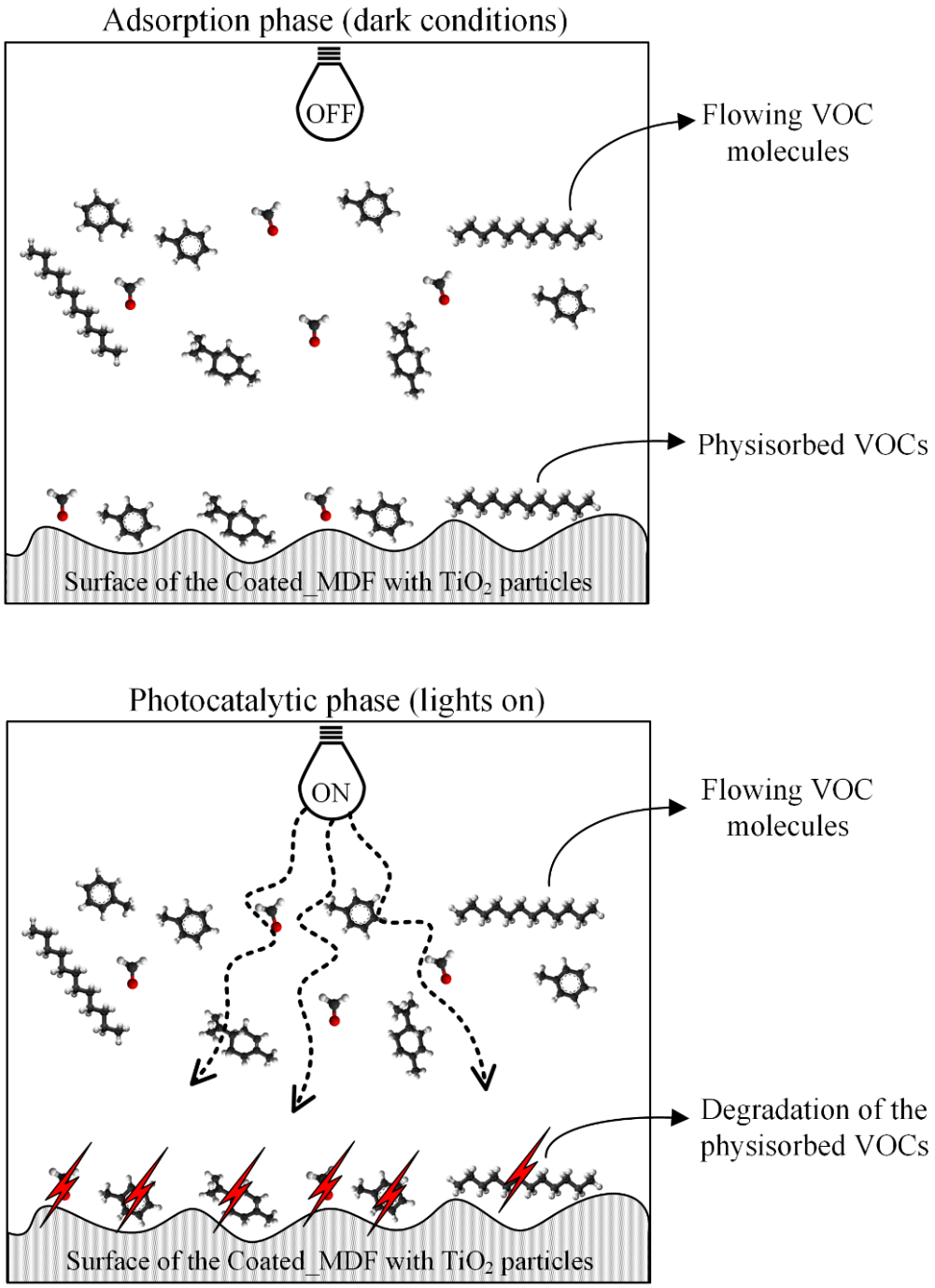

Figure 8.12 Illustration of the adsorption and photocatalytic phases of the PC panel.

8.2. Physico-chemical properties of the volatile organic compounds

Taking into account all of the data with the regard to the adsorption and desorption behaviour of natural building materials, a common observation was made in all chapters of this thesis:

- Most adsorbed VOC: formaldehyde > dodecane > limonene > toluene.

The interactions between materials and VOCs discussed in this section are of a physical nature only. Therefore, data for formaldehyde adsorption/desorption by the natural wool or lime mortars with wool incorporated is not taken into account due to the chemisorption mechanism.

In Table 8.3, some physico-chemical properties of the selected VOCs for this research are presented to support the current discussion. Formaldehyde was the most adsorbed organic pollutant by all of the natural building materials studied, due to its polarity, high vapour pressure and also water solubility - with only one exception (Mortar_P). In the case of building materials that have good capacity to buffer moisture, they will have an even greater ability to adsorb formaldehyde due to the combination of the physical adsorption of formaldehyde and water molecules and then, in addition to that, absorption of more formaldehyde molecules onto the adsorbed water. Also, the size of a formaldehyde molecule is smaller than the other VOCs which means that this molecule can reach even smaller pores in the materials' microstructures compared to larger molecules which will not fit in.

In the case of the group of non-polar molecules (toluene, limonene and dodecane), dodecane was the most adsorbed pollutant, exhibiting a significant difference to the other molecules. Most of the materials did not adsorb any toluene at all, and adsorbed only a small amount of limonene, although they adsorbed significant amounts of dodecane, at similar levels to formaldehyde for some materials. Dodecane has the lowest vapour pressure and water solubility from this group of three non-polar VOCs. This means that, in the case of non-polar compounds, those physical properties do not influence the adsorption as they do for formaldehyde. Having said that, there are other reasons which explain why dodecane is the most non-polar compound adsorbed and toluene the least. Dodecane is an aliphatic compound, i.e. a linear hydrocarbon chain, and so has more oscillating charges associated with its electron cloud that can interact with the electron clouds from the material surface. It is also able to distort along its 12-carbon atoms chain, facilitating the diffusion through the materials porous microstructure and being adsorbed onto rough surfaces. Comparing the sub-group of the non-polar compounds, that is the cyclic hydrocarbons toluene and limonene, limonene was slightly preferably adsorbed by the natural building materials. Both compounds are based on a ring of

six carbon atoms. In the case of toluene, the aromatic benzene ring has a -CH_3 group bonded to one of the carbons. The cyclic terpene limonene is also composed of a ring of six carbon atoms, with one carbon-carbon double bond in the ring; as well as a -CH_3 group on one of the carbons in the ring it has a -$C(CH_2)(CH_3)$ group bonded to another of the carbons, see Table 8.3. Therefore, limonene has two double carbon-carbon bonds separated from each other. The extra unsaturated group present in the limonene molecule, as compared to toluene, may facilitate the interactions between the electron clouds of this VOC and those on the surface of the material to a greater extent, by having more interaction sites. Due to this, limonene was slightly more adsorbed than toluene.

Table 8.3 Physico-chemical properties of formaldehyde toluene, limonene and dodecane.

	Formaldehyde	**Toluene**	**Limonene**	**Dodecane**
		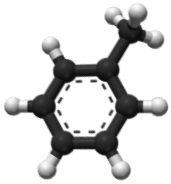	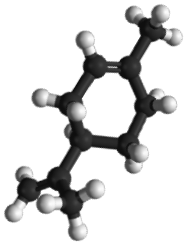	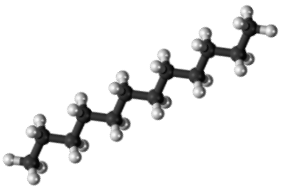
Formula	CH_2O	$C_6H_5(CH_3)$	$C_{10}H_{16}$	$C_{12}H_{26}$
Chemical conformation	Simple	Aromatic	Aromatic	Aliphatic linear chain
Polarity	Polar	Non-polar	Non-polar	Non-polar
Vapour pressure at 25 °C (mm Hg)	3890	28.4	1.45	0.135
Water solubility at 25 °C (mg/l)	400000	526	13.8	0.0037

Chapter 9

Conclusions and future recommendations

9.1. Summary and main research findings

Building materials are often identified as one of the major contributors to poor indoor air quality. This PhD research thesis has proved that the use of VOC emission-free natural building materials can improve poor IAQ by not contributing to harmful air pollutants in the first place and also by actively removing the organic pollutants emitted by other VOC sources. Use of these materials can lead to improvements in the indoor air quality of an indoor space without the need for using air purifiers which consume energy and sometimes produce other harmful gases such as ozone.

The aim of the underlying work of this PhD was to investigate how natural building materials would behave when exposed to a polluted environment and the development of novel materials with improved capacity to capture organic pollutants from the indoor air, which was successfully fulfilled.

To achieve the objectives of this PhD, several natural building materials were selected featuring different chemical composition and physical characteristics (analysed by several techniques) such as specific surface area and porosity, and classed according to their application: insulation, coating (plaster or render) and wood-based panels. In total, 18 natural building materials were investigated in Chapter 4 as the 'state of the art' materials, of which some were further developed for improved performance in an indoor environment.

TVOC and formaldehyde emissions of the 'state of the art' materials showed that the emission levels and type of organic compounds emitted depend mainly on the chemical composition of the building materials. In general, no formaldehyde was emitted by the materials other than the wood-based panels. This was attributed to the formaldehyde-based resins used by the panel manufacturers to glue the wood fibres together to form the wood board. With regard to the TVOC emissions, these were shown to be very low for all materials and the type of VOC

emitted was related to the chemical composition of the building material. For example, natural VOCs, such as α-pinene, were emitted by wood based materials such as panels and insulation materials including Hemp-lime, Hemp fibres and Wood fibreboard. The main type of VOCs emitted by the lime mortars were alcohols and aldehydes which may originate from the fuels used by the manufacturers to produce the lime powder. Some VOCs emitted by the wood-based materials were related to the degradation of the hemicellulose – acetic acid and furfural.

To study the ability of natural building materials to improve the indoor air quality and investigate their interactions with VOCs, experiments of adsorption and desorption were carried out. These experiments were performed in lab-scale environmental chambers and in a real-sized room with a volume of 30 m^3, featuring a door and a window. Both configurations had controlled inlet air flow-rate, temperature and relative humidity. The organic pollutants toluene, limonene, dodecane and formaldehyde were selected because they are commonly found in a polluted indoor environment and also have distinct physico-chemical properties. Adsorption/desorption experiments allowed simulation of realistic situations, where the natural building materials were exposed to polluted air (adsorption phase) followed by clean air (desorption phase). From the 18 state of the art materials, four were selected to investigate their adsorption/desorption: MDF, Coated_MDF, Mortar_P and Natural wool. Highly porous materials such as MDF and Mortar_P showed a better ability to capture VOCs from the air. Coated_MDF had the worst adsorption/desorption performance due to its very flat surface. Natural wool proved to be a good adsorber of formaldehyde due to its high capacity for chemisorption of organic pollutants. Materials with wider pore size distribution and smaller pore size will adsorb more VOCs because of their higher specific surface area featuring a larger number of adsorption sites. Also, because of the larger pores, the VOCs can easily diffuse through the material to reach the inner microstructure and find even more adsorption sites, as was the case for Mortar_P.

In Chapter 5, the MDF panels were modified by incorporating walnut shell. It was concluded that the addition of the walnut shell led to an increase in capacity to adsorb VOCs. By investigating the microstructure of the MDF with walnut incorporated, using scanning electron microscopy, it was concluded that the improvement in the adsorption capacity was due to the highly porous surface of the walnut shell, which is a physical characteristic.

Two clay-based plasters with the same specific surface area showed varying abilities to adsorb VOCs, (Chapter 6). This difference was attributed to their chemical composition. The clay plaster with higher clay mineral content and crystalline SiO_2 had preferable characteristics with

which to adsorb VOCs. In this same chapter, the adsorption and desorption of the lime mortar with natural wool incorporated was also investigated. It was found that the addition of wool fibres led to a decrease in the specific surface area of the lime mortar; however the effect of the lower specific surface area had only a slight effect on the adsorption of toluene, limonene and dodecane. With regard to formaldehyde it was shown that, by adding only 1 % of natural wool to the lime mortar matrix, the material had the capacity to reduce this organic pollutant by up to 93 % of its concentration in the indoor air compared to the 57 % by the Reference mortar or only 20 % by the traditional gypsum plaster.

In Chapter 7, the adsorption and desorption behaviour of lime mortar with TiO_2 particles incorporated was studied. The photocatalytic activity of lime mortars with TiO_2 particles has been studied extensively. However, its capacity to adsorb VOC under dark conditions has received much less attention and was therefore investigated in this PhD research. It was found that, by adding a small quantity of TiO_2 particles at up to 5 % of the lime mortar by weight, the uptake of VOCs increased from 27 % to 45 %. In Chapter 4 it was observed that the specimen Coated_MDF did not adsorb any VOCs due to its very flat surface. This material was then coated with TiO_2 particles and its capacity to adsorb VOC under dark conditions, and then degrade them when the lights were turned on, was investigated in the 30 m^3 chamber. The greater uptake of VOCs when the lights were on indicated that this material had the ability to adsorb VOCs and afterwards degrade them when irradiated with light.

As a final remark, the main findings of this PhD research are summarised as follows:

- ✓ Natural building materials are typically low- or zero-VOC emitters;
- ✓ Natural building materials can improve the indoor air quality by adsorbing organic pollutants passively;
- ✓ The wide range of chemical compositions of the building materials, their different physical characteristics, and the four selected VOCs with different physico-chemical properties allowed the mechanisms of interaction between with materials surface and VOC molecules to be investigated;
- ✓ Interactions between materials and VOCs depend on the materials' properties and also on physico-chemical characteristics of the VOCs, and is shown to be a combination of both factors;
- ✓ Most natural building materials are porous, with pores visible at macro- and microscale;

- ✓ Depending on the size of the pores, these can play an important role on the diffusion of the VOCs through the material to reach other available adsorption sites (macropores); or, play an important role on the adsorption of VOCs by having more adsorption sites available due to higher surface area (meso- and micropores);
- ✓ Materials with the same specific surface area showed different VOC adsorption capacities, indicating that the chemical composition of the material had an effect on the interaction between the material and the VOCs;
- ✓ For the same material, the physico-chemical properties of the VOCs influenced the adsorption/desorption behaviour, so that the more polar VOCs and VOCs with molecules featuring simple chemical conformation, e.g. a linear hydrocarbon chain, are preferably adsorbed by the material;
- ✓ Building materials with good moisture buffering properties will have good adsorption capacity for water soluble VOCs;
- ✓ By combining two building materials which have a good ability to adsorb different organic pollutants either by physisorption and/or chemisorption, the final composite material may feature outstanding VOC uptakes;
- ✓ Physical interactions between the surface of the materials and VOC molecules are based on attractive and repulsive forces which keep the VOC molecule adsorbed onto the material surface depending on the chemical composition and porosity of the building material concerned.

The main conclusions and research findings of this PhD thesis contribute to the scientific knowledge of how natural building materials can improve the indoor air quality and shows why materials have different capacities to adsorb/desorb VOCs. The outcomes of the research will guide the development of new materials for achieving better indoor air quality. Notwithstanding, some future recommendations are made in the next section.

9.2. Proposed recommendations

- ➢ It was observed that materials with good capacity to buffer moisture have a superior ability to take up water soluble VOCs. The investigation of the adsorption and desorption behaviour of these materials under dry conditions would provide further

understanding of the adsorption/desorption mechanisms. The effect of the water vapour would be eliminated and thus the intrinsic capacity of the material to adsorb water soluble VOCs could be investigated;

- A study of the diffusion of VOCs through natural building materials could be achieved by placing the material between two chambers, one chamber containing polluted air with known concentrations, and measuring the concentration of those pollutants in the other chamber;
- In the case of composite building materials such as lime mortars and clay plasters, a study of the adsorption and desorption behaviour of each constituent could be made to investigate their individual contribution;
- In the VOCs adsorption/desorption experiments, performed, the desorption phase could be continued until no more VOCs were being re-emitted by the materials. This would allow the calculation of the real desorbed mass of VOCs;
- The adsorption and desorption behaviour of the building materials tested in the 30 m^3 environmental chamber should be compared with an "empty" chamber test where no material is installed. This will inform if there is any sink effect of the chamber;
- For a full assessment of environmental performance, a study of the hygrothermal properties of these materials should be carried out.

References

Abdul-Wahab, S.A. ed., 2011. *Sick Building Syndrome*. Springer.

Abell, A.B., Willis, K.L., and Lange, D.A., 1999. Mercury Intrusion Porosimetry and Image Analysis of Cement-Based Materials. *Journal of Colloid and Interface Science*, 211, pp.39–44.

Agarwal, U.P., 2006. Raman imaging to investigate ultrastructure and composition of plant cell walls: distribution of lignin and cellulose in black spruce wood (Picea mariana). *Planta*, 224(5), pp.1141–1153.

Agrios, A.G. and Pichat, P., 2005. State of the art and perspectives on materials and applications of photocatalysis over TiO2. *Journal of Applied Electrochemistry*, 35(7–8), pp.655–663.

Alexander, P., Carter, D., and Johnson, K.G., 1951. Formation by formaldehyde of a cross-link between lysine and tyrosine residues in wool. *The Biochemical journal*, 48(4), pp.435–441.

American Society of Heating, R. and A.-C.E.T.A.I. of A.B.O. and M.A.I.S.M. and A.C.C.N.A.U.S.G.B.C. and Agency, U.S.E.P., 2009. *Indoor Air Quality Guide*.

An, Y., Zhang, J.S., and Shaw, C.Y., 1999. Measurements of VOC Adsorption / Desorption Characteristics of Typical Interior Building Materials. *HVAC & Research*, 5, pp.37–41.

Anbalagan, G., Mukundakumari, S., Murugesan, K.S., and Gunasekaran, S., 2009. Infrared, optical absorption, and EPR spectroscopic studies on natural gypsum. *Vibrational Spectroscopy*, 50(2), pp.226–230.

Anon, *ChemSpider database of the Royal Society of ChemistryNo Title* [Online]. Available from: www.chemspider.com.

Ansell, M.P., Ball, R.J., Lawrence, M., Maskell, D., Shea, A., and Walker, P., 2017. 7 – Green composites for the built environment. In: *Green Composites*. pp.123–148.

Ashby, M.F., 2013. *Materials and the Environment*. 2nd ed. Elsevier Inc.

Atkins, P.W. and De Paula, J., 2014. *Atkins' Physical chemistry.* 10th ed. Oxford University Press.

Ayrilmis, N., Buyuksari, U., Avci, E., and Koc, E., 2009. Utilization of pine (Pinus pinea L.) cone in manufacture of wood based composite. *Forest Ecology and Management*, 259(1), pp.65–70.

Van Balen, K., 2005. Carbonation reaction of lime, kinetics at ambient temperature. *Cement and Concrete Research*, 35(4), pp.647–657.

Van Balen, K. and Van Gemert, D., 1994. Modelling lime mortar carbonation. *Materials and Structures*, 27(7), pp.393–398.

Ball, R.J., El-Turki, A., and Allen, G.C., 2011. Influence of carbonation on the load dependent deformation of hydraulic lime mortars. *Materials Science and Engineering: A*, 528(7–8), pp.3193–3199.

Barak, Phillip; Nater, E.A., 2005. The Virtual Museum of Minerals and Molecules: Molecular Visualization in a Virtual Hands-On Museum [Online]. *Journal of Natural Resources and Life Sciences Education*, 34, pp.67–71. Available from: http://www.jnrlse.org.ezp2.lib.umn.edu/view/2005/e04-0042.pdf.

Baumann, M., Lorenz, L., Batterman, S., and Zhang, G.-Z., 2000. Aldehyde Emissions From Particleboard and Medium Density Fiberboard Products. *Forest Products Journal*, 50(9), pp.75–82.

Baumann, M.G.D., Batterman, S.A., and Zhang, G.-Z., 1999. Terpene emissions from particleboard and medium-density fiberboard products. *Forest products journal*, 49(1), pp.49–56.

Belarmino, D.D., Ladchumananandasivam, R., and Belarmino, L.D., 2012. Physical and Morphological Structure of Chicken Feathers (Keratin Biofiber) in Natural, Chemically and Thermally Modified Forms. *Materials Sciences and Applications*, 3, pp.887–893.

Bergaya, F. and Lagaly, G. eds., 2013. *Handbook of Clay Science*. Elsevier.

Berge, B., 2009. *The Ecology of Building Materials*. 2nd ed. Elsevier Ltd.

Berglund, B., Clausen, G., Kettrup, A., Lindvall, T., and Maroni, M., 1997. Total Volatile Organic Compounds (TVOC) in Indoor Air Quality Investigation. Report No 19. *European Communities*, pp.1–45.

Boran, S., Usta, M., and Gümükaya, E., 2011. Decreasing formaldehyde emission from medium density fiberboard panels produced by adding different amine compounds to urea

formaldehyde resin. *International Journal of Adhesion and Adhesives*, 31(7), pp.674–678.

Boran, S., Usta, M., Ondaral, S., and Gümüşkaya, E., 2012. The efficiency of tannin as a formaldehyde scavenger chemical in medium density fiberboard. *Composites Part B: Engineering*, 43(5), pp.2487–2491.

Brown, S.K., 1999. Chamber assessment of formaldehyde and VOC emissions from wood-based panels. *Indoor air*, 9(3), pp.209–215.

Callister, W.D., 2007. *Materials Science and Engineering: An Introduction*. John Willey & Sons.

Cheng, Y.H., Lin, C.C., and Hsu, S.C., 2015. Comparison of conventional and green building materials in respect of VOC emissions and ozone impact on secondary carbonyl emissions. *Building and Environment*, 87, pp.274–282.

Chiang, Y.C., Chiang, P.C., and Huang, C.P., 2001. Effects of pore structure and temperature on VOC adsorption on activated carbon. *Carbon*, 39(4), pp.523–534.

Colombo, A., De Bortoli, M., Knoppel, H., Pecchio, E., and Vissers, H., 1993. Adsorption of Selected Volatile Organic Compounds in a Carpet, a Wall Coating, and a Gypsum Board in a Test Chamber. *Indoor Air*, 3, pp.276–282.

Crump, D., Dengel, A., and Swainson, M., 2009. *Indoor Air Quality in highly energy efficient homes - a review*. IHS BRE Press on behalf of the NHBC Foundation.

Crump, D.R., Squire, R.W., and Yu, C.W.F., 1997. Sources and concentrations of formaldehyde and other volatile organic compounds in the indoor air of four newly built unoccupied test houses. *Indoor and Built Environment*, 6(1), pp.45–55.

Curling, S.F., Loxton, C., and Ormondroyd, G.A., 2012. A rapid method for investigating the absorption of formaldehyde from air by wool. *Journal of Materials Science*, 47(7), pp.3248–3251.

Dabrowski, A., 2001. Adsorption - from theory to practice. *Advances in colloid and interface science*, 93(1–3), pp.135–224.

Dai, D. and Fan, M., 2010. Characteristic and Performance of Elementary Hemp Fibre. *Materials Sciences and Applications*, 1(6), pp.336–342.

Deng, C.-S., Breen, C., Yarwood, J., Habesch, S., Phipps, J., Craster, B., and Maitland, G., 2002. Ageing of oilfield cement at high humidity: a combined FEG-ESEM and Raman

microscopic investigation. *Journal of Materials Chemistry*, 12(10), pp.3105–3112.

Dengel, A., 2014. The very air we breathe. *RICS Property Journal - Residential Environment*, pp.32–33.

Diamond, S., 2000. Mercury porosimetry - An inappropriate method for the measurement of pore size distributions in cement-based materials. *Cement and Concrete Research*, 30, pp.1517–1525.

Dickinson, R.G. and Dillon, R.T., 1929. The Raman Spectrum of Gypsum. *Chemistry*, 15, pp.695–699.

Diebold, U., 2003. The surface science of titanium dioxide. *Surface Science Reports*, 48(5–8), pp.53–229.

Downs, R.T., 2006. The RRUFF Project: an integrated study of the chemistry, crystallography, Raman and infrared spectroscopy of minerals. *19th General Meeting of the International Mineralogical Association*.

Dunlap, M., 1997. *Introduction to the Scanning Electron Microscope Theory, Practice, & Procedures*.

Edwards, D.D., Allen, G.C., Ball, R.J., and El-Turki, A., 2007. Pozzolanic properties of glass fines in lime mortars. *Advances in Applied Ceramics*, 106(6), pp.309–313.

El-Turki, A., Ball, R.J., Holmes, S., Allen, W.J., and Allen, G.C., 2010. Environmental cycling and laboratory testing to evaluate the significance of moisture control for lime mortars. *Construction and Building Materials*, 24(8), pp.1392–1397.

Elkilani, A.S., Baker, C.G.J., Al-Shammari, Q.H., and Bouhamra, W.S., 2003. Sorption of volatile organic compounds on typical carpet fibers. *Environment International*, 29(5), pp.575–585.

European Union Joint Research Centre, 2013. *Urban Air, Indoor Environment and Human Exposure: Harmonisation framework for health based evaluation of indoor emissions from construction products in the European Union using the EU-LCI concept*.

Fang, L., Clausen, G., and Fanger, P.O., 1999. Impact of temperature and humidity on chemical and sensory emissions from building materials. *Indoor air*, 9(3), pp.193–201.

Fujishima, A. and Honda, K., 1972. Electrochemical Photolysis of Water at a Semiconductor Electrode. *Nature*, 238(5358), pp.37–38.

Fujishima, A., Rao, T.N., and Tryk, D.A., 2000. Titanium dioxide photocatalysis. *Journal of Photochemistry and Photobiology C: Photochemistry Reviews*, 1(1), pp.1–21.

Fujishima, A., Zhang, X., and Tryk, D.A., 2008. TiO2 photocatalysis and related surface phenomena. *Surface Science Reports*, 63(12), pp.515–582.

Garside, P. and Wyeth, P., 2003. Identification of Cellulosic Fibres by FTIR Spectroscopy. *Studies in Conservation*, 48, pp.269–275.

Giampiccolo, A., Ibáñez Gómez, J.A., de Miguel, Y.R., Mair, S., Casado, A.M., da Silva, C.F., Tobaldi, D.M., Mayer, F., Ansell, M.P., Labrincha, J.A., and Ball, R.J., 2017. Novel TiO2-based photocatalytic lime mortar for indoor air quality improvement using visible light. *Submitted to Journal of Physics and Chemistry of Solids*.

Giampiccolo, A., Tobaldi, D.M., Ansell, M.P., and Ball, R.J., 2016. Synthesis of Co-TiO2 nanostructured photocatalytic coatings for MDF substrates. *Green Materials*, 4(4), pp.140–149.

Gonçalves, H., Gonçalves, B., Silva, L., Vieira, N., Raupp-Pereira, F., Senff, L., and Labrincha, J.A., 2014. The influence of porogene additives on the properties of mortars used to control the ambient moisture. *Energy and Buildings*, 74, pp.61–68.

Gonçalves, M.C. and Margarido, F., 2015. *Materials for Construction and Civil Engineering*. Springer.

Gunnarsen, L., Nielsen, P.A., and Wolkoff, P., 1994. Design and Characterization of the CLIMPAQ, Chamber for Laboratory Investigations of Materials, Pollution and Air Quality*. *Indoor Air*, 4(1), pp.56–62.

Gunschera, J., Markewitz, D., Koberski, U., and Salthammer, T., 2013. Catalyzed Reactions on Mineral Plaster Materials Used for Indoor Air Purification. *Clean - Soil, Air, Water*, 41(5), pp.437–446.

Gunschera, J., Mentese, S., Salthammer, T., and Andersen, J.R., 2013. Impact of building materials on indoor formaldehyde levels: Effect of ceiling tiles, mineral fiber insulation and gypsum board. *Building and Environment*, 64, pp.138–145.

Haghighat, F. and De Bellis, L., 1998. Material emission rates: Literature review, and the impact of indoor air temperature and relative humidity. *Building and Environment*, 33(5), pp.261–277.

Hammond, C., 2009. *The Basics of Crystallography and Diffraction 3rd Ed.* Oxford University Press.

Hearn, N. and Hooton, R.D., 1992. Sample mass and dimension effects on mercury intrusion porosimetry results. *Cement and Concrete Research*, 22(4), pp.970–980.

Hodgson, a T., Beal, D., and McIlvaine, J.E.R., 2002. Sources of formaldehyde, other aldehydes and terpenes in a new manufactured house. *Indoor air*, 12, pp.235–242.

Horn, W., Ullrich, D., and Seifert, B., 1998. VOC Emissions from Cork Products for Indoor Use. *Indoor Air*, 8(1), pp.39–46.

Huang, H., Haghighat, F., and Blondeau, P., 2006. Volatile organic compound (VOC) adsorption on material: Influence of gas phase concentration, relative humidity and VOC type. *Indoor Air*, 16(3), pp.236–247.

Huang, X., Wang, Y.-J., and Di, Y.-H., 2007. Experimental Study of Wool Fiber on Purification of Indoor Air. *Textile Research Journal*, 77(12), pp.946–950.

Jiang, C., Li, D., Zhang, P., Li, J., Wang, J., and Yu, J., 2017. Formaldehyde and volatile organic compound (VOC) emissions from particleboard: Identification of odorous compounds and effects of heat treatment. *Building and Environment*, 117, pp.118–126.

Jørgensen, R.B., Bjørseth, O., and Malvik, B., 1999. Chamber testing of adsorption of volatile organic compounds (VOCs) on material surfaces. *Indoor Air*, 9, pp.2–9.

Kelly, T.J., Smith, D.L., and Satola, J. a N., 1999. Emission Rates of Formaldehyde from Materials and Consumer Products Found in California Homes. *Environmental Science & Technology*, 33(1), pp.81–88.

Kim, H.S., Kim, S., Kim, H.J., and Kim, H.G., 2006. Physico-mechanical properties, odor and VOC emission of bio-flour-filled poly(propylene) bio-composites with different volcanic pozzolan contents. *Macromolecular Materials and Engineering*, 291(10), pp.1255–1264.

Kim, K.W., Kim, S., Kim, H.J., and Park, J.C., 2010. Formaldehyde and TVOC emission behaviors according to finishing treatment with surface materials using 20L chamber and FLEC. *Journal of Hazardous Materials*, 177(1–3), pp.90–94.

Kim, S., 2009. The reduction of indoor air pollutant from wood-based composite by adding pozzolan for building materials. *Construction and Building Materials*, 23(6), pp.2319–2323.

Kim, S., Kim, J.A., Kim, H.J., and Do Kim, S., 2006. Determination of formaldehyde and TVOC emission factor from wood-based composites by small chamber method. *Polymer Testing*, 25(5), pp.605–614.

Knudsen, H.N., Kjaer, U.D., Nielsen, P. a., and Wolkoff, P., 1999. Sensory and chemical characterization of VOC emissions from building products: Impact of concentration and air velocity. *Atmospheric Environment*, 33(8), pp.1217–1230.

Koivula, M., Kymäläinen, H.R., Virta, J., Hakkarainen, H., Hussein, T., Komulainen, J., Koponen, H., Hautala, M., Hämeri, K., Kanerva, P., Pehkonen, A., and Sjöberg, A.M., 2005. Emissions from thermal insulations - Part 2: Evaluation of emissions from organic and inorganic insulations. *Building and Environment*, 40(6), pp.803–814.

Labrincha, J.A., Marques, J.I., Hajjaji, W., Senff, L., Zanelli, C., Dondi, M., and Rocha, F., 2014. Novel Inorganic Products Based on Industrial Wastes [Online]. *Waste and Biomass Valorization*, 5(3), pp.385–392. Available from: http://link.springer.com/10.1007/s12649-013-9281-4.

Lee, S.C., Lam, S., and Fai, H.K., 2001. Characterization of VOCs , ozone , and PM 10 emissions from office equipment in an environmental chamber. *Building and Environment*, 36, pp.837–842.

Lennard-Jones, J.E., 1931. Cohesion. *The proceedings of the physical society*, 43(5), pp.461–482.

Lennard-Jones, J.E., 1937. The equation of state of gases and critical phenomena. *Physica*, 4(10), pp.941–956.

Lin, R.F., Blackman, G.S., Van Hove, M.A., and Somorjai, G.A., 1987. LEED intensity analysis of the structure of coadsorbed benzene and CO on Rh(111). *Acta Crystallographica Section B*, 43(4), pp.368–376.

Linstrom, P.J. and Mallard, W.G., 2011. *NIST Chemistry WebBook, NIST Standard Reference Database Number 69*. Gaithersburg MD. Available from: http://webbook.nist.go.

Lucas, S., Senff, L., Ferreira, V.M., Barroso de Aguiar, J.L., and Labrincha, J.A., 2010. Fresh state characterization of lime mortars with PCM additions. *Applied Rheology*, 20(6), p.63162.

Makowski, M. and Ohlmeyer, M., 2006. Comparison of a small and a large environmental test chamber for measuring VOC emissions from OSB made of scots pine (Pinus sylvestris

L.). *Holz als Roh - und Werkstoff*, 64(6), pp.469–472.

Mansour, E., Curling, S., Stéphan, A., and Ormondroyd, G., 2016. Absorption of volatile organic compounds by different wool types. *Green Materials*, 4(1), pp.1–7.

Maroni, M., Seifert, B., and Lindvall, T., 1995. *Indoor Air Quality: A Comprehensive Reference Book*. Elsevier Science B.V.

Masel, R.I., 1996. *Principles of adsorption and reaction on solid surfaces*. John Wiley & Sons.

Maskell, D., da Silva, C.F., Mower, K., Rana, C., Dengel, A., Ball, R.J., Ansell, M.P., Thomson, A., Peter, U., Contu, D., and Walker, P.J., 2017. Bio-based plaster for improved indoor air quality. In: *Proceedings, 2nd International Conference on Bio-based Building materials 2017, Clermond-Ferrand*.

Matsumoto, H., Shimizu, M., and Sato, H., 2009. The contaminant removal efficiency of an air cleaner using the adsorption/desorption effect. *Building and Environment*, 44(7), pp.1371–1377.

Meininghaus, R., Gunnarsen, L., and Knudsen, H.N., 2000. Diffusion and sorption of volatile organic compounds in building materials - Impact on indoor air quality. *Environmental Science and Technology*, 34(15), pp.3101–3108.

Meininghaus, R., Kirchner, S., Maupetit, F., Sallée, H., and Quenard, D., 2000. Gravimetric studies on VOC adsorption by indoor materials under near-ambient conditions. *Indoor and Built Environment*, 9(5), pp.277–283.

Meininghaus, R., Salthammer, T., and Knöppel, H., 1999. Interaction of volatile organic compounds with indoor materials - A small-scale screening method. *Atmospheric Environment*, 33(15), pp.2395–2401.

Melià, P., Ruggieri, G., Sabbadini, S., and Dotelli, G., 2014. Environmental impacts of natural and conventional building materials: A case study on earth plasters. *Journal of Cleaner Production*, 80, pp.179–186.

Menzies, D. and Bourbeau, J., 1997. Building-Related Illness. *The New England Journal of Medicine*, pp.1524–1531.

Middlebrook, W.R., 1949. The irreversible combination of formaldehyde with proteins. *The Biochemical journal*, 44(1), pp.17–23.

Modolo, R.C.E., Ferreira, V.M., Tarelho, L.A., Labrincha, J.A., Senff, L., and Silva, L., 2013.

Mortar formulations with bottom ash from biomass combustion. *Construction and Building Materials*, 45, pp.275–281.

Mølhave, L., Clausen, G., Berglund, B., Ceaurriz, J., Kettrup, A., Lindvall, T., Maroni, M., Pickering, a C., Risse, U., Rothweiler, H., Seifert, B., and Younes, M., 1997. Total Volatile Organic Compounds (TVOC) in Indoor Air Quality Investigations. *Indoor Air*, 7(19), pp.225–240.

Montana, G., Randazzo, L., and Sabbadini, S., 2014. Geomaterials in green building practices: comparative characterization of commercially available clay-based plasters. *Environmental Earth Sciences*, 71(2), pp.931–945.

Nakata, K. and Fujishima, A., 2012. TiO2 photocatalysis: Design and applications. *Journal of Photochemistry and Photobiology C: Photochemistry Reviews*, 13(3), pp.169–189.

Nakata, K., Ochiai, T., Murakami, T., and Fujishima, A., 2012. Photoenergy conversion with TiO2 photocatalysis: New materials and recent applications. *Electrochimica Acta*, 84, pp.103–111.

Nazaroff, W.W. and Weschler, C.J., 2004. Cleaning products and air fresheners: Exposure to primary and secondary air pollutants. *Atmospheric Environment*, 38(18), pp.2841–2865.

Niedermayer, S., Fürhapper, C., Nagl, S., Polleres, S., and Schober, K.P., 2013. VOC sorption and diffusion behavior of building materials. *European Journal of Wood and Wood Products*, 71(5), pp.563–571.

Ohlmeyer, M., Makowski, M., Fried, H., Hasch, J., and Schoeler, M., 2008. Influence of panel thickness on the release of volatile organic compounds from OSB made of Pinus sylvestris L. *Forest Products Journal*, 58(1–2), pp.65–70.

Pacheco-Torgal, F., 2014. Eco-efficient construction and building materials research under the EU Framework Programme Horizon 2020. *Construction and Building Materials*, 51, pp.151–162.

Pacheco-Torgal, F. and Jalali, S., 2011. *Eco-efficient Construction and Building Materials*. Springer.

Paiva, N.T., Pereira, J., Ferra, J.M., Martins, J., Carvalho, L., and Magalhães, F.D., 2014. Development of phenol formaldehyde resin with low formaldehyde emissions that respects LEED certification. *International Wood Products Journal*, 5(3), pp.161–167.

Parida, S.K., Dash, S., Patel, S., and Mishra, B.K., 2006. Adsorption of organic molecules on silica surface. *Advances in Colloid and Interface Science*, 121(1–3), pp.77–110.

Park, J.S. and Ikeda, K., 2006. Variations of formaldehyde and VOC levels during 3 years in new and older homes. *Indoor Air*, 16(2), pp.129–135.

Pirayesh, H., Khanjanzadeh, H., and Salari, A., 2013. Effect of using walnut/almond shells on the physical, mechanical properties and formaldehyde emission of particleboard. *Composites Part B: Engineering*, 45(1), pp.858–863.

Pirayesh, H., Khazaeian, A., and Tabarsa, T., 2012. The potential for using walnut (Juglans regia L.) shell as a raw material for wood-based particleboard manufacturing. *Composites Part B: Engineering*, 43(8), pp.3276–3280.

Popa, J. and Haghighat, F., 2003. The impact of VOC mixture, film thickness and substrate on adsorption/desorption characteristics of some building materials. *Building and Environment*, 38(7), pp.959–964.

Raw, G.J., Coward, S.K.D., Brown, V.M., and Crump, D.R., 2004. Exposure to air pollutants in English homes. *Journal of Exposure Analysis and Environmental Epidemiology*, 14 Suppl 1, pp.S85–S94.

Razak, N.I.A., Ibrahim, N.A., Zainuddin, N., Rayung, M., and Saad, W.Z., 2014. The influence of chemical surface modification of kenaf fiber using hydrogen peroxide on the mechanical properties of biodegradable kenaf fiber/poly(lactic acid) composites. *Molecules*, 19(3), pp.2957–2968.

Rizk, M., Verriele, M., Dusanter, S., Schoemaecker, C., Le Calve, S., and Locoge, N., 2016. Fast sorption measurements of volatile organic compounds on building materials: Part 1 - Methodology developed for field applications. *Building and Environment*, 99, pp.200–209.

Rizk, M., Verriele, M., Mendez, M., Blond, N., Dusanter, S., Schoemaecker, C., Blondeau, P., Le Calvé, S., and Locoge, N., 2016. Fast sorption measurements of volatile organic compounds on building materials: Part 2 Comparison between FLEC and CLIMPAQ methods. *Building and Environment*, 99, pp.239–251.

Rode, C., Peuhkuri, R., Mortensen, L., Hansen, K., Time, B., Gustavsen, A., Ojanen, T., Ahonen, J., Svennberg, K., and Arfvidsson, J., 2005. *Moisture buffering of building materials*. Technical University of Denmark, Department of Civil Engineering.

Rodgers, K.A. and Hampton, W.A., 2003. Laser Raman identification of silica phases comprising microtextural components of sinters. *Mineralogical Magazine*, 67(1), pp.1–13.

Rogers, G.E., 1959. Electron Microscope Studies of Hair and Wool. *Annals of the New York Academy of Sciences*, 83(3), pp.378–399.

Rouquerol, F., Rouquerol, J., Sing, K.S.W., Llewellyn, P., and Maurin, G., 2014. *Adsorption by powders and porous solids: Principles, Methodology and Applications*.

Ruiz, J., Bilbao, R., and Murillo, M.B., 1998. Adsorption of different VOC onto soil minerals from gas phase: Influence of mineral, type of VOC, and air humidity. *Environmental Science & Technology*, 32(8), pp.1079–1084.

Salthammer, T., 2016. Very volatile organic compounds: An understudied class of indoor air pollutants. *Indoor Air*, 26(1), pp.25–38.

Salthammer, T. and Fuhrmann, F., 2007. Photocatalytic surface reactions on indoor wall paint. *Environmental Science & Technology*, 41(18), pp.6573–6578.

Salthammer, T., Mentese, S., and Marutzky, R., 2010. Formaldehyde in the indoor environment. *Chemical Reviews*, 110(4), pp.2536–2572.

Salthammer, T., Schwarz, A., and Fuhrmann, F., 1999. Emission of reactive compounds and secondary products from wood-based furniture coatings. *Atmospheric Environment*, 33(1), pp.75–84.

Samet, J.M., Marbury, M.C., and Spengler, J.D., 1987. Health effects and sources of indoor air pollution. Part I. *American Review of Respiratory Diseases*, (5), pp.1486–1508.

Samet, J.M., Marbury, M.C., and Spengler, J.D., 1988. Health effects and sources of indoor air pollution. Part II. *American Review of Respiratory Diseases*, (5), pp.221–242.

Sampath, S., Uchida, H., and Yoneyama, H., 1994. Photocatalytic Degradation of Gaseous Pyridine over Zeolite-Supported Titanium Dioxide. *Journal of Catalysis*, 149(1), pp.189–194.

Senff, L., Hotza, D., and Labrincha, J.A., 2011. Effect of red mud addition on the rheological behaviour and on hardened state characteristics of cement mortars. *Construction and Building Materials*, 25(1), pp.163–170.

Senff, L., Tobaldi, D.M., Lucas, S., Hotza, D., Ferreira, V.M., and Labrincha, J.A., 2013.

Formulation of mortars with nano-SiO2 and nano-TiO2 for degradation of pollutants in buildings. *Composites Part B: Engineering*, 44(1), pp.40–47.

da Silva, C.F., Rana, C., Maskell, D., Dengel, A., Ansell, M., and Ball, R., 2016. Influence of eco-materials on indoor air quality. *Green Materials*, 4(2), pp.72–80.

da Silva, C.F., Stefanowski, B.K., Maskell, D., Ormondroyd, G.A., Ansell, M.P., Dengel, A., and Ball, R.J., 2017. Improvement of Indoor Air Quality by MDF panels containing walnut shell. *Building and Environment (under revision)*.

Sing, K.S.W., Everett, D., Haul, W., Moscou, L., Pierotti, R., Rouquerol, J., and Siemieniewska, T., 1985. Reporting physisorption data for gas/solid systems with special reference to the determination of surface area and porosity. *Pure & Appl. Chem.*, 57(4), pp.603–619.

Singer, B.C., Coleman, B.K., Destaillats, H., Hodgson, A.T., Lunden, M.M., Weschler, C.J., and Nazaroff, W.W., 2006. Indoor secondary pollutants from cleaning product and air freshener use in the presence of ozone. *Atmospheric Environment*, 40(35), pp.6696–6710.

Skinner, C., Stefanowski, B.K., Heathcote, D., Charlton, A., and Ormondroyd, G.A., 2016. Life cycle assessment of pilot-scale wood fibre production using mechanical disc refining at different pressures. *International Wood Products Journal*, 7(3), pp.149–155.

Son, Y.S., Lim, B.A., Park, H.J., and Kim, J.C., 2013. Characteristics of volatile organic compounds (VOCs) emitted from building materials to improve indoor air quality: Focused on natural VOCs. *Air Quality, Atmosphere and Health*, 6(4), pp.737–746.

Takeda, N., Ohtani, M., Torimoto, T., Kuwabata, S., and Yoneyama, H., 1997. Evaluation of diffusibility of adsorbed propionaldehyde on titanium dioxide-loaded adsorbent photocatalyst films from its photodecomposition rate. *J. Phys. Chem. B*, 101(14), pp.2644–2649.

Tichenor, B.A., Guo, Z., Dunn, J.E., Sparks, L.E., and Mason, M.A., 1991. Interaction of Vapour phase Organic Compounds with Indoor Sinks. *Indoor Air*, 1, pp.23–35.

Tobaldi, D.M., Piccirillo, C., Rozman, N., Pullar, R.C., Seabra, M.P., ??kapin, A.S., Castro, P.M.L., and Labrincha, J.A., 2016. Effects of Cu, Zn and Cu-Zn addition on the microstructure and antibacterial and photocatalytic functional properties of Cu-Zn modified TiO2 nano-heterostructures. *Journal of Photochemistry and Photobiology A: Chemistry*, 330, pp.44–54.

Tobaldi, D.M., Pullar, R.C., Škapin, A.S., Seabra, M.P., and Labrincha, J.A., 2014. Visible light activated photocatalytic behaviour of rare earth modified commercial TiO2. *Materials Research Bulletin*, 50, pp.183–190.

U.S. Environmental Protection Agency, 1991. Indoor Air Facts No. 4 Sick Building Syndrome. *EPA - Air & Radiation (6609J), Research and Development (MD-56)*, pp.1–4.

U.S. Environmental Protection Agency, 2009. *Regulation for reducing emissions from consumer products* [Online]. Available from: https://www.arb.ca.gov/consprod/regs/2008/3cp.htm#94509 [Accessed 20 January 2017].

U.S. Environmental Protection Agengy, 2016. *Formaldehyde Emission Standards for Composite Wood Products* [Online]. Available from: https://www.regulations.gov/document?D=EPA-HQ-OPPT-2016-0461-0001 [Accessed 9 February 2017].

Uhde, E. and Salthammer, T., 2007. Impact of reaction products from building materials and furnishings on indoor air quality-A review of recent advances in indoor chemistry. *Atmospheric Environment*, 41(15), pp.3111–3128.

Vieira, J., Senff, L., Gonçalves, H., Silva, L., Ferreira, V.M., and Labrincha, J.A., 2014. Functionalization of mortars for controlling the indoor ambient of buildings. *Energy and Buildings*, 70, pp.224–236.

Virta, J., Koivula, M., Hussein, T., Koponen, S., Hakkarainen, H., Kymäläinen, H.R., Hämeri, K., Kulmala, M., and Hautala, M., 2005. Emissions from thermal insulations - Part 1: Development and characteristics of the test apparatus. *Building and Environment*, 40(6), pp.797–802.

Wal, J.F., Hoogeveen, A.W., and Leeuwen, L., 1998. A Quick Screening Method for Sorption Effects of Volatile Organic Compounds on Indoor Materials. *Indoor Air*, 8, pp.103–112.

Wang, B., Yang, W., McKittrick, J., and Meyers, M.A., 2016. Keratin: Structure, mechanical properties, occurrence in biological organisms, and efforts at bioinspiration. *Progress in Materials Science*, 76, pp.229–318.

Wang, S., Ang, H.M., and Tade, M.O., 2007. Volatile organic compounds in indoor environment and photocatalytic oxidation: State of the art. *Environment International*, 33(5), pp.694–705.

Weschler, C.J., 2016. Roles of the human occupant in indoor chemistry. *Indoor Air*, 26(1),

pp.6–24.

Weschler, C.J. and Shields, H.C., 2000. The influence of ventilation on reactions among indoor pollutants: modeling and experimental observations. *Indoor air*, 10(2), pp.92–100.

Weschler, C.J. and Shields, H.C., 2003. Experiments probing the influence of air exchange rates on secondary organic aerosols derived from indoor chemistry. *Atmospheric Environment*, 37(39–40), pp.5621–5631.

Wojciechowska, E., Włochowicza, A., and Wesełucha-Birczyńskab, A., 1999. Application of Fourier-Transform Infrared and Raman Spectroscopy to Study Degradation of the Wool Fiber Keratin. *Journal of Molecular Structure*, 512(511–512), pp.307–318.

Wolkoff, P., 1998. Impact of air velocity, temperature, humidity, and air on long-term VOC emissions from building products. *Atmospheric Environment*, 32(14–15), pp.2659–2668.

Wolkoff, P., 1999. How to measure and evaluate volatile organic compound emissions from building products. A perspective. *Science of the Total Environment*, 227(2–3), pp.197–213.

Won, D., Corsi, R.L., and Rynes, M., 2001. Sorptive interactions between VOCs and indoor materials. *Indoor Air*, 11(4), pp.246–256.

World Health Organization, 1989. *Indoor air quality: Organic pollutants.* Copenhagen: WHO Regional Office for Europe (EURO Reports and Studies No. 111.).

World Health Organization, 2010. *WHO guidelines for indoor air quality: selected pollutants*. Copenhagen: World Health Organisation Regional Office for Europe.

Xu, J. and Zhang, J.S., 2011. An experimental study of relative humidity effect on VOCs' effective diffusion coefficient and partition coefficient in a porous medium. *Building and Environment*, 46(9), pp.1785–1796.

Young, D.M. and Crowell, A.D., 1962. *Physical adsorption of gases*. Butterworth & Co.

Yu, C. and Crump, D., 1998. A review of the emission of VOCs from polymeric materials used in buildings. *Building and Environment*, 33(6), pp.357–374.

Yu, C. and Crump, D., 2010. Indoor Environmental Quality - Standards for Protection of Occupants' Safety, Health and Environment. *Indoor and Built Environment*, 19(5), pp.499–502.

Yu, C. and Crump, D., 2011. Standards for Evaluating Indoor Air. *Indoor and Built*

Environment, 20(4), pp.389–392.

Yu, C.W.F., Crump, D., and Squire, R.W., 1999. The effect of introducing new materials on the indoor concentrations of VOCs and formaldehyde in an unoccupied test house. In: *Proceedings, Indoor Air 99*.

Yu, C.W.F. and Jeong Tai Kim, J.T., 2010. Building Pathology, Investigation of Sick Buildings - VOC Emissions. *Indoor and Built Environment*, 19(1), pp.30–39.

Yu, C.W.F. and Kim, J.T., 2012. Low-Carbon Housings and Indoor Air Quality. *Indoor and Built Environment*, 21(1), pp.5–15.

Zhang, J., Zhang, J., and Chen, Q., 2002. Effects of Environmental Conditions on the VOC Sorption by Building Materials - Part 1: Experimental Results. *ASHRAE Transactions*, 108(2), pp.273–282.

Zhang, L.Z., 2005. Comparisons of emissions of polar and non-polar VOCs in a room. In: *Proceedings, Indoor Air 2005*.

Zhang, Y., Luo, X., Wang, X., Qian, K., and Zhao, R., 2007. Influence of temperature on formaldehyde emission parameters of dry building materials. *Atmospheric Environment*, 41(15), pp.3203–3216.

Standards list

BS EN 1015-2:1999. Methods of test for mortar for masonry. Bulk sampling of mortars and preparation of test mortars.

BS EN 1015-3:1999. Methods of test for mortar for masonry. Determination of consistence of fresh mortar (by flow table).

BS EN 1015-11:1999. Methods of test for mortar for masonry. Determination of flexural and compressive strength of hardened mortar.

BS EN ISO 16000-9:2006. Indoor air. Determination of the emission of volatile organic compounds from building products and furnishing. Emission test chamber method.

BS EN ISO 16000-10:2006. Indoor air. Determination of the emission of volatile organic compounds from building products and furnishing. Emission test cell method.

BS EN ISO/IEC 17025:2005. General requirements for the competence of testing and calibration laboratories.

BS ISO 9277:2010. Determination of the specific surface area of solids by gas adsorption. BET method.

BS ISO 16000-3:2011. Indoor air. Determination of formaldehyde and other carbonyl compounds in indoor air and test chamber air. Active sampling method.

BS ISO 16000-6:2011. Indoor air. Determination of volatile organic compounds in indoor and test chamber air by active sampling on Tenax TA sorbent, thermal desorption and gas chromatography using MS or MS-FID.

CEN/TS 16516:2013. Construction products. Assessment of release of dangerous substances. Determination of emissions into indoor air.

ISO GUM – JCGM 100:2008. Evaluation of measurement data - Guide to the expression of uncertainty in measurement.

Appendix

A1 – IAQ uncertainty

The calculation of the uncertainty of the emissions and adsorption/desorption testing for VOCs and formaldehyde followed the guide from ISO GUM – JCGM 100:2008.

A standard uncertainty gives the probability of a measured value being true of about 68 %. Therefore, the expanded uncertainty is used to gain a level of confidence of 95 % in the case of using a coverage factor of 2 or greater than 99 % if the coverage factor is 3. The expanded uncertainty is calculated by multiplying the standard combined uncertainty with the coverage factor. The mathematical expression is shown in Equation A1:

$$U = k \times \sqrt{u1^2 + u2^2 + u3^2 + \cdots + un^2} \qquad \text{Eq. A1}$$

Where *U* is the expanded uncertainty, *k* is the coverage factor and *un* is the uncertainty of each contributor to the uncertainty.

The uncertainty inputs in common for formaldehyde and VOCs are those related to the sampling process: calibrated flow meter, timing of sampling period, drift of the sampling pump during sampling, operator bias and laboratory bias.

The combined uncertainty of the formaldehyde analysis took into account the following inputs: drift of the HPLC detector and drift of the flow meter. The drift of the HPLC detector is assessed by the daily QC solution checks. The QC tolerance was set by the laboratory to be 15 %. The experimental conditions were: sampling flow rate of 1500 ml/min during 30 min. The target concentration of formaldehyde was 100 µg/m^3. The **expanded uncertainty for formaldehyde** with a confidence level of 99 % **was 6.3 %.**

The combined uncertainty for the toluene, limonene and dodecane analysis took into account the following inputs: drift of the FID and drift of the flow meter. The analysis carried out in the MS coupled to the GC is not taken into account because it is not a quantitative analysis as is the case of the HPLC and GC. The experimental conditions were: sampling flow rate of 200

ml/min during 30 min. The target concentration of formaldehyde was 300 μg/m^3. The **expanded uncertainty for toluene, limonene and dodecane** with a confidence level of 99 % **was 6.7 %.**

A2 – Raw data of the adsorption and desorption experiments

Tables with raw data from the VOCs and formaldehyde adsorption and desorption experiments carried out in the 2-litre and 30 m^3 environmental chambers are presented below.

Table A 1 Adsorption and desorption data from 2-litre chambers - Chapter 4.

Time (h)	Chemical name	MDF	Coated_MDF	Mortar_RS	Natural wool	Ref. chamber
0	Toluene	0	0	0	0	0
0	Limonene	0	0	0	0	0
0	Dodecane	0	0	0	0	0
0	Formaldehyde	0	0	0	0	0
1	Toluene	1764	1590	1258	1736	1679
1	Limonene	2127	1730	904	2199	2140
1	Dodecane	2209	1574	498	2040	2370
1	Formaldehyde	296	608	241	294	681
24	Toluene	2285	2173	1947	2119	2169
24	Limonene	2533	2338	1874	2377	2397
24	Dodecane	2877	2519	1321	2626	2755
24	Formaldehyde	565	718	380	356	754
48	Toluene	2312	2291	2119	2175	2133
48	Limonene	2547	2558	2096	2488	2371
48	Dodecane	2652	2789	1549	2717	2598
48	Formaldehyde	581	762	431	394	772
144	Toluene	2223	2131	1934	2091	2021
144	Limonene	2547	2494	2106	2391	2225
144	Dodecane	2656	2703	1831	2619	2572
144	Formaldehyde	319	782	160	433	779
146	Toluene	172	84	482	16	13
146	Limonene	420	167	1068	48	24
146	Dodecane	721	455	1893	515	141
146	Formaldehyde	120	151	255	0	0
170	Toluene	8	15	83	7	6
170	Limonene	95	36	292	4	3
170	Dodecane	112	47	552	25	18
170	Formaldehyde	189	0	141	130	0
194	Toluene	7	9	33	7	1
194	Limonene	56	28	189	2	2
194	Dodecane	86	34	410	17	14
194	Formaldehyde	0	0	97	0	0

Table A 2 Adsorption and desorption data of the MDF panel tested in the 30 m^3 environmental chamber - Chapter 4.

	Time (h)	Toluene	Limonene	Dodecane
Outlet	0	21	2	11
	3	4005	474	464
	5	3612	431	562
	24	2178	376	539
	48	1591	356	527
	73	2422	336	551
	143	1137	280	571
	147	16	7	33
	149	16	6	29
	167	13	4	19
	192	11	3	15
	216	12	4	17
	312	4	3	12
Inlet	0	22	2	12
	3	4763	773	1371
	5	4352	717	1375
	24	2661	668	1369
	48	1807	622	1351
	73	2762	585	1403
	143	1399	498	1451
	147	17	5	21
	149	15	4	18
	167	14	4	17
	192	11	3	15
	216	12	3	15

Table A 3 Adsorption and desorption data of MDF panels modified with walnut shells tested in the 2-litre chambers - Chapter 5.

Time (h)	Chemical name	0% walnut	5%walnut	10% walnut	15% walnut	Ref. chamber
0	Toluene	0	0	0	0	0
0	Limonene	0	0	0	0	0
0	Dodecane	0	0	0	0	0
0	Formaldehyde	154	132	168	178	0
1	Toluene	1495	1421	1488	1520	1507
1	Limonene	575	546	536	505	658
1	Dodecane	347	331	306	261	584
1	Formaldehyde	365	310	298	277	562
2	Toluene	1534	1414	1565	1529	1536
2	Limonene	594	531	578	538	663
2	Dodecane	398	353	383	312	596
2	Formaldehyde	355	318	308	282	577
4	Toluene	1521	1466	1528	1564	1691
4	Limonene	601	588	593	594	657
4	Dodecane	448	430	421	390	574
4	Formaldehyde	382	337	321	293	562
24	Toluene	1564	1471	1518	1457	1821
24	Limonene	726	663	691	622	693
24	Dodecane	632	582	580	522	650
24	Formaldehyde	398	332	337	321	566
48	Toluene	1576	1524	1609	1579	1533
48	Limonene	775	729	771	778	757
48	Dodecane	972	924	957	942	1043
48	Formaldehyde	397	342	337	321	586
144	Toluene	1791	1719	1696	1784	1689
144	Limonene	1448	1393	1371	1476	1408
144	Dodecane	2475	2399	2365	2493	2518
144	Formaldehyde	418	354	351	343	573
218	Toluene	1866	1752	1809	2028	1828
218	Limonene	1993	1842	1944	2117	1973
218	Dodecane	2858	2641	2805	3042	2881
218	Formaldehyde	427	366	363	345	551
285	Toluene	1781	1718	1745	1870	1808
285	Limonene	2040	1978	2002	2147	2064
285	Dodecane	2696	2616	2658	2857	2772
285	Formaldehyde	428	382	365	340	563
286	Toluene	101	91	97	111	5
286	Limonene	357	329	455	553	20
286	Dodecane	1066	971	1219	1391	140
286	Formaldehyde	238	209	228	238	0
287	Toluene	40	37	34	37	4
287	Limonene	255	228	342	409	16
287	Dodecane	818	722	978	1130	117
287	Formaldehyde	156	141	164	200	0
289	Toluene	7	8	8	8	0

289	Limonene	173	151	210	262	9
289	Dodecane	588	495	692	854	66
289	Formaldehyde	221	187	210	220	0
309	Toluene	0	0	0	0	0
309	Limonene	34	28	23	31	0
309	Dodecane	200	176	238	306	26
309	Formaldehyde	184	148	182	192	0
333	Toluene	11	0	0	0	0
333	Limonene	7	0	0	0	0
333	Dodecane	134	0	0	0	0
333	Formaldehyde	119	102	124	120	0

Table A 4 Adsorption and desorption data of modified clay-based mortars and lime mortar with cellulose tested in the 2-litre chambers- Chapter 6.

Time (h)	Chemical name	Cell_mortar	Clay_E14	Clay_H2	Ref. chamber
0	Toluene	37	0	0	13
0	Limonene	0	0	0	0
0	Dodecane	0	0	0	0
0	Formaldehyde	0	0	0	0
2	Toluene	969	907	901	685
2	Limonene	1441	1333	1349	445
2	Dodecane	832	1012	981	453
2	Formaldehyde	168	146	130	1035
4	Toluene	1013	976	968	1140
4	Limonene	1599	1509	1529	2239
4	Dodecane	1087	1166	1153	2459
4	Formaldehyde	130	181	144	1042
24	Toluene	1038	1013	1001	1024
24	Limonene	1852	1781	1803	2136
24	Dodecane	1778	1536	1525	2438
24	Formaldehyde	270	370	340	1166
48	Toluene	1024	1038	1021	1050
48	Limonene	1950	1898	1898	2182
48	Dodecane	1946	1744	1729	2513
48	Formaldehyde	362	440	293	1132
72	Toluene	1002	975	990	1010
72	Limonene	2022	1933	1927	2152
72	Dodecane	2005	1817	1836	2551
72	Formaldehyde	320	425	336	1091
192	Toluene	963	933	939	927
192	Limonene	2170	2122	2045	2122
192	Dodecane	2284	2193	2100	2582
192	Formaldehyde	465	643	480	1213
195	Toluene	102	128	136	0
195	Limonene	693	759	723	13
195	Dodecane	1296	1026	1079	78
195	Formaldehyde	325	371	313	129
197	Toluene	49	79	113	0
197	Limonene	516	594	580	8
197	Dodecane	1052	866	867	56
197	Formaldehyde	404	335	260	19
217	Toluene	12	0	16	0
217	Limonene	222	259	265	3
217	Dodecane	323	384	387	22
217	Formaldehyde	135	183	148	0
241	Toluene	8	0	7	0
241	Limonene	119	167	178	0
241	Dodecane	197	263	275	13
241	Formaldehyde	61	86	61	0
313	Toluene	8	0	0	0

313	Limonene	18	36	57	0
313	Dodecane	93	115	116	0
313	Formaldehyde	33	0	33	0

Table A 5 Data of the VOCs adsorption and desorption of lime-based mortars modified with natural wool tested in the 2-litre chambers - Chapter 6.

Time (h)	Chemical name	Ref. mortar	TL w. mortar	1 % w. mortar	2.5 % w. mortar	Ref. chamber
0	Toluene	0	0	0	0	0
0	Limonene	0	0	0	0	0
0	Dodecane	0	0	0	0	0
1	Toluene	1720	1723	1789	1825	2649
1	Limonene	819	862	1097	1096	2545
1	Dodecane	351	397	509	455	1464
3	Toluene	2089	2075	2053	2115	2601
3	Limonene	1294	1324	1428	1520	2681
3	Dodecane	509	544	621	642	1807
5	Toluene	2160	2115	2128	2146	2624
5	Limonene	1457	1472	1631	1630	2713
5	Dodecane	624	627	772	722	1882
24	Toluene	2431	2389	2310	2406	2226
24	Limonene	2042	2043	2018	2176	2457
24	Dodecane	997	1014	1106	1191	1935
48	Toluene	1906	1985	1943	2058	1931
48	Limonene	1593	1727	1716	1822	2081
48	Dodecane	793	952	979	1022	1666
120	Toluene	2080	2058	2013	2181	2038
120	Limonene	1972	1966	1905	2074	2199
120	Dodecane	1275	1296	1292	1407	1847
168	Toluene	2266	2281	2352	2415	2211
168	Limonene	2155	2184	2198	2277	2308
168	Dodecane	1454	1532	1547	1581	1988
190	Toluene	1997	2040	1961	2160	1912
190	Limonene	1929	1969	1893	2034	2058
190	Dodecane	1338	1385	1366	1441	1794
191	Toluene	687	688	669	671	12
191	Limonene	1314	1145	1122	1125	32
191	Dodecane	1093	1031	1026	1029	222
193	Toluene	443	446	484	435	0
193	Limonene	1004	940	857	808	14
193	Dodecane	950	949	891	862	81
195	Toluene	362	353	391	356	8
195	Limonene	832	812	740	662	10
195	Dodecane	886	878	821	791	58
214	Toluene	67	83	116	122	12
214	Limonene	359	334	340	309	3
214	Dodecane	462	436	429	399	29
218	Toluene	54	68	84	100	0
218	Limonene	353	328	325	288	0
218	Dodecane	448	427	400	378	0
296	Toluene	0	0	0	0	0
296	Limonene	170	159	158	131	0
296	Dodecane	213	208	190	177	0

320	Toluene	0	0	26	0	0
320	Limonene	137	125	117	102	0
320	Dodecane	167	163	143	138	0

Table A 6 Data of the formaldehyde adsorption and desorption of lime-based mortars modified with natural wool tested in the 2-litre chambers - Chapter 6.

Time (h)	**Chemical name**	**Ref. mortar**	**TL w. mortar**	**1 % w. mortar**	**2.5 % w. mortar**	**Gypsum**	**Ref. chamber**
0	Formaldehyde	0	0	0	0	0	0
1	Formaldehyde	14	0	0	0	283	70
3	Formaldehyde	0	0	0	0	287	97
5	Formaldehyde	0	19	0	0	294	132
24	Formaldehyde	126	54	17	15	311	231
48	Formaldehyde	139	65	16	20	303	260
55	Formaldehyde	109	62	17	18	298	237
120	Formaldehyde	134	82	18	21	304	276
144	Formaldehyde	142	88	23	22	315	293
145	Formaldehyde	112	72	16	12	8	209
147	Formaldehyde	72	62	17	11	0	161
149	Formaldehyde	78	57	18	11	0	141
168	Formaldehyde	52	49	16	11	0	86
192	Formaldehyde	38	43	9	8	0	69
217	Formaldehyde	27	28	12	10	0	55

Table A 7 Data of the VOCs adsorption and desorption of clay-based plaster tested in the 30m^3 environmental chamber – Chapter 6.

	Time (h)	Toluene	Limonene	Dodecane
Centre	0	12	18	5
	2	856	919	609
	4	1000	719	654
	23	951	468	895
	29	937	524	1087
	47	934	542	1235
	118	813	447	1076
	121	205	153	582
	124	61	71	405
	142	4	9	191
	148	3	7	194
	169	2	3	134
	173	2	2	97
	191	2	2	107
Inlet	0	0	0	0
	2	1189	1040	2088
	23	1000	619	1971
	118	843	570	1947
	121	7	7	25
	142	1	1	10

Table A 8 Data of the adsorption and desorption of lime-based mortars modified with TiO_2 particles tested under dark conditions in the 2-litre chambers - Chapter 7.

Time (h)	Chemical name	ETD	ETDK2	ETKD3	ETDK5	Ref. chamber
0	Toluene	0	0	0	0	0
0	Limonene	0	0	0	0	0
0	Dodecane	0	0	0	0	0
0	Formaldehyde	0	0	0	0	0
1	Toluene	674	674	674	624	891
1	Limonene	257	269	235	208	659
1	Dodecane	136	141	134	118	596
1	Formaldehyde	172	170	154	160	569
24	Toluene	799	806	804	812	829
24	Limonene	542	546	554	545	632
24	Dodecane	278	281	325	283	608
24	Formaldehyde	368	315	282	290	621
50	Toluene	790	790	770	783	795
50	Limonene	589	592	574	573	612
50	Dodecane	403	410	380	325	568
50	Formaldehyde	339	330	296	338	596
96	Toluene	706	681	708	705	728
96	Limonene	534	517	538	529	542
96	Dodecane	387	375	368	330	460
96	Formaldehyde	385	356	316	364	586
168	Toluene	774	778	783	760	793
168	Limonene	562	563	568	551	559
168	Dodecane	375	365	376	341	460
168	Formaldehyde	317	309	326	358	631
170	Toluene	161	162	169	178	3
170	Limonene	301	309	350	351	7
170	Dodecane	195	208	217	219	26
170	Formaldehyde	181	179	131	254	28
194	Toluene	9	10	10	2	0
194	Limonene	45	60	58	80	0
194	Dodecane	83	106	97	130	0
194	Formaldehyde	83	56	63	96	0
218	Toluene	10	13	11	10	0
218	Limonene	24	36	29	38	4
218	Dodecane	91	98	109	122	8
218	Formaldehyde	59	61	70	76	0

Table A 9 Data of the photocatalytic MDF panel tested in the 30m^3 environmental chamber (adsorption-photocatalysis and desorption) - Chapter 7.

	Time (h)	Toluene	Limonene	Dodecane
Centre	0	0	0	0
	1	537	530	108
	3	868	559	200
	5	1058	557	297
	24	1199	483	394
	48	1137	488	453
	72	1082	476	447
	144	1078	453	404
	191	1031	460	404
	192	1056	480	477
	194	1064	500	489
	196	1143	533	519
	215	1004	450	425
	239	938	432	407
	311	908	423	388
	335	855	404	366
	359	820	388	358
	361	457	263	328
	363	202	136	246
	365	109	90	210
	384	7	16	116
	408	5	8	85
	480	0	3	43
Inlet	0	0	0	0
	1	1194	876	608
	3	1191	665	613
	5	1247	582	632
	24	1217	530	620
	48	**1120**	**509**	**592**
	72	1170	535	613
	144	1133	563	680
	191	1066	556	659
	192	1074	566	677
	194	1191	637	790
	196	1226	666	812
	215	1029	538	629
	239	1013	544	636
	311	930	515	607
	335	864	484	554
	359	850	477	568

	361	11	7	15
	363	9	5	14
	365	6	5	13
	384	0	0	0
	408	0	0	0
	480	0	0	0